HYDROTREATING HEAVY OILS OVER A COMMERCIAL HYDRODEMETALLATION CATALYST

by

Seokhwan Kwak

A dissertation to the faculty of
The University of Utah
in partial fulfillment of the requirements for the degree of

Doctor of Philosophy

Department of Chemical and Fuels Engineering

The University of Utah

August 1994

ABSTRACT

A Uinta Basin bitumen was hydrotreated over a sulfided Ni-Mo on alumina commercial hydrodemetallation catalyst. The catalyst was on-stream continuously for more than 1,000 hours. The data were obtained with the reactor operating as a fixed bed reactor in the upflow mode to ensure complete wetting of the catalyst and nearly isothermal operation.

The deactivation of the catalyst was monitored by the decline in the API gravity of the total liquid product with time-on-stream at a standard set of conditions. The primary process variables studied were reactor temperature (620-685 K; 656-775 °F), liquid weight hourly space velocity (0.24-1.38 h^{-1}) and total reactor pressure (11.3-16.7 MPa; 1634-2423 psia). The hydrogen/oil ratio was fixed in all experiments at 890 m^3/m^3 (5000 scf H_2/bbl).

The extent of heteroatom and metals removal, residuum (>1000 °F) conversion and molecular weight reduction were determined as a function of process operating variables. Simulated distillation of the hydrotreated total liquid products was used to compute residuum conversion and product distributions. Conradson carbon residue conversion and pour point reduction were also determined as functions of process operating conditions.

Hydrodenitrogenation, hydrodesulfurization, hydrodemetallation and residuum conversion data were analyzed using a modified power rate law model. The apparent kinetic parameters were obtained by combined non-linear regression and ordinary differential equation solver techniques for the analysis of laboratory data. Simple first-order power rate law expressions for

hydrodenitrogenation and hydrodesulfurization were obtained for bitumen hydrotreating over the hydrodemetallation catalyst. Higher than first-order kinetic data for residuum conversion and nickel removal were organized by invoking two parallel first-order reactions for the facile and refractory fractions. A molecular weight reduction model was proposed to examine the extent of residuum conversion to gas-oil, middle distillate and gases. The first-order rate constants were also determined.

The hydrodemetallation catalyst was less active for nitrogen, sulfur and residuum conversion than the hydrodenitrogenation catalyst. Nitrogen, sulfur, and metals removal; residuum conversion; and product distributions are discussed for bitumen hydrotreating over the hydrodemetallation and hydrodenitrogenation catalysts.

TABLE OF CONTENTS

HYDROTREATING HEAVY OILS OVER A COMMERCIAL HYDRODEMETALLATION CATALYST

by

Seokhwan Kwak

A dissertation to the faculty of
The University of Utah
in partial fulfillment of the requirements for the degree of

Doctor of Philosophy

Department of Chemical and Fuels Engineering

The University of Utah

August 1994

ABSTRACT

A Uinta Basin bitumen was hydrotreated over a sulfided Ni-Mo on alumina commercial hydrodemetallation catalyst. The catalyst was on-stream continuously for more than 1,000 hours. The data were obtained with the reactor operating as a fixed bed reactor in the upflow mode to ensure complete wetting of the catalyst and nearly isothermal operation.

The deactivation of the catalyst was monitored by the decline in the API gravity of the total liquid product with time-on-stream at a standard set of conditions. The primary process variables studied were reactor temperature (620-685 K; 656-775 °F), liquid weight hourly space velocity (0.24-1.38 h^{-1}) and total reactor pressure (11.3-16.7 MPa; 1634-2423 psia). The hydrogen/oil ratio was fixed in all experiments at 890 m^3/m^3 (5000 scf H_2/bbl).

The extent of heteroatom and metals removal, residuum (>1000 °F) conversion and molecular weight reduction were determined as a function of process operating variables. Simulated distillation of the hydrotreated total liquid products was used to compute residuum conversion and product distributions. Conradson carbon residue conversion and pour point reduction were also determined as functions of process operating conditions.

Hydrodenitrogenation, hydrodesulfurization, hydrodemetallation and residuum conversion data were analyzed using a modified power rate law model. The apparent kinetic parameters were obtained by combined non-linear regression and ordinary differential equation solver techniques for the analysis of laboratory data. Simple first-order power rate law expressions for

hydrodenitrogenation and hydrodesulfurization were obtained for bitumen hydrotreating over the hydrodemetallation catalyst. Higher than first-order kinetic data for residuum conversion and nickel removal were organized by invoking two parallel first-order reactions for the facile and refractory fractions. A molecular weight reduction model was proposed to examine the extent of residuum conversion to gas-oil, middle distillate and gases. The first-order rate constants were also determined.

The hydrodemetallation catalyst was less active for nitrogen, sulfur and residuum conversion than the hydrodenitrogenation catalyst. Nitrogen, sulfur, and metals removal; residuum conversion; and product distributions are discussed for bitumen hydrotreating over the hydrodemetallation and hydrodenitrogenation catalysts.

TABLE OF CONTENTS

THE UNIVERSITY OF UTAH GRADUATE SCHOOL

SUPERVISORY COMMITTEE APPROVAL

of a dissertation submitted by

Seokhwan Kwak

This dissertation has been read by each member of the following supervisory committee and by majority vote has been found to be satisfactory.

March 8, 1994 — Chair: Francis V. Hanson

3/8/94 — Milind D. Deo

March 8, 1994 — A. Lamont Tyler

March 8, 1994 — Franklin E. Massoth

March 8, 1994 — Edward M. Eyring

THE UNIVERSITY OF UTAH GRADUATE SCHOOL

FINAL READING APPROVAL

To the Graduate Council of the University of Utah:

I have read the dissertation of Seokhwan Kwak in its final form and have found that (1) its format, citations and bibliographic style are consistent and acceptable; (2) its illustrative materials including figures, tables, and charts are in place; and (3) the final manuscript is satisfactory to the supervisory committee and is ready for submission to The Graduate School.

June 15, 1994
Date

Francis V. Hanson
Chair, Supervisory Committee

Approved for the Major Department

A. Lamont Tyler
Chair/Dean

Approved for the Graduate Council

Ann W. Hart
Dean of The Graduate School

LIST OF TABLES

LIST OF FIGURES

ACKNOWLEDGMENTS

I give my deep appreciation to my wife, Hyejeong Ihn Kwak, parents, Byongkwang Kwak and Soonjo Kim, and parents-in-law, Wonsik Ihn and Jeongmin Oh, for their tremendous support and patience throughout this endeavor. I especially dedicate this work to my wife. I cannot fully express the debt that I owe to her and I extend my love and respect to her.

I am grateful to my dissertation advisor, Professor Francis V. Hanson, for his guidance and help in the completion of this study. Special appreciation and thanks are due to him for his constant assistance, encouragement, faith and patience during the difficult stages of this research. I would like to express special appreciation to my supervisory committee: Professors Milind D. Deo, Franklin E. Massoth, A. Lamont Tyler and Edward M. Eyring.

Extreme gratitude is expressed to Dr. Daniel C. Longstaff for his assistance in conducting the experiments and providing thoughtful suggestions and discussions which were helpful in the completion of this work.

I extend my thanks to Dr. John Ward in UNOCAL Corporation for providing the HDM catalyst and for helpful suggestions and discussions.

The United States Department of Energy/Morgantown Energy Technology Center/Laramie Projects Office is also thanked for financial support.

I express appreciation to Mr. Jiazhi Pu for his support in the modeling and simulation work. Gratitude is extended to Dr. John Fletcher, Dr. Deepak Deshpande, Dr. Chi-Hsing Tsai, Dr. Larry Neer and Mr. Brett Jenkins for their helpful discussions and assistance in product analysis. Thanks are also due to

Dr. Yongseung Yun, Dr. Hoil Ryu, Mr. Hwal Song and Mrs. Jeesun Han, Mr. Chungwoo Kim, and all members of the Oil Sand Research Laboratory at the University of Utah for their kind friendship and support.

CHAPTER 1

INTRODUCTION

Heavy oils and bitumens are known for their high molecular weight and high concentrations of heteroatomic species such as nitrogen, sulfur and oxygen and metals such as Ni, V. and As. The heteroatomic species are a cause for environmental concern since they form SO_x and NO_x during combustion. Both metals and heteroatomic species are a concern in refinery processes such as catalytic cracking, hydrocracking and reforming by poisoning the catalysts.

In catalytic upgrading, heteroatoms are removed as H_2S and NH_3 via desulfurization and denitrogenation; however, in hydrodemetallation (HDM), metals are deposited on the catalyst as sulfides and cause irreversible fouling of the catalyst. This catalyst deactivation has a serious impact on the economics of residuum hydroprocessing because catalysts poisoned by metal deposition must be replaced whereas coked catalysts can be reused after regeneration. Therefore metals which are concentrated in the high molecular weight resin and asphaltene fractions ultimately determine the lifetime of the catalyst. Recent hydrotreating processes for upgrading heavy feedstocks have focused on catalysts having a low tendency toward coke formation and catalysts which can tolerate higher metal deposition [1].

A commercial hydrodemetallation catalyst which had a large pore diameter and volume was used in this study due to the nature of the Whiterocks bitumen: high molecular weight and high residuum content. These

characteristics of heavy feeds may cause maldistribution of the feedstock over the surface of the catalyst bed in conventional trickle-bed laboratory reactor operation. The resulting coning in the inlet region of the reactor and the consequent incomplete wetting of the catalyst may lead to the determination of erroneous apparent kinetic parameters and to misleading conclusions regarding the influence of process variables on conversion and product distribution and yields. Furthermore, lower superficial velocities in laboratory reactors at the same space velocity relative to the commercial reactor could lead to partial wetting of the catalyst. Therefore, the kinetic parameters for heteroatom removal and residuum conversion for bitumen and bitumen-derived heavy oil were determined in an reactor which operated upflow in the plug-flow mode.

The objective of this study was to determine the influence of process operating variables, temperature, pressure and residence time or space velocity on denitrogenation, desulfurization and residuum conversion and on product distributions and yields. The determination of apparent kinetic parameters was also undertaken.

CHAPTER 2

LITERATURE SURVEY

Origin of Bitumen

The potential hydrocarbon resource that occurs in oil sand deposits have been variously estimated on a worldwide basis as being in excess of 3 trillion (3 x 10^{12}) barrels of petroleum equivalent and the oil sand resource for the United States has been estimated to be in excess of 52 million barrels [2].

Oil sand is a general term for any rock material, loose or consolidated, that contains the bitumen in pores or fractures. It is usually composed of 85 wt% of rock matrix which is mostly quartz or carbonate sand-sized particles and the heavy oil called bitumen [3]. The bitumen has a reddish brown to black color and exists in semisolid under natural reservoir conditions due to its high viscosity. It contains more heteroatoms and metals and less volatiles than conventional petroleum crude oil. This bitumen must be recovered from the oil and upgraded to produce high quality hydrocarbon values.

Bitumen Separation Technologies

Bitumen can be recovered from oil sands by either in-situ thermal enhanced oil recovery processes or by aboveground recovery processes.

In-Situ Processes

In-situ thermal enhanced oil recovery processes can be divided into three types: 1) heating alone to reduce the viscosity of bitumen to release it from the rock, 2) solvent (or chemically active solution) injection to flush the bitumen from the rock and 3) combinations of heating and solvent injection.

Steam or hot water injection [4,5] and in-situ combustion (fire flooding) [6] belong to the first category. In steam injection processes minor changes occur in bitumen properties except for pour point and viscosity reduction [4,5]. However, when steam is introduced into the formation at high pressures, cracking may occur to some extent in addition to distillation. In-situ combustion usually causes significant physical and chemical changes in bitumen due to the coking and combustion of a portion of the bitumen to provide heat to mobilize bitumen and/or the bitumen-derived heavy oils. In-situ combustion includes a number of options: forward and reverse and wet and dry combustion [6].

Chemical processes which use chemicals or chemically active solutions for mobilizing bitumen result in minor changes in bitumen properties other than viscosity. In these processes, the chemical should be recovered and cleaned up for reuse in view of the high cost of the injected chemicals.

Aboveground Processes

The first step in all aboveground processes is mining or quarrying followed by size-reduction. The size and quantity along with the cost of this equipment are all enormous.

There are ways of recovering bitumen-derived heavy oils from oil sands after mining or quarrying: extraction using water and/or chemical solvents [7,8,9] and pyrolysis or thermal processing [10]. The extraction processes do not significantly influence the physical and chemical properties of bitumen; however,

the final mineral-free product is little different from the original reservoir fluid [7,8,9]. Pyrolysis or thermal processing results in significant physical and chemical changes to the bitumen-derived liquids recovered from the oil sands relative to the bitumen. A sufficient heat should be introduced in this type of processes to volatilize a portion of bitumen, thus, being separated from the oil sand; at the same time the heavier or higher boiling fractions of the bitumen will be thermally decomposed [10].

The alternative schemes for production of a refinery feedstock from oil sands are summarized in Figure 2.1.

Chemical Composition of Bitumen and Petroleum Resids

Definitions of heavy oils are usually based on the API gravity or viscosity at reservoir conditions and are frequently quite arbitrary [11]. The term "heavy oil" has often been used to describe conventional petroleum crude oils which have API gravities of less than 20 °API and which require thermal stimulation to induce mobility in the reservoir. The bitumen in oil sands which require surface mining followed by extraction or pyrolysis to recover hydrocarbon values are also defined to be heavy oils. Heavy oils are generally darker than conventional crudes and may even black.

Speight [2] classified the heavy oils according to the following density-gravity system:

- Heavy crude oil
  - Density-gravity range from 1,000 kg/m^3 to more than 934 kg/m^3 (10 °API to < 20 °API)
- Extra heavy crude oil (may also include atmospheric residua (boiling range 613 K to 923 K))

Figure 2.1

Alternative Schemes for Production of a Refinery Feedstock from Oil Sands

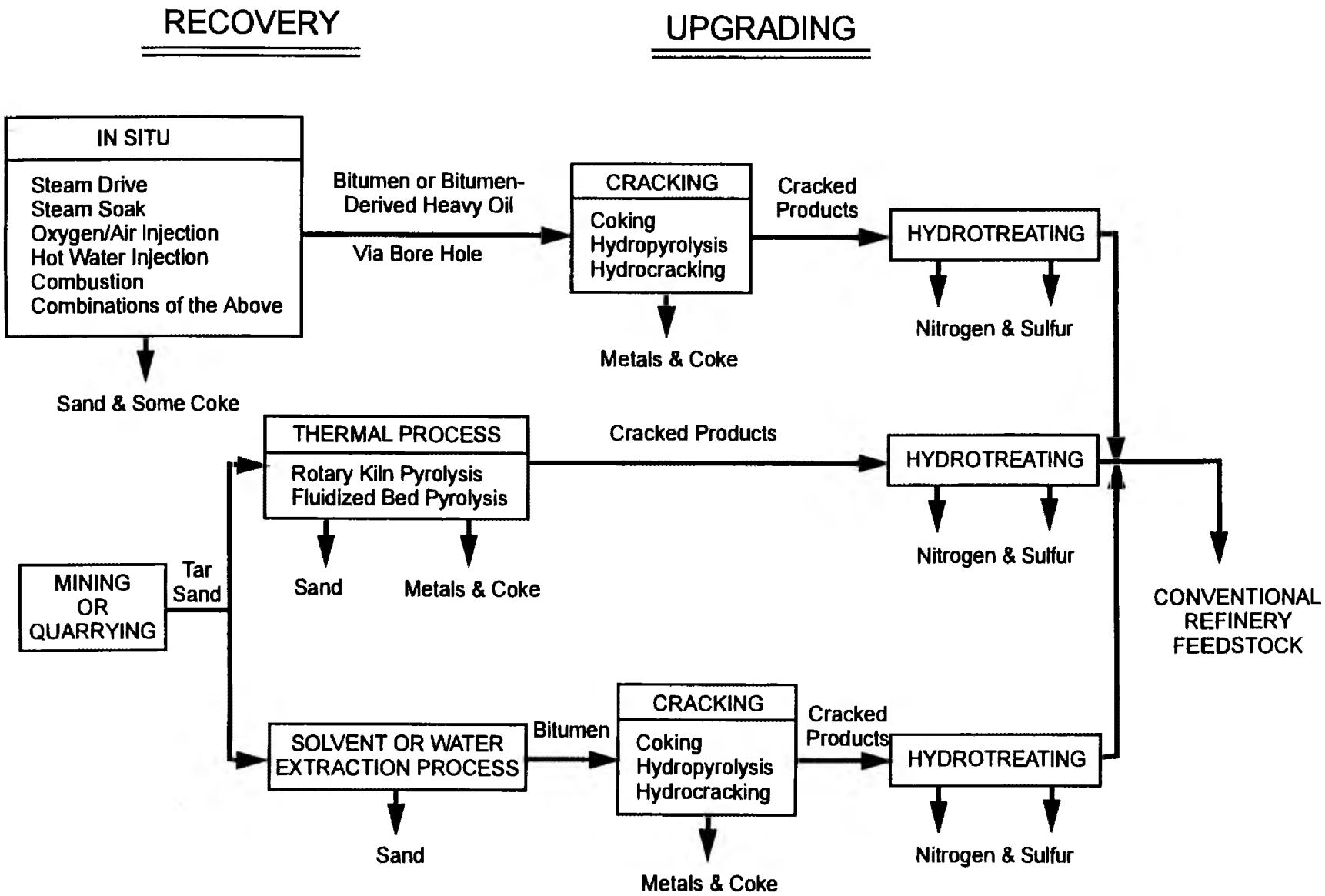
RECOVERY
UPGRADING
IN SITU
Steam Drive
Steam Soak
Oxygen/Air Injection
Hot Water Injection
Combustion
Combinations of the Above
Bitumen or Bitumen-Derived Heavy Oil
Via Bore Hole
CRACKING
Coking
Hydropyrolysis
Hydrocracking
Cracked Products
HYDROTREATING
Nitrogen & Sulfur
Metals & Coke
Sand & Some Coke
THERMAL PROCESS
Rotary Kiln Pyrolysis
Fluidized Bed Pyrolysis
Cracked Products
HYDROTREATING
Nitrogen & Sulfur
Sand
Metals & Coke
MINING OR QUARRYING
Tar Sand
CONVENTIONAL REFINERY FEEDSTOCK
SOLVENT OR WATER EXTRACTION PROCESS
Bitumen
CRACKING
Coking
Hydropyrolysis
Hydrocracking
Cracked Products
HYDROTREATING
Nitrogen & Sulfur
Sand
Metals & Coke

- Density-gravity greater than 1,000 kg/m^3 (<10 °API)
- Maximum viscosity of 10,000 mPa s (cp)

• Oil sand bitumen or natural asphalt (may also include vacuum residua (boiling range>783 K)):

- Density-gravity greater than 1,000 kg/m^3 (<10 °API)
- Viscosity greater than 10,000 mPa s (cp).

Beaton [12] defined residuum as the bottom fraction that remains after atmospheric or vacuum distillation of a crude oil. The atmospheric and vacuum residuum differs in their nominal initial boiling points which are 617 K (650°F) and 811 K (1000°F), respectively. Asphaltene constituents and vanadium and nickel organometallic compounds distinguish residuum from the lighter fractions of crude oils. Residuum must undergo significant upgrading as they are generally less valuable in their natural state than lighter crude fractions.

Beaton and Bertolacini [1] demonstrated that sulfur contents vary between 1% to 6%, with 4% typical in the petroleum residuum and the typical residuum contains 20% oils (the most catalytically reactive fraction), 65% resin (intermediate reactive fraction), and 15% asphaltenes (the least reactive fraction). Most studies on the composition of residuum begin with fractionation of the materials into several compound-type classes by techniques such as gel permeation and liquid chromatography.

The bitumen in oil sands differs from crude oil in heteroatom concentrations and in the proportions of hydrogen and carbon. Bitumens have higher nitrogen and oxygen concentrations and lower hydrogen-to-carbon ratios than conventional crude oils due to the heavier, complex hydrogen-deficient constituents. These differences are reflected on the high Conradson carbon residue (CCR) and asphaltene contents of bitumen. These chemical differences

are reflected in physical properties: high viscosity, high specific gravity, and high pour point [10,13-17].

The properties of a conventional crude oil, a Canadian bitumen, a Utah bitumen and an atmospheric petroleum resid are compared in Table 2.1.

Uinta Basin Oil Sands

Although the United States does not have oil sand deposits which comparable in size with those of Canada and Venezuela, there are several large deposits in the state of Utah.

As can be seen in Table 2.1., the Uinta Basin bitumen has a higher hydrogen content and contains about three times as much nitrogen, but only about one-tenth as much sulfur, as the Athabasca bitumen [14]. It also has a lower vanadium content, but slightly higher nickel content [16-18]. The Uinta Basin bitumens originated in a non-marine environment (lacustrine) thus they are richer in saturates than Athabasca bitumens which originated in a marine environment [17]. The bitumens usually differ not only in depositional environment, but in age. The bitumens that had lower saturate molecular weight distributions were reported to be older [18]. The higher concentrations of mono-, di- and tricyclic saturates in Athabasca bitumen [19] may simply be the result of greater degradation of higher molecular weight saturates in the bitumen. These results are consistent with the high H/C ratio of Whiterocks oil sands bitumen [20].

The distinguishing property of the Uinta Basin oil sand bitumens are the viscosities. The Uinta Basin bitumens are at least one to two orders of magnitude more viscous than the Athabasca bitumen [21]. This high viscosity affects recovery and upgrading process and makes handling of the primary bitumen difficult.

Table 2.1

Comparison of Athabasca and Uinta Basin Bitumens with Petroleum Resid and Conventional Crude Oil

Property	Conventional Crude Oil	Athabasca Bitumen	Uinta Basin Bitumen	Safaniya Atmospheric Residuum (617 K+)
Reference	[13]	[14]	[10]	[15]
Gravity, °API	25-37	7.4	10.3	13.9
Conradson carbon, wt%	1-2	12.7	13.0	13.2
Ash, wt%	0.0	0.9	0.8	
Elemental analysis				
C, wt%	86	83.1	85.0	84.9
H, wt%	13.5	9.8	11.4	11.1
N, wt%	0.2	0.4	1.3	0.2
S, wt%	0.1-2.0	4.5	0.4	3.6
Ni, ppm	-	68	75 [17]	24.3
V, ppm	-	234	2 [17]	86.0
Fe, ppm	2-10	408	-	-
H/C Atomic Ratio	1.9	1.4	1.6	1.6

The physical and chemical properties of bitumens extracted from Utah oil sands are presented in Table 2.2 [10].

Heavy Oil Upgrading Technology

The decline in demand for residual fuel oils and the increase in heavier crude supplies worldwide indicates that the development of heavy oil upgrading technologies for converting heavy residuum to lighter and/or more valuable materials are necessary [22-24].

There are several ways to categorize heavy oil upgrading technology [25,26]. Traditionally upgrading processes have been classified according to whether carbon is rejected from or hydrogen is added to the feedstock. Carbon rejection aims to remove asphaltene and carbon residues in the form of coke, pitch, or extra heavy, aromatic oils by thermal cracking whereas hydrogen addition is intended to increase hydrogen/carbon ratio via hydrotreating.

Upgrading processes can be grouped as follows:

- catalytic processes (hydrotreating (HT), hydrocracking)
- noncatalytic processes (hydrovisbreaking, donor-solvent processes, hydropyrolysis)
- catalytic cracking (FCC); and
- thermal processes (visbreaking, coking)

Finally there are other non-refining processes in which heavy oils and residuum can be utilized:

- combustion
- partial oxidation
- steam reforming
- solvent deasphalting (SDA)

Table 2.2

Properties of Extracted Bitumen from Utah Oil Sands [10]

Property	PR Spring Rainbow I	Sunny-side	Whiterocks	Asphalt Ridge	Circle Cliffs
Bitumen Content, wt%	14.1	8.5	8.0	10.9	3.6
Gravity, °API	7.8	5.5	10.3	14.4	14.3
Conradson Carbon, wt%	14.0	14.8	13.0	-	23.3
Ash, wt%	3.3	2.4	0.8	0.04	0.10
Pour Point, K	372	-	-	-	332
Viscosity, cps	8269[a]	7373[b]	29245[c]	2015[d]	23012[e]
Simulated Distillation					
Volatility, wt%	39.9	32.4	22.1	-	31.2
IBP-478K, wt%	1.3	0.9	0.9	-	0.0
478K-617K, wt%	5.1	7.3	3.3	-	3.4
617K-811K, wt%	25.6	24.0	18.8	-	27.8
>811 K Residue, wt%	68.1	67.6	77.9	-	68.8
Elemental analysis					
C, wt%	84.7	83.3	85.0	85.2	83.2
H, wt%	11.2	10.8	11.4	11.7	9.8
N, wt%	1.3	0.7	1.3	1.0	0.4
S, wt%	0.5	0.6	0.4	0.6	4.9
Atomic H/C Ratio	1.60	1.56	1.61	1.65	1.42
MW, g/mol	702.0	1042.0	-	668.0	744.0
Gradient elution chromatography					
Saturates, wt%	9.5	13.2	15.3	10.0	13.4
MNA/DNA Oils, wt%	10.2	21.0	8.5	11.4	21.1
PNA Oils, wt%	11.4	5.9	11.9	4.4	9.1
Soft Resins, wt%	13.9	13.9	16.7	18.4	9.5
Hard Resins, wt%	1.1	5.6	2.6	1.2	3.6
Polar Resins, wt%	2.0	1.7	2.7	3.7	3.8
Asphaltenes, wt%	31.3	29.8	31.2	39.9	33.0
Noneluted Asphaltenes, wt%	20.6	8.9	11.1	11.1	6.5

[a] Measured at 373 K
[b] Measured at 338 K
[c] Measured at 347 K
[d] Measured at 493 K
[e] Measured at 363 K

- olefin processes (non-tubular, tubular)

The various heavy oil and residuum upgrading process schemes are summarized in Figure 2.2.

Hydroprocessing

Catalytic Hydroprocessing

Catalytic hydroprocessing includes hydrotreating and hydrocracking. Hydrotreating includes hydrodesulfurization (HDS), hydrodenitrogenation (HDN), and hydrodemetallation (HDM). Co/Mo catalysts are recommended where HDS is the primary objective because Co exhibits better selectivity for desulfurization than Ni and Ni/Mo catalysts are more suitable in applications where mild hydrogenation or nitrogen removal is required because Ni exhibits better hydrogenation than Co.

Since the initial developments for the production of low-sulfur fuel oil (LSFO) in the late 1960s catalytic residuum hydroprocessing has played an important role in producing low sulfur fuel oil in accordance with environmental regulations. It should be noted that these restrictions have become stricter since the 1970s. Quann et al. [27] reported that the capacity of residuum hydrotreating is increasing with the total free world capacity has increased from approximately 200,000 barrels per stream day (BPSD) in 1970 to 1,200,000 BPSD in 1986 [27].

In residuum desulfurization processes the distillate and naphtha yields are low even though conversion of gas-oils to light products occurs. Recently high severity residuum hydrotreater operations have been used to attain 80 to 95% sulfur conversion [28-30]. Thus, the current trend in catalytic residuum hydrotreating is to use an HDM catalyst at severe operating conditions rather than using an HDS catalyst at moderate conditions [1].

Figure 2.2

Summary of Heavy Oil Upgrading Processes

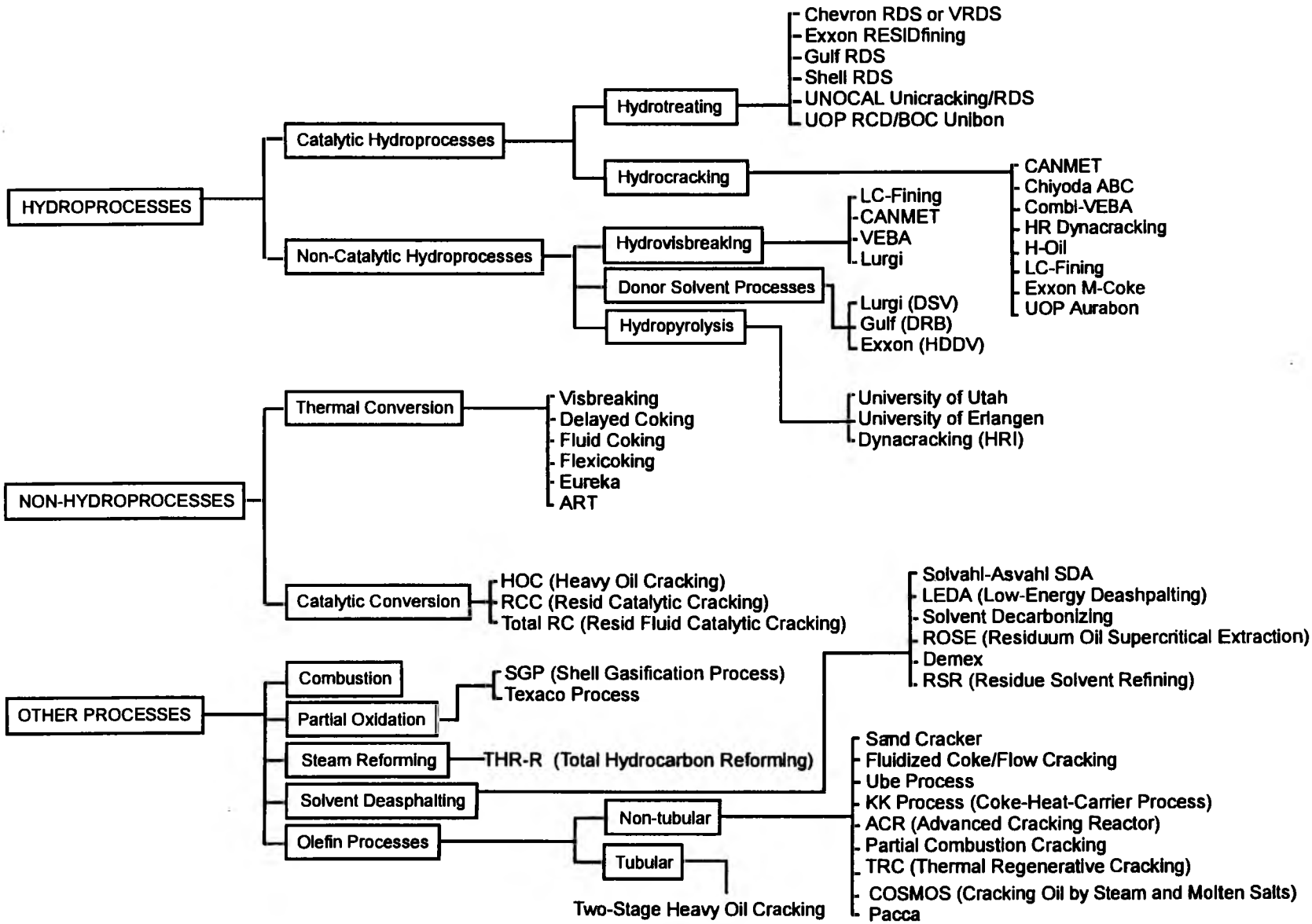
HYDROPROCESSES
Catalytic Hydroprocesses
Hydrotreating
Chevron RDS or VRDS
Exxon RESIDfining
Gulf RDS
Shell RDS
UNOCAL Unicracking/RDS
UOP RCD/BOC Unibon
Hydrocracking
CANMET
Chiyoda ABC
Combi-VEBA
HR Dynacracking
H-Oil
LC-Fining
Exxon M-Coke
UOP Aurabon
Non-Catalytic Hydroprocesses
Hydrovisbreaking
LC-Fining
CANMET
VEBA
Lurgi
Donor Solvent Processes
Lurgi (DSV)
Gulf (DRB)
Exxon (HDDV)
Hydropyrolysis
University of Utah
University of Erlangen
Dynacracking (HRI)
NON-HYDROPROCESSES
Thermal Conversion
Visbreaking
Delayed Coking
Fluid Coking
Flexicoking
Eureka
ART
Catalytic Conversion
HOC (Heavy Oil Cracking)
RCC (Resid Catalytic Cracking)
Total RC (Resid Fluid Catalytic Cracking)
OTHER PROCESSES
Combustion
SGP (Shell Gasification Process)
Texaco Process
Partial Oxidation
Steam Reforming
THR-R (Total Hydrocarbon Reforming)
Solvent Deasphalting
Solvahl-Asvahl SDA
LEDA (Low-Energy Deashpalting)
Solvent Decarbonizing
ROSE (Residuum Oil Supercritical Extraction)
Demex
RSR (Residue Solvent Refining)
Olefin Processes
Non-tubular
Sand Cracker
Fluidized Coke/Flow Cracking
Ube Process
KK Process (Coke-Heat-Carrier Process)
ACR (Advanced Cracking Reactor)
Partial Combustion Cracking
TRC (Thermal Regenerative Cracking)
COSMOS (Cracking Oil by Steam and Molten Salts)
Pacca
Tubular
Two-Stage Heavy Oil Cracking

Typical residuum hydrotreating operating conditions are a temperature range of 623-713 K (350-440°C), a pressure range of 5.2-20.7 MPa (750-3000 psi) and a space velocity range of 0.1-2 h^{-1} LHSV. Hydrogen consumptions range from 550 to 2500 [scf/bbl] [27]. Beaton and Bertolacini [1] reported operating temperatures between 672-728 K (750-850°F, about 400-450°C), hydrogen partial pressures from 9.7 to 17.2 MPa (1400-2500 psi), and liquid hourly space velocities ranging from 0.1 to 0.5 h^{-1} for residuum hydrotreating.

Chevron RDS or vacuum residuum desulfurization (VRDS) [22], Exxon RESIDfining [31], Gulf RDS [32], Shell RDS [33], UNOCAL Unicracking/RDS [34], and UOP reduced crude desulfurization/black oil conversion (RCD/BOC) Unibon [35] are the current commercial residuum hydrotreating processes.

The combination of two processes exhibits advantages over single processes. The combination of residuum hydrotreating-fluidized catalytic cracking (FCC) [36] and residuum hydrotreating-delayed coking [37] are typical examples. The residuum hydroprocessing-coking combination produces higher yields of upgraded liquid products which are lower in heteroatoms and higher in hydrogen-to-carbon ratio with less coke formation than the coking process alone. This makes these products superior feedstocks to the downstream process. In this process the effective catalyst lifetime and tolerance is more important than high activity of the catalyst. The produced coke is of a higher quality and can be used in the production of high-value anode-grade coke.

In residuum hydroprocessing the boiling range reduction is accompanied by heteroatom removal. The main difference between residuum hydrotreating and hydrocracking processes is the boiling range reduction. In the residuum hydrotreating, heteroatom removal occurs to improve the quality of petroleum liquid and boiling range conversions below 25% are achieved whereas in residuum hydrocracking boiling range reduction is commonly about 50%.

Hydrocracking processes differ from catalytic cracking in variety of feedstocks relative to catalytic cracking and in its incorporation of a metal sulfide catalyst and hydrogen at a total pressure of 5.5-17.2 MPa (800-2500 psig). Commercial heavy oil hydrocracking processes include LC-Fining [38], H-Oil [39], VEBA-Combi [40], CANMET [41], UOP Aurabon [42], HFC [43], M-Coke [44], and Chiyoda asphaltenic bottom cracking (ABC) [45]. Operating variable ranges include temperatures of 703-743 K (430-470°C), pressures of 7.6-20.7 MPa (1100-3000 psig), LHSV's of 0.5-1.0 h^{-1} and hydrogen consumptions of 500-1500 [scf/bbl] [25].

Noncatalytic Hydroprocessing

Noncatalytic hydroprocessing includes hydrovisbreaking, donor-solvent processes, and hydropyrolysis.

The basic concept in hydrovisbreaking is to increase the solubility of hydrogen in oil with temperature and pressure. Hydrovisbreaking gives better conversions and paraffin/olefin ratios than visbreaking and operates in the same temperature-time range as hydrocracking.

Donor-solvent processes involve the dehydrogenation of the feed with solvent and the formation of hydrogen radicals which are then available for cracking reactions. The licensors for this process includes Lurgi (Donor Solvent Visbreaking (DSV)) [46], Gulf (Chevron) (Donor Refined Bitumen (DRB)) [47], and Exxon (Hydrogen Donor Visbreaking (HDDV)) [48].

Hydropyrolysis upgrades the feedstock by hydrogen addition with little or no coke formation. Hydropyrolysis operates at temperatures of 773-973 K (500-700°C), pressures of 4.1-12.4 MPa (600-1800 psig), and retention times below 1 minute. This hydropyrolysis process has been used at the University of Erlangen [49] and HRI (Dynacracking) [50] to upgrade petroleum residuum.

Most of these hydroprocessing processes are not still available at the commercial scale.

Thermal and Nonhydrogen Processes

The carbon/hydrogen ratio of petroleum feed can be upgraded by thermal processes through the formation of coke or unsaturated/aromatic hydrocarbons (hydrogen disproportionation). Thermal processes have the advantage of flexibility of feed selection over catalytic processes which require higher quality feeds due to the catalytic deactivation. The disadvantages of the thermal processes are related to the production of significant amounts of unsalable products. Thermal conversion processes for heavy oil upgrading including Visbreaking [51], Delayed Coking [52], Fluid Coking [53], Flexicoking [54], and Eureka [55] are in commercial operation. The catalytic nonhydrogen processes, heavy oil cracking (HOC) [56], residual catalytic cracking (RCC) [57], and total residuum cracking (RC) [58] are in commercial operation.

Other Processes

Other processes include combustion, partial oxidation, steam reforming, and solvent deasphalting. Heavy oils are frequently used as refinery fuels. Noncatalytic partial oxidation process is used in generation of synthesis gas by producing an additional hydrogen source [59]. One of the typical steam reforming process for producing synthesis gas from heavy oil is THR-R (Total Hydrocarbon Reforming) developed by Toyo Engineering Co. [60]. ASHVAL's Solvahl-asvahl solvent deasphalting (SDA) [61], Foster Wheeler's low-energy deasphalting (LEDA) [62], Kellogg's Solvent Deasphalting [63], Kerr-McGee's residuum oil supercritical extraction (ROSE) [64], UOP's Demex [65], Lummus

Crest's residue solvent refining (RSR) [66] are the representative processes for solvent deasphalting.

Reactors in Residuum Hydroprocessing

The most common reactor designs for residuum hydroprocessing include fixed beds, ebullieted or expanded beds and slurry beds, and moving-bed reactors. The types of reactors used in resid hydroprocessing are tabulated in Table 2.3.

Hydroprocessing Catalysts

Hydrotreating catalysts were developed primarily for processing petroleum feedstocks and typically contain 1 to 8 wt% and 3 to 20 wt% of a group VIII and VIB metal oxides on a support having a high-surface-area such as alumina. The metal oxides have been used as the active phase either in combination or alone in either supported or unsupported forms. In particular Co-Mo, Ni-Mo, Ni-Co-Mo and Ni-W have focused wide applications. The individual catalyst properties such as pore volume, pore size distribution, metal loading atomic ratio and surface area play important roles in the catalyst's activity, deactivation and stabilization [67].

The Co-Mo supported on gamma alumina catalyst has been widely used in hydrodesulfurization of petroleum liquids due to its activity and selectivity. Richardson [68] reported that Co-Mo catalyst on alumina is superior in HDS and that the activity varies with the concentration of metals with an apparent optimum Co-Mo weight ratio of 1/5. Conventional HDS catalysts contain 3% CoO, 14% MoO_3 metal oxides and is supported on gamma alumina which has surface areas as high as 200-300 m^2/g and small pore diameters in the range 80-120 Å

Table 2.3

Types of Reactors in Residuum Hydroprocessing [25,69]

Reactor Type	Process
Fixed Bed	Chevron RDS and VRDS [22]
	Exxon RESIDfining [31]
	Gulf RDS [32]
	Shell RDS [33]
	UNOCAL Unicracking/RDS [34]
	UOP RCD/BOC Unibon [35]
Ebullieted Bed	H-Oil [39]
Expanded Bed	C-E Lummus/Cities Service LC-Fining
	licensed by AMOCO [38]
Slurry Reactor	Canadian DOE CANMET [41]
	Exxon M-Coke [44]
	UOP Aurabon [42]
Moving Bed or Bunker Reactor	Shell RDS [25]

[1]. The Ni-Mo catalyst is well known for its hydrogenation activity and has been used in hydrodenitrogenation of petroleum feedstocks. Phosphorous has been used as a promoter in hydrotreating process.

Hydrodemetallation catalysts typically contain larger pore diameters (180-250 Å in meso pore range) and lower surface areas of 150 m^2/g than HDS catalysts. The HDM catalysts have lower metal contents than HDS catalysts with the intention of dematallation and maintaining catalyst activity [70].

Noncylindrical extrudates such as quadralobes exhibit better diffusion characteristics, improved activities and lower pressure drops across the catalyst bed than cylindrical, non-shaped catalysts [71].

Precipitation and impregnation are two typical methods for preparing hydrotreating catalysts [72]. In precipitation, solutions of the desired components are mixed with a precipitation agent and dried in air at 339-478 K. They are then extruded or pelleted, calcined and activated. The precipitation agent is used to promote the formation of either a coprecipitate or a gel, depending upon conditions. In impregnation, solutions of the desired constituents are in contact with either a dried porous support or a wet precipitate or gel and the excess solution is removed. The catalyst is subsequently dried and calcined. The calcination temperature, generally in the range 589-1033 K, may affect the structure and activity of the catalyst [68]. Pellet size and pore structure of the support are also important [73].

Particle Size and Reaction Rate

Catalyst size and shape are important considerations in optimizing catalyst performance considering that HDM reactions are typically diffusion limited. For large particle size residuum hydrotreating catalysts, the reaction rates are controlled by intraparticle diffusion. The factor controlling intraparticle

diffusion is the rate of heteroatomic species diffusion since the rate of hydrogen in the oil is known to be greater than that of heteroatoms in the catalyst [74]. Arey et al. [75] observed no effect of increasing the bulk-liquid flow rates on desulfurization rates and reported that diffusion of hydrogen through the liquid phase was not limiting. They also found that desulfurization was markedly improved by reducing particle size and they attributed it to the increased utilization of the interior region of the catalyst.

Kato et al. [76] investigated the relation between catalyst size and the rate constant for desulfurization of Khafji atmospheric residuum. When the volume of the catalyst bed was constant, the rate constant, k, increased in proportion to 1/d for values of 1/d up to approximately 1 where d is the average diameter of the catalyst particle. When 1/d exceeded 1, the influence of catalyst particle size significantly diminished.

Shah and Paraskos [77] observed no difference in desulfurization rate for catalysts having particle sizes of 0.5 to 0.6 mm and 0.8 mm when 50% Kuwait atmospheric reduced crude oil was hydrotreated in a down-flow fixed bed reactor. Particles smaller than 0.8 mm (1/32 in.) are typically not used in commercial fixed-bed reactors because of excessive pressure drop or the potential for plugging of the catalyst bed by particulates found in residuum feeds [78]. Therefore the optimum catalyst should compromise physical properties such as surface area, pore radius, pore volume with feedstock characteristics [79].

Surface Area, Pore Structure and Pore Size Distribution

The catalyst surface area, pore volume, pore size distribution and the ratio of molecular size to pore size are considered to be significant factors

influencing hydrotreating. These properties influence the diffusivity of the liquid feed whereas reactivities of metal compounds influence the reaction kinetics.

Riley [80] reported a general classification of catalysts according to median pore diameters: 1) small pore catalysts have median pore diameters less than 100 Å; 2) intermediate pore catalysts have median pore diameters between 100-150 Å; and 3) large pore catalysts have median pore diameters above 150 Å. Physical properties of the catalysts reflect the properties of the support. Bulk densities range from 0.4 to 0.7 g/ml, whereas pore volumes vary from 0.4 to 1.5 ml/g and surface areas typically range from 50 to 300 m^2/g. The average pore diameters of hydrotreating catalysts range from 40 to 400 Å but catalysts with bimodal pore structures may contain some pores as large as 1000 to 10,000 Å [27].

Residuum Hydroprocessing Catalysts

Since residuum typically contains a significant amount of high molecular weight resins and asphaltenes as well as nitrogen, sulfur, and metal containing species, the catalyst used to hydrotreat residuum must have optimum physical properties to permit the activity to be maintained over a long period even when excessive amounts of coke and metals deposit. In other words, the physical properties should be appropriate to the reaction environment in addition to the activity, selectivity, and stability required of the catalyst in the residuum hydrotreating catalyst [67].

Richardson and Alley [81] reported that when hydroprocessing a residuum containing 12% of its sulfur in the asphaltene fraction, the refractoriness of the feed was determined by the asphaltenic sulfur for the sulfur conversion levels above 90%. This refractoriness was attributed to the small pores of the catalyst. The refractoriness for desulfurization at lower conversion

levels was attributed to sterical hindrance involving aromatic sulfur compounds such as substituted thiophene, benzothiophenes, and dibenzothiophenes. Schuit and Gates [82] reported the effectiveness factor of two cylindrical catalysts (1.6 mm diameter) which had mean pore diameters of 78 Å and 103 Å in their study of hydrodesulfurization of a Middle East residuum. The effectiveness factor of the former was estimated to be 0.4 and that of the latter to be 0.8 .

Inoguchi et al. [83] investigated the influence of catalyst physical properties on desulfurization of Khafji atmospheric residuum and have shown that pores having diameters less than 40 Å did not affect activity while pores having diameters of 100 Å or larger did affect the activity. Desulfurization conversions of 60 to 70% were obtained with catalysts having pore sizes of 100 to 150 Å.

Hydrodemetallation Catalysts

In residuum hydrotreating processes, catalysts which have a tendency for low coke formation and high metal deposition tolerance are required. When the metal species permeate the catalyst pore structure, maximum metals tolerance can be obtained even though the metal deposition would still poison the active site of the catalyst. However, when metal penetration is shallow due to fast reaction or controlled pore size, the pore mouth would soon be plugged by metal deposition leaving active sites unused in the inner portions of the catalyst [84].

When the run-length is limited by the metals capacity of catalyst, the HDM catalyst which allows maximum metal-bearing molecule penetration and uniform metal deposition is preferred. However, when the run-length is not controlled by catalyst metal capacity, catalysts with high activity for HDM and moderate activity for HDS and Ramsbottom carbon conversion are desirable. High-activity HDM

catalysts which also have high HDS and Ramsbottom carbon removal activities are usually used for the feeds which contains low-metals [85]. Catalyst surface activity may be manipulated to alter the ratio of HDM activity to metal compound diffusivity with a predictable impact on optimum pore size. The increase of Ni and V penetration into the HDM catalyst can be accomplished by lowering the intrinsic surface activity. This is done by varying the quantity, chemical composition, or distribution of active catalytic metals.

Plumail et al. [86] determined that the optimum pore diameter for demetallation of Boscan crude on a unimodal pore size catalyst was 150 to 200 Å. Hydrodesulfurization activity was highest on catalysts with pores of 100 Å, suggesting a difference in molecular size between the sulfur- and vanadium-bearing molecules. Riley [15] reported that pore structure controlled Ni and V removal in hydrotreating a Safaniya atmospheric residuum. Metals removal activity increased with increasing pore size from 100 to 150 Å in narrow-pore-size distribution $CoMo/Al_2O_3$ catalysts.

Catalysts prepared by Hardin et al. [87] contained two pore regimes: large interparticle pores corresponding to intergranular voids with diameters of 10,000 Å and larger and intragranular pores of diameter 500 Å and smaller. Catalysts characterized by median pore diameters of 200 Å exhibited maximum activity for Ni and V removal from Athabasca bitumen. This observation was explained on the basis of catalyst surface area. As pore size increases, the catalyst surface area decreases and as does the number of active sites. Decreasing the pore size increases the surface area but also increases the diffusional resistance to the sites. Bimodal catalysts having micropore diameters ranging from 100 to 320 Å and macropores of 1000 Å and greater also exhibit maxima in hydrodevanadation (HDV) activity in the range 150 to 200 Å average pore diameter, similar to the unimodal catalyst. HDV activity over bimodal catalysts is

markedly enhanced, up to 50%, relative to the unimodal catalysts. The introduction of macropores increases asphaltene accessibility to the micropores of the catalyst, enabling conversion by depolymerization and cracking and by demetallation.

The pore structure of the catalyst is the controlling parameter for metals removal for large pore size catalysts. Vanadium removal is somewhat easier to accomplish than nickel removal which implies that either the vanadium is in a smaller molecular species than the nickel or the nickel is more tightly held by the molecule [27]. Apparently the selectivity for vanadium removal with small pore catalysts is independent of pore size [80]. Howell et al. [85] reported that Ni compounds in both Arabian Heavy and Maya feedstocks penetrated more deeply and deposit more uniformly than V counterparts.

The selection of the optimum HDM catalyst should be determined by residuum feed properties, process operating conditions, and product quality requirements [88]. A compensation effect is operative between the increase in activity due to an increase in surface area and the decrease due to diffusional resistance; hence, the existence of an optimum pore size.

Bench Scale Hydrotreating Reactor

Effect of Liquid Holdup and Catalyst Wetting

Satterfield [89] reported that the liquid holdup is a measure of the effectiveness of contact between liquid and solid catalyst and can be defined as the ratio of the volume of liquid present in the reactor to the volume of the empty reactor. The liquid present in the catalysts pores accounts for the internal holdup while that present outside the catalyst pellets is responsible for the external holdup.

Satterfield and Way [90] proposed that the external liquid holdup can be correlated in terms of the superficial velocity and viscosity of the fluid. According to Koros [91] complete catalyst wetting cannot be attained in a pilot-plant scale reactor whereas it may be attained in a commercial reactor.

Schwartz et al. [92] used tracers to make liquid holdup measurements in trickle bed reactors. The observed liquid holdups were 45-60% and 25-40% with porous and nonporous packing; respectively, for liquid fluxes in the range 0.3 to 5 kg/m^2 s. The general trend observed was an increase in liquid holdup with increasing liquid flow rate. Mears [93] proposed a model based on incomplete catalyst wetting and suggested it was a better criteria for assessing the effects of dynamic conditions in the reactor. In narrow diameter laboratory reactor, as well as in large commercial units, the liquid trends to migrate towards the wall resulting in partial wetting of the catalyst bed. Satterfield and Ozel [94] provided visual evidence for non-uniform wetting of the catalyst particles in packed beds. Also, diluting the pilot-scale catalyst bed with fine inert material such as silicon carbide (SiC) had a minimal effect on reducing axial dispersion and channeling, and did not improve the catalyst wetting at normal operating conditions with a bitumen-derived coker gas-oil [95].

Yui and co-workers [95,96] studied the kinetics of HDS, HDN and mild hydrocracking (MHC) in pilot-scale trickle-bed reactors. Yui et al. [96] reported that plug-flow was not attained with catalyst dilution and proposed that the plug-flow model used for reaction kinetics should be modified by including a power term for space velocity, $WHSV^{\alpha}$, to compensate for nonplug-flow. Yui et al. [96] also proposed that the effect of hydrogen partial pressure should be represented by a power-rate law term, $p_{H_2}{}^{\beta}$.

The empirical power, α, has been determined in pilot-scale reactors [95,96] to be between 0.3 to 1.0. Various values of alpha have been reported in

the literature for undiluted trickle-bed reactors; 0.6 [97], 0.68 [93], 0.5 to 0.9 [98]. Yui et al. [99] also reported the power term for space velocity to be 1.0 for HDS and HDN and 0.5 for mild hydrocracking (MHC) for bitumen-derived coker and hydrocracker heavy gas-oils.

Montagna and Shah [79] reported that for catalyst particles of 20/30 mesh size the liquid holdup or catalyst wetting effects are negligible in explaining the hydrotreating kinetics for 56% reduced crude. Henry and Gilbert [97] reported that at constant process operating conditions the increased utilization of catalyst achieved by decreasing the catalyst particle size can be attributed to an increase in liquid holdup.

Axial and Radial Dispersion and Backmixing in Packed Beds

Axial liquid dispersion was investigated by Scott [100] who reported that a height to column diameter ratio (H/D) of 25 to 1 was necessary to minimize axial dispersion problems in packed towers.

The model widely used for explaining the axial mixing in fixed beds is the one parameter piston diffusion (PD) model which superimposed plug-flow with a "Fick's diffusion" type of process [101]. The Peclet number (Pe) is the parameter by which the residence distribution of the liquid is described:

$$Pe = \frac{D_p \cdot u}{E} \qquad (2\text{-}1)$$

where, D_p is the particle diameter, u is the linear liquid velocity in the interstices and E is the dispersion coefficient. When this parameter is based on the particle diameter, it is called the Bodenstein number (Bo):

$$Bo = \frac{d_s \cdot u}{D_a} \tag{2-2}$$

where, d_s is the spherical catalyst particle diameter and D_a is the axial eddy diffusivity [102]. Many investigators have shown that the Bodenstein number can be correlated by the Reynolds number (Re):

$$Re = \frac{D_p \cdot u \cdot \rho}{\mu} \tag{2-3}$$

where, ρ is the density, and μ is the viscosity of the liquid [103-105]. In most instances the investigations have taken place in the Reynolds number range from 1 to 100 whereas small-scale trickle-flow reactor experiments typically operate at in the Reynolds number range from 0.001 to 0.1 [102].

Satterfield [106] states that liquid and gas radial dispersion attains a constant value above a particle Reynolds Number of about 100 and axial dispersion attains a constant value above a Reynolds Number of about 10. Small-scale laboratory experiments normally fall well below the critical Reynolds Number of 100 for radial dispersion unless special provisions are taken to ensure that the criterion is met.

Schwartz and Roberts [107] indicate that radial distribution problems may exist in trickle-flow reactors. Although they define the concept as "contacting efficiency" they did not present a method for prediction of their contacting efficiency but suggest an experimental program to determine the efficiency and develop a correlation.

The deviation from plug-flow as a function of Reynolds number has been quantified by Mears in terms of a minimum value for Peclet number [93,108].

The following criterion was suggested to determine the minimum h/d_p ratio required to establish the reactor length within 5% of that needed for plug-flow:

$$\frac{h}{d_p} > \frac{20n}{Bo} \ln \frac{C_o}{C_f} \qquad (2\text{-}4)$$

where h is the catalyst bed length, d_p is the catalyst particle diameter, n is the reaction order and C_o and C_f are the inlet and outlet reactant concentrations. Mears applied the criterion to bench scale hydrotreating units processing a straight run gas-oil feed at a temperature of 644 K (700°F), a pressure of 10.3 MPa (1500 psia) and a LHSV of 2.0 h^{-1}. A minimum h/d_p of 350 was calculated.

Comparisons of Upflow with Downflow Operation

There may be a deviation in the test data of the pilot-plant relative to the results of commercial operation even when they are obtained under same conditions of temperature and space velocity. This is due to the low superficial mass velocities in a test unit which result in poor liquid-solid contact along with low rate constants which vary with the catalyst bed length and liquid velocity [93,97]. Satterfield [89] showed that under commercial conditions the effectiveness of catalyst wetting is ideal only if a sufficiently high superficial liquid mass velocity is used. Although criteria on wetting and back-mixing for bench-scale catalyst testing units were met [71,109] in diluted downflow experiments with shaped catalysts it was reported that downflow experiments in bench-scale gave poor reproducibility and the method of catalyst packing changed reaction orders. This indicates ineffective catalyst wetting and liquid maldistribution [110]. Catalyst testing in the upflow mode can be used to overcome these problems in some instances [79,89].

A comparison of a bench-scale reactor operated in the upflow versus downflow mode for desulfurization of a heavy coker gas-oil by Takematsu and Parsons [111] indicated that the upflow mode gave superior performance and more consistent kinetics for desulfurization. This was attributed to the fact that upflow maximized the residence time of the heavy liquid fractions.

De Wind et al. [110] reported that close to 100% effective wetting of catalyst with liquid and good liquid distribution were obtained at low mass velocities using the upflow mode and concluded that upflow testing does improve catalyst wetting. The small scale reactor data and catalyst wetting efficiency were comparable to commercial downflow hydrotreaters. Thus, they recommend the upflow mode operation in bench-scale evaluation of hydrotreating catalysts in small units and at low space velocities. Testing in the upflow mode indicated that catalyst wetting efficiency was independent of space velocity and that at the conversions obtained in the upflow mode, dilution has no beneficial effect on catalyst utilization.

The upflow mode may also provide other benefits. If a catalyst gradually becomes deactivated by the deposition of polymeric or heavy materials, the upflow reactor may maintain activity longer by more effectively washing off these deposits. Heat transfer between liquid and solid may also be more effective in upflow than in downflow operation. This is of particular importance if reaction is rapid and highly exothermic. If reactants are present in both the gas and liquid phases over a range of operating conditions in which pores of the catalyst pellets are filled with liquid, an upflow reactor would be expected to exhibit a lower reaction rate than a partially-wetted trickle bed or one in which the solid catalyst is deliberately designed so as not to be wetted by the liquid phase. Some upflow reactor designs may lead to fluidization of the catalyst unless the catalysts are held in place by mechanical means [89].

Trickle-bed operation has several advantages. Pressure drop through the bed is less which reduces pumping costs and in the downflow operations the catalyst bed remains in place.

Chemistry and Reaction Mechanisms of Hydroprocessing

The presence of sulfur and nitrogen species in residuum reduces the quality of the refined products and poses environmental concerns due to the formation of SO_x and NO_x emissions during combustion. The heteroatoms (S, N) also act as catalyst poisons, causing rapid deactivation in catalytic conversion steps such as catalytic cracking and reforming [112]. Typical organosulfur compounds, organonitrogen compounds (both basic and nonbasic) and porphyrin type nickel analogs are shown in Figure 2.3.

Hydrodenitrogenation

The nitrogen in petroleum residuum, bitumens, coal-derived liquid, and shale oils can be divided into two types; heterocyclic aromatic compound and nonheterocyclic organonitrogen compounds such as aliphatic amines and nitriles. The former are dominant in heavy oils and are more difficult to denitrogenate than the latter and thus play a significant role in hydrodenitrogenation (HDN) processes involving heavy feeds [113].

Nitrogen is more difficult to remove than other heteroatoms such as sulfur or oxygen because of wider variations in adsorptivity and reactivity [114]. These variations are attributed to the two types of nitrogen species in petroleum: pyridinic and pyrrolic. These two classes of nitrogen heterocyclics have different electronic configurations. The pyridinic ring containing nitrogen compounds (six-membered) exhibit a strong basic nature since the unshared pair of electrons

Figure 2.3

Typical Heteroatom Species Present in Petroleum.

ORGANOSULFUR COMPOUNDS


Thiophene

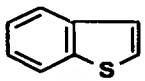
Benzothiophene

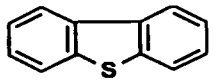
Dibenzothiophene

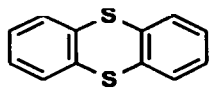
Thianthrene

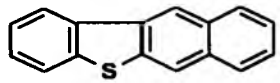
Benzonaphtholthiophene

ORGANONITROGEN COMPOUNDS

Basic Compounds [Six-Membered-Compounds]


Pyridine

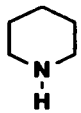
Piperidine

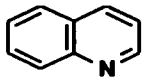
Quinoline

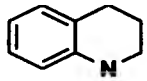
Tetrahydroquinoline

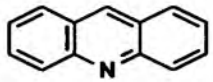
Acridine

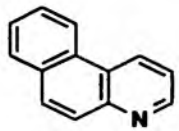
Benzoquinoline

Non-Basic Compounds [Five-Membered-Compounds]

- Non-Heterocyclic


Pyrrole

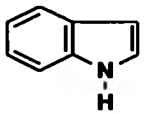
Indole

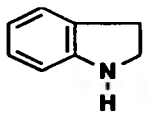
Indoline

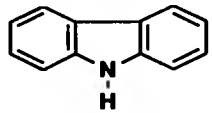
Carbazole

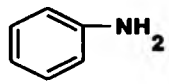
Aniline

NICKEL ANALOGS OF MODEL METALLOPORPHYRINS

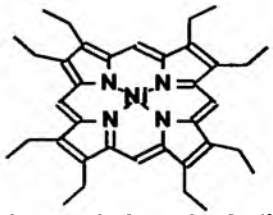
Ni-octaethylporphyrin (Ni-OEP)

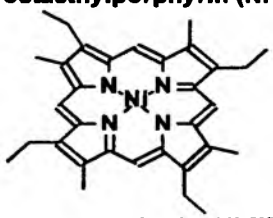
Ni-etioporphyrin (Ni-EP)

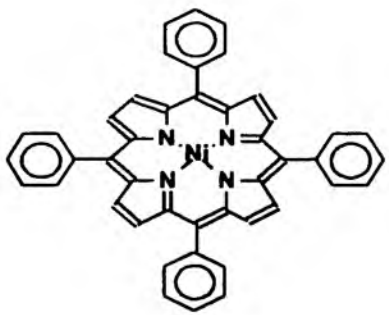
Ni-tetraphenyloporphyrin (Ni-TPP)

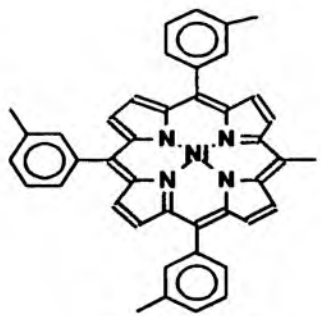
Ni-tetra(3-methylphenyl)porphyrin (Ni-T3MPP)

associated with the nitrogen are not involved in the π cloud and therefore available to share with acids. The basic nitrogen can therefore accept surface protons from the acidic site on the catalyst (Brönsted acidity) or donate unpaired electrons to electron-deficient surface sites (Lewis acidity). However, the pyrrolic ring type nitrogen heteroaromatics (five-membered) exhibit nonbasic characteristics since the extra pair of electrons on nitrogen is involved in the π cloud of the ring so that they can not interact with acids [115,116].

Typical catalysts used to accomplish HDN include Ni-Mo/Al_2O_3. The reaction chemistry for heterocyclic organonitrogen species removal indicates that the nitrogen atom containing ring must be hydrogenated before the hydrogenolysis of the carbon-nitrogen bond [113]. This is because hydrogenation of the heteroring facilitates carbon-nitrogen bond scission by reducing the bond energy of the carbon-nitrogen bond [116]. Large HDN rates can be obtained by increasing the equilibrium concentrations of saturated heteroring compounds with high hydrogen partial pressure [117].

The reactions in which nitrogen is removed from aniline derivatives are important in the denitrogenation networks because the pathways involving these reactions are those requiring the lowest hydrogen consumption. Investigations of the HDN of anilines indicate that both direct hydrogenolysis and HDN via hydrogenated intermediates may occur [118,119]. The hydrogen consumption depends strongly on the extent of hydrogenation of the aromatic rings.

Generally kinetics govern the removal of nitrogen rather than thermodynamics at reaction conditions currently used for commercial hydrotreating. Deep removal of nitrogen from moderately-refractory feedstocks can generally be achieved when a sufficiently long reaction time is used [114]. The reaction pathways for HDN of pyridine [120] and quinoline [119] are shown in Figure 2.4.

Figure 2.4

Possible Reaction Pathways for HDN of Pyridine [120] and Quinoline [119]

Reaction Pathways for Pyridine HDN Proposed by Hanlon [120]

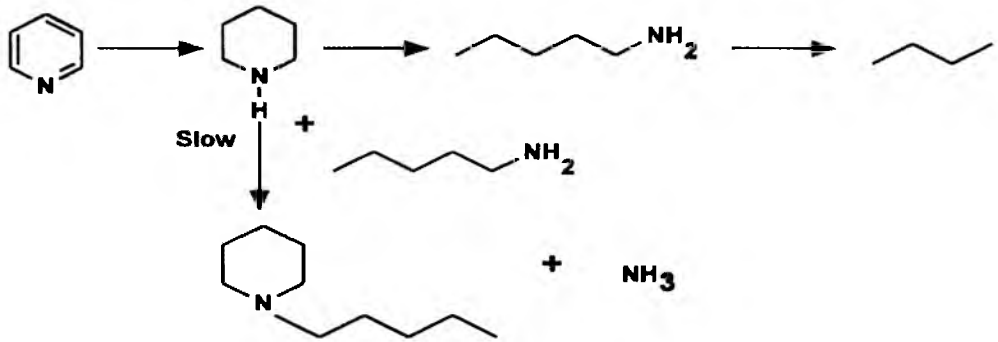

Reaction Network for Quinoline HDN Proposed by Satterfield and Yang [119]

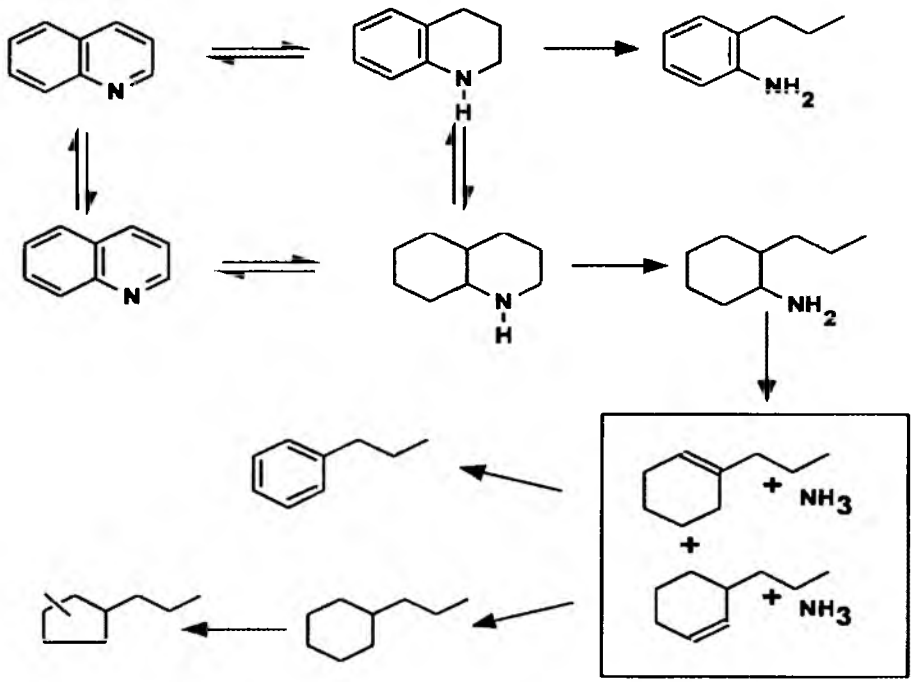

Hydrodesulfurization

Hydrodesulfurization (HDS) has been used not only for removing sulfur from naphtha reformer feedstocks but also for reducing the sulfur contents of heavy oils used as fuel refinery feedstocks and as power plant feedstocks.

Gates et al. [112] reported on the chemistry of thiophenic compound conversion since these are the least reactive organosulfur compounds in petroleum and other fossil fuels. Beaton and Bertolacini [1] showed that like the metals, about 73% of the total sulfur is distributed in the resin fraction of a typical vacuum residuum. Bar Vise and Whitehead [121] reported that sulfur-containing compounds are more volatile than metal-bearing compounds. More than 20% of the sulfur appears in 773 K minus fraction, with less than 50% of the sulfur occurring in the 923 K plus fraction.

Unlike nitrogen removal which requires the heteroatom ring hydrogenation before the hydrogenolysis of the carbon-nitrogen bond, sulfur removal occurs either with or without hydrogenation of the heterocyclic ring. Also, thermodynamics would govern the HDS pathways involving prior hydrogenation of the ring since hydrogenation of the sulfur-containing rings of organosulfur compounds is equilibrium-limited at practical HDS temperatures [117]. The HDS of organosulfur compounds is exothermic and essentially irreversible under the reaction conditions employed industrially (e.g., 613-698 K (340-425°C) and 5.6-17.2 MPa (55-170 atm)) [122]. Reaction pathways for HDS of thiophene [112], benzothiophene [123] and dibenzothiophene [124] are presented in Figure 2.5.

Hydrodemetallation

Heavy oil feedstocks contain not only heteroatoms but also the trace metals in the form of organometallic compounds [125]. The metals in heavy oils poison the catalyst in hydrotreating processes and the resulting metal deposition

Figure 2.5

Possible Reaction Pathways for HDS of Thiophene [112],
Benzothiophene [123] and Dibenzothiophene [124]

Thiophene reaction pathways suggested by Gates et al. [112]

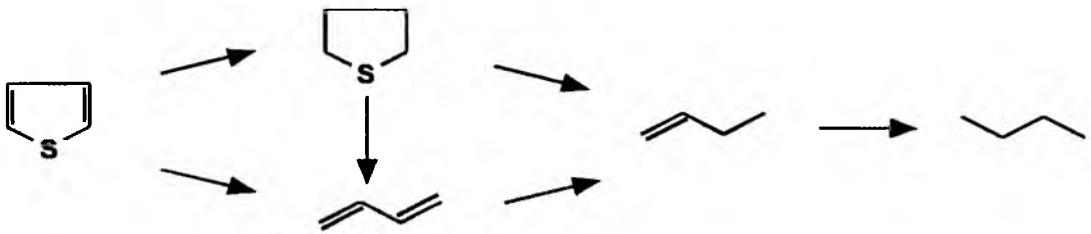

Reaction network for benzothiophene proposed by Van Parijs et al. [123]

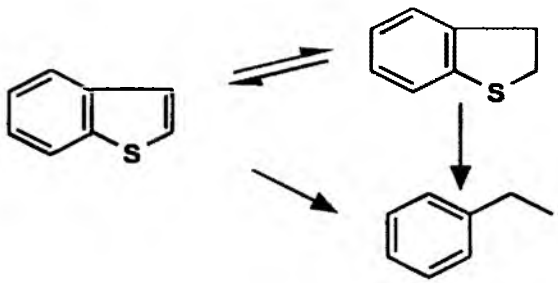

Reaction network for dibenzothiophene proposed by Houalla et al. [124]

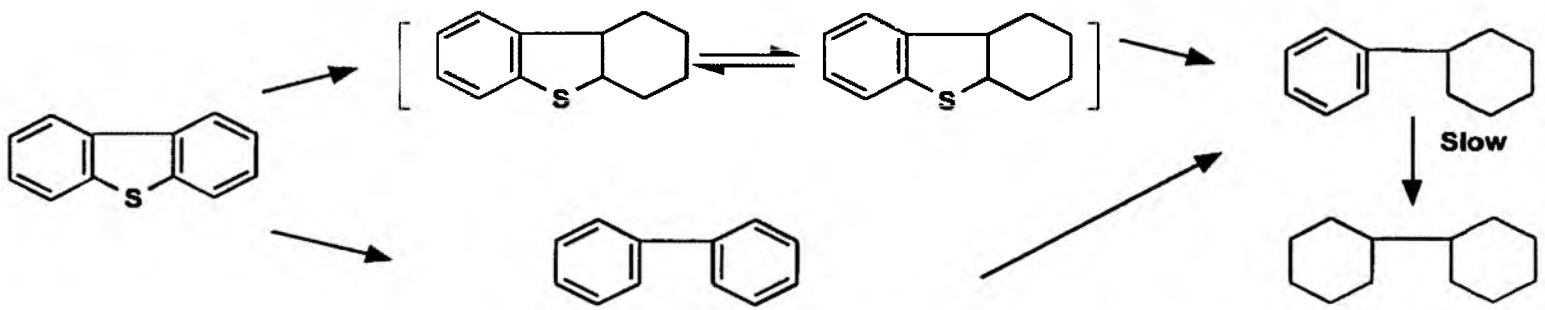

ultimately determines the catalysts' useful operating lifetime because the metal contaminants can not be removed as gases (H_2S and NH_3) as in desulfurization and denitrogenation, respectively. For example, reducing metal content via HDM is essential when heavy oils are fed to the fluid catalytic cracking unit because it would poison the cracking catalyst and erode the furnace linings and turbine blades.

Metals are usually present in the 811 K plus (1000°F$^+$) fraction of the heavy oils whereas sulfur and nitrogen are distributed over the entire boiling range. The abundance of nickel and vanadium compounds in heavy oils have stimulated the interest in residuum hydroprocessing.

Metal Compounds

Unlike sulfur and nitrogen compounds in petroleum which are distributed in the aromatic, resin and asphaltene fractions, more than 85% of the nickel and vanadium compounds are found in the resin and asphaltene fractions [126]. Beaton and Bertolacini [1] showed that nickel and vanadium reside primarily in the resin and asphaltene fractions of the residuum fractions.

There are two main types of nickel and vanadium compounds in petroleum feedstocks: one is metal porphyrins and the other is nonporphyrin metal species. The metal porphyrins differs from nonporphyrin metal species in properties such as polarity, molecular weight and structure. The nonporphrin metals have higher polarities, higher molecular weights and lower volatility than the metal porphyrins. Dean and Whitehead [127] have shown that most Ni and V appeared as nonporphyrins in 923 K plus (650°C$^+$) fraction of Middle East crudes and only 5% of the metals in the asphaltenes are present as metalloporphyrins This indicated that nonporphyrin metals associate with the highly polar asphaltene fraction. Sugihara et al. [128] also observed that the

nonporphyrin metals are associated with the asphaltenes due to high polarity in his study of metal porphyrins in Boscan asphaltenes using gel permeation chromatograph (GPC) and other techniques.

The basic form of porphyrin is called porphrite ($C_{20}H_{14}N_4$) which has four pyrrole groups in a closed ring and connected to the α-carbon by methine-carbon atoms. The metalloporphyrins are also divided into two categories, a deoxophylloerythroetioporphyrin (DPEP) and an etioporphyrin (Etio) series [128-130].

The basic skeleton of nonporphrin metal compounds has not been well identified. It is reported that they are composed of various forms of metals from inorganic to polar organic compounds [128]. Two main types of nickel and vanadium compounds have been proposed by Yen [129]: one includes arylporphyrins, hydroporphyrins, and porphyrin-degraded products and the other includes tetradentate-mixed ligands in Ni and V complexes.

Catalytic Hydrodemetallation

Hung and Wei [131] reported that total metal removal was less than the overall disappearance of feed porphyrins in their study of hydrodemetallation of porphyrins. This observation was attributed to the production of intermediate (hydrogenated metalloporphyrin termed metallochlorin) during the hydrotreating process.

Agrawal and Wei [74] found that vanadium removal is much faster than the nickel removal in their kinetic study of hydrodemetallation of nickel and vanadium porphyrins. The fast vanadium removal is due to its reactive moieties and concentration at the surface of the catalyst. However, nickel species are distributed more evenly over the catalyst than vanadium and this resulted in lower removal. They also proposed that an initial reversible hydrogenation

would be followed by terminal hydrogenolysis step in hydrodemetallation process.

Galiasso et al. [132] reported that the depolymerization of asphaltene structures followed by transport of metal species to catalytic sites is rate controlling in reactions of porphyrinic and nonporphyrinic molecules during hydrodemetallation of heavy crude oils rather than the intrinsic demetallation chemistry.

Proposed demetallation reaction pathways for Ni-etioporphyrin (a) and Ni-tetra (3-methylphenyl) porphyrin (b) [133] are presented in Figure 2.6.

Figure 2.6

Possible Reaction Pathways for HDM of Ni-etioporphyrin and Ni-tetra (3-methylphenyl) porphyrin [133].

DEMETALLATION REACTION PATHWAYS [133]

(a) Ni-etioporphyrin

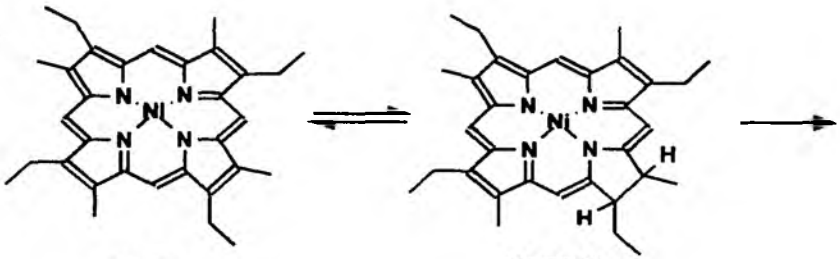

NI-EP **NI-EPH$_2$**

(b) Ni-tetra(3-methylphenyl)porphyrin

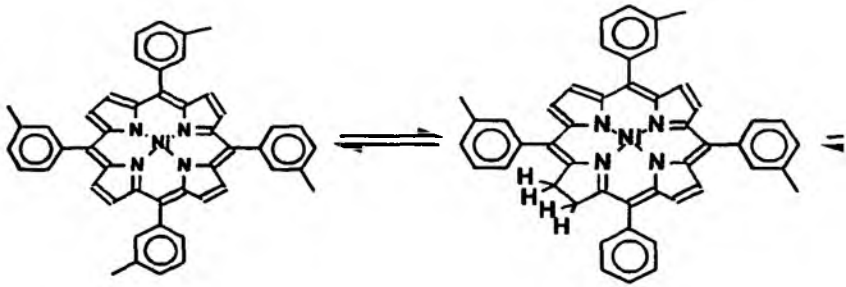

Ni-P **Ni-PH$_2$**

Deposit

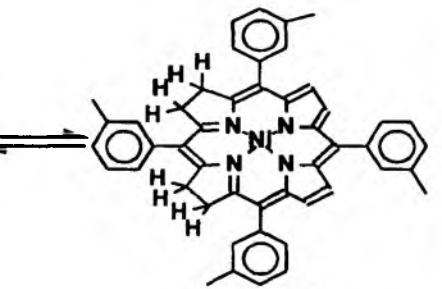

Deposit

Ni-PH$_4$

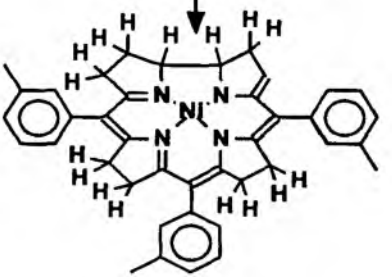

Deposit

CHAPTER 3

EXPERIMENTAL APPARATUS AND PROCEDURE

Feedstock Preparation

Ore Acquisition

The bitumen prepared for this study was obtained by solvent extraction of the Whiterocks oil sand. The oil sand ore was obtained from the Northeast section of the Fausett quarry on the Whiterocks deposit in the Uinta Basin. The mined oil sand ore was transported in polyethylene lined, 209 liter (55 gallon) drums to the Oil Sand Research Laboratory at the University of Utah. The drums were sealed to minimize oxidative degradation of the bitumen. The ore was crushed and sieved prior to extraction.

Solvent Extraction

Bitumen was separated from the oil sand by toluene extraction. Three 5-liter and five 4-liter Soxhlet extractors were used to extract the bitumen. Whatman cellulose extraction thimbles (90 mm diameter x 200 mm length) were completely filled with 800 to 1,000 g of fresh oil sands. Filter paper covers were placed on top of each thimble to prevent sand from being transferred from the thimbles into the solvent reservoir. Toluene (ACS grade, EM Science) was used as a extracting solvent. Approximately 2,000-2,500 cm^3 of toluene was poured into the solvent reservoir until the toluene level was about 2.5 cm above the top of the Glas-Col heating mantle. Four or five boiling chips were placed in the

solvent reservoir to prevent bumping and the outer wall of the thimble was cleaned. Each thimble was then wrapped with sharkskin filter paper to filter fines and the thimble and sharkskin filter paper were placed in an extractor. The assembled extractor containing fresh oil sand was wrapped with aluminum foil and the reboiler temperature controller set point was set to 55% of full scale. The extractor was checked frequently until condensed toluene started to drip from the condenser onto the top of the extraction thimble. Approximately 12 hours were required to complete the extraction. During extraction, water was collected and separated from the toluene in the trap mounted between the extractor and the water cooled condenser to produce a water-free bitumen-toluene solution.

The extent of bitumen extraction was determined by monitoring the color of toluene dripping from the thimble. When the toluene solution was clear it was determined that extraction was complete. The heating mantle switch was turned off and the aluminum foil was removed. The water and toluene were drained from the trap. The sharkskin and thimble cover were dried and placed in an appropriate disposal vessel. The extracted sand in the thimble was dried and stored in the designated receptacle for disposal. These procedures were repeated until the eighth extraction was completed.

After the eighth extraction, the extractor was cooled to room temperature and the toluene-bitumen solution was poured into 5-gallon plastic containers which were sealed and stored for rotary-evaporation and distillation. The extractor was cleaned completely with toluene and the procedure was repeated. Sufficient toluene-bitumen solution was collected to produce 57 liters (15 gallons) of solvent-free bitumen. Approximately five drums of the crushed Whiterocks oil sand ore were extracted during a 4-month period to produce the toluene-bitumen solution. The toluene-bitumen solution was allowed to stand for

3 days to permit mineral fines to settle from the solution before evaporation and recovery of the toluene.

Safety precautions were rigorously followed during the extraction procedure:

- Safety glasses, gloves and laboratory apron were worn to avoid contact with the solvent when handling toluene, toluene-wetted thimbles and sand.
- The handling of thimbles and extracted sand was done in the hood.
- The assembly and disassembly of the extractor were done cautiously due to the fragile nature of the glass extractors.
- The presence of fines in the toluene-bitumen solution was avoided as they might cause bumping of the solution in the reboiler.

Rotary Evaporation

Toluene was removed from the toluene-bitumen solutions by rota-evaporation followed by batch distillation. A Büchi EL 131 rotary evaporator with a Büchi 460 water bath was used to remove the solvent. A Precision Scientific vacuum pump (Model S35) was connected to the evaporator to evaporate toluene at subatmospheric conditions. This was done to facilitate solvent recovery. The pump operated at 100-150 torr and the evaporator speed and water-bath temperature were 120 rpm and 353 K, respectively. The previous study revealed that about 6-8 wt% toluene still remained in the bitumen after rotary evaporation [18]. This residual toluene was removed by vacuum distillation.

Distillation

A Semi-Cal high temperature distillation apparatus (Series 3650) by Reliance Glass Works, Inc. and a Precision Scientific vacuum pump were used for vacuum distillation. This tilting-funnel fractionating column was filled with Heli-Pak packing (stainless steel wire-coil packing; Podbielniak Inc.). The 12-liter kettle was filled with 8 liters of the toluene-bitumen solution to allow sufficient vapor space for disengagement of liquid. The kettle temperature was monitored by J-type thermocouples and the heating mantle was controlled with three variable transformers. The kettle pressure was monitored with a mercury manometer. The reflux ratios were varied with a solenoid valve timer.

The column and kettle were purged with argon to prevent air oxidation of the bitumen during distillation. The system was evacuated and the kettle heater was activated. It has been reported that bitumen would thermally crack when the kettle temperature reaches 620-650 K (347-377°C) [18]. Two methods have been proposed to avoid cracking the bitumen in the kettle at the termination of the distillation process. The first was to shut down the heating mantle when the kettle temperature reached 595 K (322°C). This method assumed a 25°C temperature overshoot might occur in the kettle. The second method was to stop heating the kettle when the desired reflux temperature was reached. Two assumptions were made to calculate the target reflux temperature at which distillation should be stopped. The first was that the lightest material in the Whiterocks bitumen is C_{11} naphthene which has the same vapor pressure properties as hexylcyclopentane. The second was that the toluene used in the extraction contained impurities like xylene. Therefore, a 50/50 mixture of xylene and hexylcyclopentane was used with the Antoine equation and Raoult's law to calculate the end point temperature at a specified system pressure. This temperature was considered as the final reflux temperature.

The system pressure during the distillation was held between 60-80 torr which was sufficient to distill the toluene while maintaining the kettle temperature below the bitumen thermal cracking temperature. The reflux ratios were selected based on a compromise between efficient and rapid separation. The initial reflux ratio was 5; it was increased to 10 near the end of the distillation and was 20 at the end point to give a sharp separation. Approximately 15 batch distillations were made to remove the solvent from the bitumen-solvent solution.

The kettle and reflux temperatures and the cumulative amount of the overhead liquid collected were measured during the distillation. The reflux temperature and the reflux ratios versus the volume of liquid distilled are plotted in Figure 3.1.

The concentrated bitumen was analyzed by simulated distillation to determine residual toluene concentration. The overhead product was also examined to determine the amount of light ends distilled overhead. The toluene in the residual bitumen and the light ends in the overhead fraction were less than the detectable limits (< 0.1 wt%) indicating that toluene removal was complete and that the bitumen was characteristic of the reservoir fluid.

The solvent-free bitumen was collected and stored in a 15-gallon drum. Due to the bitumen viscosity, the drum was wrapped with a Brisk Heat Drum Heater (Model DHCH 11) and heated to 373 K when transferring bitumen to the liquid feed burettes. The bitumen was blanketed with nitrogen to prevent air oxidation during storage.

Figure 3.1

Reflux and Kettle Temperatures versus Volume of Liquid Distilled

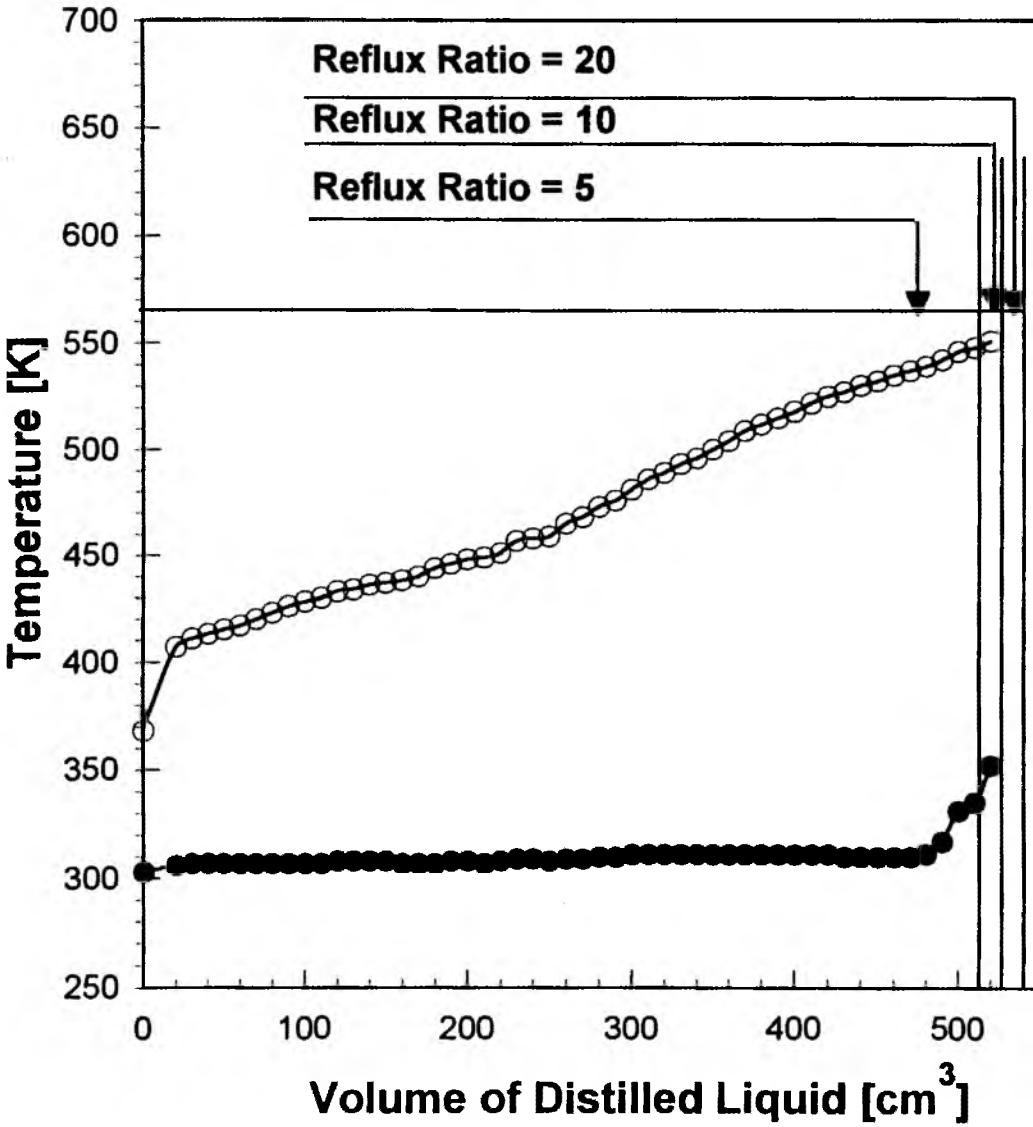
Reflux Ratio = 20
Reflux Ratio = 10
Reflux Ratio = 5
Temperature [K]
700
650
600
550
500
450
400
350
300
250
0
100
200
300
400
500
Volume of Distilled Liquid [cm3]

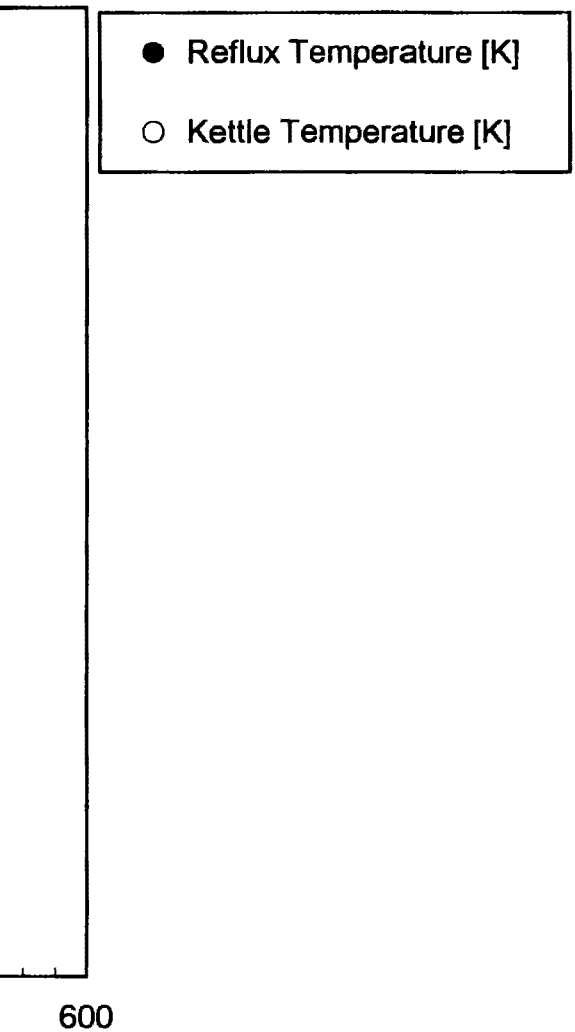
● Reflux Temperature [K]
○ Kettle Temperature [K]
600

Experimental Equipment

The hydrotreating reactor system used in this study consisted of four distinct sections; the liquid feed system, the hydrogen feed system, the catalytic reactor and the product recovery and sampling system. The hydrotreater was designed for both upflow and downflow operating modes by placing three-way manifold valves at the reactor inlet and outlet. The hydrogen and liquid feeds were fed to the reactor in the upflow mode in this study. The product gases and liquids were separated in a high pressure vapor-liquid separator. The gases were withdrawn through a back pressure regulating valve (BPRV) and the liquid product was withdrawn through the high pressure separator liquid level control valve (Annin valve). The process flow diagram for the hydrotreating unit and a schematic of the control panel are presented in Figures 3.2 and 3.3, respectively.

Liquid Feed System

Two heat traced Ace Glass, Inc. Instatherm burettes were used as feedstock reservoirs and to meter the bitumen feed rate to the hydrotreating unit. The smaller burette had a capacity of 500 cm^3 (110 volts, 2 amps maximum), and was used during mass balances and to set feed rates to the unit. The larger burette had a capacity of 4,000 cm^3 (120 volts, 5 amps maximum) and was used as a feed reservoir for overnight, unattended operation. A Model 52 Proportional Controller (Love Controls Co.) was used to control the temperature of the fluids in the burettes.

The specific gravity of the bitumen in the heated burettes was measured at 417 K (144°C) with a Streamline Hydrometer (H-B Instrument Co.; 19-31 °API range). The specific gravity was calculated according to the following equation:

Figure 3.2

Process Flow Diagram of the Hydrotreating Unit

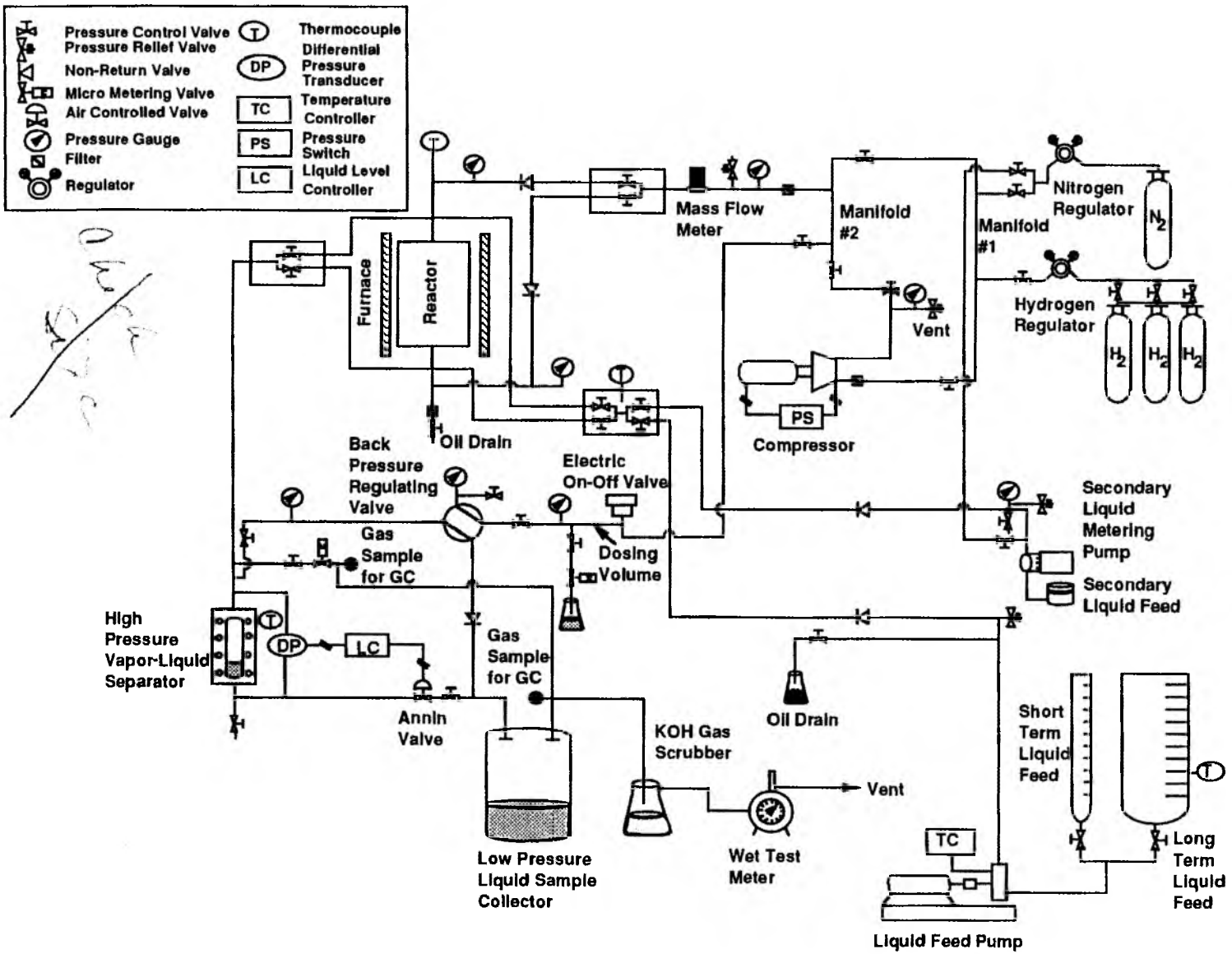
Pressure Control Valve
Pressure Relief Valve
Non-Return Valve
Micro Metering Valve
Air Controlled Valve
Pressure Gauge
Filter
Regulator
Thermocouple
Differential Pressure Transducer
Temperature Controller
Pressure Switch
Liquid Level Controller
Mass Flow Meter
Manifold #2
Manifold #1
Nitrogen Regulator
Hydrogen Regulator
Vent
Furnace
Reactor
Oil Drain
Compressor
Back Pressure Regulating Valve
Electric On-Off Valve
Gas Sample for GC
Dosing Volume
Secondary Liquid Metering Pump
Secondary Liquid Feed
High Pressure Vapor-Liquid Separator
Annin Valve
Gas Sample for GC
Oil Drain
KOH Gas Scrubber
Short Term Liquid Feed
Long Term Liquid Feed
Low Pressure Liquid Sample Collector
Wet Test Meter
Liquid Feed Pump

Figure 3.3

Diagram of Hydrotreating Unit Control Panel

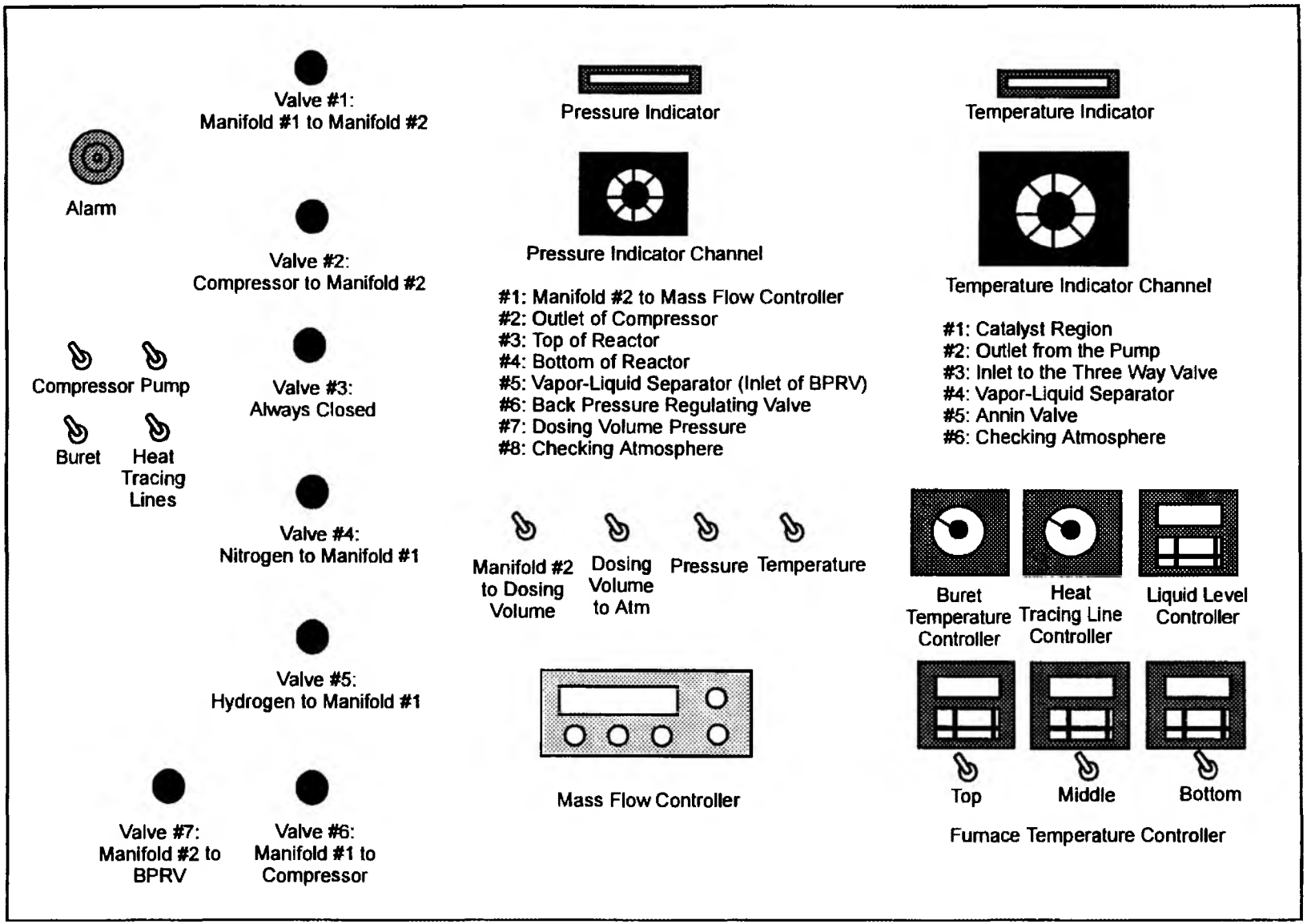
Valve #1:
Manifold #1 to Manifold #2
Alarm
Valve #2:
Compressor to Manifold #2
Compressor
Pump
Valve #3:
Always Closed
Buret
Heat
Tracing
Lines
Valve #4:
Nitrogen to Manifold #1
Valve #5:
Hydrogen to Manifold #1
Valve #7:
Manifold #2 to
BPRV
Valve #6:
Manifold #1 to
Compressor
Pressure Indicator
Pressure Indicator Channel
#1: Manifold #2 to Mass Flow Controller
#2: Outlet of Compressor
#3: Top of Reactor
#4: Bottom of Reactor
#5: Vapor-Liquid Separator (Inlet of BPRV)
#6: Back Pressure Regulating Valve
#7: Dosing Volume Pressure
#8: Checking Atmosphere
Manifold #2
to Dosing
Volume
Dosing
Volume
to Atm
Pressure
Temperature
Mass Flow Controller
Temperature Indicator
Temperature Indicator Channel
#1: Catalyst Region
#2: Outlet from the Pump
#3: Inlet to the Three Way Valve
#4: Vapor-Liquid Separator
#5: Annin Valve
#6: Checking Atmosphere
Buret
Temperature
Controller
Heat
Tracing Line
Controller
Liquid Level
Controller
Top
Middle
Bottom
Furnace Temperature Controller

$$°API = \frac{141.5}{s.g.\{60°F / 60°F\}} - 131.5 \qquad (3\text{-}1)$$

The API gravity and the specific gravity were 23.3 °API and 0.9144 g/cc, respectively, at 417 K (144°C). A Durcometer U Type proportioning pump (Duriron Company, Inc.) was used to pump the bitumen from the burettes to the reactor at the desired flow rate. A standard digital stroke adjustment, graduated in percent of stroke length, permitted reproducible setting of the stroke. The maximum operating discharge pressure of the pump was 34.3 MPa (5,000 psig) and the minimum flow rate was 20 cm^3/h at 13.8 MPa (2,000 psig).

The pump was primed using the valve at the outlet of the pump. Check valves were installed between the pump and the pump outlet manifold to prevent back flow of hydrogen into the liquid feed system. A pressure relief valve was installed at the pump outlet to avoid damage if the heat tracing failed and the transfer lines between the pump and the reactor inlet plugged with bitumen.

Heat Tracing Lines

The Whiterocks bitumen has a viscosity of about 10,000 cp at room temperature and about 1,500 cp at 361 K (190°F) [18]. Liquid transfer lines, valves, and the pump head were heat traced with 25 gauge Nichrome wire to heat the bitumen and lower its viscosity. The liquid product sampling line was also heat traced. This precaution permitted uninterrupted operation and circumvented plugging of transfer lines due to cold spots. The Nichrome wire had a resistivity of 0.83 ohm/cm (2.1 ohm/in) and was coated with glass fabric to avoid shorting on metal surfaces. Fiberglass tape was used to attach the wire to the system.

A proportional controller was used to control temperature of the heat traced lines. The heat tracing was divided into two sections; section A (lines A1 through A13), which included the lines from the pump to the reactor inlet and section B (lines B1 through B14), which included the lines from the reactor outlet to the liquid product recovery system. These two sections were connected in parallel. The spacing of the wire in each section was determined by the nature of the fluids flowing in the section.

The resistance of the heat-trace wires in each section is indicated in Table 3.1. Typical temperatures of heat traced lines for the base case operating condition at a controller setting was 343 K (70°C) are reported in Table 3.2. A schematic of heat traced sections A and B is presented in Figure 3.4.

Hydrogen Feed System

Hydrogen was compressed to the reactor inlet pressure by a Whitey Laboratory Compressor (Model LC10) whose maximum output pressure was 20.7 MPa (3,000 psig). The sealed diaphragm construction of this compressor was ideally suited for pumping hydrogen since leaks could not be tolerated. The compressor power supply was designed to turn the compressor off if the inlet pressure fell below 1.38 MPa (200 psig) to prevent damage since the inlet pressure limit was 0.35 MPa (50 psig). The regulator pressure and the compressor outlet pressure were controlled to provide a fixed hydrogen supply of 890 m^3/m^3 (5,000 scf/bbl) to the reactor. Typically the hydrogen supply pressure to the compressor inlet was 3.4 to 5.5 MPa (500-800 psig).

The initial hydrogen cylinder pressures were 13.8 MPa (2,000 psig). When the cylinder pressure fell below 5.5 MPa (800 psig), the hydrogen cylinders were changed. The hydrogen cylinder exchange was done in such a way that the lines were purged of air.

Table 3.1

Resistance of the Heat-Trace Wires in Each Section

	Resistance (Ohms)
A Section	
A1-A2	9.5
A3-A4	22.5
A5-A6	5.6
A7-A8	22.5
A9-A10	2.1
A11-A12	5.5
Total in A Section	74.9
B Section	
B1-B2	1.1
B3-B4	13.6
B5-B6	10.4
B7-B8	29.8
B9-B10	8.7
B11-B12	10.8
Total in B Section	82.0

Table 3.2

Typical Temperatures of Heat Traced Lines at the Base Case Condition

Temperature Indicator Channel Number	Section Description	Temperatures [K]
#1	Catalyst Bed Temperature	642
#2	Pump-Reactor Inlet Transfer Line	402
#3	Three-Way Valve at Reactor Inlet	420
#4	Vapor-Liquid Separator	352
#5	Annin Valve	380
#6	Room Temperature	289

Figure 3.4

Schematic of Heat Traced Lines

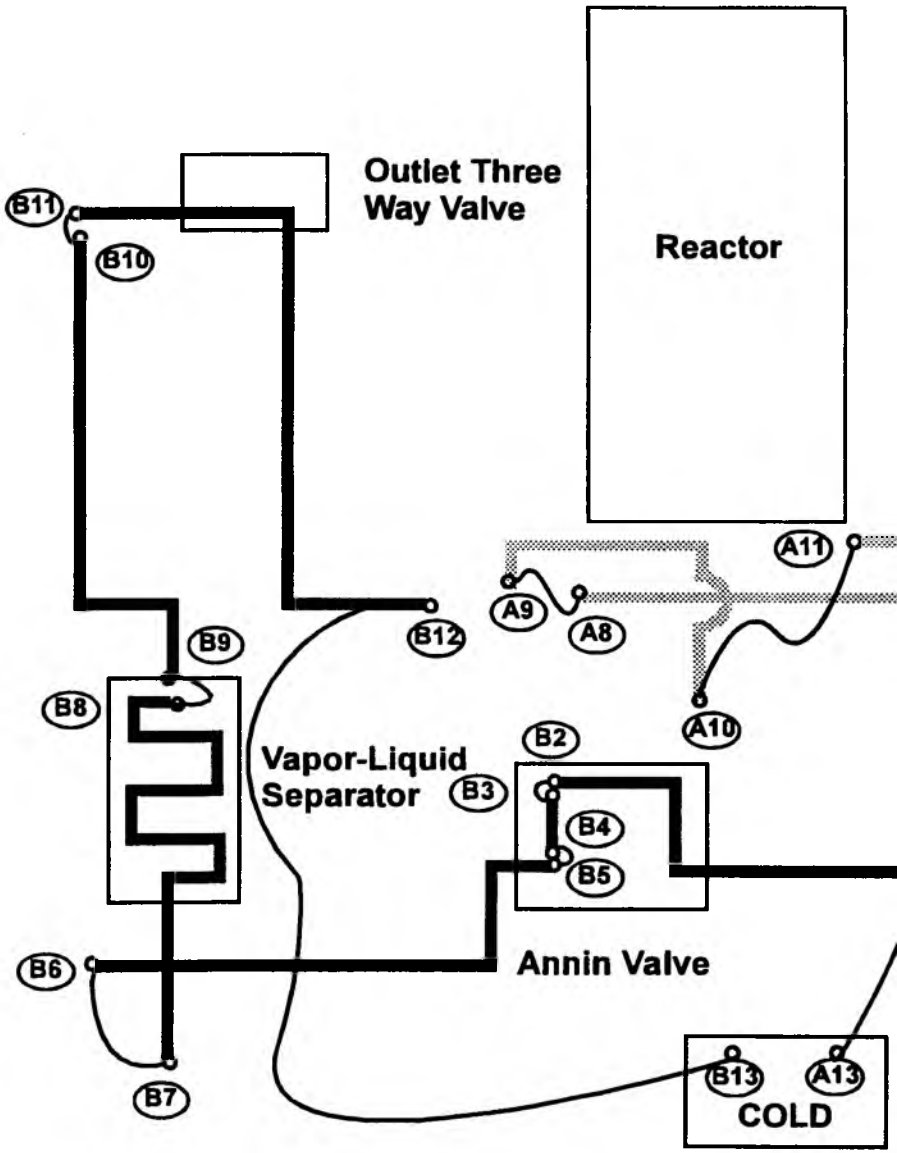
Outlet Three
Way Valve
Reactor
B11
B10
B9
B8
B12
A9
A8
A11
A10
B2
Vapor-Liquid
Separator
B3
B4
B5
B6
Annin Valve
B7
B13
A13
COLD

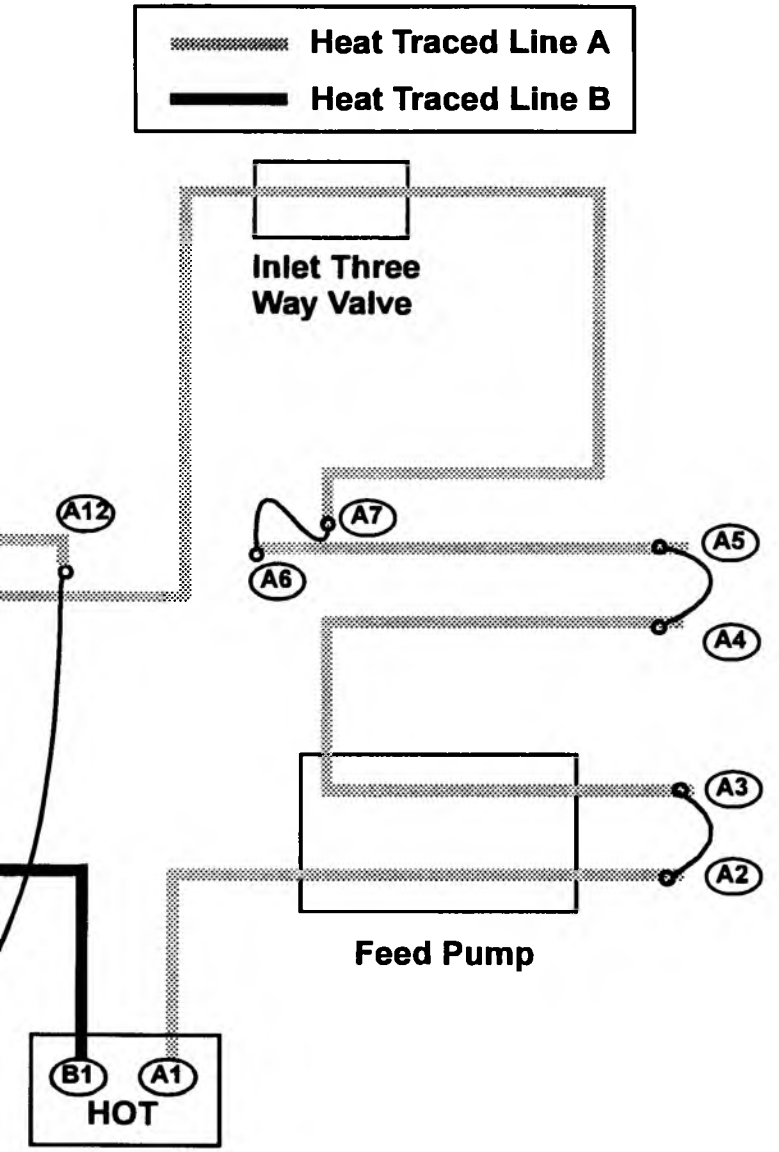
Heat Traced Line A
Heat Traced Line B
Inlet Three
Way Valve
A12
A7
A6
A5
A4
A3
A2
Feed Pump
B1
A1
HOT

Calibration of Mass Flow Controller

Hydrogen flow was controlled with a Brooks mass flow controller (Emerson Electric Co.). The mass flow controller valve was located between the compressor outlet and the reactor inlet manifold valves. Check valves were installed in the gas inlet lines to the reactor to prevent the backflow of liquid into the mass flow controller. Pressure relief valves were installed on the outlet of the compressor and on the inlet of the mass flow controller to protect the controller in the event of system overpressurizing.

The mass flow controller was calibrated at 13.7 MPa by measuring the hydrogen flowrate from the reactor in the absence of hydrogen consumption. Hydrogen flowrate was measured with a wet testmeter at different mass flow controller settings. The calibration curve for the mass flow controller is presented in Figure 3.5.

Reactor

A packed-bed tubular reactor was used in this study to simulate a refinery reactor. This type of reactor is superior to a batch autoclave even though both are governed by the same kinetics [89]. The reactor held 100 cm^3 of catalyst and was rated for operation at 20.7 MPa (3,000 psig) hydrogen at 773 K (500°C). The bitumen was fed into the reactor in the upflow mode to ensure complete wetting of the catalyst and to permit isothermal operation.

The reactor was made of seamless 316 stainless steel tubing which had an inside diameter of 2.54 cm (1 in) and a wall thickness of 0.95 cm (0.37 in). A 0.32 cm (0.13 in) outside diameter thermowell which held a movable thermocouple was located on the centerline of the reactor. The reactor was flanged at each end and sealed by copper and aluminum gaskets.

Figure 3.5

Mass Flow Meter Reading versus Volumetric Hydrogen Flow Rate

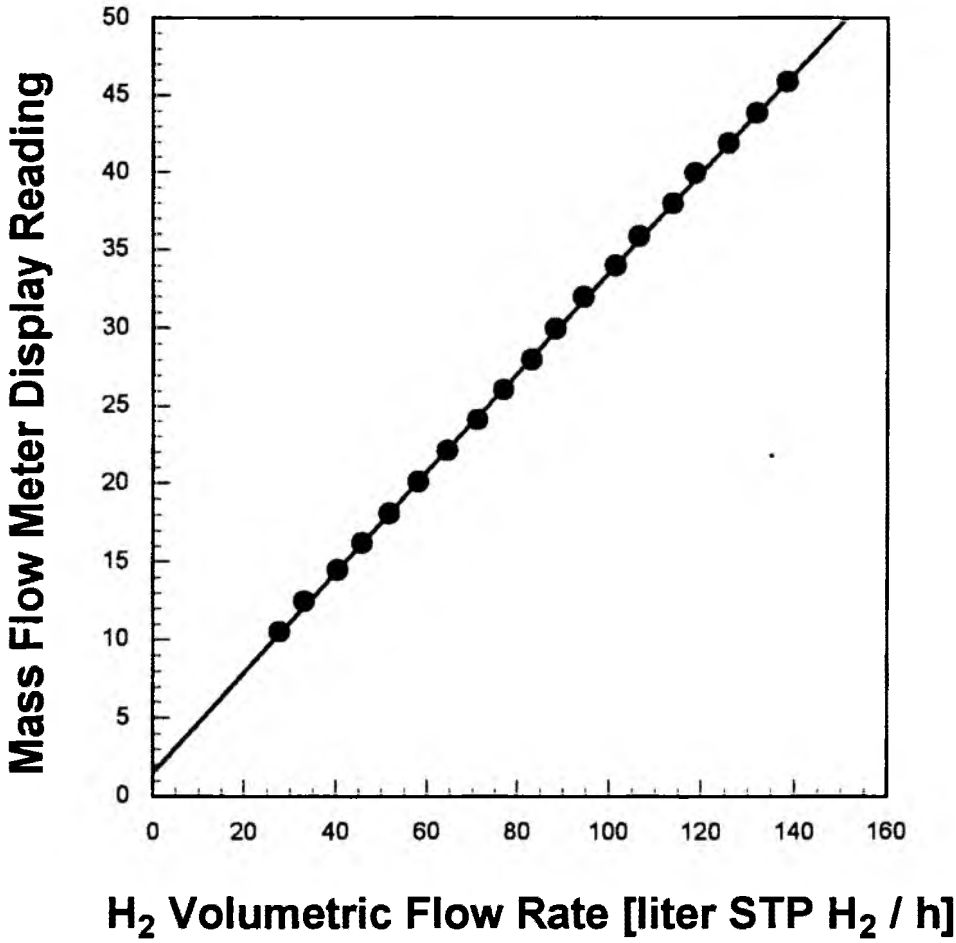
Mass Flow Meter Display Reading
50
45
40
35
30
25
20
15
10
5
0
0
20
40
60
80
100
120
140
160
H2 Volumetric Flow Rate [liter STP H2 / h]

The copper gasket was used to seal the bottom (inlet) flanges because the inlet gas contained no hydrogen sulfide (H_2S) or ammonia (NH_3). The aluminum gasket was used to seal the top (outlet) flanges because copper might interact with the hot H_2S and/or NH_3 leaving the reactor and aluminum is corrosion resistant. The aluminum gaskets showed no signs of corrosion even after 1,000 hours at temperatures in the range 620-685 K (656-775°F) in the presence of ammonia, hydrogen sulfide and water.

A 0.95 cm (0.38 in) stainless steel tube was welded in the center of the inlet and outlet cap-flanges to serve as the feed inlet and product outlet lines.

Reactor Temperature Control System

A three-zone Lindberg furnace was used to provide the heat to the reactor. Three UDC 2000 Mini-Pro Universal Digital Controllers were used to control the temperature of each section. The reactor temperature was monitored by DP 285J temperature display, Omega Engineering Co., using a movable thermocouple.

The catalyst was located in the middle (30.5 cm (12 in)) furnace zone. The bottom zone (15.2 cm (6 in)) served as the preheater and the top zone (15.2 cm (6 in)) was used as a trim heater to maintain the catalyst zone isothermal. The setting of the top section was set above the desired isothermal temperature to diminish heat losses through the reactor head. An aluminum shield was used as a heat sink to moderate temperature fluctuations due to cycling of the furnace heating element and to maintain an isothermal temperature profile in the catalyst bed. A schematic of the reactor is presented in Figure 3.6.

Figure 3.6

Schematic Diagram of Upflow Catalytic Reactor

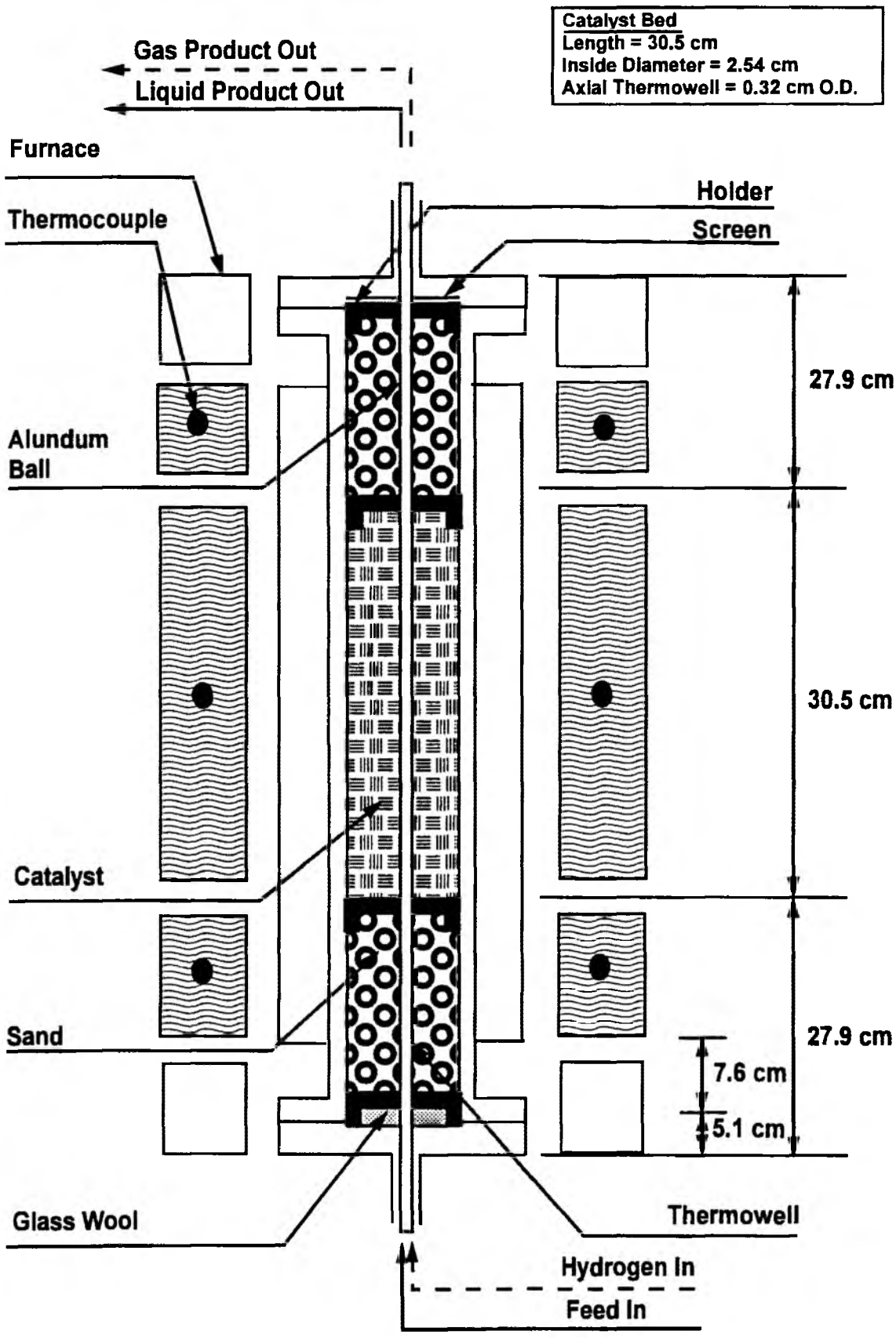
Catalyst Bed
Length = 30.5 cm
Inside Diameter = 2.54 cm
Axial Thermowell = 0.32 cm O.D.
Gas Product Out
Liquid Product Out
Furnace
Thermocouple
Holder
Screen
Alundum
Ball
27.9 cm
30.5 cm
Catalyst
Sand
27.9 cm
7.6 cm
5.1 cm
Glass Wool
Thermowell
Hydrogen In
Feed In

Reactor Pressure Control System

The system pressure was maintained by a back pressure regulating valve (BPRV) and was monitored by an Omega Engineering Model DP-354 pressure indicator. Pressure gauges were located in the feedline from the pump, in the transfer line to the reactor, in the transfer line from the reactor, and at the back pressure regulating valve as indicated in Figure 3.2. A Mity Mite Back Pressure Regulating Valve with a pressure rating of 20.7 MPa (3,000 psig) controlled the total system pressure. The system was pressurized to the desired value by admitting nitrogen to the dome of BPRV.

A schematic of the pressure control system is presented in Figure 3.7. Initially valves a, b and c were opened while valves d was closed. The compressor delivered nitrogen to the dome of the BPRV until the pressure gauge B reading reached the desired value, then all the valves were closed. The system pressure was controlled with a BPRV which functioned by controlling the flow of the vapor product exiting from the vapor-liquid separator. The BPRV functioned as an on-off valve due to the movement of the Teflon diaphragm which deflected to permit vapor product to exit the system through the BPRV orifice. The system pressure at which the BPRV would open to release vapor product was determined by the pressure on the dome side of the diaphragm. When the process pressure was greater than the dome pressure the diaphragm would deflect to permit the vapor to leave the system through the BPRV orifice. The operation of the BPRV permitted steady control of the system pressure (±0.01 MPa).

At the start of each run the dome pressure was loaded with nitrogen to the base case pressure (13.7 MPa). During reactor operation the system pressure was occasionally raised or lowered depending on the desired reactor conditions.

Figure 3.7

Schematic of System Pressure Control System

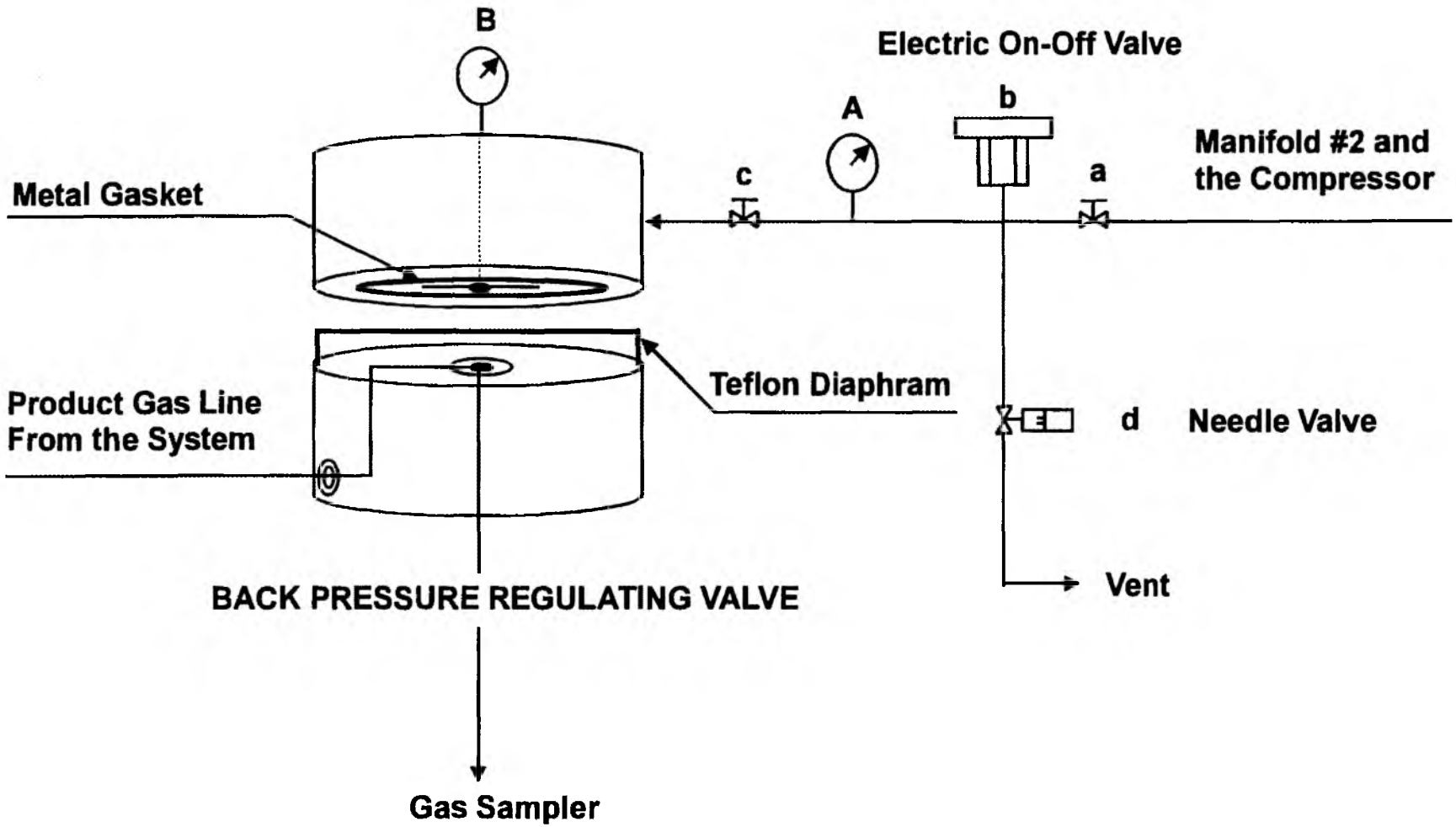
B
Electric On-Off Valve
A
b
Manifold #2 and
the Compressor
c
a
Metal Gasket
Teflon Diaphram
Product Gas Line
From the System
d
Needle Valve
Vent
BACK PRESSURE REGULATING VALVE
Gas Sampler

The dome pressure was changed in the following manner to permit a steady transition from one operating pressure to another:

- The dosing volume was pressurized with gas in manifold 1 to a pressure 0.1-1.2 MPa (15-30 psi) higher than the BPRV. Valve c between the dosing volume and the BPRV was opened. The immediate effect of opening this valve was to increase the BPRV dome pressure 0.05-0.1 MPa (7-14 psi) which in turn increased the system pressure by the same amount. The valve between the BPRV and the dosing volume was only opened when the dosing volume pressure was greater than the BPRV dome pressure to avoid a sudden and uncontrolled drop in the system pressure.
- If the system pressure was to be lowered, then the pressure on the dosing volume/BPRV was slowly vented through the needle valve (valve d) until the dome (and the system) reached the desired pressure. This step was conducted slowly (rate of pressure decreased < 0.07 MPa/min) to permit hydrogen dissolved in elastomeric rubber gaskets and O-rings to diffuse out of the matrix.
- If the system pressure was to be increased, then valves (valves a and b) between manifold #2 and the dosing volume were opened. The dosing volume/BPRV dome pressure was then gradually increased until it was 0.05-0.1 MPa higher than the desired BPRV dome pressure. At that point, the valves between manifold #2 and the dosing volume were shut.
- Because the system pressure responds slower than the dosing volume pressure, the system pressure was permitted to rise until vapor product started to exit the BPRV. Then the additional pressure (0.05-0.1 MPa) in

the connected dosing volume/BPRV dome was slowly vented through the needle valve.

- After adjustments on the BPRV dome pressure were completed the valve between the BPRV and the dosing volume was shut.

Liquid Product Separation and Sampling System

A liquid level control system on the high pressure separator was used to withdraw the total liquid product from the system. The system pressure was dropped from 13.8 MPa (2,000 psig) upstream of the control valve to atmospheric pressure downstream at the low pressure separator. A Wee Willie Model 5061 (Annin) control valve manufactured by the Masoneilan Division of the McGraw-Edison Co. was used in concert with a DP liquid level sensor-controller to control the withdrawal of liquid from the system.

The building supply air pressure which was normally 0.5-0.6 MPa (70-80 psig) was regulated to 0.16 MPa (23 psig) for the I/P converter through a 0.04-0.3 MPa (5-40 psig) Masoneilan Dresser regulator and also provided air pressure (0.21 MPa (30 psig)) to the Annin valve. A Pneumotive air compressor fitted with a Solberg air filter and a Speedaire Reducing Regulator was used to provide instrument air in the event that the building air compressor shut down. The compressor starter was set to turn on the compressor when the building air pressure dropped below 0.17 MPa (25 psig) and to shut down the compressor when the instrument air pressure reached 0.31 MPa (45 psig).

A Bailey Type BC Transmitter (BC2/3/4), Bailey Controls Co., measured the differential pressure across the Brooks high pressure vapor-liquid separator. The separator was rated for a maximum pressure of 41.3 MPa (6,000 psig) maximum pressure. The transmitter sent 4-20 mA current output to the Masoneilan Dresser I/P converter through the Honeywell UDC 3000 Universal

Digital Controller which was used to control the liquid level. The I/P converter converted this 4-20 mA signal to 0.02-0.1 MPa (3-15 psig) air signal which controlled the output to the positioner on the Annin valve. The Annin valve had a series A trim which permitted a theoretical C_v range of 0.001 and 0.01 and had a variable maximum stroke length from 0.025 to 0.38 cm (0.01-0.15 in). A schematic of the Annin control valve system is presented in Figure 3.8.

The NH_3 and H_2S in the exit gases were absorbed in a bubbler which contained a 2 molar solution of KOH (potassium hydroxide) before passing through the wet test meter or being vented to the hood.

Safety System

A safety alarm was incorporated into the system since it was intended for continuous operation; that is, more than 1,000 hours on stream. If the liquid level reached the maximum permitted level in the vapor-liquid separator, the Sonalert alarm, Mallory Co., was activated and the pump was shut down to prevent flow of bitumen through the BPRV.

Air-flow in the vicinity of the hydrotreater was maintained by continuous operation of the hood. A commercial fan was used to ventilate the hydrotreater during periods of operation to move hydrocarbon vapors and/or hydrogen to the hoods.

Experimental Procedure

Catalyst Loading

The reactor furnace was divided into three independently controlled regions; the preheater zone, the catalyst bed zone and the exit trim heater zone. The reactor was flanged at both the inlet and outlet. Aluminum and copper

Figure 3.8

Schematic of Annin Valve

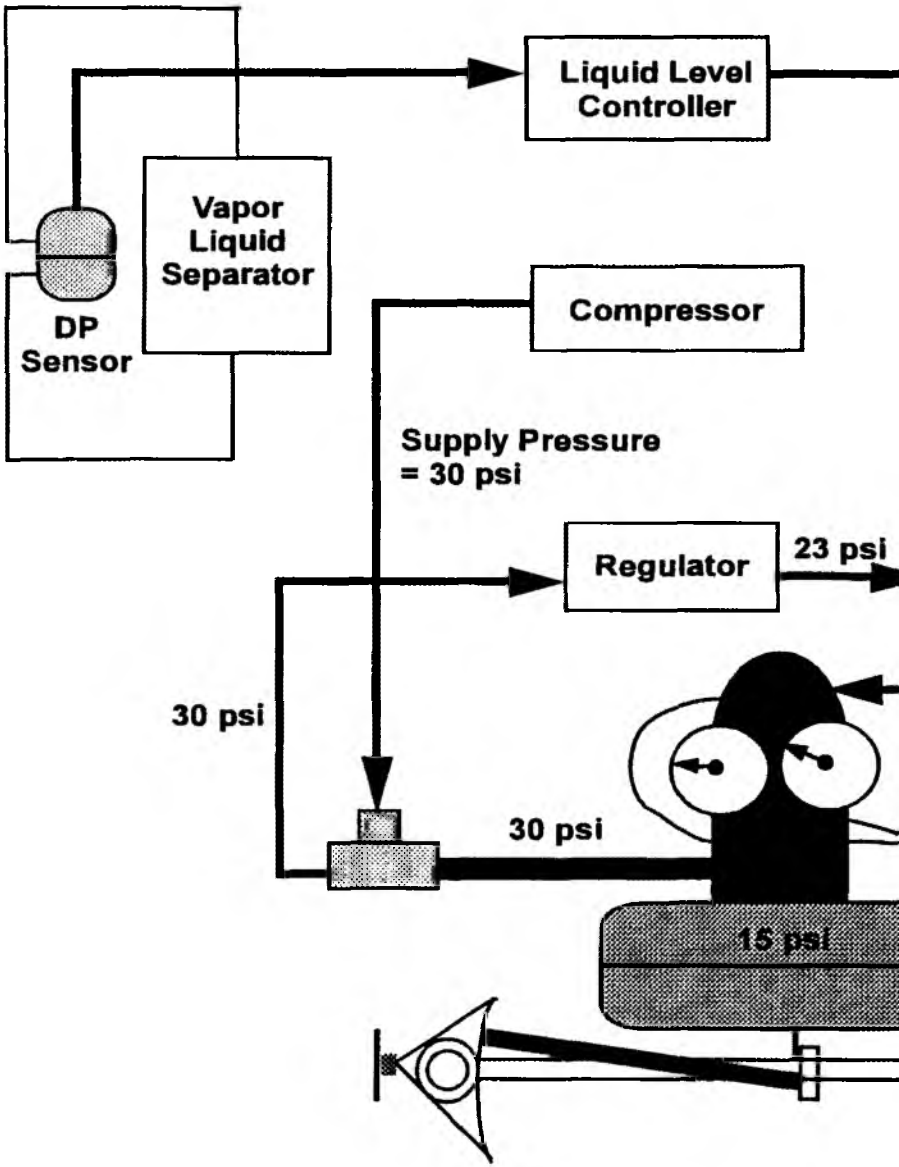
Liquid Level Controller
Vapor Liquid Separator
DP Sensor
Compressor
Supply Pressure = 30 psi
Regulator
23 psi
30 psi
30 psi
15 psi

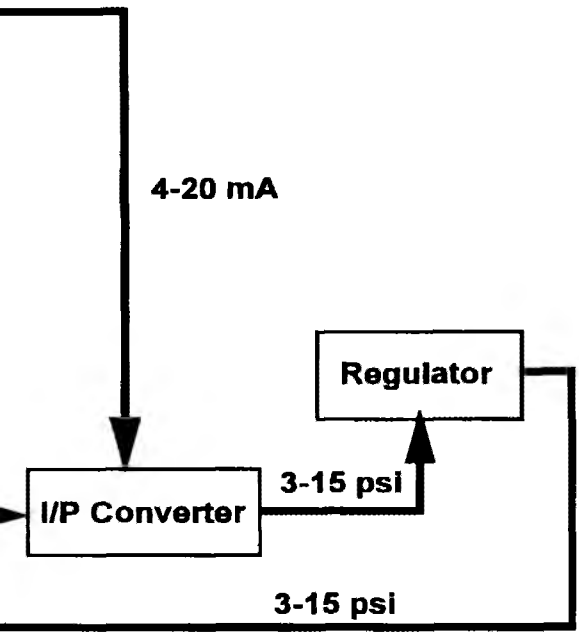
4-20 mA
Regulator
3-15 psi
I/P Converter
3-15 psi

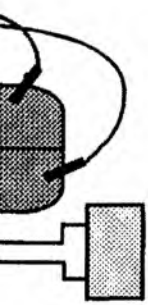

gaskets were used to seal the flanges to the unit which were set using a torque wrench. The torque wrench force was increased from 10 lb_f-in to 60 lb_f-in increments of 10 lb_f-in.

Alpha alumina balls (0.05 cm (0.13 in)) were placed in the preheater and exit zones of the reactor. The balls in the preheater zone also served to support the catalyst bed. Sand (white SiO_2; -50+70 mesh) from Aldrich Chemical Co. was placed in the interstices of the α-alumina balls to reduce the void volume and to induce higher liquid superficial velocities.

The exit zone was filled with 126.7 cm^3 of alundum balls and 34.8 cm^3 of fine sand. The reactor was tapped frequently during loading to distribute the sand throughout the alundum balls in the reactor. A pan-shaped holder fitted with a 65-mesh screen (equivalent to 212 mm opening) was used to hold the alundum balls and sand in place. The HDM catalyst bed was not diluted with sand to avoid catalyst bed plugging due to coking of the large molecular weight species in the bitumen. The catalyst charge was 152 cm^3 and was placed in the central region of the reactor. The reactor was tapped during catalyst loading to ensure proper packed density. The catalyst bed was held in place by a screen. Finally, 128.3 cm^3 of alundum balls and 35.3 cm^3 of sand were placed in the preheater zone. The reactor body was connected to the unit.

Pressure Test

The reactor system was pressure tested prior to catalyst sulfiding to minimize hydrogen leaks. The pressure test was conducted by increasing the BPRV pressure from atmospheric pressure to 6.9 MPa (1,000 psig) at atmospheric temperature. Nitrogen was used to pressurize the system. After the nitrogen pressure stabilized the system was isolated. The isolated section consisted of the line from the nitrogen regulator to the inlet of the reactor, the

reactor and the line from outlet of the reactor to vapor-liquid separator and the line from vapor-liquid separator to the BPRV inlet line.

The unit pressure was monitored. If there was no loss of pressure over 16 hours the system pressure was increased to 13.8 MPa (2,000 psig). The system pressure was monitored overnight (16 hours). If a significant leak was indicated in any segment of the unit, the line was removed, replaced and the pressure test was performed again. The BPRV section was also pressure tested. Once the system was pressure tight sulfiding could be performed.

Catalyst Sulfiding

The hydrotreating catalyst was presulfided in-situ before contact with the liquid feed. The catalyst sulfiding procedure consisted of contacting the catalyst with a sulfiding solution and hydrogen to reduce and sulfide the supported metal oxide component. After sulfiding, the active component of the metal in the catalyst changed from metal oxide to metal sulfide. The sulfiding solution was 2 wt% dimethyldisulfide in kerosene. The kerosene was obtained from the Flying J Refinery in North Salt Lake City, Utah. The dimethyldisulfide used in this study was in a 99 vol% purity obtained from Aldrich Chemical Company, Inc. The solution was prepared in a hood due to the toxicity of dimethyldisulfide. A 4-liter bottle was filled with 2,400 g of kerosene and the desired amount of dimethyldisulfide solution (72 g) was added and stirred for an hour to form a completely mixed solution.

The catalyst sulfiding procedure was recommended by the manufacturer. The conditions were a system pressure of 6.2 MPa (900 psig), 890 m^3(STP)/m^3 (5,000 ft^3/bbl) hydrogen-to-oil ratio, and 1.0 h^{-1} liquid hourly space velocity (LHSV). A mass flow controller was used to maintain the feed rate and hydrogen-to-oil ratio. The sulfiding procedure is illustrated in Figure 3.9.

Figure 3.9

Catalyst Sulfiding Sequence

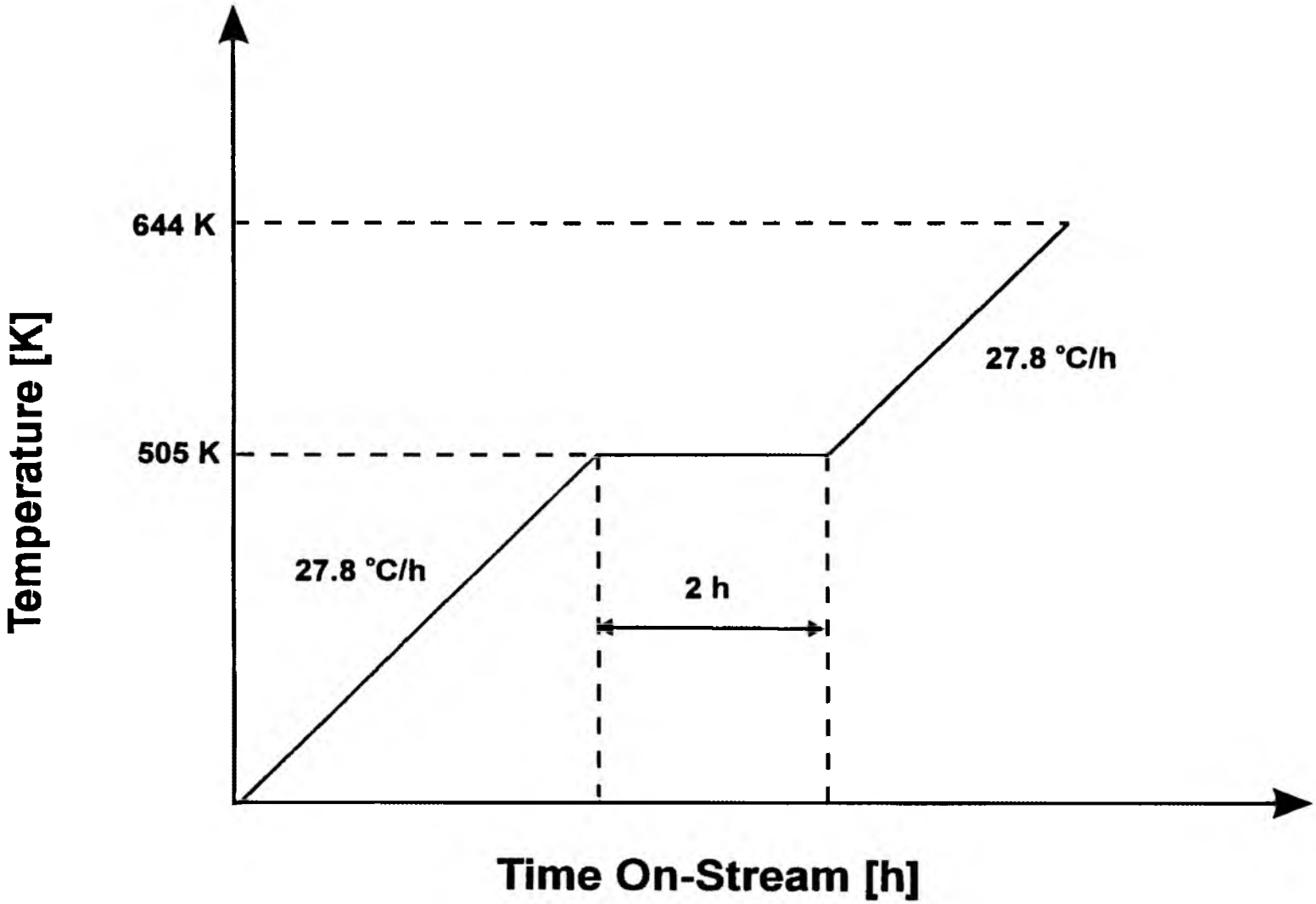
644 K
505 K
27.8 °C/h
27.8 °C/h
2 h
Temperature [K]
Time On-Stream [h]

Sulfiding was started at ambient temperature and the catalyst was heated to 505 K (450°F) at a rate of 27.8 °C/h (50 °F/h). The catalyst was held at 505 K for 2 hours. At 478 K (400°F) sulfur uptake by the catalyst increases dramatically; thus, the extended period at 505 K was to ensure complete sulfiding of the catalyst. The initial set points for the three temperature controllers were 550 K (530°F) (bottom), 489 K (420°F) (middle) and 533 K (500°F) (top). The heating rate was checked and adjusted every twenty minutes by monitoring the reactor temperature in the catalyst bed as the reactor heated up to 505 K. After holding the reactor temperature at 505 K for 2 hours, the completion of sulfiding was confirmed by the presence of hydrogen sulfide in the exit gas sampler. The hydrogen sulfide was detected by the color change of copper wool in the sampler from red to black.

The sulfiding solution feed was then stopped and the reactor temperature was lowered to 494-500 K (430-440°F). The bottom and top temperature controllers were set at 494 K (430°F). The middle section controller set point was kept at 489 K (420°F). The hydrogen feed was reversed to force the sulfiding solution out of the reactor and a small amount of hydrogen (mass flow meter reading was 2.0) was fed to the reactor to maintain hydrogen pressure overnight.

The low hydrogen flow was intended to avoid sulfur stripping by hydrogen. Subsequently, hydrogen was introduced to the reactor in the upflow mode at 890 m^3/m^3 (5,000 scf/bbl) and the sulfiding solution was introduced to the reactor at 1.0 h^{-1} LHSV. The reactor temperature was increased from 505 K (450°F) to 644 K (700°F) at a rate of 27.8 K/h (50 °F/h). At 644 K the liquid pump was turned off and the hydrogen feed was reversed to flush the sulfiding solution out of the reactor and the reactor temperature was lowered to 617 K (650°F).

Experimental Strategy and Reactor Startup

The effects of operating variables on the extent of denitrogenation, desulfurization, demetallation, residuum conversion and the product distribution and yields were determined.

Initially, the catalyst was deactivated and stabilized for 8 days at the base case conditions; 642 K (696°F), 0.45 h^{-1} and 13.7 MPa (1980 psig). At this point it was assumed that the catalyst was stabilized because the change in °API gravity with time was negligible. When liquid product started to exit from the reactor system through Annin valve, it was considered to be zero time on stream. The conditions during the initial catalyst deactivation study are presented in Table 3.3. The initial catalyst deactivation, as a function of time on-stream is shown in Figure 3.10.

After the initial catalyst deactivation period, as indicated by the API gravity of the total liquid product, the process variable experiments were conducted in a cyclic mode. A specific operating variable experiment was performed followed by an experiment at the base case condition to determine if the catalyst deactivated during the process variable experiment.

In order to select the optimum operating conditions and to cover as many operating conditions as possible with a limited number of experiments, two variables were fixed while the other variable was varied within a reasonable range. A 3-D representation of the set of operating conditions used in this study is presented in Figure 3.11. The API gravities of the total liquid products produced in the process variable experiments and at the base case conditions with respect to time on-stream are presented in Figure 3.12. The process variable experiments were performed in a random manner to avoid systematic errors; that is, the same operating variable was not studied in sequence. The sequence of experiments performed in this study is presented in Table 3.4.

Table 3.3

Conditions for Initial Catalyst Deactivation

Run No.	T K (°F)	WHSV[a] h^{-1}	LHSV h^{-1}	P MPa (psig)	TOS[b] h
D-1	641 (694)	0.90	0.53	13.7 (1987)	8
D-2	640 (693)	0.86	0.51	13.6 (1975)	29
D-3	641 (694)	0.86	0.50	13.7 (1980)	53
D-4	640 (693)	0.86	0.50	13.6 (1966)	74
D-5	640 (693)	0.82	0.48	13.5 (1955)	116
D-6	640 (693)	0.83	0.49	13.6 (1975)	139
D-7	640 (693)	0.92	0.54	13.6 (1975)	167
D-8	642 (696)	0.78	0.46	13.7 (1985)	188

[a] Weight hourly space velocity

[b] Time elapsed since oil was started over catalyst

Figure 3.10

API Gravity versus Time On-Stream

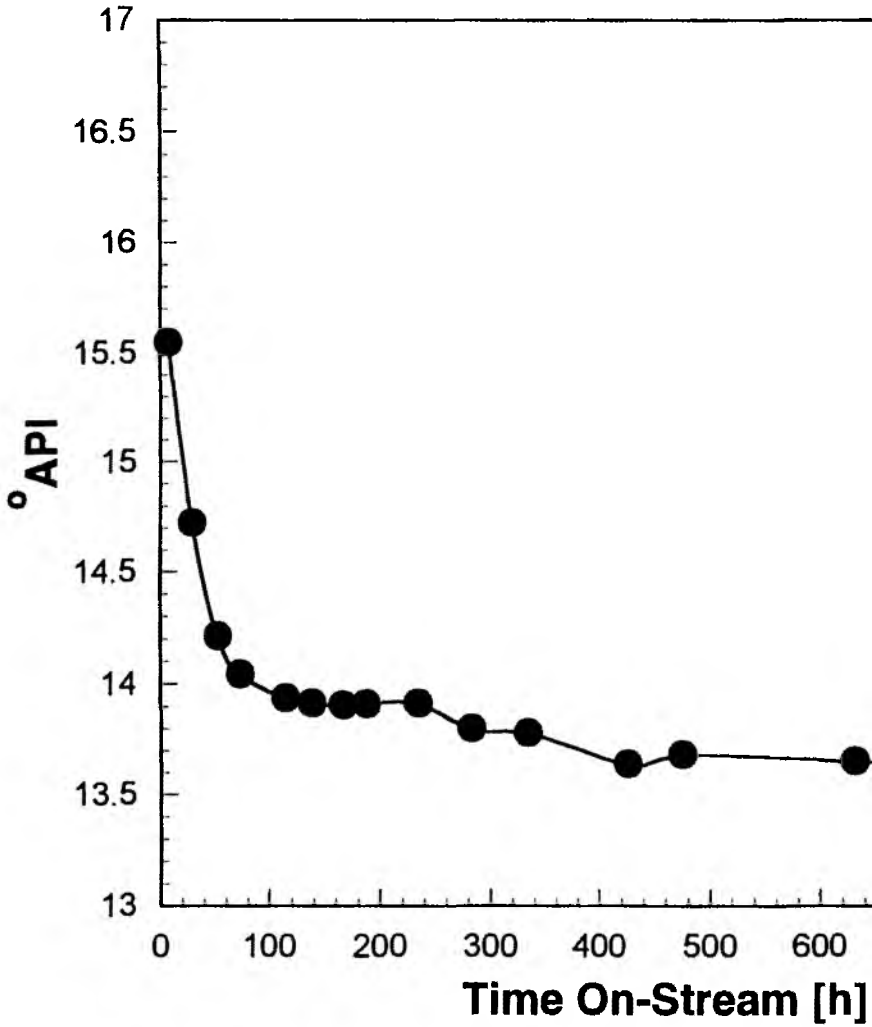
17
16.5
16
15.5
15
14.5
14
13.5
13
°API
0
100
200
300
400
500
600
Time On-Stream [h]

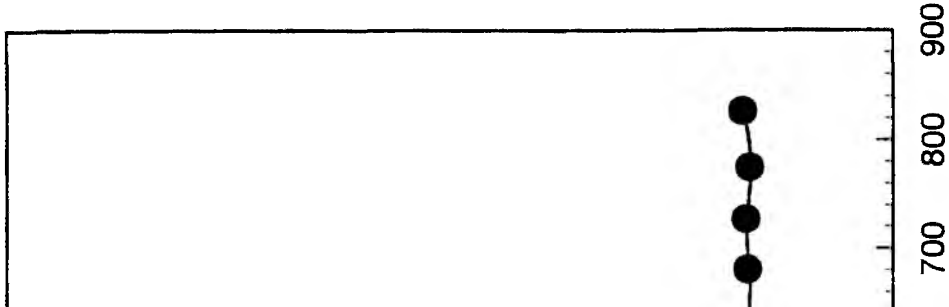
900
800
700

Figure 3.11

Operating Conditions Used in This Study

Common Point (Run D-11)
Temperature = 664 [K]
WHSV = 0.76 [h^{-1}]
Pressure = 13.7 [MPa]

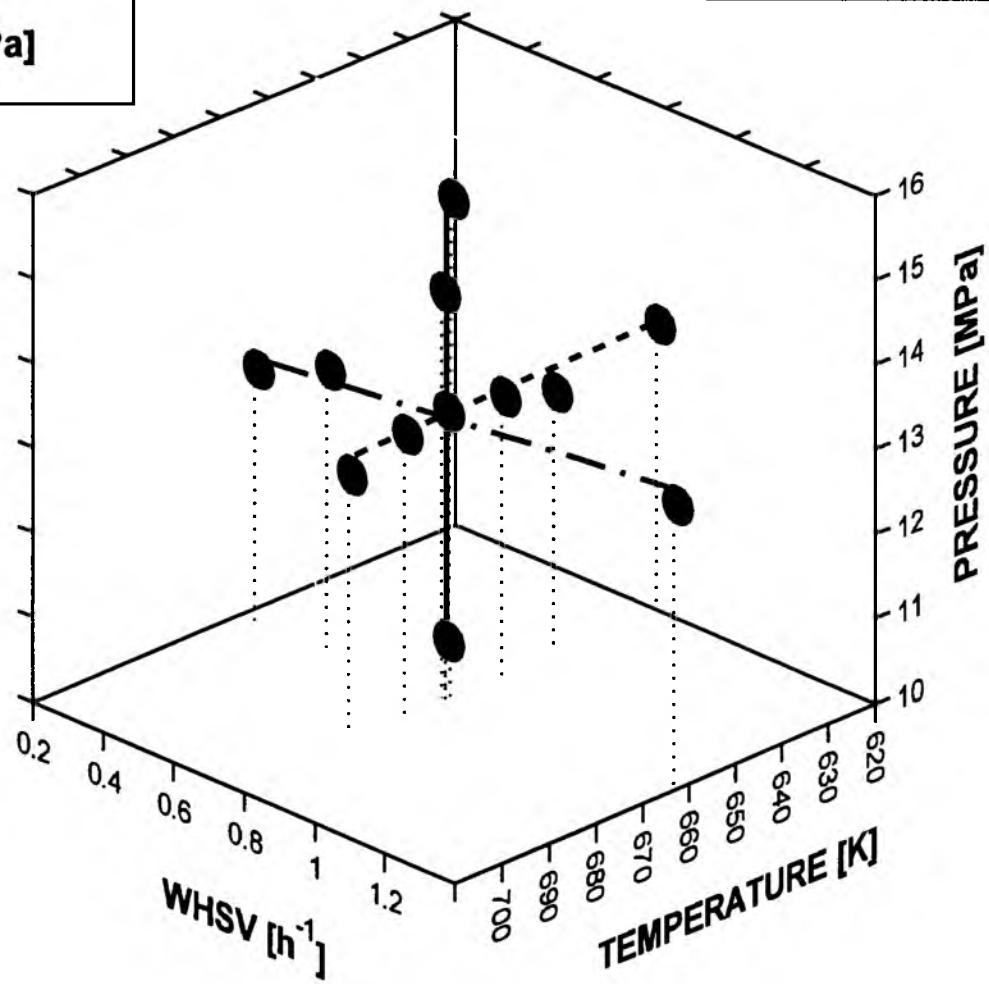

Figure 3.12

Total Liquid Product API Gravities as a Function of Time On-Stream

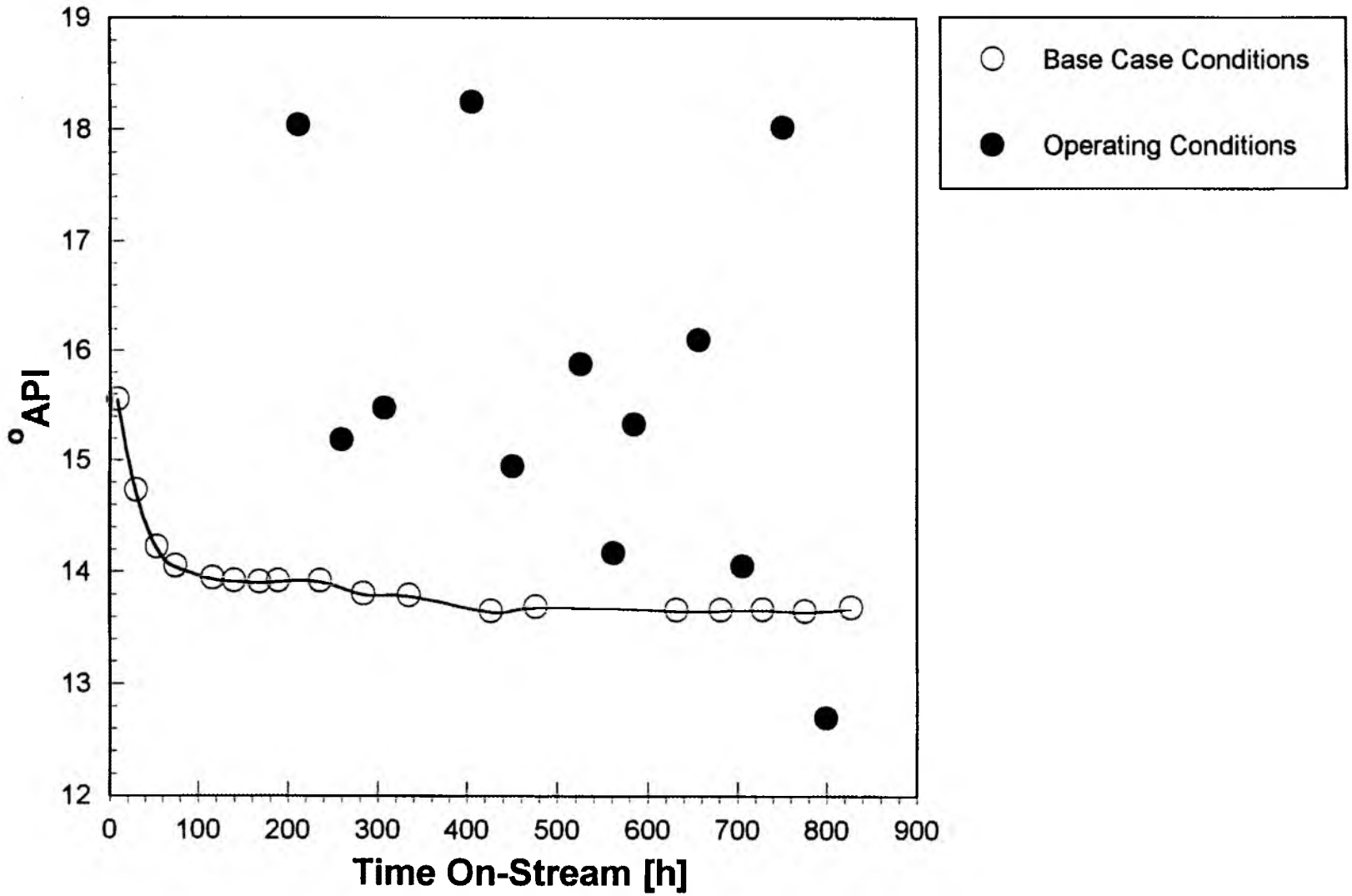
19
18
17
16
15
14
13
12
°API
0
100
200
300
400
500
600
700
800
900
Time On-Stream [h]
Base Case Conditions
Operating Conditions

Table 3.4

Sequence of Experiments Performed

Run No.	T, K (F)	WHSV (LHSV), h^{-1}	P, MPa (psig)	TOS[a], h
D-9	686 (775)	0.75 (0.44)	13.7 (1987)	211
D-10	642 (697)	0.77 (0.45)	13.7 (1980)	235
D-11	665 (737)	0.77 (0.45)	13.8 (1995)	259
D-12	643 (697)	0.78 (0.46)	13.6 (1975)	283
D-13	664 (736)	0.77 (0.45)	16.7 (2423)	306
D-14	642 (696)	0.78 (0.46)	13.6 (1975)	334
D-15	666 (739)	0.24 (0.14)	13.6 (1971)	405
D-16	642 (696)	0.77 (0.45)	13.7 (1984)	426
D-17	665 (737)	0.77 (0.45)	11.3 (1634)	450
D-18	642 (697)	0.77 (0.45)	13.6 (1972)	475
D-19	665 (738)	0.43 (0.25)	13.7 (1983)	525
D-20	653 (716)	0.77 (0.45)	13.6 (1974)	561
D-21	665 (737)	0.76 (0.45)	15.3 (2220)	584
D-22	642 (696)	0.76 (0.45)	13.7 (1988)	631
D-23	673 (752)	0.76 (0.44)	13.7 (1989)	656
D-24	642 (695)	0.78 (0.46)	13.6 (1977)	681
D-25	662 (732)	1.38 (0.81)	13.6 (1978)	705
D-26	642 (696)	0.78 (0.46)	13.6 (1972)	727
D-27	685 (773)	0.76 (0.45)	13.7 (1984)	750
D-28	641 (694)	0.77 (0.45)	13.7 (1981)	775
D-29	620 (656)	0.77 (0.45)	13.7 (1980)	799
D-30	641 (695)	0.79 (0.46)	13.6 (1976)	827
Production Run of 18 °API Total Liquid Product.				
D-31	686 (775)	0.66 (0.39)	13.5 (1965)	849
D-32	686 (774)	0.70 (0.41)	13.5 (1962)	870
D-33	685 (773)	0.75 (0.44)	13.5 (1960)	895
D-34	687 (777)	0.75 (0.44)	13.5 (1957)	919
D-35	695 (792)	0.76 (0.44)	13.5 (1954)	943
D-36	698 (797)	0.66 (0.39)	13.6 (1972)	966
D-37	697 (796)	0.61 (0.36)	13.6 (1972)	992

[a] Time on-stream.

The API gravities of the hydrotreated products were determined according to the Syncrude Analytical Method [134].

Operating Procedure

Daily experimental operations consisted of a mass balance followed by changing the reaction conditions for overnight unattended operation. It was assumed that the catalyst activity at each reaction condition was stabilized after overnight operation (16 hours) and that representative samples were taken during the subsequent mass balance.

Mass Balances

A representative sample was collected for subsequent analysis at a specific set of reaction conditions during each mass balance. The mass balance procedure was as follows:

- The gas chromatograph was activated and the sample collection system was prepared to acquire a sample of the gas from vapor-liquid separator. The procedure is described in Product Oil and Gas Analysis Section.
- The empty Erlenmeyer liquid sample collection flask (500 cm^3) and the condensable vapor collection tube (60 cm^3) were weighed.
- The liquid feed level in the large burette and the time were recorded and the constant overnight feed rate was calculated. It was assumed that the catalyst activity was at steady state since it had been at run conditions for more than 16 hours.
- Deionized water was boiled for the bath in which API gravity of the liquid product collected during mass balance would be measured.

- The hydrogen cylinder pressure was checked. If the hydrogen cylinder pressure was below 5.5 MPa (800 psig), all three cylinders were replaced.
- The small burette was filled with bitumen from the storage drum and the pump feedline was switched from the large to the small burette for the mass balance. The initial volume of feed in the small burette and the starting time of the mass balance were recorded. The liquid sampler was connected to the product line.
- The temperature profile along the catalyst bed was recorded. The detailed procedure is described in the following section (Temperature Measurement). A gas sample from the liquid-vapor separator line was collected and injected into the GC for analysis.
- The gas collector in the liquid nitrogen trap to the product line was connected and a gas sample was collected. The gas sample was collected over 1 hour and the gas flowrate was measured with the wet test meter (Precision Scientific, Inc.). The atmospheric pressure and temperature were recorded and the volumetric hydrogen flowrate exiting the reactor at STP was calculated. A gas sample collected from the liquid nitrogen trap vent line was injected for GC analysis.
- The gas collector and the liquid nitrogen trap were removed from the unit. The amount of gas collected in the liquid nitrogen trap was determined and the rate of gas production was measured.
- A representative liquid sample was collected for 3 to 4 hours. The liquid collection reservoir was disconnected from the system and was replaced by a polypropylene container (19 liter (5 gallon)) for overnight operation. The liquid level in the small burette was recorded and the LHSV during the mass balance was calculated. The mass balance was calculated from

the gas and liquid products collected. All wt% mass balances were in the range 98 to 100 wt% in this study.

- The reaction conditions were changed to those selected for the next experiment. The conditions were checked frequently so that the catalyst system would be equilibrated for the following day's mass balance.
- The hydrogen and oxygen flow to the GC were discontinued and the GC was turned off. Helium flow was continued for 2 hours until the column temperature returned to ambient.
- The API gravity of the total liquid product was determined to assess the deactivation of the catalyst as a function of the time on-stream.

Temperature Measurement

The temperature profile of the catalyst bed was measured along the axis of the reactor with a movable J-type thermocouple. The thermocouple moved inside of the 0.05 cm (1/8 in) O.D. thermowell to measure the temperature in the catalyst region. The three heating elements in the furnace were controlled to give a uniform temperature throughout the reactor length. A typical experimental catalyst bed temperature profile is presented in Figure 3.13. The temperature profile along the length of the catalyst region was almost isothermal. The kinetic average temperature was calculated from the temperature profile.

The kinetic average temperature ($T_{k,e}$) is the temperature of an isothermal reactor required to give the same conversion obtained in a nonisothermal reactor. The following equation was used to calculate the kinetic average temperature:

$$\int_0^L \exp[-E_a / RT_{k,e}]dl = \int \exp[-E_a / RT(l)]dl \qquad (3\text{-}2)$$

Figure 3.13

Typical Temperature Profiles in the Catalyst Zone

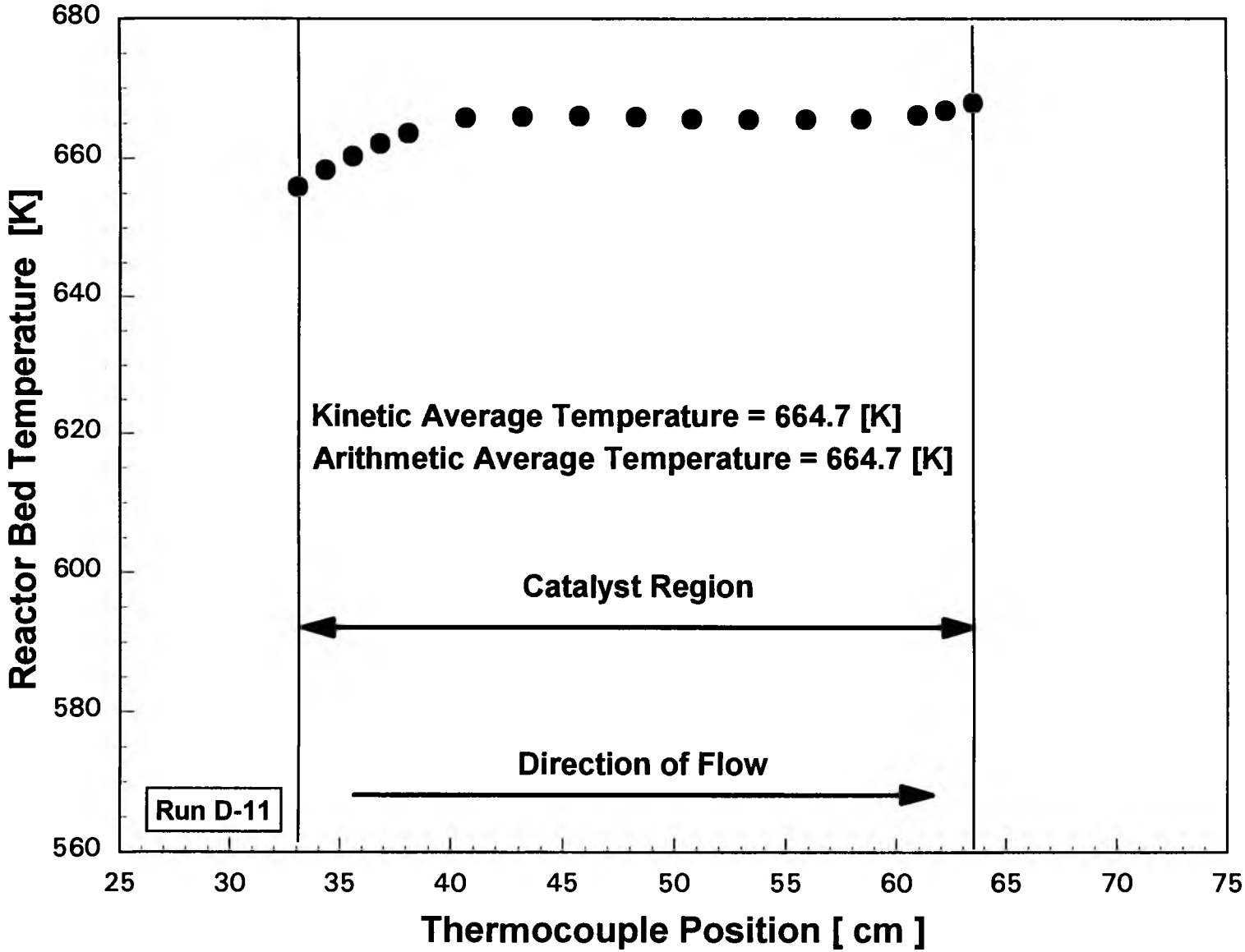
Reactor Bed Temperature [K]
680
660
640
620
600
580
560
25
30
35
40
45
50
55
60
65
70
75
Thermocouple Position [cm]
Kinetic Average Temperature = 664.7 [K]
Arithmetic Average Temperature = 664.7 [K]
Catalyst Region
Direction of Flow
Run D-11

where, T(l) is the measured axial temperature gradient across the reactor; R is the gas constant; l is the length of the reactor at each measurement; L is the total length of the reactor; and E_a is the activation energy.

The kinetic ($T_{k,e}$) and arithmetic average temperatures ($T_{a,e}$) were calculated as follows:

$$\frac{1}{T_{k,e}} = (-\frac{R}{E_a}) \ln[\frac{1}{L}\int_0^L \exp[-E_a / RT(l)]dl \quad (3\text{-}3)$$

$$T_{a,e} = \frac{1}{L}\int_0^L T(l)dl \quad (3\text{-}4)$$

The activation energy for hydrodenitrogenation of bitumen-derived liquid, E_a=106 kJ/mol, was determined in a previous study [18] and was used here to calculate the kinetic average temperature. The kinetic average temperature is not strongly dependent upon the value of the activation energy, E_a. This assumption should be valid because $T_{Axial}=T_{max}-T_{min}$ is small as can be seen in Figure 3.13. The calculation was based on Trapezoidal Rule using the weighting functions.

The arithmetic average temperature was only slightly higher (0.06 K (0.1°F) at most) than the kinetic average temperature. Thus, the reactor operated essentially isothermally.

Sample Purging

The total liquid product samples collected during the mass balances were purged to remove H_2S and NH_3 which were dissolved in the hydrotreated liquid

so as to minimize the uncertainty when elemental analyses of these samples were performed.

About 25 g of the total liquid product was placed in a 60 cm^3 test tube fitted with a side arm. The test tube was placed in a 250 ml Erlenmeyer flask containing 175 cm^3 of water. The ammonia and hydrogen sulfide were stripped from the sample with helium at a flowrate of 50 cm^3/min. The helium was bubbled through the sample for 4 hours while the water in the flask was boiling. The purged liquid and the stripped light ends which were recovered in a cold water trap were mixed to form the final sample. These samples were sent to the Galbraith Lab for elemental analysis.

Overnight Operating Procedure

After completion of each mass balance and the collection and preparation of material balance samples, the temperature and pressure were reset for the next experiment. The space velocity was adjusted because the feed rate was affected by the temperature and pressure adjustments. The total liquid product was collected overnight in 19 liter (5 gallon) plastic container and the catalyst attained a steady state at the new reactor conditions. Even though the system was designed to operate unattended overnight, it was periodically checked to minimize the possibility of reactor upsets.

Shutdown

After the conclusion of the process variable study a high temperature (775-797 K (685-698°F)) and low LHSV (0.36-0.43 h^{-1}) run was made to produce a high API gravity (18 °API) total liquid product for subsequent hydrocracking and catalytic cracking experiments. After 150 hours on-stream in the production run the compressor failed, hydrogen flow was lost and, severe coking occurred

in the reactor inlet region; thus the bitumen hydrotreating run (Run D) was terminated.

All heat tracing lines were shut off and the system was allowed to return to the ambient temperature. In addition, the reactor pressure was slowly decreased. Kerosene was pumped through the reactor to flush out the bitumen-derived heavy oil. The kerosene flush was discontinued when the color of the liquid exiting from the system changed from black to yellow. Hexane was used as a second flush solution at a reactor temperature of 400 K and a reactor pressure of 1.4 MPa (200 psig). The hexane was pumped through the system until the liquid exiting from the system was colorless. The catalyst was then dried in flowing nitrogen and cooled to ambient temperature.

The reactor was disconnected and removed from the system and the catalyst was removed from the reactor. The catalyst particles were no longer individual pellets but rather were fused due to severe external coking. It was presumed that the coking took place at the time of the compressor failure.

Product Gas and Liquid Analysis

The gas samples produced during mass balances were analyzed by gas chromatography. The liquid samples were analyzed by simulated distillation. Carbon, hydrogen, nitrogen, sulfur, and metals contents were determined along with pour point, Conradson carbon residue, and composition-type analyses.

Gas Product Analysis

The gas from the high pressure vapor-liquid separator was analyzed with a Carle Analytical GC Series SX , Model 211 (FID) (Carle Instruments, Inc.), which was connected to IBM AT computer for integration. The Carle GC was

turned-on each day as part of the mass balance procedure. The helium flow pressure was then started at 0.37 MPa (53 psig) when the column temperature reached 331 K. When the column temperature reached (331 K), the hydrogen flow was started at 0.07 MPa (10 psig) above the run pressure, 32 psig. The FID was ignited after purging the hydrogen line, for 1 to 2 minutes. The air flow was started at 20 psig and the hydrogen flow pressure was reduced to the normal operating pressure (0.22 MPa (32 psig)). Two gas samples from the system were injected, one was taken at a point before the gas collector and the other was taken from after the gas collector in the liquid nitrogen trap. These two samples were necessary because the liquid nitrogen trap did not collect a small amount of the light hydrocarbon gases, methane and ethane. This observation was factored into the calculation of hydrogen consumption.

The FID response factors were used to correct the GC analysis [135]. The FORTRAN program called HYDROGEN.FOR was written to calculate hydrogen consumption for various mass balance and is presented in Appendix A.

Liquid Product Analysis

Simulated Distillation

The molecular weight distribution of the liquid products was determined by simulated distillation using a Hewlett Packard 5890 Series II Gas Chromatograph with an HP 3396 Series II Integrator and an HP 7673 Controller. The GC was connected to an IBM XT Personal Computer for data logging. A Fused Silica Capillary Column, 5 m long and 0.53 mm ID with a 0.1 mm thick film, by Supelco Inc., was used to separate the sample to carbon number 60 (C_{60}). The column was calibrated using an HP boiling point calibration sample No. 1, for the C_5 to C_{40} paraffins and Supelco, Inc. boiling point calibration sample for paraffins up to

C_{60}. The column retention time calibrations were performed three times before bitumen and hydrotreated total liquid product analyses were performed. The normal paraffin boiling point distributions corresponding to carbon numbers were obtained from the literature [136]. Then tabulated retention times for the paraffin standard samples were used in the program, SIMDIS.BAS, which is described in Appendix B. The oven temperature program was started at 308 K and held at this temperature for 4.5 minutes. The oven was then heated at the rate of 12 °C/h until the final temperature of 653 K was reached and maintained for 8.75 minutes. The same program was used for both the sample and blank runs. The hydrotreated liquid sample was warmed and dichloromethane (EM Science Co.) was added to obtain a representative sample for GC injection.

The simulated distillation procedures for the hydrotreated total liquid products were repeated in the following manner:

- First conditioning run
- First blank run
- Sample only run
- Second conditioning run
- Second blank run
- Sample and internal standard run

Column conditioning was required after a sample injection to remove all uneluted materials left on the column owing to the heavy nature of the hydrotreated total liquid product.

The initial oven temperature for the conditioning run was 308 K. The oven was then heated at 50 °C/h to 653 K and temperature was maintained at 653 K for 90 minutes to remove the uneluted material from the previous run.

Blank runs were also necessary after conditioning to obtain the stabilized base lines. The Basic program called ZEROBLNK.BAS was written to subtract the baseline from the sample peak. The sample plus internal standard run was conducted to the correct retention times for the high carbon number materials. The C_{14} through C_{17} paraffin mixture was used as an internal standard. The weight ratios for mixtures of the bitumen, the hydrotreated total liquid product and the internal standard are tabulated in Table 3.5. About 10 hours were required to analyze one sample.

The raw data acquired from the GC, which has ".BNC" extension and was not readable by IBM PC, was integrated using a Basic program called SLICE6.BAS and resulted in files which had ".RPT" extension. The .RPT extension files were readable by an IBM PC, and through the SIMDIS.BAS program in the PC, they were transferred into ASCII text files and tabulated. The basic programs including SIMDIS.BAS and ZEROBLNK.BAS are shown in Appendix A.

Elemental Analysis

The bitumen feed and the hydrotreated total liquid products were sent to Galbraith Laboratory, Inc. for elemental analysis. The analyses performed included carbon, hydrogen, nitrogen, sulfur, nickel, vanadium, and arsenic. The hydrotreated samples were nitrogen and sulfur stripped prior to analysis to remove dissolved ammonia and hydrogen sulfide.

The nitrogen analysis was conducted on a LECO FP-428 Nitrogen Analyzer (50-100 mg sample size). The range of the instrument was 0.1 to 100 wt% nitrogen with a reproducibility of ±0.1 % [137].

The sulfur analysis was done by an Oxygen Bomb/Ion Chromatography method [138,139] due to the low ppm range, 0-3500 ppm of the samples. A

Table 3.5

Mixture Ratios for Internal Standard and Representative Samples

Sample I.D.	Amount of Sample [wt%]	Amount of Internal Standard [wt%]
Feed+IS	74.2	25.8
D-11+IS	69.5	30.5
D-13+IS	66.4	33.6
D-15+IS	64.3	35.7
D-17+IS	68.6	31.4
D-18+IS	73.7	26.3
D-19+IS	65.6	34.4
D-20+IS	67.7	32.3
D-21+IS	65.5	34.5
D-23+IS	67.7	32.3
D-25+IS	75.0	25.0
D-27+IS	68.7	31.3
D-29+IS	69.2	30.8

Dionex Model 10/14 Ion Chromatograph was used. Carbon and hydrogen analyses were performed with a Perkin-Elmer 240 Elemental Analyzer [140]. The amount of arsenic of the feed was in the ppm range and was analyzed by Atomic Absorption Spectroscopy using a Perkin Elmer 5000 AA; and a HGA 500 Graphite Furnace [141,142]. The nickel and vanadium analyses were performed by Inductively Coupled Plasma Emission Spectroscopy using a Perkin-Elmer P II instrument [143,144].

Pour Point and Conradson Carbon Residue Measurement

Conradson carbon residues were measured according to ASTM D 189-IP 13 [145]. The pour points were measured by the Pycnometer Method described in the Syncrude Analytical Methods Handbook [134].

CHAPTER 4

RESULTS AND DISCUSSION

This chapter describes the extent of heteroatom removal, residuum conversion, product distributions and yield of hydrotreated Whiterocks bitumen over a commercial HDM catalyst as a function of process variables. Also, a comparison of bitumen hydrotreating over a small pore (HDN) catalyst [18,146] and a large pore (HDM) catalyst was generated to determine the effect of metal loading and pore size distribution on hydrotreating. This comparison is based on two experiments in which bitumen was hydrotreated at similar conditions [18, 146]. The kinetics of nitrogen, sulfur and residuum conversion for the hydrotreating of a bitumen-derived heavy oil over the HDN catalyst will also be discussed [18,147]. The Whiterocks bitumen-derived heavy oil was produced in a fluidized-bed pyrolysis reactor [18,147,148].

Properties of Bitumen, Bitumen-Derived Liquid and Hydrotreated Products over HDM and HDN Catalysts

There are significant differences in the properties between commercial HDM and HDN catalysts as indicated in Table 4.1. The HDM catalyst has double the median pore diameter and less than half of the metal loadings as the HDN catalyst.

The large pore diameter of the HDM catalyst diminishes deactivation due to coke formation and metal deposition relative to the HDN catalyst for a fixed

Table 4.1

Properties of UNOCAL Quadralobe HDM and HDN Catalysts

	HDM Catalyst	HDN Catalyst [18,147-149]
Pore Volume, cc/g (by Mercury Porosimetry)	0.72	0.55
Surface Area, m^2/g	155	241
Mean Pore Diameter, Å	180	90
Average Characteristic Dimension, cm	0.16	0.16
MoO_3, wt%	6.2	12.8
NiO, wt%	1.0	3.3
P_2O_5, wt%	0.0	0.8
Unimodal Pore Structure	yes	yes

feedstock and set of operating parameters. It also reduces the diffusion barrier to the transport of heteroatoms, metal compounds and residuum molecules to the interior, active surface of the catalyst. Quann et al. [27] reported that metal removal reactions in conventional 0.16 cm (=1/16 inch) hydrotreating catalysts are generally diffusion limited.

The metals in the catalyst serve as sites for catalytic hydrogenation in the hydrotreating process. Therefore, the lower surface area and metals loading of the HDM catalyst was expected to exhibit lower catalytic activity than higher metals content HDN catalyst. An HDM catalyst also has a larger pore volume. The UNOCAL HDM and HDN catalysts were quadralobe shaped extrudates with unimodal pore structures. The quadralobe catalyst was selected for this study since it has been demonstrated that shaped catalysts exhibit improved diffusion characteristics relative to cylindrical extrudates [71].

Selected physical and chemical properties of the feedstocks are presented in Table 4.2. The analyses indicate that the two bitumen samples were quite similar. The bitumen-derived liquid contained significantly less residuum than the bitumen samples as indicated by simulated distillation analysis and it had only about 31% of the residuum content of the bitumen.

The differences in the feedstocks are also reflected in the Conradson carbon residues (CCR) and the asphaltene contents. The asphaltene contents were determined as pentane insolubles in this study. The Conradson carbon residue and the asphaltene content of the bitumen-derived liquid were 79% and 64%; respectively, of the values determined for the bitumen. Elemental analyses indicated that the pyrolysis process in which the bitumen-derived heavy oil was produced resulted primarily in molecular weight and boiling range reduction without selective deposition of heteroatomic species in the carbonaceous residue; however, nickel compounds were deposited in the carbonaceous

Table 4.2

Selected Feedstock Properties

	Whiterocks Bitumen over HDM Catalyst	Whiterocks Bitumen over HDN Catalyst [18,146,149]	Whiterocks Bitumen-Derived Liquid over HDN Catalyst [18,147,149]
Liquid Gravity, °API	11.7	11.4	18.5
CCR, wt%	10.2	8.8	8.1
Pour Point, K(°F)	319(115)	330(135)	250(-10)
Asphaltenes[a], wt%	4.4	5.0	2.8
Simulated Distillation			
Volatility, wt%	42.2	43.3	82.2
C_5-478 K(400°F), wt%	1.9	0.0	4.9
478 K(400°F)-616 K(650°F), wt%	6.0	6.3	42.2
616 K(650°F)-811 K(1000°F), wt%	34.3	37.0	35.6
>811 K(1000°F), wt%	57.8	56.7	17.8
Elemental Analysis			
C, wt%	85.1	85.5	85.9
H, wt%	11.6	11.0	11.1
N, wt%	1.3	1.1	1.0
S, ppm	3334	3700	3200
Ni, ppm	72	78	9
V, ppm	<10	4	<1
As, ppm	3	3	3
H/C Atomic Ratio	1.6	1.5	1.6

[a] Pentane Insolubles

residue.

The processing conditions required to hydrotreat the bitumen were more severe than those required for the bitumen-derived liquid. The process operating variable range for bitumen hydrotreating over both the HDM and HDN [18,146,149] catalysts and for bitumen-derived liquid hydrotreating over the HDN catalyst [18,147,149] are summarized in Table 4.3 and in Figure 4.1.

The extent of nitrogen removal was the key reactivity parameter followed during the course of this study; however, the key operating parameter followed on the catalyst testing unit during the run was the specific gravity of the total liquid product. The nitrogen content of the total liquid products produced during hydrotreating the Whiterocks bitumen and bitumen-derived liquid over HDM and HDN catalysts is plotted as a function of API gravity in Figure 4.2. The similarity between the trends indicates that the nitrogen-gravity correlation for the hydrodenitrogenation of bitumen and bitumen-derived liquid could be used with confidence as an online guide to estimate the real time influence of changes in operating variables during the course of the study.

Although the bitumen-derived liquid data [18,147] were obtained under the same sets of conditions as the bitumen data [18,146], the hydrotreated bitumen-derived liquid samples are clustered at lower product nitrogen levels than the hydrotreated bitumen samples. Clearly, the bitumen nitrogen is more refractory than the bitumen-derived liquid nitrogen. The difference is most likely due to the higher molecular weight of the bitumen.

Table 4.3

Process Operating Variable Ranges and Base Case Conditions
for Bitumen and Bitumen-Derived Liquid Hydrotreating

	Bitumen [18,146,149]	Bitumen-Derived Liquid [18,147,149]
Base Case Conditions		
Temperature, K(°F)	642(696)	618(653)
Pressure, MPa(psia)	13.7(1980)	13.7(1980)
WHSV, h^{-1}	0.76	0.78
LHSV, h^{-1}	0.45	0.48
Process Variable Ranges		
Temperature, K(°F)	616-711(650-820)	
Pressure, MPa(psia)	11.0-16.9(1600-2450)	
WHSV, h^{-1}	0.24-1.38	
LHSV, h^{-1}	0.14-0.81	

Figure 4.1

Operating Conditions for Bitumen and Bitumen-Derived Liquid Hydrotreating over HDM and HDN Catalysts

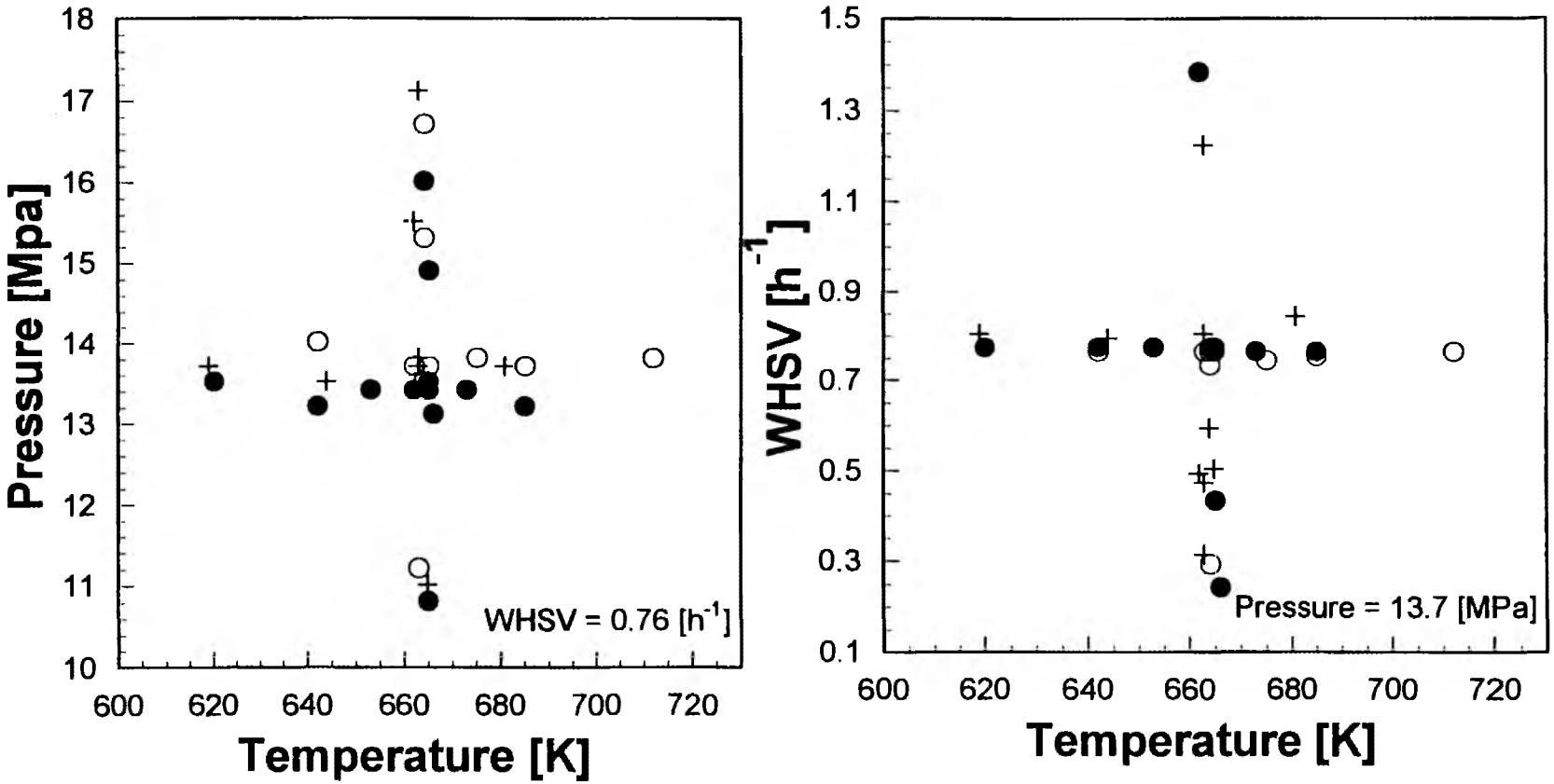
Pressure [Mpa]
Temperature [K]
WHSV = 0.76 [h-1]
WHSV [h-1]
Temperature [K]
Pressure = 13.7 [MPa]
Bitumen HT over an HDM Catalyst
Bitumen HT over an HDN Catalyst [18,146]
Bitumen-Derived Liquid HT over an HDN Catalyst [18,147]

Figure 4.2

Nitrogen Concentration versus Total Liquid Product API Gravity

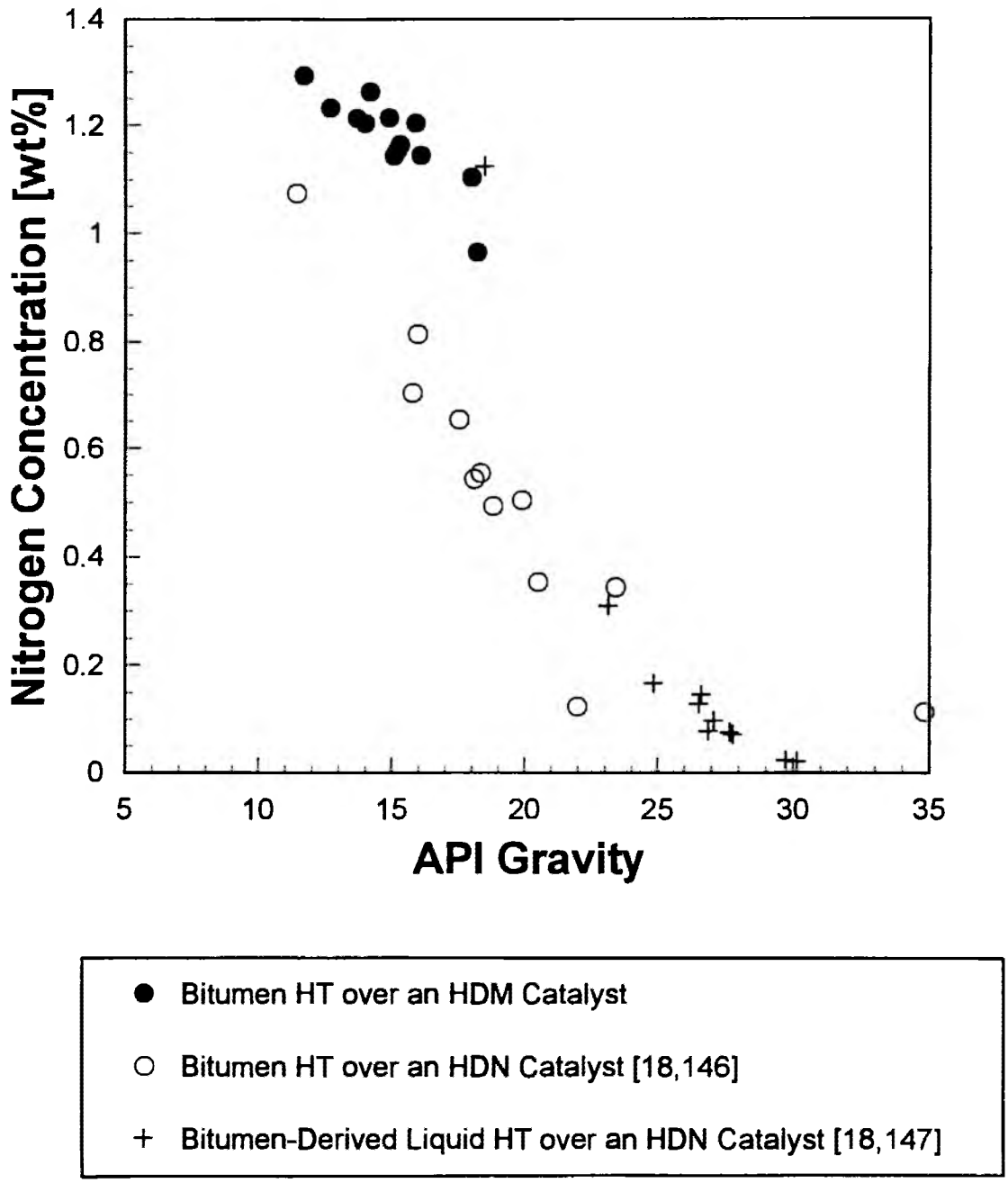
Nitrogen Concentration [wt%]
1.4
1.2
1
0.8
0.6
0.4
0.2
0
5
10
15
20
25
30
35
API Gravity
Bitumen HT over an HDM Catalyst
Bitumen HT over an HDN Catalyst [18,146]
Bitumen-Derived Liquid HT over an HDN Catalyst [18,147]

Hydrotreated Bitumen over an HDM Catalyst

The chemical and physical properties of the hydrotreated total liquid products produced from bitumen and bitumen-derived liquid at various reaction conditions over an HDN catalyst were reported by Longstaff and co-workers [18,147-149].

The total liquid products produced were upgraded relative to the bitumen (Tables 4.4 through 4.6) as a result of hydrotreating the bitumen over an HDM catalyst. The HDM catalyst selectively removed nickel in the feed under all reaction conditions. The maximum nickel removal was 81.8% at low WHSV, 0.24 h^{-1} and a temperature of 666 K. Sulfur removal occurred to a greater extent than nitrogen removal which seems to be reasonable considering the need for hydrogenation of the ring prior to nitrogen removal. Sulfur removal ranged from 14.9% to 77.4% whereas nitrogen removal ranged from 2.3% to 29.0%. It is interesting to note that at the least severe conditions there appeared to be an increase in the sulfur content of the hydrotreated total liquid product relative to the bitumen. This may be related to the low sulfur content in the feed. The maximum Conradson carbon residue conversion, 43.4%, was achieved at low WHSV of 0.24 h^{-1} and a temperature of 666 K.

The pour point of the total liquid product was 279 K at 685 K whereas it was 319 K for the bitumen. This change indicated that the HDM catalyst exhibited little cracking activity under the conditions used in this study. The API gravity was increased from 11.7 to 18.3 °API at low WHSV of 0.24 h^{-1}. Residuum conversion ranged from 10.6% to 61.2%.

Table 4.4

Elemental Analysis of the Bitumen and the Hydrotreated Total Liquid Products Produced over a Commercial HDM Catalyst

Run I.D.	Temperature [K]	Pressure [MPa]	WHSV [h^{-1}]	C [wt%]	H [wt%]	N [wt%]	S [ppm]	Ni [ppm]	H/C[a] [-]
Whiterocks Bitumen				85.1	11.6	1.29	3334	72	1.6
Temperature:									
D-29	**620**	13.7	0.77	85.3	11.4	1.23	4220	39	1.6
D-18	**642**	13.6	0.77	85.4	10.7	1.21	2390	40	1.5
D-20	**653**	13.6	0.77	86.1	11.6	1.26	2720	55	1.6
D-11	**665**	13.8	0.77	85.5	11.8	1.15	2030	23	1.7
D-23	**673**	13.7	0.76	85.5	11.7	1.14	1930	25	1.6
D-27	**685**	13.7	0.76	85.8	11.3	1.10	2220	30	1.6
Pressure:									
D-17	665	**11.3**	0.77	85.8	12.0	1.21	2140	31	1.7
D-11	665	**13.8**	0.77	85.5	11.8	1.15	2030	23	1.7
D-21	665	**15.3**	0.76	85.4	11.6	1.16	1880	25	1.6
D-13	664	**16.7**	0.77	85.9	11.9	1.14	1980	22	1.7
WHSV:									
D-15	666	13.6	**0.24**	86.2	12.2	0.96	790	14	1.7
D-19	665	13.7	**0.43**	85.4	11.5	1.20	1720	20	1.6
D-11	665	13.8	**0.77**	85.5	11.8	1.15	2030	23	1.7
D-25	662	13.6	**1.38**	85.6	11.2	1.20	2850	33	1.6

[a] Atomic Ratio

Table 4.5

Selected Properties of the Bitumen and the Hydrotreated Total Liquid Products Produced over a Commercial HDM Catalyst

Run I.D.	Temperature [K]	Pressure [MPa]	WHSV [h^{-1}]	Conradson Carbon Residue [wt%]	Pour Point [K]	API Gravity [°API]
Whiterocks Bitumen				10.2	319	11.7
Temperature:						
D-29	**620**	13.7	0.77	10.1	315	12.7
D-18	**642**	13.6	0.77	9.4	307	13.7
D-20	**653**	13.6	0.77	9.2	299	14.2
D-11	**665**	13.8	0.77	8.5	287	15.2
D-23	**673**	13.7	0.76	8.1	283	16.1
D-27	**685**	13.7	0.76	7.6	279	18.0
Pressure:						
D-17	665	**11.3**	0.77	8.6	288	14.9
D-11	665	**13.8**	0.77	8.5	287	15.2
D-21	665	**15.3**	0.76	8.4	287	15.3
D-13	664	**16.7**	0.77	8.0	284	15.5
WHSV:						
D-15	666	13.6	**0.24**	6.1	281	18.3
D-19	665	13.7	**0.43**	7.9	284	15.9
D-11	665	13.8	**0.77**	8.5	287	15.2
D-25	662	13.6	**1.38**	8.9	295	14.0

Table 4.6

Yield of Distillate Fractions Produced in Bitumen Hydrotreating over an HDM Catalyst

Run I.D.	Temperature [K]	Pressure [MPa]	WHSV [h^{-1}]	C_1-C_4 [wt%]	C_5-478 K [wt%]	478-616 K [wt%]	616-811 K [wt%]	> 811K [wt%]	H_2 consumption [l/l]
Feed Composition				-	1.9	6.0	34.3	57.8	
Temperature:									
D-29	**620**	13.7	0.77	1.5	0.7	6.7	38.8	52.2	6
D-18	**642**	13.6	0.77	1.2	4.8	7.2	40.9	46.5	24
D-20	**653**	13.6	0.77	0.8	1.1	8.7	44.0	44.1	31
D-11	**665**	13.8	0.77	1.3	1.5	10.2	48.2	38.1	41
D-23	**673**	13.7	0.76	2.0	1.5	13.1	51.1	31.9	47
D-27	**685**	13.7	0.76	3.3	5.3	15.4	49.5	25.9	55
Pressure:									
D-17	665	**11.3**	0.77	1.7	5.0	9.4	43.7	38.9	28
D-11	665	**13.8**	0.77	1.3	1.5	10.2	48.2	38.1	41
D-21	665	**15.3**	0.76	1.2	4.0	9.7	48.0	36.8	43
D-13	664	**16.7**	0.77	1.3	6.2	10.7	45.6	34.7	66
WHSV:									
D-15	666	13.6	**0.24**	3.8	3.1	15.2	52.6	23.5	75
D-19	665	13.7	**0.43**	2.4	1.5	10.7	52.5	32.5	48
D-11	665	13.8	**0.77**	1.3	1.5	10.2	48.2	38.1	41
D-25	662	13.6	**1.38**	0.9	1.8	8.4	42.1	46.5	31

Upflow Mode Operation

Laboratory-scale catalytic reactors are frequently used to simulate commercial reactors. However, plug-flow operation is difficult to attain in the trickle-bed mode due to low length-to-diameter ratios of laboratory-scale reactors [89,95,99,150,151]. The reactor diameter used in this study was 2.54 cm and the catalyst was confined to a section of the reactor 30.4 cm long which gave a reactor diameter-to-catalyst particle diameter ratio of 16. It has been reported [89] that hydrodynamic problems associated with liquid distribution and wall flow decrease with an increase in the reactor diameter-to-particle diameter ratio above 10. A reactor diameter-to-particle diameter ratio of 16 would have been expected to have been sufficient to ensure minimal liquid distribution and wall effects for intermediate petroleum feedstocks (°API gravity > 20 °API). However, heavy oils (°API gravity > 10 °API; μ < 10,000 cps) and bitumens (°API gravity < 10 °API; μ > 10,000 cps) may exhibit coning and incomplete wetting of the catalyst even when the reactor diameter-to-particle diameter is 16. The criterion for minimum reactor length which minimizes axial dispersion in shallow, trickle-bed reactors was developed by Mears [108] and is given by Equation (4-1):

$$\frac{L}{d_s} > \frac{20n}{Bo} \ln \frac{C_f}{C_p} \qquad (4\text{-}1)$$

where L is the length of reactor bed, d_s is the equivalent spherical diameter of the catalyst particles, n is the order of reaction, Bo is the Bodenstein number or the liquid particle Peclet number, C_f is the feed concentration, and C_p is the product concentration. The Mears criterion [108] was used to assess the feasibility of operating the laboratory reactor used to study the hydrotreating of bitumen and

bitumen-derived liquid in the trickle-bed mode. Even though the criterion was satisfied for downflow or trickle bed operation, the low superficial mass velocities in the reactor may lead to inefficient catalyst utilization, especially for shaped catalysts [110]. Wind et al. [110] proposed that reversing the direction of liquid flow from downflow to upflow in a laboratory-scale reactor would improve catalyst utilization comparable to that attained in commercial units. It also was shown that the utilization of shaped catalysts would vary less in the upflow than in the downflow mode owing to improved wetting, reduced channelling and reduced back-mixing. Thus, the upflow mode which improves catalyst utilization, eliminates channelling and simulates commercial downflow reactor behavior was chosen for these studies.

Plug-Flow Equations

The rate expressions for hydrodenitrogenation, hydrodesulfurization and hydrodemetallation contain a power-law dependence on hydrogen partial pressure. It was, therefore, necessary to estimate the hydrogen partial pressure at the various process operating conditions.

Vapor phase hydrogen fugacities were determined using the Grayson-Streed method [152]. Flash calculations were performed using the Process Simulation Program developed by Simulation Sciences Inc. [153] and parameters calculated by Longstaff [18,146,147] and Hwang [154]. The calculations indicated that vapor phase was predominately hydrogen (Table 4.7) at the reaction conditions employed to hydrotreat the Whiterocks bitumen and bitumen-derived liquid. This is mainly due to the H_2/oil ratio (=890 m^3/m^3; 5,000 scf/bbl) used in this study.

Table 4.7

Influence of Operating Variables on Vapor Composition during Bitumen Hydrotreating over an HDM Catalyst

Run I.D.	Temperature [K]	Pressure [MPa]	WHSV [h^{-1}]	Vapor [mol%]	Liquid [mol%]	H_2 [mol% in vapor]
Temperature:						
D-29	**620**	13.7	0.77	94.6	5.4	98.8
D-18	**642**	13.6	0.77	94.6	5.4	97.3
D-20	**653**	13.6	0.77	94.3	5.7	98.2
D-11	**665**	13.8	0.77	94.1	5.9	98.2
D-23	**673**	13.7	0.76	94.2	5.8	98.0
D-27	**685**	13.7	0.76	94.4	5.6	96.3
Pressure:						
D-17	665	**11.3**	0.77	95.0	5.0	96.2
D-11	665	**13.8**	0.77	94.1	5.9	98.2
D-21	665	**15.3**	0.76	93.9	6.1	97.6
D-13	664	**16.7**	0.77	93.7	6.3	96.0
WHSV:						
D-15	666	13.6	**0.24**	94.2	5.8	96.4
D-19	665	13.7	**0.43**	94.0	6.0	98.0
D-11	665	13.8	**0.77**	94.1	5.9	98.2
D-25	662	13.6	**1.38**	94.3	5.7	98.6

Evaluation of Plug-Flow Assumption

The plug-flow assumption for the upflow operating mode was evaluated using two models; one assumes plug-flow and a second accounts for possible deviations from plug-flow [95,99].

Plug-Flow nth Order Kinetics

The rate expressions for heteroatom removal contain a power-law dependence on hydrogen partial pressure. The rate expression for nth order plug-flow is given by:

$$\frac{dC_i}{d\tau} = -k\, C_i^n P_{H_2}^{\beta} \qquad (4\text{-}2)$$

where C_i is an appropriate representation of the bitumen or bitumen-derived liquid concentration, k is the apparent rate constant, n is a reaction order, P_{H_2} is hydrogen partial pressure and β is a power term for hydrogen partial pressure. The solution of the plug-flow equation for nth order kinetics is given by:

$$\ln\frac{C_{i,feed}}{C_{i,prod}} = \frac{k\, P_{H_2}^{\beta}}{WHSV} \qquad \text{for } n=1 \qquad (4\text{-}3)$$

$$\frac{1}{C_{i,prod}^{n-1}} - \frac{1}{C_{i,feed}^{n-1}} = \frac{(n-1)\, k\, P_{H_2}^{\beta}}{WHSV} \qquad \text{for } n\neq 1 \qquad (4\text{-}4)$$

where $k = k_o \exp(-\frac{E}{RT})$, n is reaction order, $C_{i,feed}$ is the feed concentration, $C_{i,prod}$ is the product concentration, k_o is the pre-exponential factor, E is the apparent activation energy and R is the Universal gas constant.

Nonplug-Flow nth Order Kinetics

Yui and Sanford [95,99] recommended that the WHSV should be replaced by $WHSV^{\alpha}$ to compensate for deviations from plug-flow behavior. These deviation arise because of the lower superficial mass velocities achieved in the laboratory-scale reactors relative to those obtained in the commercial reactor when it was operated in a trickle-bed mode. The integrated equation for nonplug-flow, nth order kinetics is given by

$$\ln\frac{C_{l,feed}}{C_{l,prod}} = \frac{k\,P_{H_2}^{\beta}}{WHSV^{\alpha}} \qquad \text{for } n=1 \qquad (4\text{-}5)$$

$$\frac{1}{C_{l,prod}^{n-1}} - \frac{1}{C_{l,feed}^{n-1}} = \frac{(n-1)\,k\,P_{H_2}^{\beta}}{WHSV^{\alpha}} \qquad \text{for } n\neq 1 \qquad (4\text{-}6)$$

where $k = k_o \exp(-\frac{E}{RT})$.

The kinetic parameters were determined by a nonlinear regression technique which used the Levenberg-Marquardt method [155]. Subroutines from the MINPACK package were used [156]. The results, presented in Table 4.8, indicated that the exponent (α) on the WHSV was very close to 1 for the hydrotreating of bitumen and bitumen-derived liquid over both HDM and HDN catalyst when the reactor was operated in the upflow mode. Thus, the plug-flow equation was valid for use in this study. The fact that the value of α was slightly greater than one is attributed to experimental error.

Furthermore, when the terms on the left-hand side in Equations (4-3) through (4-6) are plotted against (1/WHSV) or $1/(WHSV)^{\alpha}$, the resulting straight lines should pass through the origins if the plug-flow assumption is valid. The plots for heteroatom removal for the bitumen-derived liquid and the bitumen (Figure 4.3) demonstrate that the fixed-bed catalytic reactor used in this study

Table 4.8

Values of the Power α on the Space Velocity to Account for Deviations from Plug-Flow Operation

	Empirical Power Term for Space Velocity
Bitumen Hydrotreating over an HDM Catalyst	
Hydrodenitrogenation	0.99
Hydrodesulfurization	1.00
Residuum conversion	0.97
Hydrodemetallation (Ni Removal)	0.92
Bitumen Hydrotreating over an HDN Catalyst	
Hydrodenitrogenation	1.05
Hydrodesulfurization	1.08
Residuum conversion	0.97
Bitumen-Derived Liquid Hydrotreating over an HDN Catalyst	
Hydrodenitrogenation	0.95
Hydrodesulfurization	1.01
Residuum conversion	0.98

Figure 4.3

Test of Plug-Flow Assumption for HDN and HDS of Bitumen and Bitumen-Derived Liquid over an HDN Catalyst

Hydrodenitrogenation of Bitumen-Derived Liquid over an HDN catalyst

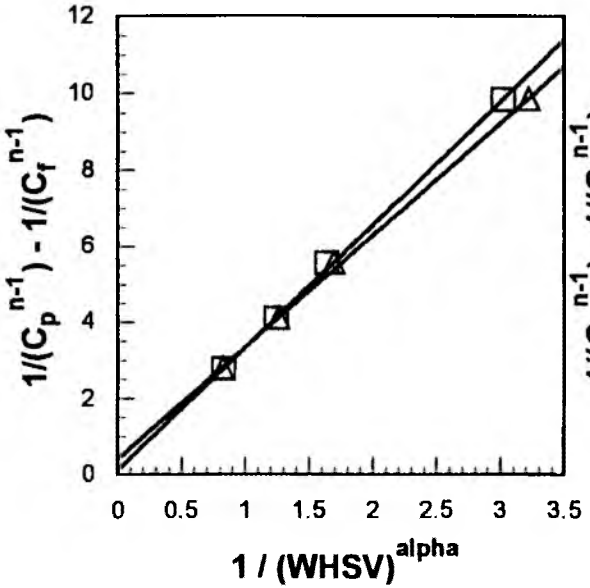

Hydrodesulfurization of Bitumen over an HDN catalyst

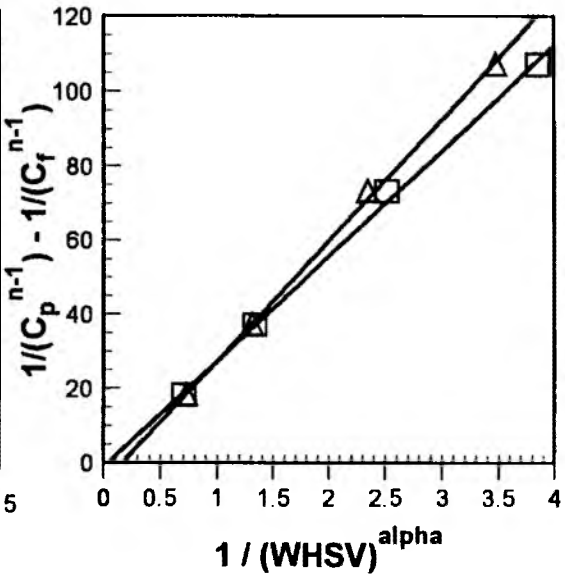

Nickel Removal of Bitumen over an HDM catalyst

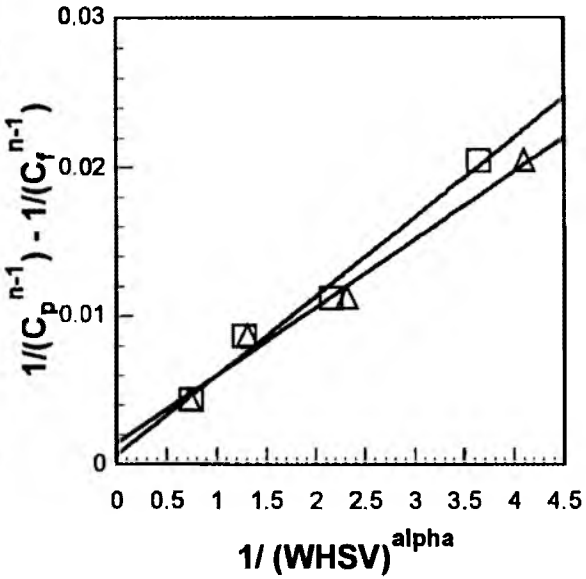

△ Plug-Flow Approach (nth order)

□ Nonplug Flow Approach (nth order)

operated under plug-flow conditions when the feed was introduced in upflow mode. Thus, the plug-flow assumption is valid for the upflow operating mode in the laboratory-scale reactor and the plug-flow equation (4-3) was used to analyze the data.

Alternative Kinetic Representation

Nickel removal from bitumen over an HDM catalyst and HDS for bitumen and HDN for bitumen-derived liquid over an HDN catalyst exhibited reaction orders greater than one when the data was analyzed by an nth order kinetic approach. Also, residuum conversion for bitumen and bitumen-derived liquid [18,147] over both the HDM and HDN [18,146] catalysts were found to follow higher than first-order kinetics. This indicated that a range of reactivities for heteroatom and residuum compounds was being observed [157]. When a significant fraction of the heteroatomic and/or the residuum species are present in unreactive fractions such as asphaltenes, the removal and/or conversion kinetics can be represented by two parallel first-order reactions.

The basis of the alternative model is to assume that the feedstock consists of two reactive lumps or fractions; a facile fraction and a refractory fraction. The rate of removal or conversion of the refractory fraction is presumed to be considerably slower than that of the facile fraction. For the case of HDN of bitumen-derived liquid [18,147], this can be partly attributed to partial dehydrogenation of nitrogen containing compounds during bitumen pyrolysis. Therefore, the conversion or removal of species which gave an apparent order greater than unity was modeled by two parallel first-order reactions [158].

This model has been used to explain hydroprocessing kinetics [81,82, 159-161]. Richardson et al. [81] proposed that, although the desulfurization rate of different individual sulfur compounds follow first-order rate expressions, when

these compounds are simultaneously desulfurized the combined results provide an apparent second-order behavior. Oleck and Sherry [159] also reported a similar observation for the desulfurization of an atmospheric reduced Arabian Light crude oil. The desulfurization of nonasphaltenic sulfur compounds is extremely fast and that of asphaltenic sulfur compounds is slow. Both are first-order reactions and the whole may be regarded as a second-order reaction. Frye and Mosby [160] reported that the desulfurization data for three compounds found in a cycle oil feedstock were well organized by a first-order model. Therefore, residuum desulfurization can be considered to be a series of first-order reactions of decreasing rate constants such that the sequence of reactions leads to an apparent second-order dependence [161]. Richardson and Alley [81] suggested that the apparent order with respect to space-time depends on the ratio of the fastest and slowest reactions.

The reaction scheme is presented in equation (4-7).

$$\mathrm{A} \left| \begin{array}{ll} \mathrm{A_1} = \gamma\,\mathrm{A} & \xrightarrow{k_1} \mathrm{B} \\ \mathrm{A_2} = (1-\gamma)\,\mathrm{A} & \xrightarrow{k_2} \mathrm{B} \end{array} \right. \qquad (4\text{-}7)$$

where A_1 represents the facile portion of the heteroatom or residuum fraction in the feedstock and A_2 represents the refractory portion. The reaction scheme is written such that the apparent first-order rate constant k_1 is larger than the apparent first-order rate constant k_2. The parameter γ is the facile fraction of the heteroatom or residuum fraction which is more reactive and $1-\gamma$ is the refractory fraction which is less reactive. The integrated rate expression is given by Equation (4-8).

$$\frac{C_{i,prod}}{C_{i,feed}} = \gamma \exp\left[-\frac{k_1 P_{H_2}^{\beta}}{WHSV^{\alpha}}\right] + (1-\gamma)\exp\left[-\frac{k_2 P_{H_2}^{\beta}}{WHSV^{\alpha}}\right] \qquad (4\text{-}8)$$

where the rate constants are given by the Arrhenius equation

$$k_1 = k_{1o} \exp\left(-\frac{E_1}{RT}\right)$$

$$k_2 = k_{2o} \exp\left(-\frac{E_2}{RT}\right)$$

and k_{1o} and E_1 and k_{2o} and E_2 are the pre-exponential factors and apparent activation energies for facile and refractory heteroatom or residuum fractions, respectively.

The kinetic parameters determined for the two-parallel first-order reactions scheme for HDS, HDN, HDM and residuum conversion are presented in Table 4.9. The objective function [162,163] (OF) which represented the minimization of the function defined in Equation (4-9) was computed.

$$OF = \sum_{i=1}^{n} \left| C_p^{exp} - C_p^{model} \right|^2 \qquad (4\text{-}9)$$

The values for objective function indicated that the two-parallel first-order reactions provided a reasonable representation of the data. Experimental and calculated values for Ni removal over an HDM catalyst for both the nth order and two parallel first-order reactions representation are compared in Figure 4.4.

Table 4.9

Apparent Kinetic Parameters for the Alternative Kinetic Representation

	Bitumen Hydrotreating over an HDM Catalyst		Bitumen Hydrotreating over an HDN Catalyst [18,146]	Bitumen-Derived Liquid Hydrotreating over an HDN Catalyst [18,147]
	HDM	Residuum Conversion	HDS	HDN
γ	0.67	0.74	0.7	0.8
k_{10}	9.8×10^{4}	1.3×10^{12}	4.3×10^{11}	3.8×10^{12}
k_{20}	8.5×10^{5}	7.9×10^{8}	6.3×10^{12}	1.6×10^{11}
E_1 [kJ/mol]	94	124	142	160
E_2 [kJ/mol]	81	177	170	158
OF	6.0×10^{-6}	12.8	1.4×10^{-4}	1.2×10^{-3}

Figure 4.4

Observed versus Predicted Nickel Content of the Total Liquid Product Produced during Bitumen Hydrotreating over an HDM Catalyst

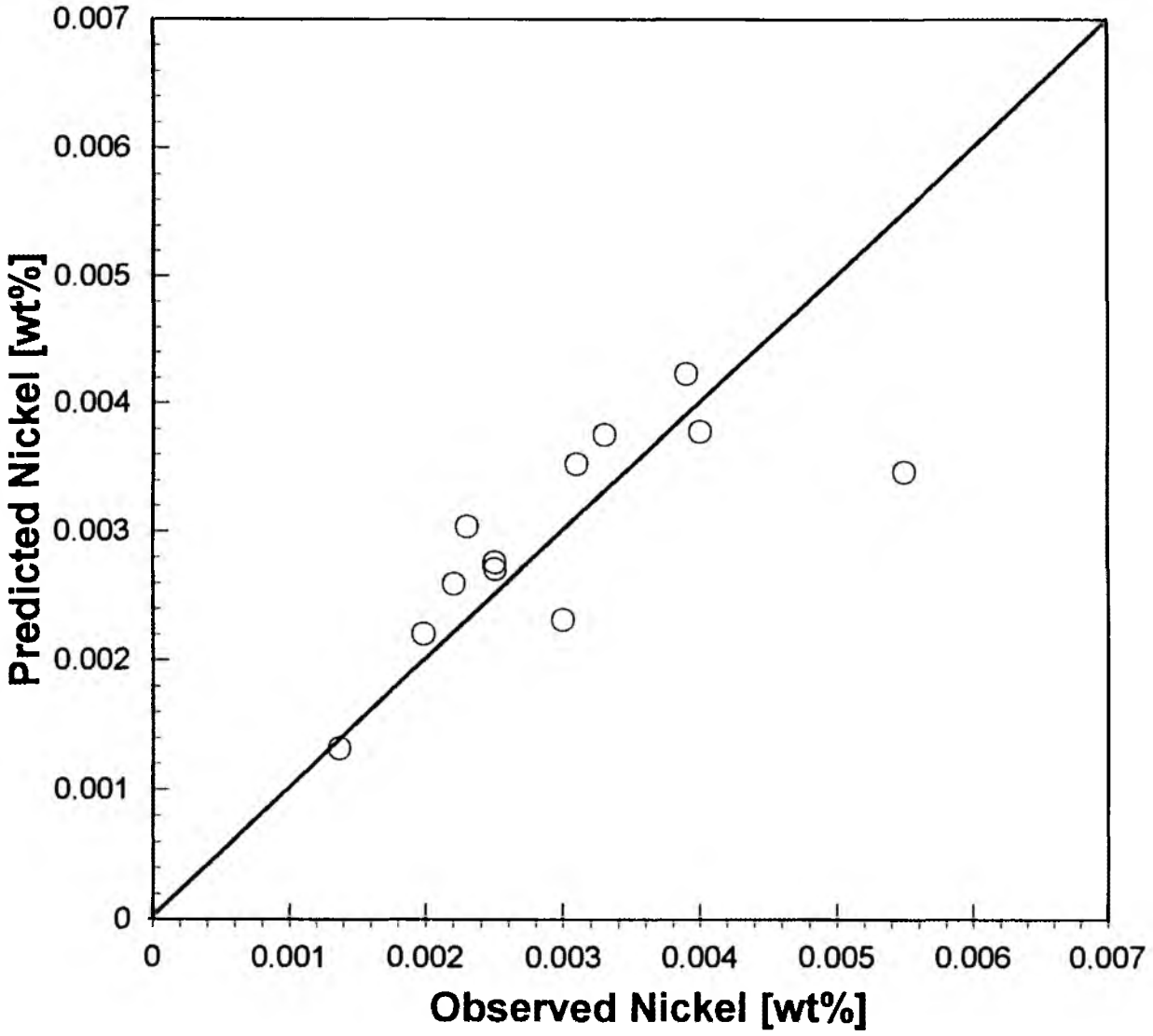
0.007
0.006
0.005
0.004
0.003
0.002
0.001
0
Predicted Nickel [wt%]
0
0.001
0.002
0.003
0.004
0.005
0.006
0.007
Observed Nickel [wt%]

Computation of Kinetic Parameters

Two methods were used to obtain the kinetic parameters for hydrotreating bitumen and bitumen-derived liquid. The first was a conventional kinetic analysis using a graphical method (Longstaff et al. [18,147]) and the other was a nonlinear regression analysis. The conventional analysis consisted of fixing two operating variables, and changing one variable to obtain data from which the required kinetic parameters were calculated. This method clearly detects the effect of each operating variable; however, many experiments are required since two variables are fixed in each set of experiments. The kinetic parameters for the general plug-flow equations were determined simultaneously by nonlinear regression analysis thus the need to fix two variables at a time was avoided. However, the effect of each variable is not clearly demonstrated. In addition, due to a limited number of data points and the relatively large number of parameters which must be simultaneously determined, the final results may be misleading.

The kinetic parameters for hydrodenitrogenation determined by conventional and nonlinear regression kinetic analyses for HDN of bitumen and bitumen-derived liquid are presented in Table 4.10.

Process Variable Studies

The two most important reactions taking place in bitumen hydrotreating are thermal cracking to lighter products and catalytic hydrogenation related to the removal of heteroatoms [12,164]. Both of these reactions are dependent upon the residence time of the feedstock in the reactor and/or the contact time, the temperature of the reaction and the hydrogen partial pressure in the reactor.

Table 4.10

Comparison of Kinetic Parameters for Hydrodenitrogenation

	Bitumen HDN over an HDM Catalyst		Bitumen HDN over an HDN Catalyst [18,146]		Bitumen-Derived Liquid HDN over an HDN Catalyst [18,147]	
	Conventional	Nonlinear	Conventional	Nonlinear	Conventional	Nonlinear
n	1.0	1.2	1.0	0.8	1.5	1.7
α	1.0	0.99	1.0	1.05	1.0	0.95
β	1.1	1.5	0.7	0.8	0.6	1.1
k_o	2.8×10^{4}	7.3×10^{4}	1.3×10^{7}	4.5×10^{4}	3.4×10^{9}	8.5×10^{6}
E_a [kJ/mol]	71	98	92	75	113	96
OF	7.7×10^{-2}	5.4×10^{-3}	1.5×10^{-1}	4.3×10^{-2}	1.5×10^{-1}	2.3×10^{-3}

The primary process variables investigated in this study were the liquid hourly space velocity, the reactor temperature and the hydrogen partial pressure.

Space Velocity

The space velocity experiments were conducted at a fixed reaction temperature (664 K) and pressure (13.7 MPa) and the effect of space velocity on product distribution and yields is presented in Table 4.11. The effect of space velocity plays a important role in bitumen hydrotreating over an HDM catalyst. In the space velocity ranges studied here, heteroatom removal and residuum conversion increased significantly at lower space velocities. Abdul-Halim et al. [165] reported that LHSV exerted a greater influence on the sulfur removal than temperature at relatively low temperatures. Tables 4.11 and 4.12 represent that the increments of hydrogen consumption from 31 to 75 m^3/m^3 made 29% of nitrogen removal possible. Also, residence time increments by a factor of six led to 77% of sulfur and 82% nickel removals over a low activity HDM catalyst. Decreasing trends were shown in Conradson carbon residue conversion as WHSV decreased. At 0.24 h^{-1} WHSV, there was about 43% reduction in CCR during hydrotreating.

The product distribution and yields are presented in Figure 4.5. The scatter in the naphtha yields may have been related to the loss of this fraction when the total liquid product samples were stripped of NH_3 and H_2S prior to elemental analysis. Residuum content is significantly decreased as the residence time of the liquid increased; about 61% residuum conversion was achieved at 0.24 h^{-1} WHSV. The gas, naphtha and distillate fractions monotonically increased with increasing residence time. The gas-oil yield exhibited a maximum at a residence time of 2.3 hours. The maximum in gas-oil

Table 4.11

Effect of WHSV on Product Distribution and Yields

at 664 K (735 °F) and 13.7 MPa (1980 psia)

Run No.	D-15	D-19	D-11	D-25
Process operating conditions				
WHSV, h^{-1}	0.24	0.43	0.77	1.38
τ, h	4.1	2.3	1.3	0.7
Temperature, K	666	665	665	662
Pressure, MPa	13.6	13.7	13.8	13.6
API gravity	18.3	15.9	15.2	14.0
Specific gravity	0.945	0.960	0.965	0.972
Pour Point, K	281	284	287	295
CCR, wt%	6.1	7.9	8.5	8.9
H_2 consumption, m^3/m^3	75	48	41	31
Elemental Analysis				
C, wt%	86.2	85.4	85.5	85.6
H, wt%	12.2	11.5	11.8	11.2
N, wt%	0.96	1.20	1.15	1.20
S, wt%	0.08	0.17	0.20	0.29
Ni, ppm	14	20	23	33
H/C atomic ratio	1.7	1.6	1.7	1.6
Product yield distribution				
Volatility, wt%	76.5	67.5	61.9	53.5
C_1-C_4, wt%	3.8	2.4	1.3	0.9
C_5-478 K, wt%	3.1	1.5	1.5	1.8
478-616 K, wt%	15.2	10.7	10.2	8.4
616-811 K, wt%	52.6	52.5	48.2	42.1
> 811 K, wt%	23.5	32.5	38.1	46.5
Liquid yield, vol %	98.4	100.4	99.7	99.4

Table 4.12

Heteroatom Removal and Residuum and Conradson Carbon Conversions of the Bitumen over a Commercial HDM Catalyst

Run I.D.	Temperature [K]	Pressure [MPa]	WHSV [h^{-1}]	N [%]	S [%]	Ni [%]	Residuum [%]	Conradson Carbon Residue [%]
Temperature:								
D-29	**620**	13.7	0.77	5.6	-	46.4	10.6	1.7
D-18	**642**	13.6	0.77	7.4	29.2	45.1	20.6	9.0
D-20	**653**	13.6	0.77	2.3	18.4	23.6	23.6	9.6
D-11	**665**	13.8	0.77	11.9	39.8	68.4	34.9	17.8
D-23	**673**	13.7	0.76	14.1	43.5	66.1	46.2	22.7
D-27	**685**	13.7	0.76	16.9	35.1	59.4	56.4	27.5
Pressure:								
D-17	665	**11.3**	0.77	8.2	37.2	57.9	34.2	17.7
D-11	665	**13.8**	0.77	11.9	39.8	68.4	34.9	17.8
D-21	665	**15.3**	0.76	10.7	44.0	65.5	36.9	18.5
D-13	664	**16.7**	0.77	12.8	41.4	69.9	40.9	23.3
WHSV:								
D-15	666	13.6	**0.24**	29.0	77.4	81.8	61.2	43.4
D-19	665	13.7	**0.43**	10.8	50.5	73.6	46.1	26.1
D-11	665	13.8	**0.77**	11.9	39.8	68.4	34.9	17.8
D-25	662	13.6	**1.38**	7.3	14.9	54.4	19.9	13.0

Figure 4.5

Effect of WHSV on Product Distribution and Yields

at 664 K (735°F) and 13.7 MPa (1980 psia)

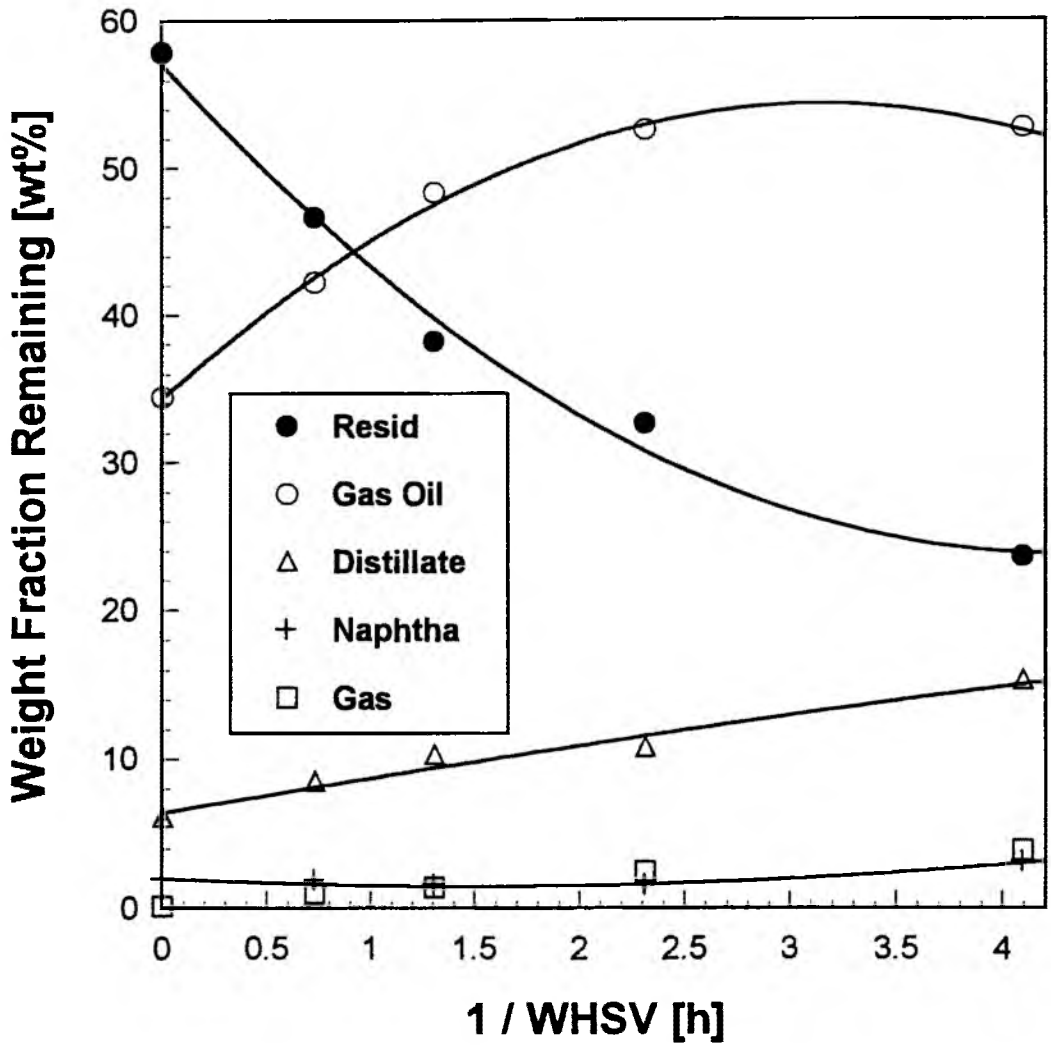
Weight Fraction Remaining [wt%]
60
50
40
30
20
10
0
0
0.5
1
1.5
2
2.5
3
3.5
4
1 / WHSV [h]
Resid
Gas Oil
Distillate
Naphtha
Gas

yields has been reported by other workers [18,146,164] and implies that gas-oil is formed from residuum and subsequently cracks to produce distillate, naphtha and gas.

The effect of WHSV on the conversion of nitrogen and sulfur at 664 K and 13.7 MPa is shown in Figure 4.6. The plots of the natural logarithm of the fractions of nitrogen and sulfur remaining versus residence time (reciprocal of space velocity) were straight lines and passed through 1 on the log scale y-axis. This indicated that both HDN and HDS removal from bitumen over an HDM catalyst followed first-order kinetics. Also, the differences in the slopes of Figure 4.6 indicates that sulfur removal from the bitumen is easier than nitrogen removal.

First-order nitrogen removal kinetics over an HDN catalyst has been reported previously [15,95,99]. Yui and his coworkers [95,99] showed first-order kinetics for HDN of bitumen-derived coker and hydrocracker heavy gas-oils and Riley [15] reported first-order nitrogen dependence for HDN of heavy oils. The consistent observation of first-order kinetics implies a uniform refractoriness for nitrogen compounds in the bitumens; bitumen-derived liquids, and heavy oils studied.

Hydrotreating studies with different petroleum residua using Co-Mo-alumina catalysts have shown that the hydrodesulfurization reaction may follow apparent first-order [166], pseudo-second order [167] or second-order [168] kinetics with respect to sulfur compounds. Higher than first-order or second-order kinetics for HDS in heavy oil hydrotreating is supported by the majority of experimental results [73]. HDS of Syncrude bitumen-derived coker and hydrocracker heavy gas-oil obeyed an apparent 1.5 order [95,99] over a NiMo catalyst in a trickle-bed reactor. The ranges of the reaction conditions were 623-673 K, 0.7-1.5 h^{-1} LHSV and 7-11 MPa. Second-order kinetics were reported for

Figure 4.6

First-Order Kinetic Plots for Nitrogen and Sulfur Removal over an HDM Catalyst at 664 K (735°F) and 13.7 MPa (1980 psia)

HDN Reaction Follows First Order Kinetics Over an HDM Catalyst

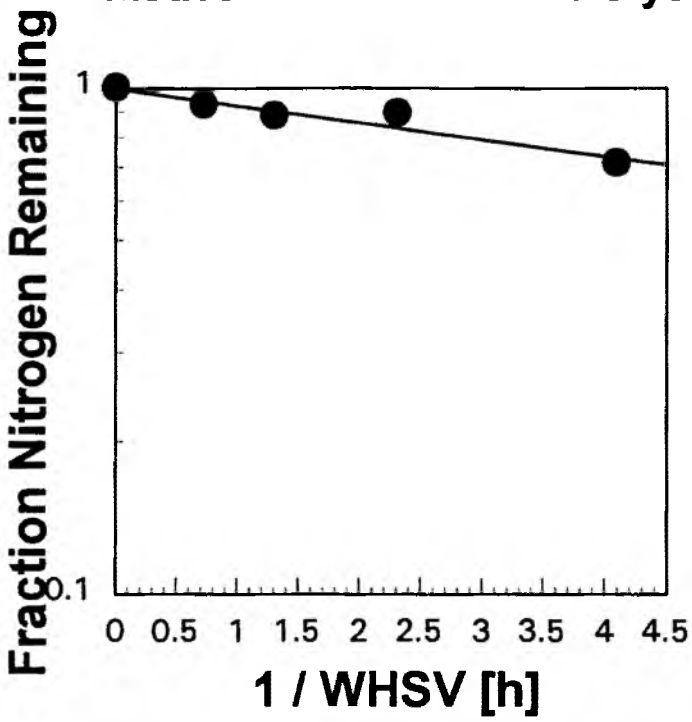

HDS Reaction Follows First Order Kinetics Over an HDM Catalyst

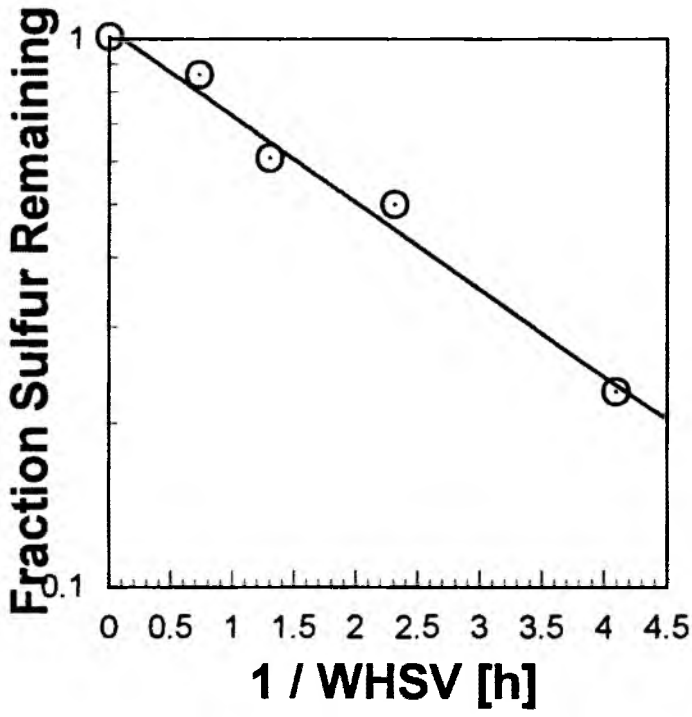

HDS in coal conversion studies [169] and for HDS in petroleum residuum studies [170-172]. Abdul-Halim [165] used second-order kinetics to organize sulfur removal data for deasphalted oil and Wei et al. [158] used two parallel first-order reactions to obtain apparent overall second-order dependence for HDS.

As indicated earlier, it was found that bitumen HDS over an HDM catalyst followed first-order kinetics. The first-order behavior may be related to the naphthenic nature of the Uinta Basin bitumens compared with conventional heavy oils. George [173] reported that HDS and HDN of feedstocks derived from coprocessing of heavy oil and coal (24 °API; 703 K) followed irreversible first-order kinetics at 673 K, 5 h^{-1} LHSV, and 13.3 MPa over a commercial NiMo catalyst. Billon et al. [166] also obtained the first-order kinetics for the HDS of petroleum residuum over a CoMo catalyst.

In contrast with nitrogen and sulfur removal, nickel removal and residuum conversion of Whiterocks bitumen over an HDM catalyst did not follow first-order kinetics. Nickel removal and residuum conversion followed higher than first-order kinetics overall. Oleck and Sherry [159] reported that a good fit of the reaction rate data was obtained with second-order kinetics for nickel and vanadium removal from Lagomedio (Venezuelan) atmospheric residuum over $CoMo/Al_2O_3$ catalysts.

A first-order kinetic plot (Figure 4.7) for nickel removal indicated two distinct regions. This implies that there may be two different classes of nickel species in the feed. One class of nickel reacts considerably faster than the other class of nickel compounds and each compounds follow first-order behavior. Because both classes of compounds react simultaneously apparent overall second-order behavior would be expected. Thus, two parallel first-order reactions involving the two classes of nickel compounds (or lumps) was used as

Figure 4.7

First-Order Kinetic Plot for Nickel Removal over an HDM Catalyst at 664 K (735°F) and 13.7 MPa (1980 psia)

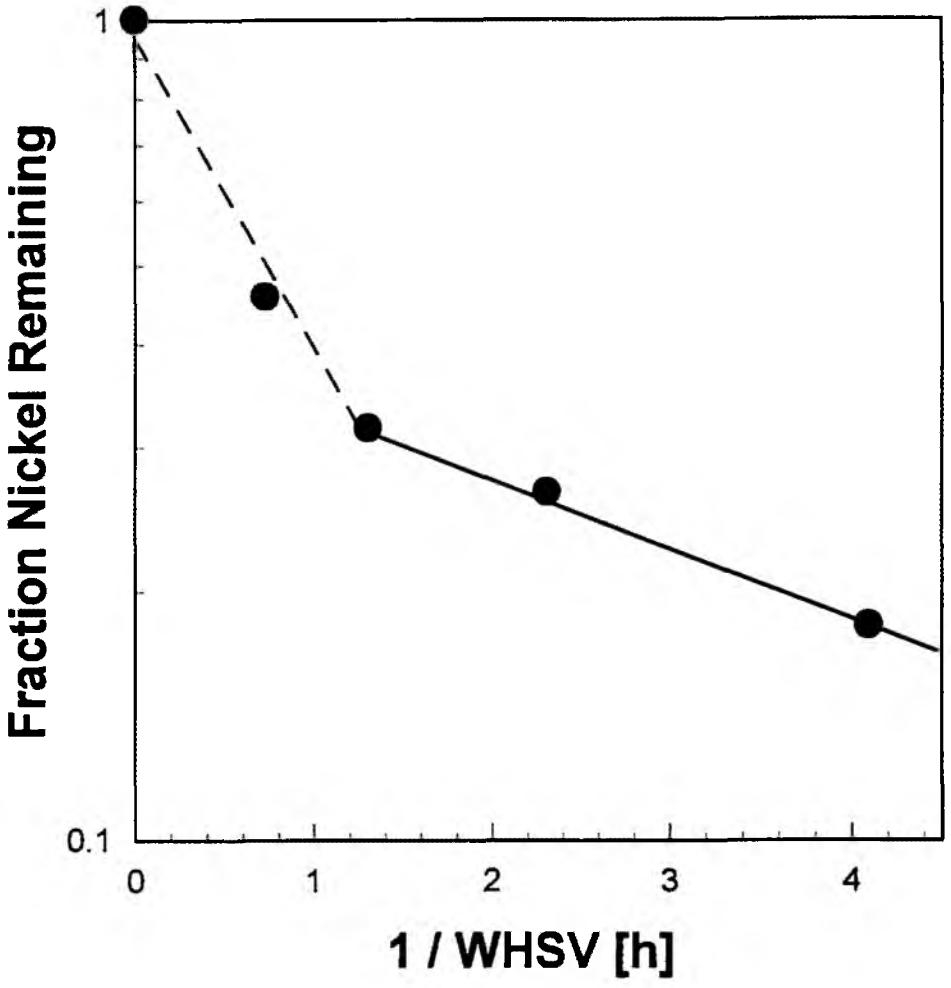
Fraction Nickel Remaining
1
0.1
0
1
2
3
4
1 / WHSV [h]

an alternative scheme to represent nickel removal. This representation has been employed by several researchers for analyzing HDM data [158,174].

The simultaneous occurrence of several first-order metal removal reactions with different rates can lead to an apparent reaction order greater than unity just as in hydrodesulfurization [175]. Metal profiles indicating the presence of "easy" and "hard" to remove metal species have been reported for V [176]. Metalloporphyrins, metal species sometimes referred to as "easy" metals, are readily removed resulting in sharp metal gradients near the exterior surface of the pellets at the reactor entrance. The more refractory, "hard" compounds yield more uniform profiles. The liquid phase in the vicinity of the reactor outlet is depleted of the "easy" Ni species and the relatively uniform metal-deposition profiles reflect deposition from the refractory or "hard" Ni compounds. Galiasso et al. [132] reported that pure metalloporphyrins in clean systems are up to 10 times more reactive than naturally occurring metalloporphyrins in petroleum resins and 100 to 500 times more reactive than nickel and vanadyl compounds in Kuwait atmospheric residuum [131].

The kinetic parameter estimation results indicated that the refractory fractions of residuum and nickel were 0.74 and 0.67, respectively. The rate constants at 664 K indicate that the facile residuum and nickel fractions are 7 and 117 times more reactive than those in refractory fractions, respectively. This large difference in rate constants resulted in the apparent higher than first-order kinetics for nickel removal and residuum conversion over an HDM catalyst, even though the refractory nickel and residuum fractions were more than twice the facile nickel and residuum fractions.

Temperature

The effect of temperature on product distribution and yields at a fixed space velocity (0.76 h^{-1} WHSV) and pressure (13.7 MPa) is presented in Table 4.13. Increasing temperature favorably affected the heteroatom removal reaction rates and promoted an increase in the thermal conversion of residuum. Sooter [177] observed that the desulfurization of raw anthracene oil, over a $CoMo/Al_2O_3$ catalyst at 6.9 MPa (1000 psig), increased from 48% to 84% when temperature was increased from 589 K (600°F) to 644 K (700°F). The low sulfur and nickel contents in the feed in this study account for the scatter in the sulfur and nickel data for the total liquid product. The API gravity increased from 12.7 to 18.0 °API as the temperature increased from 620 to 685 K. The increase in API gravity was accompanied by an increase in hydrogen consumption from 6 to 55 m^3/m^3. The levels of heteroatom removal and residuum conversion were lower in the temperature range studied than those obtained for the WHSV range studied. This may be due to the relatively low temperature range used in this study (620-685 K) compared to the temperature range used in commercial residuum hydroprocessing (620-713 K) [1,27]. Space velocity appears to exert a greater impact on heteroatom removal at low temperatures than the reactor temperature range itself. The nitrogen content decreased only by 17% , the sulfur content decreased by 44% and the nickel content decreased by 68%. The relatively high nickel removal is related to the selectivity of the HDM catalyst used in this study for demetallation and the low metals loading is reflected in heteroatom conversion. Residuum conversion at 685 K and 0.76 h^{-1} WHSV (56%) was comparable to that obtained at 665 K and 0.24 h^{-1} WHSV (61%). This indicated that temperature and residence time exhibit a synergism for residuum conversion whereas heteroatom removal over the HDM catalyst was more dependent on residence time than on temperature. The Conradson carbon

Table 4.13

Effect of Temperature on Product Distribution and Yields

at 0.76 h^{-1} WHSV and 13.7 MPa (1980 psia)

Run No.	D-29	D-18	D-20	D-11	D-23	D-27
Process operating conditions						
Temperature, K	620	642	653	665	673	685
WHSV, h^{-1}	0.77	0.77	0.77	0.77	0.76	0.76
τ, h	1.3	1.3	1.3	1.3	1.3	1.3
Pressure, MPa	13.7	13.6	13.6	13.8	13.7	13.7
API gravity	12.7	13.7	14.2	15.2	16.1	18.0
Specific gravity	0.981	0.975	0.972	0.965	0.959	0.947
Pour Point, K	315	307	299	287	283	279
CCR, wt%	10.1	9.4	9.2	8.5	8.1	7.6
H_2 Consumption, m^3/m^3	6	24	31	41	47	55
Elemental Analysis						
C, wt%	85.3	85.4	86.1	85.5	85.5	85.8
H, wt%	11.4	10.7	11.6	11.8	11.7	11.3
N, wt%	1.23	1.21	1.26	1.15	1.14	1.10
S, wt%	0.42	0.24	0.27	0.20	0.19	0.22
Ni, ppm	39	40	55	23	25	30
H/C atomic ratio	1.6	1.5	1.6	1.7	1.6	1.6
Product yield distribution						
Volatility, wt%	47.8	53.5	55.9	61.9	68.1	74.1
C_1-C_4, wt%	1.5	1.2	0.8	1.3	2.0	3.3
C_5-478 K, wt%	0.7	4.8	1.1	1.5	1.5	5.3
478-616 K, wt%	6.7	7.2	8.7	10.2	13.1	15.4
616-811 K, wt%	38.8	40.9	44.0	48.2	51.1	49.5
> 811 K, wt%	52.2	46.5	44.1	38.1	31.9	25.9
Liquid yield, vol %	97.4	99.5	99.4	99.7	99.5	97.3

residue shows about 28% removal at 685 K and the pour point decreased significantly as the reaction temperature increased.

The product distribution and yields are presented in Figure 4.8. The scatter in the C_1-C_4 gas yields were related to the small amount of gas produced during hydrotreating over the low activity HDM catalyst. The naphtha, distillate, and gas-oil yields increased and the residuum content decreased as the reaction temperature increased. The scatter in the naphtha yields may be related to the NH_3 and H_2S stripping procedure described in the experimental section. A maximum in the gas-oil yield was not observed as the temperature increased; however, it is expected that there would be a temperature above 685 K at which the rate of gas-oil conversion to lighter fractions would exceed the rate of residuum conversion to gas-oil.

The apparent activation energy is a measure of the response of the rate constant to temperature. The effect of temperature on the rate constant for nickel and residuum conversion over an HDM catalyst is presented in Figure 4.9. The apparent activation energies were 98 kJ/mol for HDN and 91 kJ/mol for HDS for bitumen hydrotreating over an HDM catalyst. The activation energies of both HDN and HDS suggest that HDN and HDS for this feedstock over an HDM catalyst were not limited by pore diffusion. The activation energy for CCR removal was 156 kJ/mol which may reflect the significance of thermal conversion on CCR removal. The activation energy for HDN (98 kJ/mol) was comparable to literature values [95,99].

Yui and Sanford [99] reported that the apparent activation energies for HDN of coker HGO and hydrocracker HGO were 96 kJ/mol and 75 kJ/mol, respectively. Diaz-Real [178] reported an apparent activation energy of 104 kJ/mol for HDN of a bitumen-derived heavy gas-oil over a NiMo zeolite based

Figure 4.8

Effect of Temperature on Product Distribution and Yields

at 0.76 h^{-1} WHSV and 13.7 MPa (1980 psia)

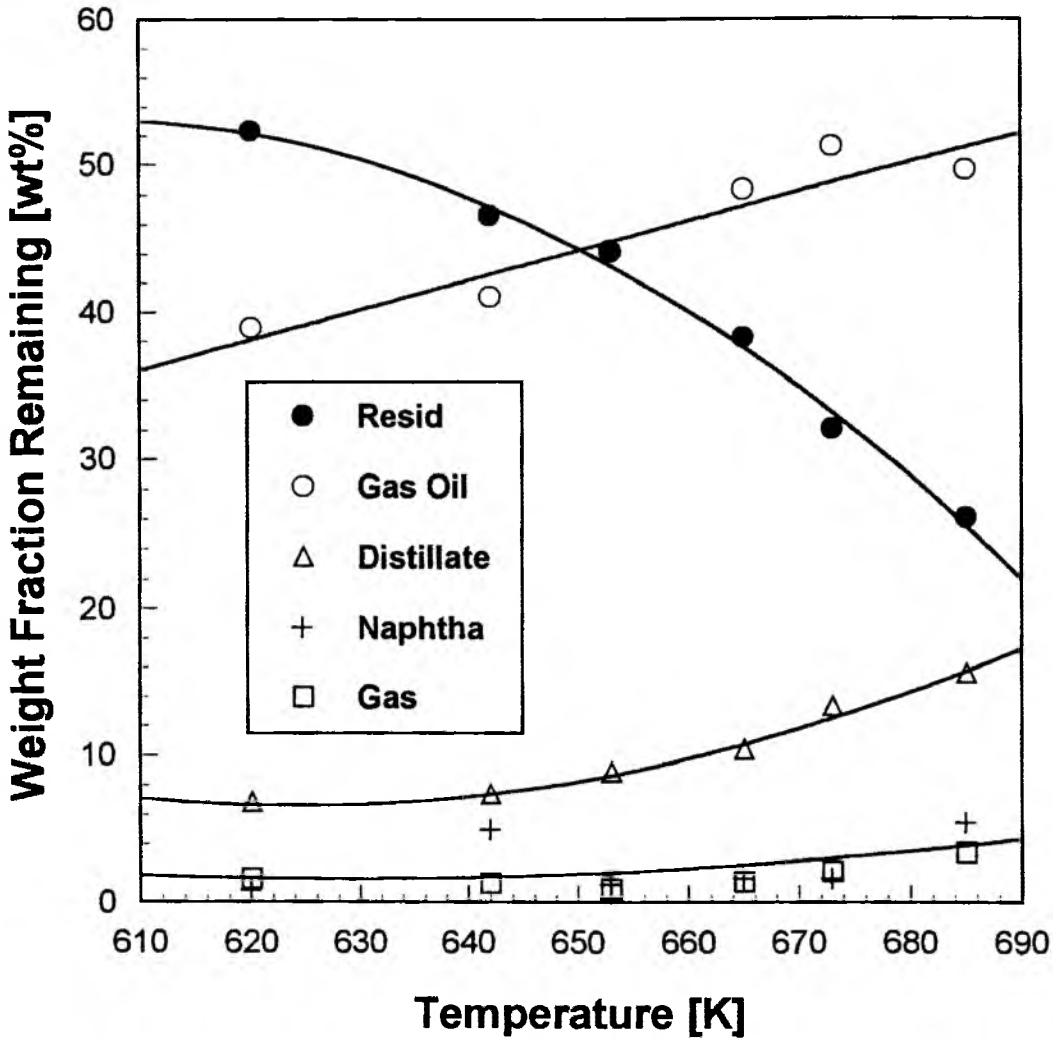
Weight Fraction Remaining [wt%]
60
50
40
30
20
10
0
610
620
630
640
650
660
670
680
690
Temperature [K]
Resid
Gas Oil
Distillate
Naphtha
Gas

Figure 4.9

Arrhenius Plots for Residuum Conversion and Nickel Removal over an HDM Catalyst at 0.76 h^{-1} WHSV and 13.7 MPa (1980 psia)

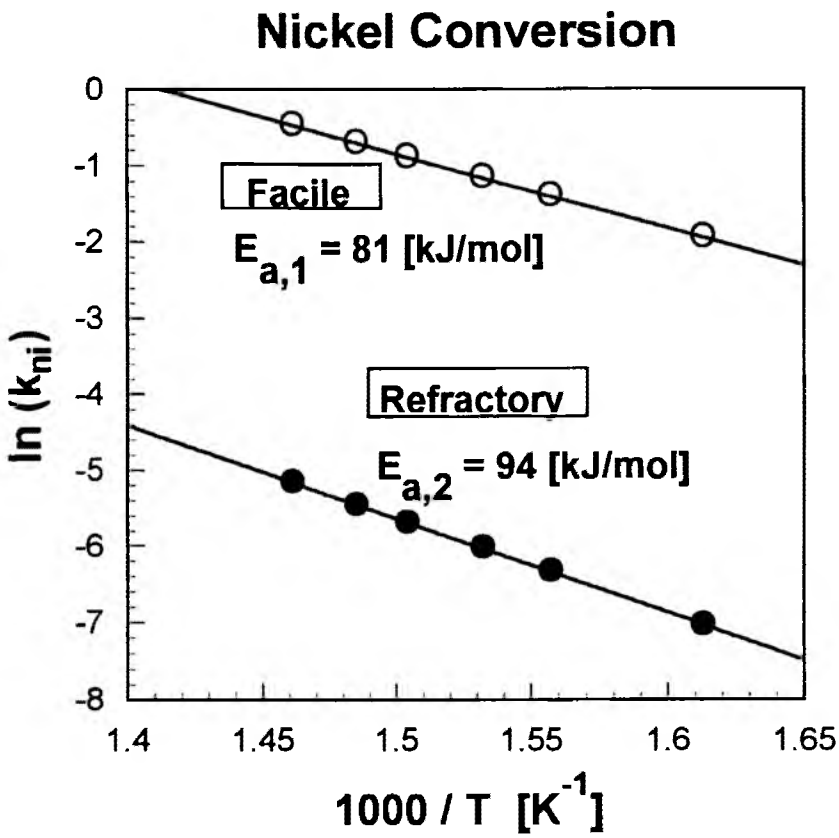
Nickel Conversion
0
-1
-2
-3
-4
-5
-6
-7
-8
ln (k_ni)
Facile
E_a,1 = 81 [kJ/mol]
Refractory
E_a,2 = 94 [kJ/mol]
1.4
1.45
1.5
1.55
1.6
1.65
1000 / T [K^-1]

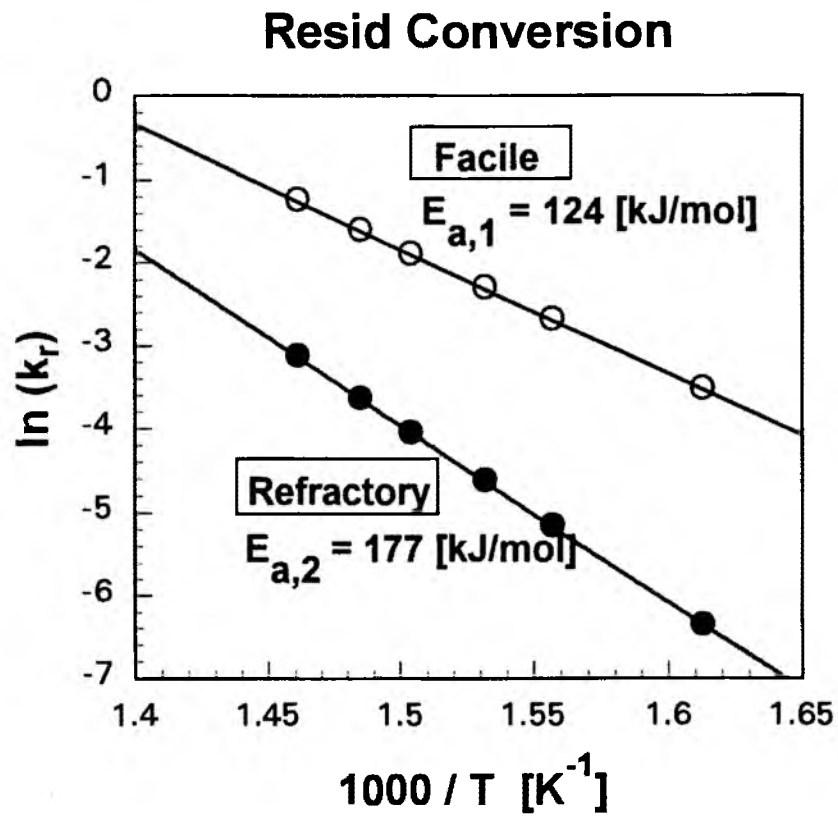
Resid Conversion
0
-1
-2
-3
-4
-5
-6
-7
ln (k_r)
Facile
E_a,1 = 124 [kJ/mol]
Refractory
E_a,2 = 177 [kJ/mol]
1.4
1.45
1.5
1.55
1.6
1.65
1000 / T [K^-1]

catalyst. Yui [95] obtained a similar apparent activation energy, 92 kJ/mol, for HDN of a bitumen-derived coker gas-oil.

The apparent activation energy (91 kJ/mol) for HDS of bitumen over an HDM catalyst in this study was somewhat lower than expected [1,76]. This may be related to the chemical composition of the residuum in the bitumen under investigation as compared to the feedstocks for which data have been reported in the literature [1,73,76,99,179]. Bridge et al. [179] reported an apparent activation energy of 125 kJ/mol for desulfurization of an atmospheric residuum from Arabian heavy crude. Beaton and Bertolacini [1] and Beuther and Schmidt [73] reported that the apparent activation energy for HDS of residuum was 117 kJ/mol and for desulfurization of a Kuwait vacuum residuum was 113 kJ/mol. Yui and Sanford [99] reported that the apparent activation energies for HDS for both bitumen-derived hydrocracker and coker HGO over a commercial NiMo catalyst was 129 kJ/mol.

Residuum conversion of bitumen over an HDM catalyst was found to follow higher than first-order kinetics thus two parallel first-order reactions were used to correlate residuum conversion data. Residuum conversion is primarily a thermal reaction thus the higher value of the apparent activation energy than catalytic conversion would be expected [180]. The activation energies for the facile and refractory fractions of the Whiterocks bitumen residuum in bitumen hydrotreating over an HDM catalyst ranged from 124 kJ/mol to 177 kJ/mol, respectively. The fractions of facile and refractory residuum were 0.26 and 0.74, respectively.

In this study the apparent activation energies for the removal of the facile and refractory nickel species were 81 and 94 kJ/mol, respectively. These values of activation energy seem to be reasonable compared with literature values. Quann et al. [27] reported that apparent activation energies for global metal

removal ranged from 42 to 158 kJ/mol depending on the reaction order. For first-order kinetics the activation energies vary from 42 to 75 kJ/mol. Hung et al. [131] reported activation energies of 115 and 142 kJ/mol for Ni-Etio porphyrin and Ni-TPP porphyrin, respectively, over a $CoMo/Al_2O_3$ catalyst. The temperature ranged from 553 to 623 K and the hydrogen partial pressure ranged from 4 to 12 MPa. Morales et al. [181] reported that the activation energy for VO-TPP porphyrin was 58-60 kJ/mol with $CoMo/Al_2O_3$, Co/Al_2O_3, Mo/Al_2O_3 catalysts in the temperature range 423-573 K and the hydrogen partial pressure range 1.4-7.4 MPa.

Pressure

The effects of hydrogen partial pressure on product distribution and yields at a fixed space velocity and reaction temperature are presented in Table 4.14. The WHSV and temperature were maintained at 0.76 h^{-1} and 665 K, respectively, in these experiments. Heteroatom removal was only slightly influenced by increasing the pressure relative to the WHSV and temperature. The API gravity and pour point of the total liquid products changed little with respect to increasing pressure, that is; the API gravity of the liquid product increased from 14.9 to 15.5 °API and the pour point decreased from 288 to 284 K as the pressure increased from 11.3 MPa to 16.7 MPa.

The hydrogen consumption increased from 28 to 66 m^3/m^3 as the pressure increased from 11.3 to 16.7 MPa (Figure 4.10). Hydrogen consumptions in the same range were observed in the WHSV experiments, that is; an increase from 31 to 75 m^3/m^3 as the WHSV decreased from 1.38 to 0.24 h^{-1} at 665 K and 13.7 MPa. However, the extent of residuum conversion at high hydrogen consumption was significantly different (~50% greater) when space

Table 4.14

Effect of Pressure on Product Distribution and Yields

at 0.76 h^{-1} WHSV and 664 K (735 °F)

Run No.	D-17	D-11	D-21	D-13
Process operating conditions				
Pressure, MPa	11.3	13.8	15.3	16.7
Temperature, K	665	665	665	665
WHSV, h^{-1}	0.77	0.77	0.76	0.77
τ, h	1.3	1.3	1.3	1.3
API gravity	14.9	15.2	15.3	15.5
Specific gravity	0.966	0.965	0.964	0.963
Pour Point, K	288	287	287	284
CCR, wt%	8.6	8.5	8.4	8.0
H_2 consumption, m^3/m^3	28	41	43	66
Elemental Analysis				
C, wt%	85.8	85.5	85.4	85.9
H, wt%	12.0	11.8	11.6	11.9
N, wt%	1.21	1.15	1.16	1.14
S, wt%	0.21	0.20	0.19	0.20
Ni, ppm	31	23	25	22
H/C atomic ratio	1.7	1.7	1.6	1.7
Product yield distribution				
Volatility, wt%	61.1	61.9	63.2	65.3
C_1-C_4, wt%	1.7	1.3	1.2	1.3
C_5-478 K, wt%	5.0	1.5	4.0	6.2
478-616 K, wt%	9.4	10.2	9.7	10.7
616-811 K, wt%	43.7	48.2	48.0	45.6
> 811 K, wt%	38.9	38.1	36.8	34.7
Liquid yield, vol %	99.5	99.7	99.4	100.0

Figure 4.10

Reactor Pressure versus Hydrogen Consumption for Bitumen Hydrotreating over an HDM Catalyst

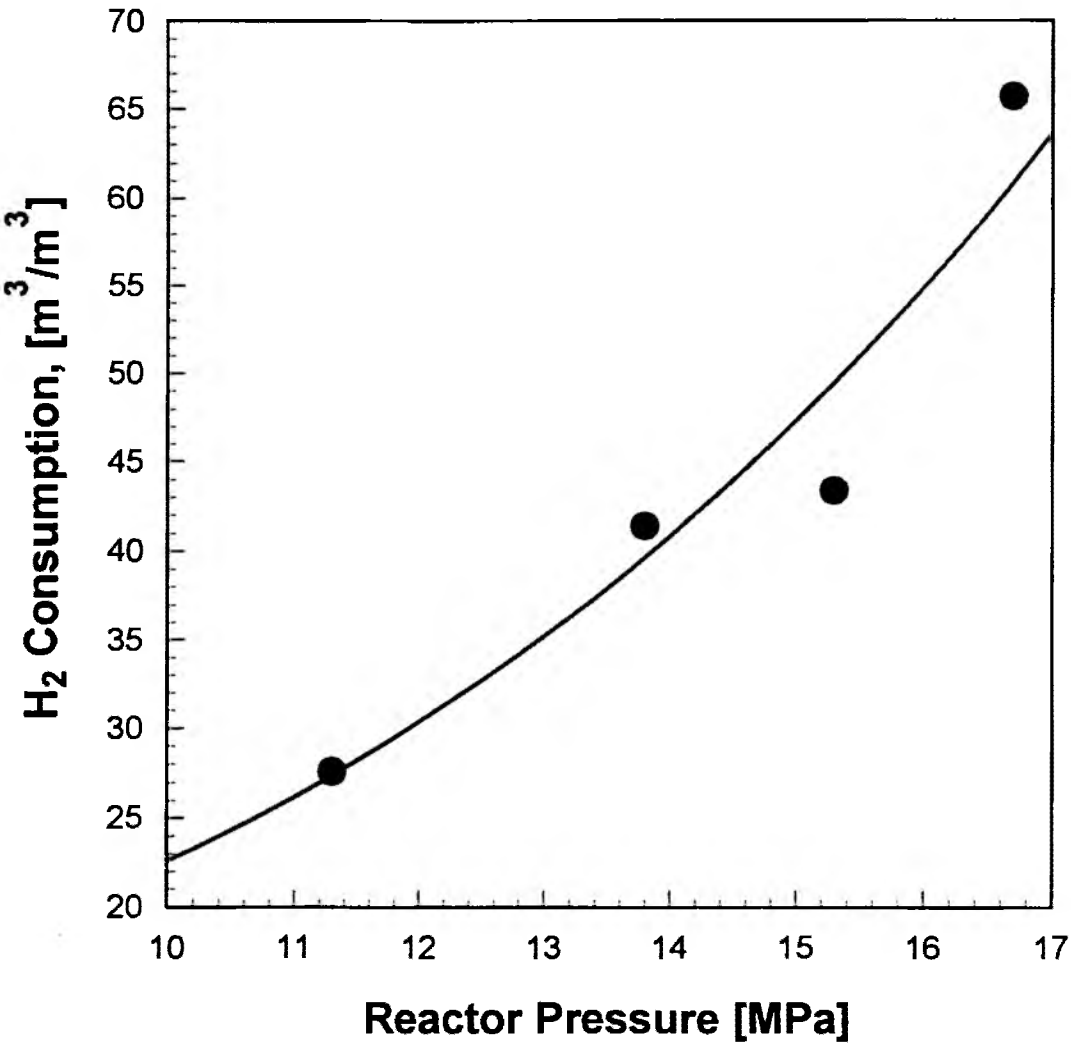
70
65
60
55
50
45
40
35
30
25
20
10
11
12
13
14
15
16
17
H2 Consumption, [m3/m3]
Reactor Pressure [MPa]

velocity was the independent variable than when pressure was the independent variable.

The high hydrogen consumption and low residuum conversion observed when pressure was varied could be due to aromatic ring hydrogenation in the absence of cracking and/or extensive denitrogenation and desulfurization, 13% and 44%, respectively; and was not the result of saturating cracked products. Beuther and Schmid [73] reported an improvement in desulfurization with increasing hydrogen pressure, however, the response to pressure diminished with increasing pressure at pressure above 6.9 MPa. A similar trend was observed in this study over the pressure range investigated. The residuum and CCR conversions were 41% and 23%, respectively, in this study.

Speight [11] reported that heteroatom removal rates are enhanced by an increase in hydrogen partial pressure in accord with model compound studies. Both feedstock and degree of heteroatom removal may influence the magnitude of the hydrogen response. The heavier feedstocks require substantially more hydrogen addition to achieve a fixed level of upgrading relative to conventional feedstocks. Simultaneous removal of other heteroatoms, aromatics saturation, and nonselective hydrocracking of petroleum are responsible for hydrogen consumption.

Figure 4.11 shows the hydrogen partial pressure dependence for reaction rate for nitrogen, sulfur, and Conradson carbon residue conversion. The hydrogen partial pressure dependence (β) for bitumen hydrotreating over an HDM catalysts in Equation (4-2) were 1.5 for nitrogen, 0.7 for sulfur, and 1.8 for nickel removal and 0.8 for residuum and CCR conversions.

The high value for the nitrogen removal confirms the presumption [113,114,116] that aromatic ring hydrogenation is required prior to hydrogenolysis of the carbon-nitrogen bond. This step is not necessarily

Figure 4.11

Hydrogen Partial Pressure Dependence for Reaction Rate

for Nitrogen, Sulfur, and CCR Conversion

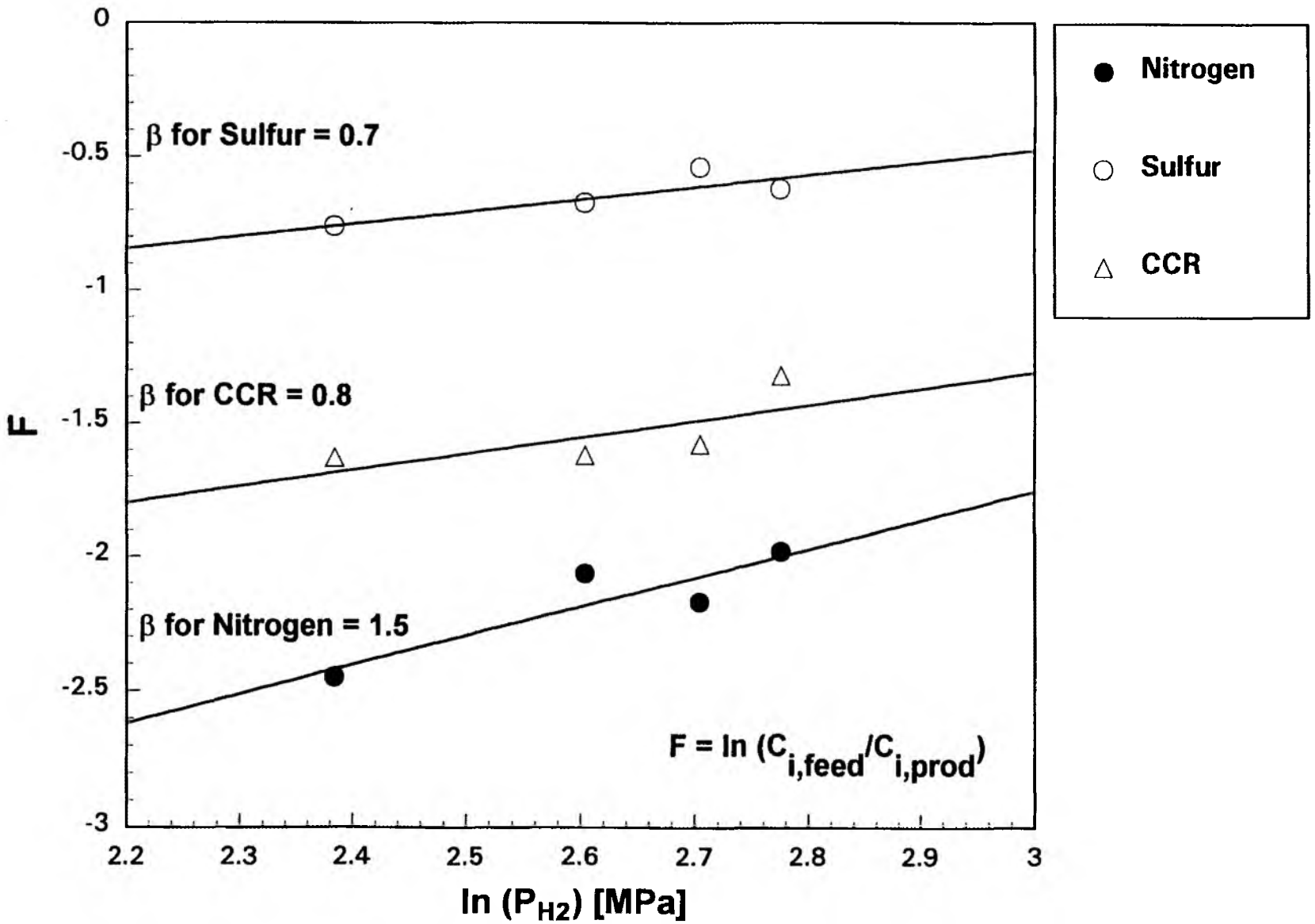
0
-0.5
-1
-1.5
-2
-2.5
-3
F
β for Sulfur = 0.7
β for CCR = 0.8
β for Nitrogen = 1.5
F = ln (C i,feed/C i,prod)
2.2
2.3
2.4
2.5
2.6
2.7
2.8
2.9
3
ln (P H2) [MPa]
Nitrogen
Sulfur
CCR

required for the sulfur removal and accordingly sulfur removal results in a lower hydrogen dependence. Residuum conversion is largely dependent on the thermal cracking and hydrogen is consumed in preventing retrograde polymerization.

Yui et al. [95,99] reported that the hydrogen partial pressure power ranged from 1.2 to 1.8 for HDN and from 0.6 to 1.1 for HDS when bitumen-derived coker and hydrocracker gas-oils were hydrotreated. Beaton and Bertolacini [1] reported that desulfurization of residuum responded in a first-order manner to pressure. The low hydrogen partial pressure dependence for HDS of the Whiterocks bitumen compared with literature values (0.7 versus unity) may be related to the naphthenic nature of the Uinta Basin bitumens. This may indicate that hydrogenation becomes more important as the number of aromatic rings increases in the average feed molecule.

Nickel in petroleum exists as soluble organometallic complexes that fall into two categories; metal porphyrins, and nonporphyrin metal complexes. Dean and Whitehead [127] have shown that the majority of the nickel species are present in the 617 K^+ fraction and are nonporphyrins. The reactivity of the high molecular weight nonporphyrin nickel in an aromatic hydrocarbon structure is therefore sensitive to hydrogen partial pressure. The reported hydrogen partial pressure dependence [131, 181] for HDM varied from 1 to 2.2. The order for nickel removal is likely a function of the rate-limiting metal removal step. The values of hydrogen partial pressure dependence determined in this study are in agreement with these values and seem to be reasonable.

Catalyst Deactivation Rate

The deactivation or aging rate for Whiterocks bitumen hydrotreating over the HDM catalyst was calculated to be 0.18°C/day over approximately 600 hours on-stream which was similar to the deactivation rate obtained over an HDN catalyst (0.20°C/day) [18,147]. The deactivation rate for Whiterocks bitumen-derived liquid hydrotreating over the HDN catalyst [18,147] was also estimated to be the same with those of bitumen hydrotreating over both the HDN [18,146] and HDM catalyst. The similarity in the deactivation rates for the BDL-HDN, BIT-HDN and BIT-HDM systems despite the larger pore size, lower surface area and lower metal loadings of the HDM catalyst relative to the HDN catalyst and the fact that the bitumen-derived liquid contained 1/3 less residuum than the bitumen was puzzling. It is presumed that it may be related to the combinations of thermal and catalytic conversion required to upgrade these heavy oil feedstocks.

Process Variable Effect on Pour Point

The pour point of the hydrotreated total liquid product generally decreased as the temperature and pressure increased, and the space velocity decreased. Temperature and space velocity had the greatest effect on pour point (Figure 4.12). The effect of pressure on pour point was minimal.

Effect of Catalyst and Feed on Conversion

The API gravity was used to correlate the extent of sulfur and nitrogen removal and residuum conversion in the hydrotreated liquid products using two different catalysts (HDM and HDN) and two different feeds (BDL and BIT).

As can be seen in Figures 4.13 through 4.15, heteroatom and residuum conversions correlate with the total liquid product API gravities. Figures 4.13 and 4.14 indicate that the HDM catalyst was less active for heteroatom

Figure 4.12

Pour-Point of Hydrotreated Total Liquid Product
as a Function of Operating Variables

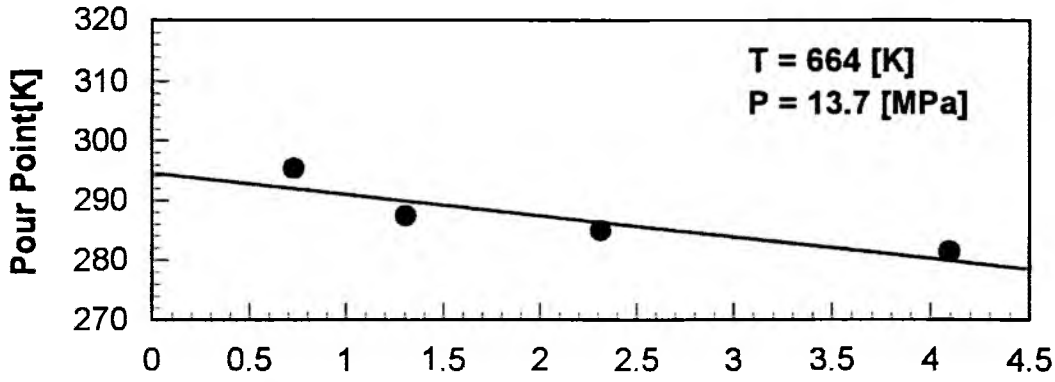
Pour Point[K]
320
310
300
290
280
270
T = 664 [K]
P = 13.7 [MPa]
0
0.5
1
1.5
2
2.5
3
3.5
4
4.5
1/WHSV [h]

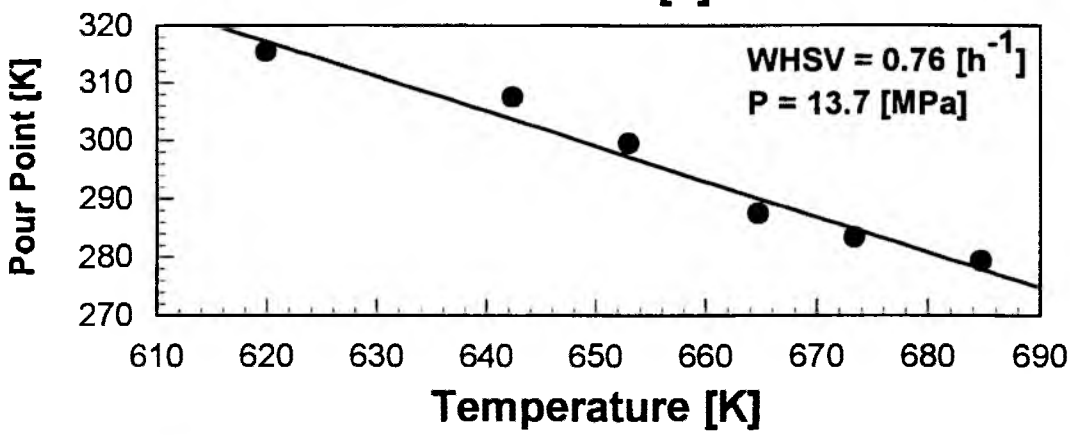
Pour Point [K]
320
310
300
290
280
270
WHSV = 0.76 [h-1]
P = 13.7 [MPa]
610
620
630
640
650
660
670
680
690
Temperature [K]

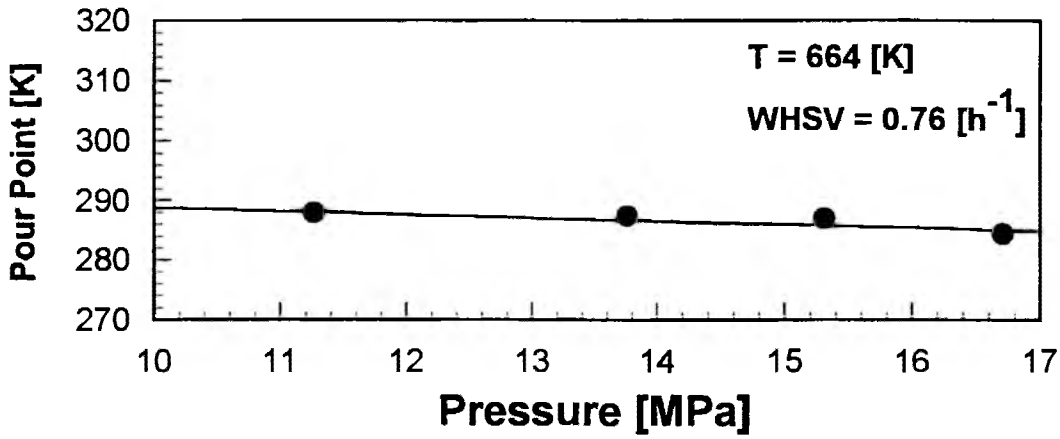
Pour Point [K]
320
310
300
290
280
270
T = 664 [K]
WHSV = 0.76 [h-1]
10
11
12
13
14
15
16
17
Pressure [MPa]

Figure 4.13

Nitrogen Conversion versus API Gravity

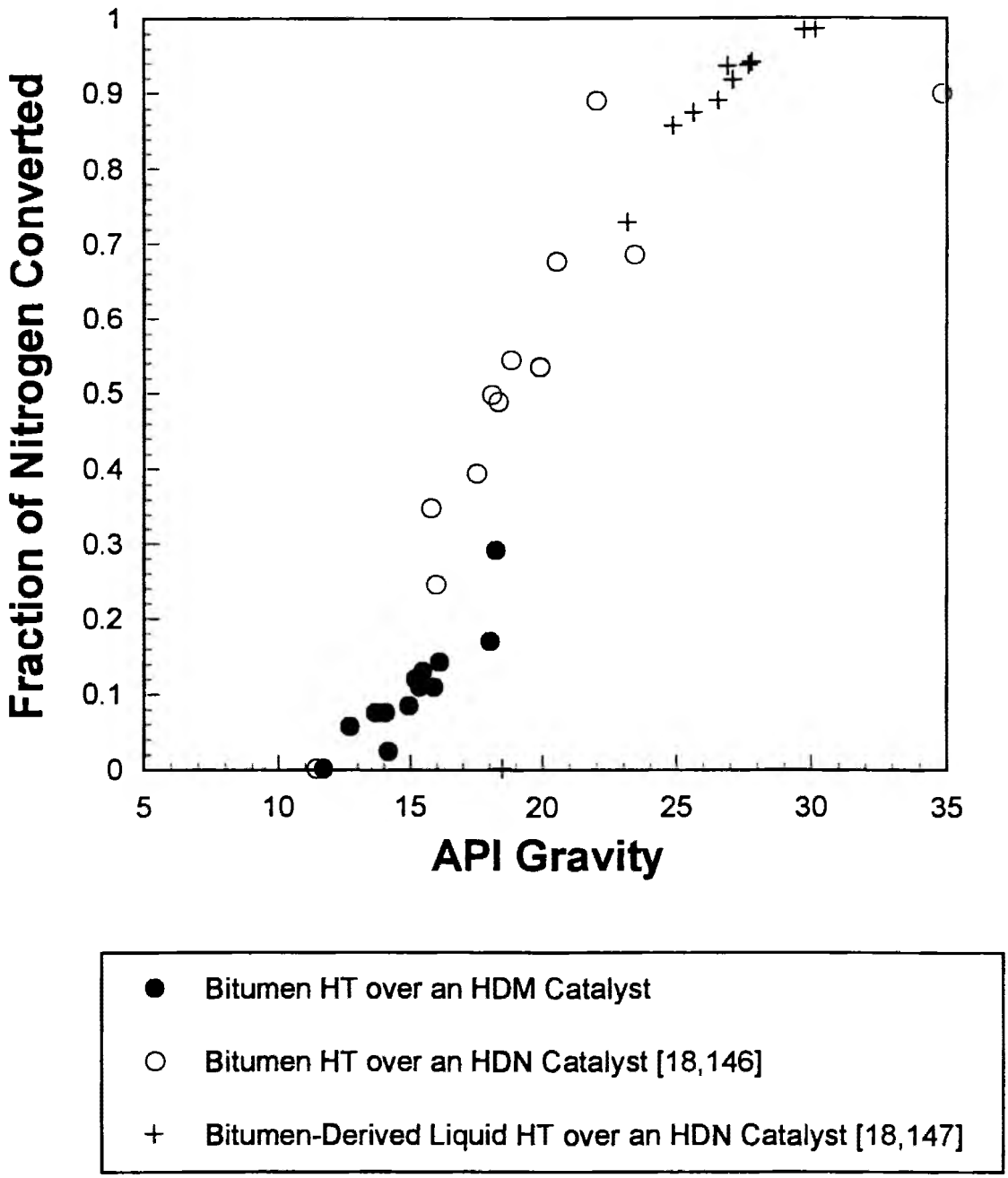
Fraction of Nitrogen Converted
1
0.9
0.8
0.7
0.6
0.5
0.4
0.3
0.2
0.1
0
5
10
15
20
25
30
35
API Gravity
Bitumen HT over an HDM Catalyst
Bitumen HT over an HDN Catalyst [18,146]
Bitumen-Derived Liquid HT over an HDN Catalyst [18,147]

Figure 4.14

Sulfur Conversion versus API Gravity

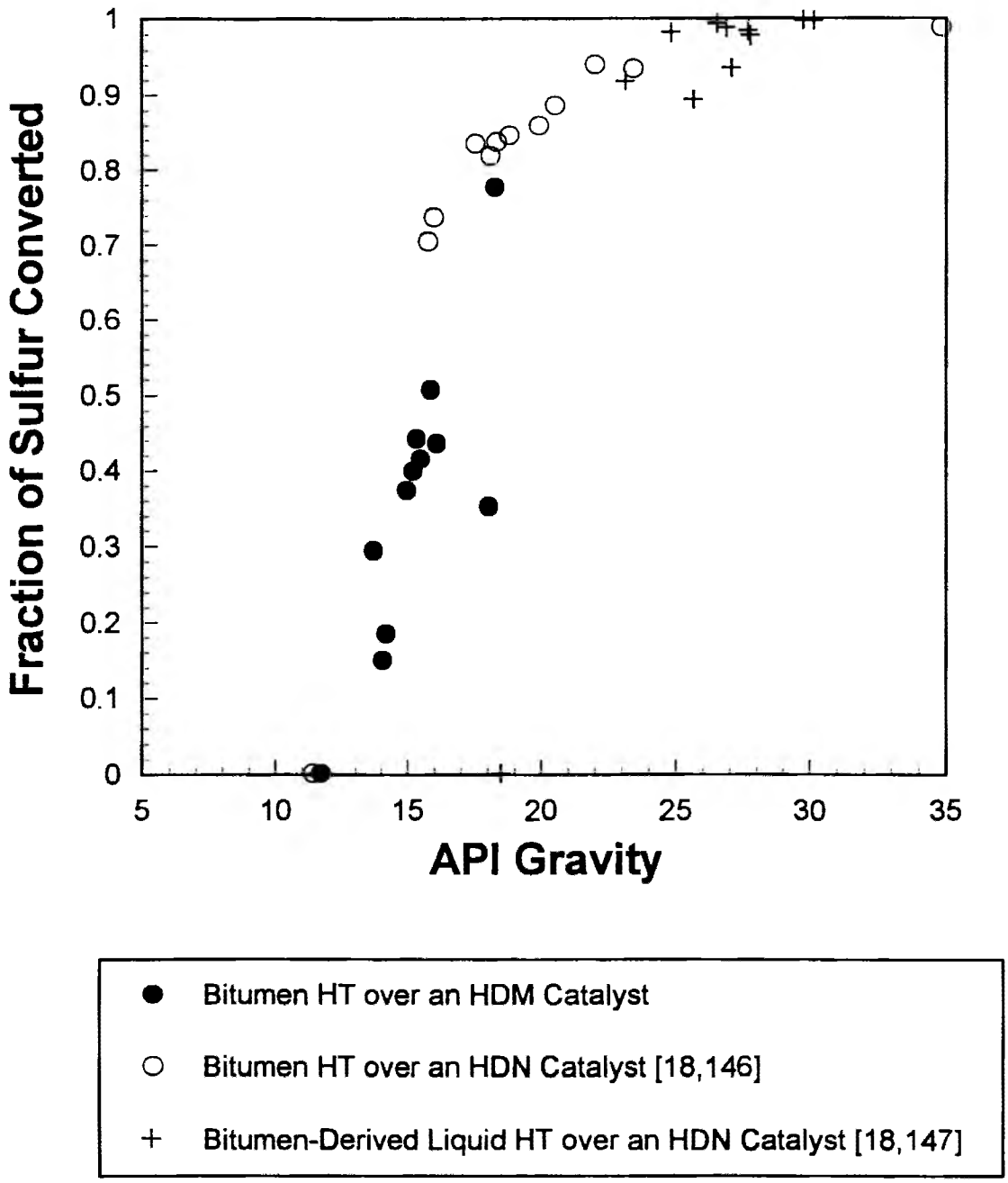
Fraction of Sulfur Converted
1
0.9
0.8
0.7
0.6
0.5
0.4
0.3
0.2
0.1
0
5
10
15
20
25
30
35
API Gravity
Bitumen HT over an HDM Catalyst
Bitumen HT over an HDN Catalyst [18,146]
Bitumen-Derived Liquid HT over an HDN Catalyst [18,147]

Figure 4.15

Residuum Conversion versus API Gravity

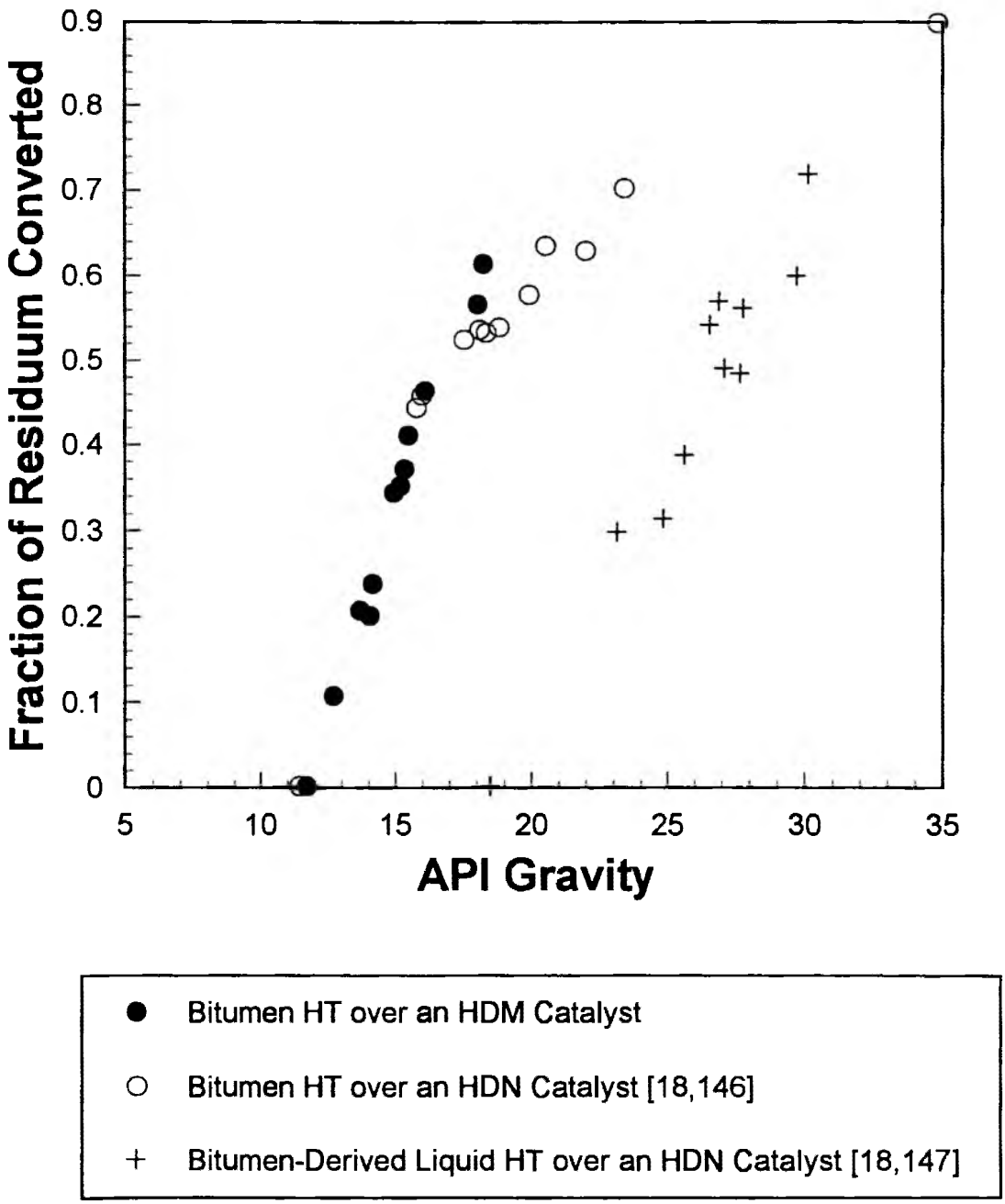
Fraction of Residuum Converted
0.9
0.8
0.7
0.6
0.5
0.4
0.3
0.2
0.1
0
5
10
15
20
25
30
35
API Gravity
Bitumen HT over an HDM Catalyst
Bitumen HT over an HDN Catalyst [18,146]
Bitumen-Derived Liquid HT over an HDN Catalyst [18,147]

conversion when processing bitumen. Heteroatom removal appeared to represent a continuum for both catalysts (HDN and HDM) and both feedstocks (BDL and BIT) whereas residuum conversion for BDL over the HDN catalyst was distinctly different from residuum conversion for BIT over both the HDN and HDM catalysts. This difference is related to the thermal history of the BDL [148]: pyrolysis of the Whiterocks oil sand to produce the BDL resulted in a significant reduction in boiling range and residuum content; however, it had little influence on heteroatom concentration.

The higher nitrogen and sulfur conversions of bitumen-derived liquid [18,147] compared with those of bitumen over an HDN catalyst [18,146] are likely related to the molecular weight differences between the two feeds which ultimately influenced their reactivities. This explanation seems possible considering that both feedstocks have the same origin and these two experiments were performed at the same operating conditions. The influence of molecular weight on reactivity for heteroatom removal has been discussed previously [182,183]: nitrogen and sulfur conversions are limited by steric hindrance and diffusional constraints. These steric hindrance and diffusional constraints were applied to the results of bitumen hydrotreating over an HDN catalyst [18,146]. These factors seemed to result in the lower conversion of heteroatoms in bitumen than in bitumen-derived liquid over an HDN catalyst. Thus, molecular weight reduction is required prior to heteroatom removal to convert high nitrogen content bitumen to liquid fuels catalytically.

Residuum conversion plots for bitumen and bitumen-derived liquid over an HDN catalyst [18,146,147] in Figure 4.15 exhibit the parallel curves. The displacement of the bitumen-derived liquid curve is related to the molecular weight reduction which occurred during the fluidized bed pyrolysis of the oil sand to produce the bitumen-derived liquid.

The effect that catalyst selection plays on residuum conversion appears to contrast with the work of other researchers [166,184-186] which indicated that residuum conversion is primarily thermal. The residuum conversion in hydrotreating bitumen over an HDN catalyst gives a higher value than that over an HDM catalyst. In addition, the Arrhenius plot for whole residuum conversion shows that the first-order activation energies for bitumen hydrotreating were found to be 132 and 83 kJ/mol for HDM and HDN catalysts, respectively. If residuum conversion is only due to thermal reaction, these two values should be the same. The higher apparent activation energy observed for residuum conversion during the bitumen hydrotreating over an HDM catalyst implies the increasing influence that thermal cracking exhibits when the catalytic activity of the system is reduced. All these results indicate for catalyst/oil systems operating in the ranges of temperature studied that residuum conversion is affected by catalyst selection.

There are two possible explanations for the catalytic effect on residuum conversion. One is related to process operating variables; this study was conducted at lower temperatures (620-685 K) than those reported in the literature (620-713 K) [1,27]. The importance of thermal cracking in the overall residuum conversion would be emphasized if this study had been carried out at higher temperatures. This is basically due to the fact that thermal cracking exhibits a higher activation energy than catalytic cracking.

The second possible explanation is that the catalyst-to-oil ratio used in this study is higher than those used in the literature [1,27]. The system in this study has a very highly concentrated catalyst region which is not diluted. Also, the fixed-bed reactor used in this study had a higher catalyst-to-oil ratio than were used in the dilute catalyst systems such as stirred autoclaves, ebullieted beds or diluted packed beds. In dilute catalyst systems, catalytic cracking is

suppressed whereas thermal cracking remains the same as in the concentrated catalyst systems. Consequently, if thermal and catalytic reactions are approximately equal, it is not possible to compare the results from these two different systems.

Effect of Catalyst and Feed on Selectivity

The effect of catalyst and feed selection on the extent of heteroatom removal are shown in Figures 4.16 to 4.18. Sulfur conversions exceed nitrogen conversions as expected since sulfur compounds are known to be more reactive than nitrogen compounds [114]. Heteroatom conversion was lower over the HDM and HDN catalysts when bitumen was used as the feedstock relative to the conversions attained with the bitumen-derived liquid [18,147]. This is due to the steric and diffusional effects which reduce accessibility of heteroatom containing moieties in BIT-HDN system and lower activity of catalyst incorporated in BIT-HDM system.

Residuum conversion in bitumen hydrotreating over an HDM catalyst was reduced relative to an HDN catalyst; however, it was not as significant as the reductions in heteroatom removal. Thermal conversion is not greatly influenced by mass transfer or steric barriers whereas heteroatom removal is more sensitive to catalyst activity, i.e., metal loading, than residuum conversion.

Bitumen hydrotreating over an HDM catalyst indicated that residuum conversion surpassed nitrogen conversion in all cases and was almost the same as sulfur conversion as can be seen in Figure 4.18. In this sense, the results of the bitumen-derived liquid and bitumen hydrotreating over an HDN catalyst demonstrated that heteroatom conversion is more sensitive to catalyst selection than is residuum conversion [18,146,147]. This is because cracking can proceed via a thermal pathway which is unavailable for heteroatom conversion.

Figure 4.16

Nitrogen, Sulfur and Residuum Conversion versus API Gravity for Bitumen-Derived Liquid over an HDN Catalyst System [18,147]

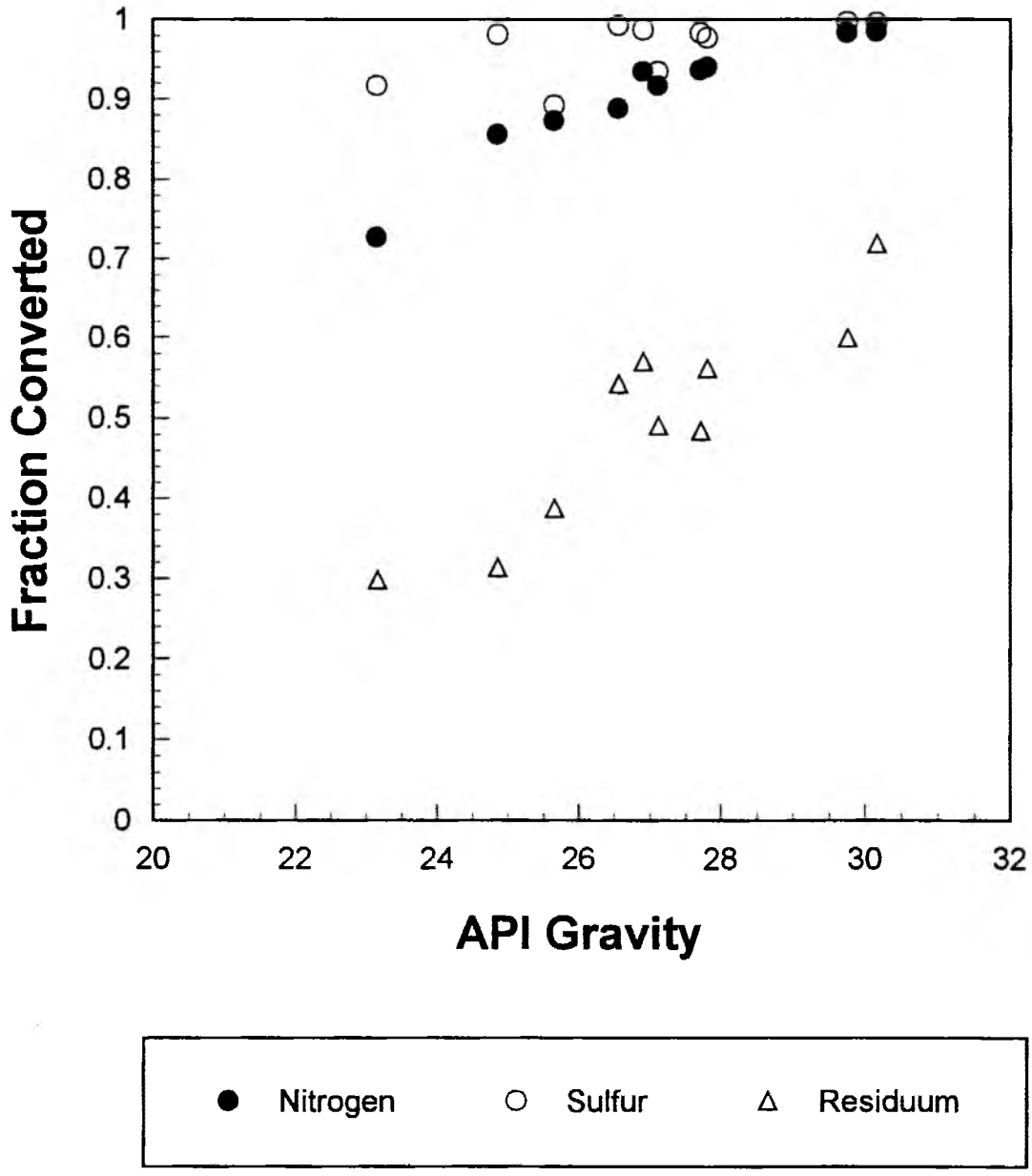
Fraction Converted
1
0.9
0.8
0.7
0.6
0.5
0.4
0.3
0.2
0.1
0
20
22
24
26
28
30
32
API Gravity
Nitrogen
Sulfur
Residuum

Figure 4.17

Nitrogen, Sulfur and Residuum Conversion versus API Gravity for Bitumen over an HDN Catalyst System [18,146]

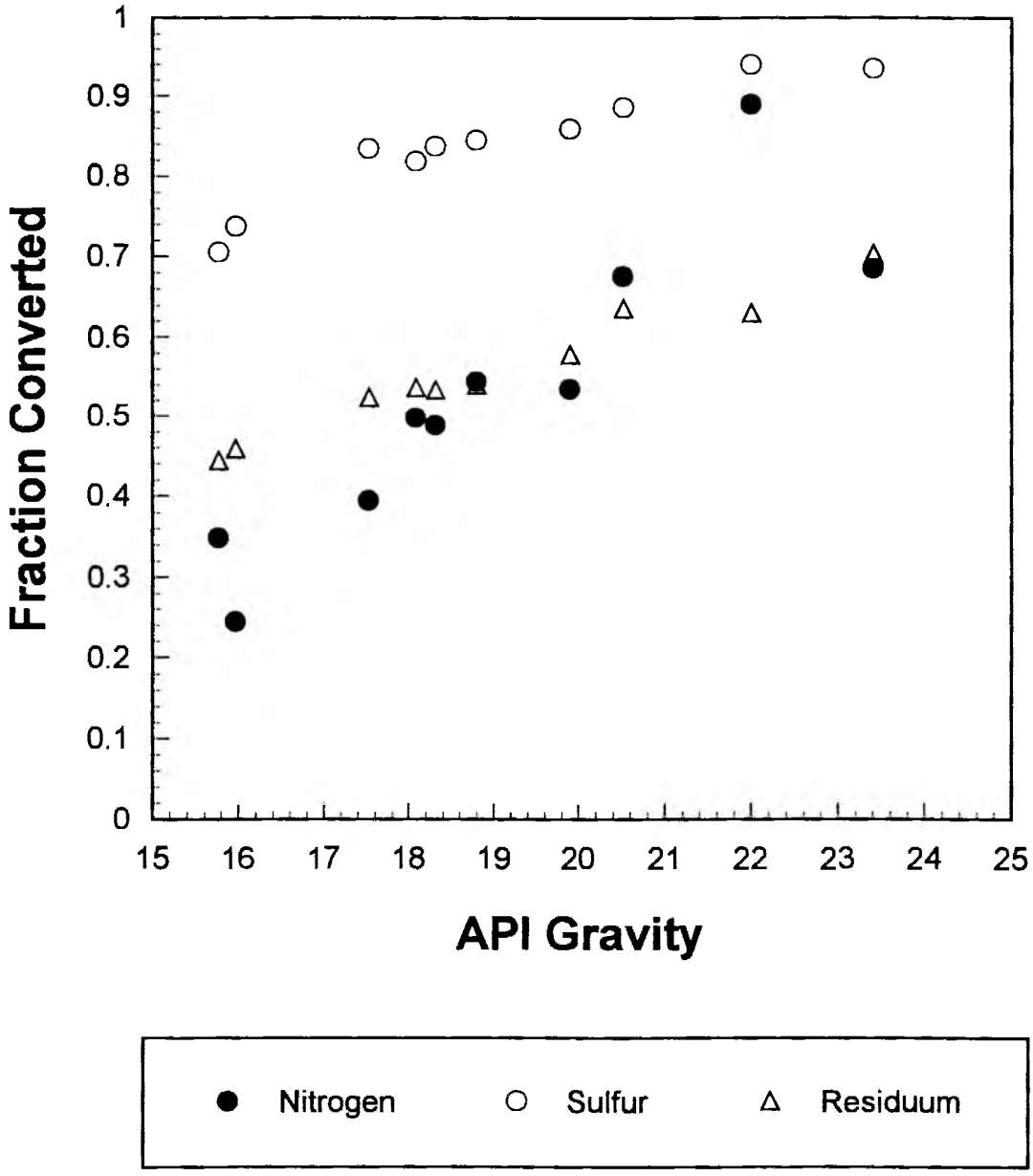
Fraction Converted
1
0.9
0.8
0.7
0.6
0.5
0.4
0.3
0.2
0.1
0
15
16
17
18
19
20
21
22
23
24
25
API Gravity
Nitrogen
Sulfur
Residuum

Figure 4.18

Nitrogen, Sulfur and Residuum Conversion versus API Gravity for Bitumen over an HDM Catalyst System

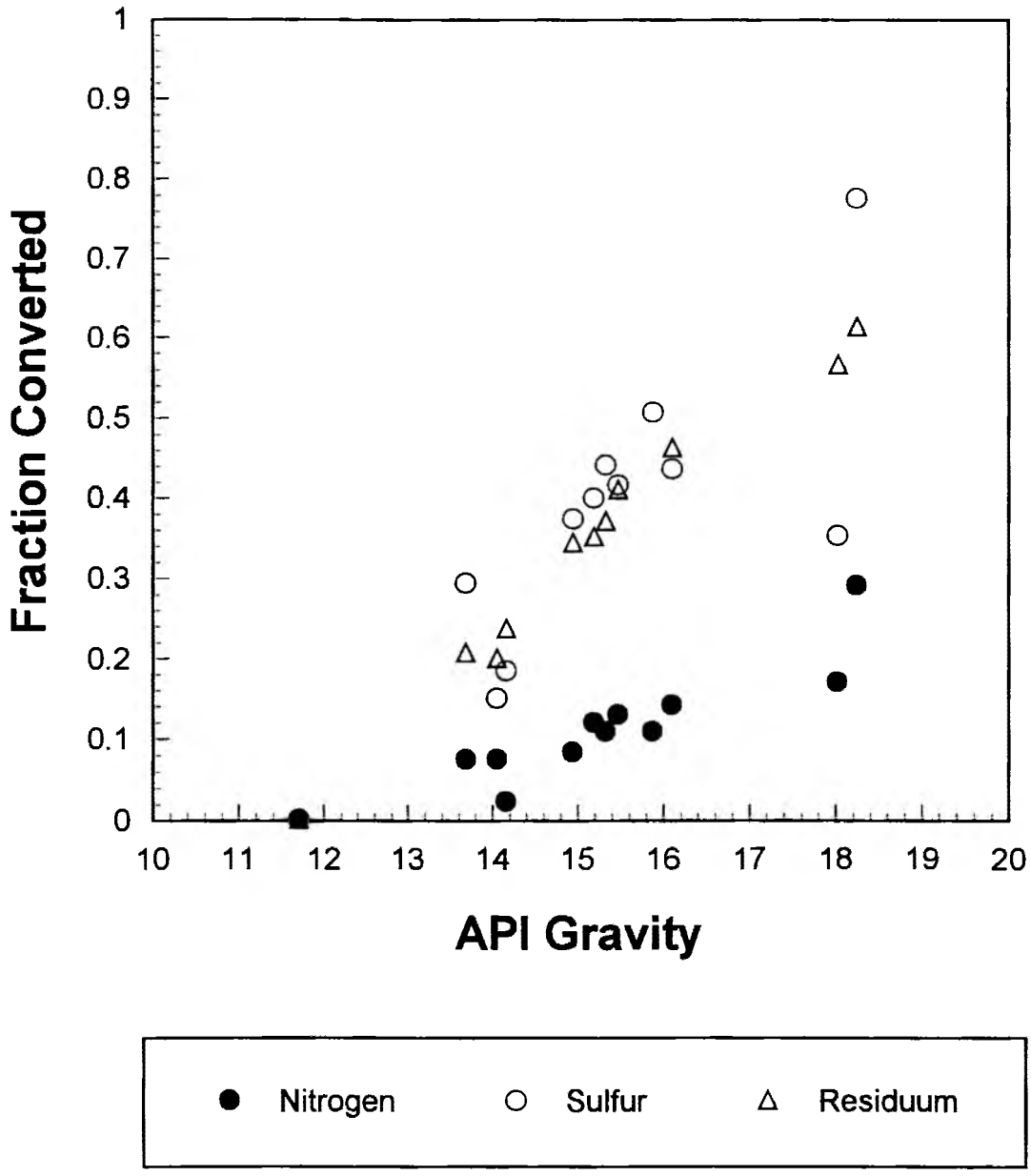
Fraction Converted
1
0.9
0.8
0.7
0.6
0.5
0.4
0.3
0.2
0.1
0
10
11
12
13
14
15
16
17
18
19
20
API Gravity
Nitrogen
Sulfur
Residuum

Molecular Weight Reduction Model for Residuum Conversion

The residuum conversion reaction involves a free-radical mechanism to convert residuum molecules to hydrocarbon gases, naphthas, distillates, and gas-oils. Hydrogen must be present to prevent retrograde polymerization reactions. Mosby et al. [164] showed that the thermal cracking of residuum is not a single first-order reaction and that these cracking reactions are irreversible. The refractory and facile residuum were assumed to crack to form all product fractions (gas-oil, distillate, naphtha, and gases). The rate constants from the model correlate well with intuition in that lower molecular weight reactants have smaller rate constants, and the overall model closely predicts pilot plant results. Mosby et al. [191] reported that the gas-oil yield goes through a maximum at about 30% at 683 K (770°F). This is due to cracking of the gas-oil fraction to lighter products at the higher temperatures. Thermal reaction pathways have been discussed by Savage [187] and Bunger [188], who investigated the reactions of hydrogen during the hydropyrolysis of heavy crudes.

In order to represent the product distributions as a function of process variables, the bitumen and hydrotreated total liquid products were grouped into four lumps; the residuum fraction (R) which boils above 811 K (538°C), the gas-oil fraction (O) with boiling range between 548-811 K (275°C-538°C), the middle distillate fraction (D) which includes C_5 to 548 K (275°C) boiling material, and gases (G) which includes NH_3, H_2S and C_1 to C_4 hydrocarbon gases.

The twelve possible reactions involving these four lumps are shown in the following scheme:

$$
\begin{array}{lll}
R \xrightarrow{1} O & R \xrightarrow{2} D & R \xrightarrow{3} G \\
O \xrightarrow{4} R & O \xrightarrow{5} D & O \xrightarrow{6} G \\
D \xrightarrow{7} R & D \xrightarrow{8} O & D \xrightarrow{9} G \\
G \xrightarrow{10} R & G \xrightarrow{11} O & G \xrightarrow{12} D
\end{array}
\tag{4-10}
$$

Two assumptions were made to simplify the reaction scheme. First, each reaction was assumed to obey irreversible first-order kinetics, so that reactions 4, 7, 8, 10, 11, and 12 were excluded. The second assumption was that the middle distillate fractions and gases are secondary products. Therefore, reactions 2 and 3 were also disregarded in the final scheme. Accordingly, the simplified reaction scheme for molecular weight reduction can be represented as follows:

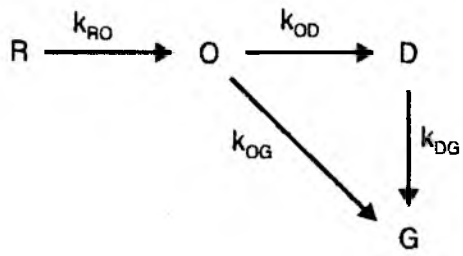

(4-11)

The differential equations describing the system are given by the following equations:

$$\frac{dC_R}{dt} = -k_{RO}C_R \tag{4-12}$$

$$\frac{dC_O}{dt} = k_{RO}C_R - (k_{OD} + k_{OG})C_O \tag{4-13}$$

$$\frac{dC_D}{dt} = k_{OD}C_O - k_{DG}C_D \tag{4-14}$$

$$\frac{dC_G}{dt} = k_{OG}C_O + k_{DG}C_D \tag{4-15}$$

where C_R, C_O, C_D, and C_G represent concentrations of residuum, gas-oils, middle distillates, and gases, respectively. The apparent first-order rate constants; k_{RO}, k_{OD}, k_{OG}, and k_{DG}, represent the conversions of residuum to gas-oil, gas-oil to middle distillate, gas-oil to gases and middle distillates to gases, respectively. Reaction rates are usually expressed in terms of molar concentrations for well-defined chemical species and reaction schemes. However, the conversions adopted for lumped kinetic representations of complex reaction schemes are in terms of mass fractions.

The results of the analysis are presented in Table 4.15. The rate of conversion of residuum to gas-oil was about four times greater than that of gas-oil conversion to middle distillates and gases. The production of gases from middle distillates was minimal.

The experimental and calculated values for the residuum, gas-oil, middle distillate, and gas fractions for the molecular weight reduction scheme matched reasonably well (Figures 4.19 and 4.20). The objective function defined in Equation (4-9) was used for computing the differences of the experimental and calculated values [162,163].

Table 4.15

Irreversible First-Order Rate Constants and Objective Functions for the Proposed Molecular Weight Reduction Model at 664 K (735°F) and 13.7 MPa (1980 psia)

	Rate Constants [h^{-1}]
k_{RO}	0.28
k_{OD}	0.04
k_{OG}	0.03
k_{DG}	0.002
	Objective Function (OF)
Residuum Fraction	3.6×10^{-3}
Gas-Oil Fraction	2.9×10^{-3}
Middle Distillate Fraction	1.1×10^{-3}
Gases Fraction	4.8×10^{-5}

Figure 4.19

Experimental versus Calculated Yield of Reactant Lumps for Hydrotreating Whiterocks Bitumen over an HDM Catalyst at 664 K (735°F) and 13.7 MPa (1980 psia)

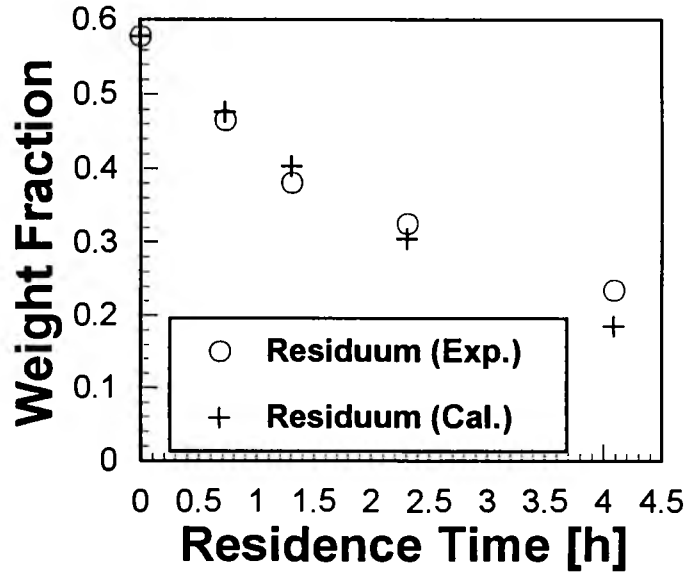
Weight Fraction
0.6
0.5
0.4
0.3
0.2
0.1
0
Residuum (Exp.)
Residuum (Cal.)
0 0.5 1 1.5 2 2.5 3 3.5 4 4.5
Residence Time [h]

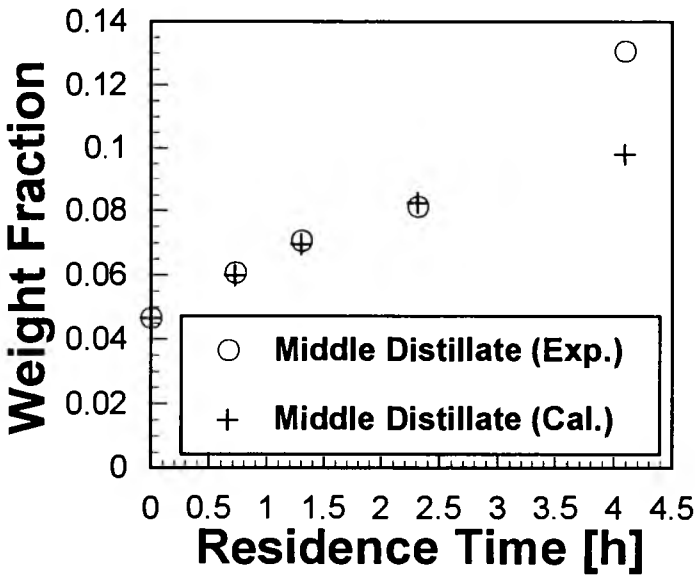
Weight Fraction
0.14
0.12
0.1
0.08
0.06
0.04
0.02
0
Middle Distillate (Exp.)
Middle Distillate (Cal.)
0 0.5 1 1.5 2 2.5 3 3.5 4 4.5
Residence Time [h]

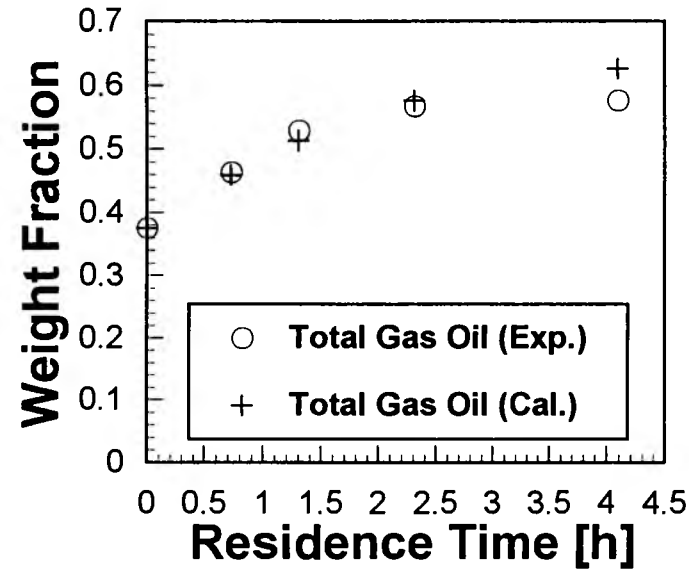
Weight Fraction
0.7
0.6
0.5
0.4
0.3
0.2
0.1
0
Total Gas Oil (Exp.)
Total Gas Oil (Cal.)
0 0.5 1 1.5 2 2.5 3 3.5 4 4.5
Residence Time [h]

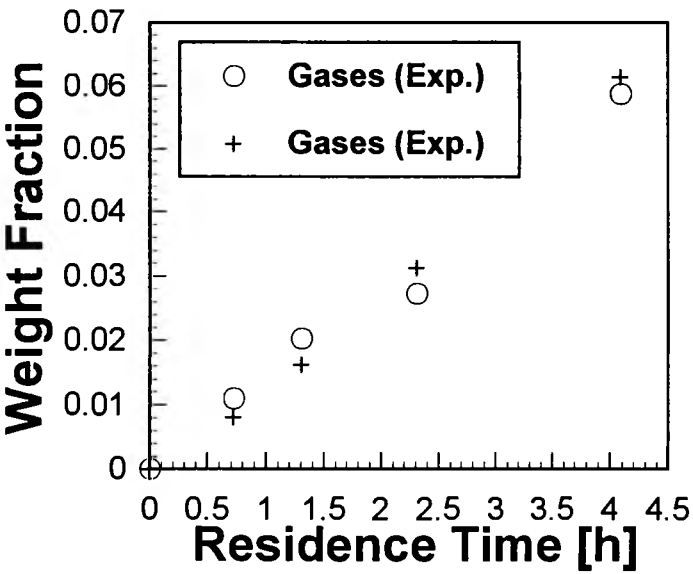
Weight Fraction
0.07
0.06
0.05
0.04
0.03
0.02
0.01
0
Gases (Exp.)
Gases (Exp.)
0 0.5 1 1.5 2 2.5 3 3.5 4 4.5
Residence Time [h]

Figure 4.20

Plot of Experimental versus Calculated Values for Residuum Conversion

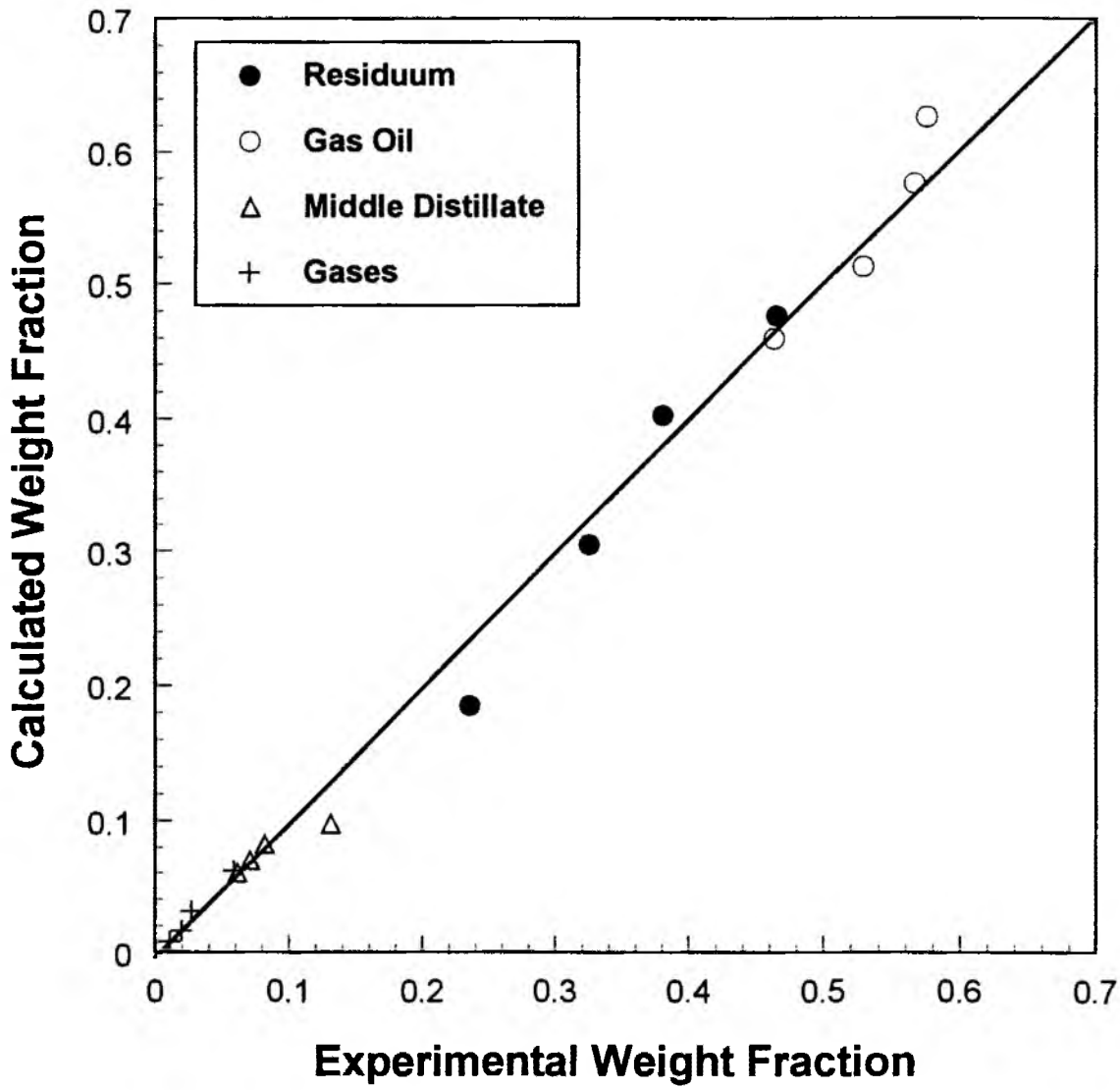
Residuum
Gas Oil
Middle Distillate
Gases
Calculated Weight Fraction
Experimental Weight Fraction
0
0.1
0.2
0.3
0.4
0.5
0.6
0.7

CHAPTER 5

CONCLUSIONS

1. The plug-flow assumption is appropriate for the hydrotreating of bitumen and bitumen-derived liquid over both HDM and HDN catalysts in the upflow operating mode.
2. The HDM catalyst was effective for nickel and sulfur removal with the Whiterocks bitumen. However, it was ineffective for denitrogenation. Bitumen HDN and HDS followed pseudo first-order kinetics over a commercial HDM catalyst. Nickel removal and residuum conversion gave apparent higher than first-order kinetics. The data were organized by invoking parallel first-order reactions: one involving a facile fraction as reactant and the second involving a refractory fraction as reactant. The activation energies for residuum conversion and metal removal, 124 kJ/mol for facile residuum, 177 kJ/mol for refractory residuum, 81 kJ/mol for facile nickel and 94 kJ/mol for refractory nickel, suggested that residuum conversion and metal removal for bitumen over an HDM catalyst were not limited by pore diffusion.
3. HDM catalyst deactivation was about 0.18°C/day during bitumen hydrotreating over a commercial HDM catalyst.
4. Sulfur conversion appears to be linked to residuum conversion because residuum conversion facilitates conversion of sulfur in higher molecular weight moieties.

5. During hydroprocessing, gas, distillate and naphtha are produced; residuum is converted; and, gas-oil is both converted and produced. The proposed molecular weight reduction model organized the Whiterocks bitumen hydrotreating data reasonably well.
6. Conradson Carbon Residue removal was found to obey first-order kinetics and its activation energy and hydrogen partial pressure dependence indicated that thermal reaction largely influenced its conversion.
7. Pour point reduction during hydroprocessing was most sensitive to temperature and space velocity. The influence of pressure on pour point was minimal.
8. Larger median pore diameters in the HDM catalyst do not result in higher conversion compared with HDN catalyst when hydrotreating bitumen because of the lower activity of the catalyst. Since thermal reactions are emphasized with an HDM catalyst, heteroatom conversion lags behind residuum conversion compared that with an HDN catalyst.
9. Although thermal cracking is important in residuum conversion, some residuum conversion is catalytic. This is in disagreement with the known model that thermal and catalytic reactions can be treated as largely independent and separable. This disagreement can be explained by the fact that the diluted catalyst systems do not have sufficient catalyst concentrations to promote a noticeable increase in activity in residuum removal; this is particularly true at high temperatures when thermal cracking plays a more significant role in residuum conversion.
10. Residuum cracking is less sensitive to catalyst selection than heteroatom conversion because residuum conversion can proceed through a thermal pathway which, for the most part, is not available for heteroatom conversion.

APPENDIX A

BASIC PROGRAMS FOR SIMULATED DISTILLATION OF LIQUID PRODUCTS

(SIMDIS.BAS, ZEROBLNK.BAS)

```
83    REM
85    REM         THIS IS "SIMDIS.BAS" PROGRAM
86    REM
90    REM VERSION TO USE HALF-AND-HALF INTERVALS
94    REM VERSION FOR THE SHORT COLUMN, USING THE
95    REM SHORT RETENTION TIMES
100   REM PROGRAM = SHORTSMD.BAS (SHORT SIMULATED DISTILLATION.BASIC)
101   REM
102   REM
103   REM                                          BY SEOKHWAN KWAK
104   REM
105   REM
110   REM ******** CAUTION *********
120   REM *** THIS PROGRAM USES LONG VARIABLE NAMES, THIS IS NOT
130   REM *** SUPPORTED IN SOME VERSIONS OF BASIC, WHICH READ AS FEW
140   REM *** AS TWO SIGNIFICANT CHARACTERS IN A VARIABLE NAME.
150   REM *** THIS MAY LEAD TO VERY DIFFICULT TO FIND BUGS.
160   REM ******** END OF CAUTION **********
170   REM *** THIS PROGRAM WRITTEN FOR MICROSOFT QBASIC
180   REM
190   REM
200   DIM RETENTIONTIME(99), BOILINGPOINT(99), BLANK(3500)
210   DIM SAMPLE(3500), ISSAMPLE(3500), CARBONNUMBER(99)
220   DIM CUMAREA(99), PEAKAREA(99), E(3500), CUM(99)
230   DIM NORMPEAKAREA(99)
240   REM
250   REM
260   REM READ PARAFFIN PROPERTY DATA
270   GOSUB 1000
280   REM
290   REM
300   REM GET THE VARIOUS FILENAMES
310   GOSUB 3000
320   REM
330   REM
340   REM CALCULATE PEAK LOCATIONS, ETC...
350   GOSUB 4000
360   REM
370   REM
380   REM LOAD DATA FROM SAMPLE (ETC...) FILES, SUBTRACT BLANK
390   GOSUB 5000
400   REM
410   REM
420   REM CALCULATE TOTAL AND PARTIAL SAMPLE AREAS
430   GOSUB 6000
440   REM
450   REM
460   REM CALCULATE UNELUTED FRACTION
470   GOSUB 7000
480   REM
490   REM
500   REM CALCULATE PEAK AND CUMULATIVE AREAS
510   GOSUB 8000
520   REM
```

```
530   REM
540   REM PRINT RESULTS
550   GOSUB 9000
560   REM
570   REM
580   STOP
590   REM
600   REM
1000  REM SUBROUTINE FOR PROGRAM INDEX, CARBON NUMBER,
1010  REM RETENTION TIME(MIN), NORMAL BP (F)
1020  DATA 01, 20, 13.27, 651
1030  DATA 02, 21, 13.84, 673
1040  DATA 03, 22, 14.40, 695
1050  DATA 04, 23, 14.94, 716
1060  DATA 05, 24, 15.48, 736
1070  DATA 06, 25, 15.98, 755
1080  DATA 07, 26, 16.48, 774
1090  DATA 08, 27, 16.98, 791
1100  DATA 09, 28, 17.47, 808
1110  DATA 10, 29, 17.95, 824
1120  DATA 11, 30, 18.42, 840
1130  DATA 12, 31, 18.86, 856
1140  DATA 13, 32, 19.30, 871
1150  DATA 14, 33, 19.74, 884
1160  DATA 15, 34, 20.17, 898
1170  DATA 16, 35, 20.66, 912
1180  DATA 17, 36, 21.15, 925
1190  DATA 18, 37, 21.60, 936
1200  DATA 19, 38, 22.05, 948
1210  DATA 20, 39, 22.43, 960
1220  DATA 21, 40, 22.80, 972
1230  DATA 22, 41, 23.18, 982
1240  DATA 23, 42, 23.55, 993
1250  DATA 24, 43, 23.88, 1003
1260  DATA 25, 44, 24.20, 1013
1270  DATA 26, 45, 24.58, 1023
1280  DATA 27, 46, 24.95, 1033
1290  DATA 28, 47, 25.33, 1042
1300  DATA 29, 48, 25.70, 1051
1310  DATA 30, 49, 26.00, 1059
1320  DATA 31, 50, 26.30, 1067
1330  DATA 32, 51, 26.63, 1075
1340  DATA 33, 52, 26.95, 1083
1350  DATA 34, 53, 27.23, 1090
1360  DATA 35, 54, 27.50, 1098
1370  DATA 36, 55, 27.80, 1105
1380  DATA 37, 56, 28.10, 1112
1390  DATA 38, 57, 28.33, 1119
1400  DATA 39, 58, 28.55, 1126
1410  DATA 40, 59, 28.83, 1132
1420  DATA 41, 60, 29.10, 1139
1730  INPUT "MAX C-NUMBER INDEX ELUTED, C60 = 41:  ", MAXINDEX
1740  FOR I = 1 TO MAXINDEX
1750  READ TRASH
```

```
1760   READ CARBONNUMBER(I)
1770   READ RETENTIONTIME(I)
1780   READ BOILINGPOINT(I)
1790   NEXT I
1800   RETURN
1810   REM
1820   REM
1830   REM
1840   REM
3000   REM GET VARIOUS FILENAMES
3010   INPUT "SUBTRACT A BLANK RUN (1 = YES, 0 = NO)   ", FLAG2
3020   PRINT
3030   IF (FLAG2 = 1) THEN INPUT "BLANK RUN FILENAME  ", SBLANK$
3040   INPUT "SAMPLE (ONLY) RUN FILENAME  ", SSAMPLE$
3050   INPUT "SAMPLE + INTERNAL STANDARD FILENAME   ", SISSAMPLE$
3055   INPUT "OUTPUT FILENAME  ", OUTPUT$
3060   PRINT
3070   IF (FLAG2 = 1) THEN OPEN SBLANK$ FOR INPUT AS #10
3080   OPEN SSAMPLE$ FOR INPUT AS #11
3090   OPEN SISSAMPLE$ FOR INPUT AS #12
3094   OPEN OUTPUT$ FOR OUTPUT AS #13
3095   PRINT #13, "SUBTRACT A BLANK RUN (1 = YES, 0 = NO)   ", FLAG2
3096   PRINT #13, "SAMPLE (ONLY) RUN FILENAME  ", SSAMPLE$
3097   PRINT #13, "SAMPLE + INTERNAL STANDARD FILENAME   ", SISSAMPLE$
3098   PRINT #13, "OUTPUT FILENAME  ", OUTPUT$
3099   PRINT #13,
3100   RETURN
3110   REM
3120   REM
3130   REM
3140   REM
4000   REM CALCULATE SOME PEAK LOCATIONS
4010   INPUT "CHROMATOGRAM TIME IN MINUTES   ", CHROMATOGRAMTIME
4015   PRINT #13, "CHROMATOGRAM TIME IN MINUTES   ", CHROMATOGRAMTIME
4020   TIMEFACTOR = 30
4030   REM TIMEFACTOR = # OF "SLICES" IN ONE MINUTE
4040   MAXI = CHROMATOGRAMTIME * TIMEFACTOR
4050   INPUT "A TIME BEFORE FIRST I-S PEAK IN MIN. (5 MIN.?)   ", FIRSTPEAK
4060   INPUT "A TIME AFTER LAST I-S PEAK IN MIN. (13 MIN.?)   ", LASTPEAK
4062   PRINT #13, "A TIME BEFORE FIRST I-S PEAK IN MIN.   ", FIRSTPEAK
4064   PRINT #13, "A TIME AFTER LAST I-S PEAK IN MIN.   ", LASTPEAK
4070   FIRSTI = FIRSTPEAK * TIMEFACTOR
4080   LASTI = LASTPEAK * TIMEFACTOR
4090   RETURN
4100   REM
4110   REM
4120   REM
4130   REM
5000   REM LOAD DATA FROM SAMPLE (ETC...) FILES, SUBTRACT BLANK
5010   FOR I = 1 TO MAXI
5020   IF (FLAG2 = 1) THEN INPUT #10, TRASH, TRASH, BLANK(I)
5030   INPUT #11, TRASH, TRASH, SAMPLE(I)
5040   INPUT #12, TRASH, TRASH, ISSAMPLE(I)
5050   IF (FLAG2 = 1) THEN SAMPLE(I) = SAMPLE(I) - BLANK(I)
```

```
5060  IF (FLAG2 = 1) THEN ISSAMPLE(I) = ISSAMPLE(I) - BLANK(I)
5070  NEXT I
5080  RETURN
5090  REM
5100  REM
5110  REM
5120  REM
6000  REM CALCULATE TOTAL AND PARTIAL SAMPLE AREAS
6010  SAMPAREA = 0
6020  ISSAMPAREA = 0
6030  FOR I = 1 TO MAXI
6040  SAMPAREA = SAMPAREA + SAMPLE(I)
6050  ISSAMPAREA = ISSAMPAREA + ISSAMPLE(I)
6060  NEXT I
6070  PARSAMPAREA = SAMPAREA
6080  PARISSAMPAREA = ISSAMPAREA
6090  FOR I = FIRSTI TO LASTI
6100  PARSAMPAREA = PARSAMPAREA - SAMPLE(I)
6110  PARISSAMPAREA = PARISSAMPAREA - ISSAMPLE(I)
6120  NEXT I
6130  RETURN
6140  REM
6150  REM
6160  REM
6170  REM
7000  REM CALCULATE UNELUTED FRACTION
7010  INPUT "SAMPLE WEIGHT = ", SAMPWT
7020  INPUT "INTERNAL STANDARD WEIGHT = ", ISSAMPWT
7022  PRINT #13, "SAMPLE WEIGHT = ", SAMPWT
7024  PRINT #13, "INTERNAL STANDARD WEIGHT = ", ISSAMPWT
7030  ISFRAC = ISSAMPWT / (ISSAMPWT + SAMPWT)
7040  UNELUTED = (1 / ISFRAC) * (ISSAMPAREA - (SAMPAREA * PARISSAMPAREA /
      PARSAMPAREA)) - ISSAMPAREA
7050  TEMP = ISSAMPAREA - SAMPAREA * PARISSAMPAREA / PARSAMPAREA
7060  PLUSFRAC = UNELUTED / (UNELUTED + (ISSAMPAREA - TEMP))
7070  PRINT "PLUS FRACTION = "; PLUSFRAC
7075  PRINT #13, "PLUS FRACTION = "; PLUSFRAC
7080  RETURN
7090  REM
7100  REM
7110  REM
7120  REM
8000  REM CALCULATE PEAK AND CUMULATIVE AREAS
8005  RETENTIONTIME(MAXINDEX + 1) = 2 * RETENTIONTIME(MAXINDEX) -
      RETENTIONTIME(MAXINDEX - 1)
8010  FOR I = 1 TO MAXINDEX
8020  CUMAREA(I) = 0
8030  FOR J = 1 TO (RETENTIONTIME(I) + RETENTIONTIME(I + 1)) * TIMEFACTOR / 2
8040  CUMAREA(I) = CUMAREA(I) + SAMPLE(J)
8050  NEXT J
8060  NEXT I
8070  FOR I = 2 TO MAXINDEX
8080  PEAKAREA(I) = CUMAREA(I) - CUMAREA(I - 1)
8090  NORMPEAKAREA(I) = PEAKAREA(I) / SAMPAREA
```

```
8100  NEXT I
8110  PEAKAREA(1) = CUMAREA(1)
8120  NORMPEAKAREA(1) = PEAKAREA(1) / SAMPAREA
8130  FOR I = 1 TO MAXINDEX
8140  CUMAREA(I) = CUMAREA(I) / SAMPAREA
8150  NEXT I
8160  RETURN
8170  REM
8180  REM
8190  REM
8200  REM
9000  REM PRINT RESULTS
9010  PRINT "CARBON #       NORMAL BP       MASS FRAC  CUMULATIVE FRAC "
9015  PRINT #13, "CARBON #       NORMAL BP       MASS FRAC     CUMULATIVE FRAC"
9020  FOR I = 1 TO MAXINDEX
9030  ACTUALPEAKAREA = NORMPEAKAREA(I) * (1 - PLUSFRAC)
9040  ACTUALCUMAREA = CUMAREA(I) * (1 - PLUSFRAC)
9050  PRINT CARBONNUMBER(I), BOILINGPOINT(I), ACTUALPEAKAREA,
      ACTUALCUMAREA
9055  PRINT #13, CARBONNUMBER(I), BOILINGPOINT(I), ACTUALPEAKAREA,
      ACTUALCUMAREA
9060  NEXT I
9070  PRINT "C"; CARBONNUMBER(MAXINDEX); " PLUS FRACTION = "; (1 -
      ACTUALCUMAREA)
9080  PRINT #13, "C"; CARBONNUMBER(MAXINDEX); "PLUS FRACTION = "; (1 -
      ACTUALCUMAREA)
9090  RETURN
```

```
83      REM
85      REM         THIS IS "ZEROBLNK.BAS" PROGRRAM.
86      REM
91      REM
92      REM
93      REM                                          BY SEOKHWAN KWAK
94      REM
100     INPUT "SAMPLE FILENAME:  ", F1$
110     INPUT " BLANK FILENAME:  ", F2$
120     INPUT "OUTPUT FILENAME:  ", F3$
130     F1$ = F1$ + ".RPT"
140     F2$ = F2$ + ".RPT"
145     INPUT "CHROMATOGRAM TIME (MIN):  ", TYME
150     OPEN F1$ FOR INPUT AS #10
160     OPEN F2$ FOR INPUT AS #11
170     OPEN F3$ FOR OUTPUT AS #12
171     INPUT "AMOUNT OF START OF RUN TO ZERO OUT (MIN):   ", ZTIME
172     FOR I = 1 TO (ZTIME * 30)
173     PRINT #12, USING "########.####"; TRASH1
174     PRINT #12, USING "########.####"; TRASH2
175     PRINT #12, USING "########.#####"; 0
176     NEXT I
180     FOR I = ((ZTIME * 30) +1 ) TO (TYME * 30)
190     INPUT #10, TRASH1, TRASH2, SAMPLE
200     INPUT #11, TRASH, TRASH, BLANK
210     RESULT = SAMPLE - BLANK
220     PRINT #12, USING "########.####"; TRASH1
230     PRINT #12, USING "########.####"; TRASH2
240     PRINT #12, USING "########.#####"; RESULT
250     NEXT I

260     STOP
```

APPENDIX B

FORTRAN PROGRAM FOR CALCULATING HYDROTREATED PRODUCT DISTRIBUTION

```
C
C       The following program is used to calculate
C       heavy oil product distributions for bitumen hydrotreated over
C       Unocal HDM catalyst including NH3, H2S, H20, C1-C4 Gases,
C       C5+ naphtha, distillate, gas oil and residuum fractions
C       by weight.
C
C                                  By Seokhwan Kwak
C
C
        implicit double precision (a-h,o-z)
        double precision ld,masbal,masbwt,lnorm,liqout
        double precision methawt,metha,naphtwt,napht
        double precision metha1,napht1,hcgas,methaar
C
C
C       Initialization....
C
        open(22, file='d13c1c6', status='unknown')
C
C       Input all feed elemental properties.....
C       where, fd=wt[in grams] of feed going to hydrotreater.
C       fdcwt, fdhwt, hdnwt, fdswt, fdowt=wt% of carbon, hydrogen,
C       nitrogen, sulfur and oxygen in the feed respectively.....
C
        write(*,10)
        write(22,10)
10      format(2x,'Amount of liquid fed into hydrotreater[grams] ?')
        read*, fd
        write(*,15) fd
        write(22,15) fd
15      format(4x,';',2x,f9.5,2x,'[grams]',/)
C
        fdcwt=85.1
        fdhwt=11.6
        fdnwt=1.360
        fdswt=0.3334
        fdowt=100.-fdcwt-fdhwt-fdnwt-fdswt
C
C
C       Calculating actual grams of C, H, O, N, S in the feed.....
C
        fdc=fd*fdcwt/100.
        fdh=fd*fdhwt/100.
        fdn=fd*fdnwt/100.
        fds=fd*fdswt/100.
        fdo=fd*fdowt/100.
C
C
C       The following step is used to calculate the mass balance and
C       normalization of the hydrotreated product.....
C
C       where,
C       ld=wt of liquid coming out of hydrotreater [grams].
```

```
C       out=wt of liquid+gas coming out of hydrotreater [grams]
C       masbwt=Mass Balance [wt%]
C       gnorm=wt of gas after normalization [grams]
C       lnorm=wt of liquid after normalization [grams]
C       snorm=wt of liquid+gas after normalization [grams].....
C
        write(*,20)
        write(22,20)
20      format(2x,'Input amount liquid going out [grams]')
        read*, ld
        write(*,25) ld
        write(22,25) ld
25      format(4x,';',2x,f9.5,2x,'[grams]',/)
C
        write(*,30)
        write(22,30)
30      format(2x,'input amount of liquid+gas going out [grams]')
        read*, out
        write(*,35) out
        write(22,35) out
35      format(4x,';',2x,f9.5,2x,'[grams]',/)
C
C
        gas=out-ld
C
        masbal=out/fd
        masbwt=masbal*100.
C
        write(*,40) masbwt
        write(22,40) masbwt
40      format(2x,'Mass balance;',2x,f9.5,/)
C
C
        gnorm=gas*1/masbal
        lnorm=ld*1/masbal
        snorm=gnorm+lnorm
C
        write(*,50)
        write(22,50)
50      format(2x,'NORMALIZATION VALUE OF GAS & LIQUID')
C
        write(*,60) gnorm
        write(22,60) gnorm
60      format(2x,'Gas;',2x,f9.5)
        write(*,70) lnorm
        write(22,70) lnorm
70      format(2x,'Liquid;',2x,f9.5)
        write(*,80) snorm
        write(22,80) snorm
80      format(2x,'gas+liquid after normalization;',2x,f9.5,/)
C
C       Calculating amount of n,s,o converted in grams....
C
        write(*,90)
```

```
      write(22,90)
90    format(2x,'Input wt% of Carbon in the product')
      read*, pdcwt
      write(*,95) pdcwt
      write(22,95) pdcwt
95    format(4x,':',2x,f9.5,2x,'[wt%]',/)
C
      write(*,100)
      write(22,100)
100   format(2x,'Input wt% of Hydrogen in the product')
      read*, pdhwt
      write(*,105) pdhwt
      write(22,105) pdhwt
105   format(4x,':',2x,f9.5,2x,'[wt%]',/)
C
      write(*,110)
      write(22,110)
110   format(2x,'Input wt% of Nitrogen in the product')
      read*, pdnwt
      write(*,115) pdnwt
      write(22,115) pdnwt
115   format(4x,':',2x,f9.5,2x,'[wt%]',/)
C
      write(*,120)
      write(22,120)
120   format(2x,'Input wt% of Sulfur in the product')
      read*, pdswt
      write(*,125) pdswt
      write(22,125) pdswt
125   format(4x,':',2x,f9.5,2x,'[wt%]',/)
C
      pdowt=100.-pdcwt-pdhwt-pdnwt-pdswt
C
      cons=fds-lnorm*pdswt/100.
      conn=fdn-lnorm*pdnwt/100.
      cono=fdo-lnorm*pdowt/100.
C
      water=cono*(18./16.)
      liqout=lnorm-water
C
      ammonia=conn*(17./14.)
      hysulf=cons*(34./32.)
      gasout=gnorm-ammonia-hysulf
C
      write(*,130) water
      write(22,130) water
130   format(2x,'Water;',2x,f9.5)
C
      write(*,140) hysulf
      write(22,140) hysulf
140   format(2x,'Hydrogen Sulfide;',2x,f9.5)
C
      write(*,150) ammonia
      write(22,150) ammonia
```

```
150     format(2x,'Ammonia;',2x,f9.5)
C
        write(*,160) liqout
        write(22,160) liqout
160     format(2x,'Liquid Product;',2x,f9.5)
C
        write(*,170) gasout
        write(22,170) gasout
170     format(2x,'Gas Product;',2x,f9.5)
C
C       Input each area of C1 to C6 for hydrotreated gas
C       from Carle Gas Chromatograph....
C
        write(*,180)
        write(22,180)
180     format(2x,'Input area of C1 from G.C.')
        read*, methaar
        write(*,185) methaar
        write(22,185) methaar
185     format(4x,';',2x,f9.5)
C
        write(*,190)
        write(22,190)
190     format(2x,'Input area of C2 from G.C.')
        read*, ethanar
        write(*,195) ethanar
        write(22,195) ethanar
195     format(4x,';',2x,f9.5)
C
        write(*,200)
        write(22,200)
200     format(2x,'Input area of C3 from G.C.')
        read*, propaar
        write(*,205) propaar
        write(22,205) propaar
205     format(4x,';',2x,f9.5)
C
        write(*,210)
        write(22,210)
210     format(2x,'Input area of C4 from G.C.')
        read*, butanar
        write(*,215) butanar
        write(22,215) butanar
215     format(4x,';',2x,f9.5)
C
        write(*,220)
        write(22,220)
220     format(2x,'Input area of C5 from G.C.')
        read*, pentaar
        write(*,225) pentaar
        write(22,225) pentaar
225     format(4x,';',2x,f9.5)
C
        write(*,230)
```

```
      write(22,230)
230   format(2x,'Input area of C6 from G.C.')
      read*, hexanar
      write(*,235) hexanar
      write(22,235) hexanar
235   format(4x,';',2x,f9.5)
C
C     Consider relative sensitivity data for hydrogen flame
C     detector [FID].....
C     Adapted from " W.A. Dietz, "Response Factors for Gas
C     Chromatographic Analysis", J. of G.C., Feb, 1987, p.68.....
C
      tmethar=methaar/0.97
      tethaar=ethanar/0.97
      tpropar=propaar/0.98
      tbutaar=butanar/1.09
      tpentar=pentaar/1.04
      thexaar=hexanar/1.03
C
      totalar=tmethar+tethaar+tpropar+
     &  tbutaar+tpentar+thexaar
C
      methawt=tmethar/totalar*100.
      ethanwt=tethaar/totalar*100.
      propawt=tpropar/totalar*100.
      butanwt=tbutaar/totalar*100.
      pentawt=tpentar/totalar*100.
      hexanwt=thexaar/totalar*100.
C
      metha=gasout*methawt/100.
      ethan=gasout*ethanwt/100.
      propa=gasout*propawt/100.
      butan=gasout*butanwt/100.
      penta=gasout*pentawt/100.
      hexan=gasout*hexanwt/100.
C
C     Input the Simulated Distillation results for
C     hydrotreated product.....
C
      write(*,240)
      write(22,240)
240   format(2x,'Input wt% of up to 400 [F] from Simdis')
      read*, naphtwt
      write(*,245) naphtwt
      write(22,245) naphtwt
245   format(4x,';',2x,f9.5)
C
      write(*,250)
      write(22,250)
250   format(2x,'Input wt% of 400 to 650 [F] from Simdis')
      read*, distiwt
      write(*,255) distiwt
      write(22,255) distiwt
255   format(4x,';',2x,f9.5)
```

```
C
      write(*,260)
      write(22,260)
260   format(2x,'Input wt% of 650 to 1000 [F] from Simdis')
      read*, gasoiwt
      write(*,265) gasoiwt
      write(22,265) gasoiwt
265   format(4x,';',2x,f9.5)
C
      write(*,270)
      write(22,270)
270   format(2x,'Input wt% of > 1000 [F] from Simdis')
      read*, residwt
      write(*,275) residwt
      write(22,275) residwt
275   format(4x,';',2x,f9.5)
C

      napht=liqout*naphtwt/100.
      disti=liqout*distiwt/100.
      gasoi=liqout*gasoiwt/100.
      resid=liqout*residwt/100.
C
      chliq=water+napht+disti+gasoi+resid
      chgas=ammonia+hysulf+metha+ethan+propa+butan+
     &  penta+hexan
C
      total=chliq+chgas
C
      write(*,280)
      write(22,280)
280   format(2x,'Is total product gas and liquid = feed amount ?')
      write(*,285) total
      write(22,285) total
285   format(4x,';',2x,f9.5)
C
C
C     Based on amount of feed (assumed to be 100 [g]),
C     calculate all gas and liquid hydrotreated products including
C     NH3, H2S, H20, C1-C4 Gases, C5+ naphtha, distillate, gas oil
C     and residuum fractions by weight.....
C
      ammonia1=(ammonia/fd)*100.
      hysulf1=(hysulf/fd)*100.
      water1=(water/fd)*100.
      metha1=(metha/fd)*100.
      ethan1=(ethan/fd)*100.
      propa1=(propa/fd)*100.
      butan1=(butan/fd)*100.
      napht1=((penta+hexan+napht)/fd)*100.
      disti1=(disti/fd)*100.
      gasoi1=(gasoi/fd)*100.
      resid1=(resid/fd)*100.
C
```

```
      hcgas=metha1+ethan1+propa1+butan1
C
      write(*,290)
      write(22,290)
290   format(2x,'wt% of ammonia in product')
      write(*,295) ammonia1
      write(22,295) ammonia1
295   format(4x,';',2x,f9.5)
C
      write(*,300)
      write(22,300)
300   format(2x,'wt% of hydrogen sulfide in product')
      write(*,305) hysulf1
      write(22,305) hysulf1
305   format(4x,';',2x,f9.5)
C
      write(*,310)
      write(22,310)
310   format(2x,'wt% of water in product')
      write(*,315) water1
      write(22,315) water1
315   format(4x,';',2x,f9.5)
C
      write(*,320)
      write(22,320)
320   format(2x,'wt% of methane in product')
      write(*,325) metha1
      write(22,325) metha1
325   format(4x,';',2x,f9.5)
C
      write(*,330)
      write(22,330)
330   format(2x,'wt% of ethane in product')
      write(*,335) ethan1
      write(22,335) ethan1
335   format(4x,';',2x,f9.5)
C
      write(*,340)
      write(22,340)
340   format(2x,'wt% of propane in product')
      write(*,345) propa1
      write(22,345) propa1
345   format(4x,';',2x,f9.5)
C
      write(*,350)
      write(22,350)
350   format(2x,'wt% of butane in product')
      write(*,355) butan1
      write(22,355) butan1
355   format(4x,';',2x,f9.5,//)
C
      write(*,357)
      write(22,357)
357   format(2x,'wt% C1 to C4 gases in product')
```

```
      write(*,359) hcgas
      write(22,359) hcgas
359   format(4x,';',2x,f9.5)
C
      write(*,360)
      write(22,360)
360   format(2x,'wt% of C5 to 400 [F] in product')
      write(*,365) napht1
      write(22,365) napht1
365   format(4x,';',2x,f9.5)
C
      write(*,370)
      write(22,370)
370   format(2x,'wt% of 400 to 650  [F] in product')
      write(*,375) disti1
      write(22,375) disti1
375   format(4x,';',2x,f9.5)
C
      write(*,380)
      write(22,380)
380   format(2x,'wt% of 650 to 1000 [F] in product')
      write(*,385) gasoi1
      write(22,385) gasoi1
385   format(4x,';',2x,f9.5)
C
      write(*,390)
      write(22,390)
390   format(2x,'wt% of >1000 [F] in product')
      write(*,395) resid1
      write(22,395) resid1
395   format(4x,';',2x,f9.5,//)
C
C
      total2=ammonia1+hysulf1+water1+hcgas+napht1+disti1+gasoi1+resid1
C
      write(*,400)
      write(22,400)
400   format(2x,'sum of total wt% of products should be 100')
      write(*,405) total2
      write(22,405) total2
405   format(4x,';',2x,f9.5)
C
C
      stop
      end
```

APPENDIX C

FORTRAN PROGRAM FOR CALCULATING HYDROGEN CONSUMPTION (HYDROGEN.FOR)

```
C
C       Program "Hydrogen.for"
C
C       This program is used to calculate hydrogen consumption
C       for hydrotreating of heavy oil over HDM catalyst.
C
C                                                  by Seokhwan Kwak
C
C
C
        implicit double precision (a-h,o-z)
        double precision metha
C
C
C       Initialization....
C
C
        open(22, file='d13h2cos', status='unknown')
C
C       Input the amount of hydrogen going into the hydrotreater and
C       the amount of hydrogen+methane+ethane+ethylene coming out of the
C       liquid nitrogen trap.....
C
        write(*,10)
        write(22,10)
10      format(2x,'Input amount of hydrogen going in l[stp]/hr')
        read*, hydin
        write(*,15) hydin
        write(22,15) hydin
15      format(4x,';',2x,f9.5,2x,'liter[stp]/hr',/)
        write(*,20)
        write(22,20)
20      format(2x,'Input amount of hydrogen+C1+C2 going out l[stp]/hr')
        read*, gasout
        write(*,25) gasout
        write(22,25) gasout
25      format(4x,';',2x,f9.5,2x,'liter[stp]/hr',/)
C
C       Enter gas chromatographic results for hydrogen+C1 to C2 gases from
C       the liquid nitrogen trap.....
C
        write(*,30)
        write(22,30)
30      format(2x,'Input area of methane')
        read*, metha
        write(*,35) metha
        write(22,35) metha
35      format(4x,';',2x,f9.5)
        write(*,40)
        write(22,40)
40      format(2x,'Input area of ethane')
        read*, ethan
        write(*,35) ethan
        write(22,35) ethan
```

```
      write(*,50)
      write(22,50)
50    format(2x,'Input area of ethylene')
      read*, ethyl
      write(*,55) ethyl
      write(22,55) ethyl
55    format(4x,':',2x,f9.5,/)
C
C     Calculate volumes of hydrogen, methane, ethane and ethylene
C     at std condition based on standard sample areas.....
C
      write(*,60)
      write(22,60)
60    format(2x,'Input atmospheric temperature [C]')
      read*, temp
      write(*,65) temp
      write(22,65) temp
65    format(4x,':',2x,f5.1,2x,'[C]')
      write(*,70)
      write(22,70)
70    format(2x,'Input atmospheric pressure [mmHg]')
      read*, press
      write(*,75) press
      write(22,75) press
75    format(4x,':',2x,f5.1,2x,'[mmHg]',/)
C
      sareac1=2.6387
      sareac2=4.7985
      sareac3=8.3760
C
      vstd1=(metha*5.e-4/sareac1)*(273.15/(temp+273.15))*(press/760.)
      vstd2=(ethan*5.e-4/sareac2)*(273.15/(temp+273.15))*(press/760.)
      vstd3=(ethyl*5.e-4/sareac3)*(273.15/(temp+273.15))*(press/760.)
      vstd4=5.e-1 - vstd1-vstd2-vstd3
C
C     Normalization and get the volume % of hydrogen only among
C     exit gas from liquid nitrogen trap.....
C
      vstd=vstd1+vstd2+vstd3+vstd4
C
      vstd11=vstd1/vstd
      vstd21=vstd2/vstd
      vstd31=vstd3/vstd
      vstd41=vstd4/vstd
C
      hydout=gasout*vstd41
C
C     Simple check of normalization result.....
C
      chtotal=vstd11+vstd21+vstd31+vstd41
C
      write(*,80) chtotal
      write(22,80) chtotal
```

```
80      format(2x,'After normalization, total volume should be
   &    1;',2x,f3.1/)
C
        write(*,90)
        write(22,90)
90      format(2x,'Input liquid feeding in [cc/hr]')
        read*, vel
        write(*,95) vel
        write(22,95) vel
95      format(4x,':',2x,f9.5,2x,'[cc/hr]',/)
C
C       Finally, calculate hydrogen consumption for heavy oil
C       hydrotreating by HDM catalyst in various units.....
C
        hydcons=(hydin-hydout)*(1000.*5.614578)/(vel)
        hydcons1=(hydin-hydout)*2./(22.4*vel*0.9144)
        hydcons2=hydcons*(28.31685/158.98729)
C
        write(*,100)
        write(22,100)
100     format(2x,'hydrogen consumption in scfH2/bblfeed')
        write(*,105) hydcons
        write(22,105) hydcons
105     format(4x,':',2x,f9.5,2x,'[scf H2/bbl feed]')
        write(*,110)
        write(22,110)
110     format(2x,'hydrogen consumption in gH2/gfeed')
        write(*,105) hydcons1
        write(22,105) hydcons1
115     format(4x,':',2x,f9.5,2x,'[g H2/g feed]')
        write(*,120)
        write(22,120)
120     format(2x,'hydrogen consumption in lH2/lfeed')
        write(*,125) hydcons2
        write(22,125) hydcons2
125     format(4x,':',2x,f9.5,2x,'[liter H2/liter feed]')
C
C
C
        stop
        end
```

APPENDIX D

FORTRAN PROGRAM FOR KINETICS OF TWO PARALLEL FIRST-ORDER REACTIONS USING NON-LINEAR REGRESSION (MINPACK SUBROUTINE)

```
C
C       This program is used to calculate kinetic parameters for hydrotreating the
C       Whiterocks bitumen over a commercial (UNOCAL) catalyst.  This program uses
C       the non-linear regression MINPACK routine and is specially made for two parallel first
C       order nickel removal reactions (facile and refractory fractions).
C
C                                                                   by Seokhwan Kwak
C
        INTEGER J,M,N,INFO,LWA,NWRITE
        INTEGER IWA(5)
        DOUBLE PRECISION TOL,FNORM,L2NORM
        DOUBLE PRECISION X(5),FVEC(12),WA(99)
        DOUBLE PRECISION ENORM,DPMPAR
        DOUBLE PRECISION TIME,CAL(12),DIFF,AAD
        DOUBLE PRECISION TIME,CALCP,EXPCP,DIFF1
        DOUBLE PRECISION T,WHSV,P,EXPT,ALPHA,BETA,CP
        COMMON /KWAKDAT/T(12), WHSV(12), P(12),EXPT(12),ALPHA,BETA,CP(12)
        EXTERNAL FCN
C
C       LOGICAL OUTPUT UNIT IS ASSUMED TO BE NUMBER 11.
C
        DATA NWRITE /11/
C
        M = 12
        N = 5
C
C       THE FOLLOWING STARTING VALUES PROVIDE A ROUGH FIT.
C
C       Here,   X(1) = gamma
C               X(2) = K10
C               X(3) = K20
C               X(4) = E1 [J mol-1]
C               X(5) = E2 [J mol-1]  .....
C
        X(1) = .1d0
        X(2) =  0.6d5
        X(3)= 0.6d6
        X(4) =  0.78d5
        X(5) = 0.89d5
C
        LWA = 150
C
C       SET TOL TO THE SQUARE ROOT OF THE MACHINE PRECISION.
C       UNLESS HIGH PRECISION SOLUTIONS ARE REQUIRED,
C       THIS IS THE RECOMMENDED SETTING.
C
        TOL = DSQRT(DPMPAR(1))*1.d4
C
        CALL LMDIF1(FCN,M,N,X,FVEC,TOL,INFO,IWA,WA,LWA)
        FNORM = ENORM(M,FVEC)
C
        OPEN(NWRITE,FILE='hdnialtr.out',STATUS='UNKNOWN')
C
        WRITE (NWRITE,1000) FNORM,INFO,(X(J),J=1,N)
```

```
      WRITE (*,1000) FNORM,INFO,(X(J),J=1,N)
C
1000  FORMAT (5X,31H FINAL L2 NORM OF THE RESIDUALS,D15.7 //
     *  5X,15H EXIT PARAMETER,16X,I10 //
     *  5X,27H FINAL APPROXIMATE SOLUTION // 3X,5D15.7)
C
      WRITE(6,9994)
      WRITE(NWRITE,9994)
9994  FORMAT(//5X, 'Time(hr)', 6X, 'Exptl.', 9X, 'Cald.',
     1  9X, 'Diff', 10X, 'AAD %',
     2  /5X, '========', 6X, '======', 9X, '=====',
     3  9X, '====', 10X, '=====')
C
      S=0.D0
      DO 5 I=1,M
      CALL CALCUL(I, N, X, CAL)
      TIME=1.D0/WHSV(I)
      DIFF=CAL(I)-EXPT(I)
      AAD=100.D0*ABS(DIFF)/EXPT(I)
      S=S+AAD
      WRITE(6, 9993) TIME, EXPT(I), CAL(I), DIFF, AAD
      WRITE(NWRITE,9993) TIME, EXPT(I), CAL(I), DIFF, AAD
9993  FORMAT(7X, F5.3, 4X, 4(1X, F12.8))
5     CONTINUE
C
      S=S/M
      WRITE(6,9992) S
      WRITE(NWRITE,9992) S
9992  FORMAT(/5X, 'AAD: ', F14.8, '%'//)
C
      WRITE(6,1112)
      WRITE(NWRITE,1112)
1112  FORMAT(//5X, 'Time(hr)', 6X, 'Cp(exp)', 9X, 'Cp(cal)',
     1  9X, 'Diff', 10X, 'L2 norm',
     2  /5X, '========', 6X, '======', 9X, '=====',
     3  9X, '====', 10X, '=====')
C
      DO 6 I=1,M
      CALL CALCUL(I, N, X, CAL)
      TIME=1.D0/WHSV(I)
      EXPCP=CP(I)
      CALCP=(CAL(I))
      DIFF1=EXPCP-CALCP
      L2NORM=DIFF1**2.D0
      S1=S1+L2NORM
      WRITE(6, 9993) TIME, EXPCP, CALCP, DIFF1, S1
      WRITE(NWRITE,9993) TIME, EXPCP, CALCP, DIFF1, S1
6     CONTINUE
C
      WRITE(6,*) S1
      WRITE(NWRITE,*) S1
C
      STOP
      END
```

```
C
C
      SUBROUTINE FCN(M,N,X,FVEC,IFLAG)
      INTEGER M,N,IFLAG,I
      DOUBLE PRECISION X(N),FVEC(M),CAL(12),EXPT
      DOUBLE PRECISION CONCPROD,CONCFEED,CP(12)
      DOUBLE PRECISION T,WHSV,P,EXPT,ALPHA,BETA,CP
      COMMON /KWAKDAT/T(12), WHSV(12), P(12),EXPT(12),ALPHA,BETA,CP(12)
C
      DATA CONCFEED/0.0072D0/
      DATA (CP(I),I=1,12)/0.0039d0,0.0040d0,0.0055d0,0.0023d0,
     &                    0.0025d0,0.0030d0,0.0033d0,0.00198d0,
     &                    0.00137d0,0.0031d0,0.0025d0,0.0022d0/
C
      DO 50 I=1,12
C
      CONCPROD=CP(I)
      EXPT(I)=CONCPROD
C
      CALL CALCUL(I,N,X,CAL)
      FVEC(I)=CAL(I) - EXPT(I)
50    CONTINUE
C
      RETURN
      END
C
C
      SUBROUTINE CALCUL(I, N, X, CAL)
      IMPLICIT REAL*8 (A-H,O-Z)
      DIMENSION X(N)
      DOUBLE PRECISION WHSVE,PRESS,TEMP,CAL(12),K1,K2
      DOUBLE PRECISION T,WHSV,P,EXPT,ALPHA,BETA,CP
      COMMON /KWAKDAT/T(12), WHSV(12), P(12),EXPT(12),ALPHA,BETA,CP(12)
C
      DATA (P(I),I=1,12)/13.4892d0,13.2361d0,13.3706d0,13.5050d0,
     &                   13.4268d0,13.1797d0,13.4434d0,13.3926d0,
     &                   13.1069d0,10.8405d0,14.9383d0,16.0327d0/
      DATA (T(I),I=1,12)/619.8550d0,642.3613d0,652.9521d0,664.7213d0,
     &                   673.3173d0,684.6519d0,662.2412d0,665.1570d0,
     &                   665.7481d0,664.6790d0,664.7027d0,664.4580d0/
      DATA (WHSV(I),I=1,12)/0.76978d0,0.76578d0,0.769456d0,0.76676d0,
     &                      0.757103d0,0.762504d0,1.37578d0,0.432506d0,
     &                      0.24429d0,0.76683d0,0.76007d0,0.771431d0/
C
      DATA CONCFEED/0.0072D0/
      DATA ALPHA,BETA/0.9164538d0,1.759649d0/
C
      TEMP=T(I)
      WHSVE=WHSV(I)
      PRESS=P(I)
C
      K1=X(2)*EXP(-(X(4)/8.314D0)*(1.D0/TEMP))
      K2=X(3)*EXP(-(X(5)/8.314D0)*(1.D0/TEMP))
C
```

```
      CAL(I)=((X(1)*EXP(-K1*PRESS**BETA/(WHSVE**ALPHA)))+(1.D0-X(1))*
     *  EXP(-K2*PRESS**BETA/(WHSVE**ALPHA)))*CONCFEED
      RETURN
      END
```

APPENDIX E

INPUT FILE FOR PROCESS SIMULATION

```
TITLE PROBLEM=HTTEMP, PROJECT=HDMBIT, USER=KWAKRJDS, DATE=JUN/10/93
DIMENSION ENGLISH, TEMP=F
PRINT INPUT=NONE, STREAM=NONE
COMPONENT DATA
 LIBID 1,HYDROGEN / 2,WATER / 3,HYSULFID / 4,AMMONIA / 5,METHANE /    *
     6,ETHANE / 7,PROPANE / 8,BUTANE / 9,PENTANE / 10,HEXANE
 TBPCUTS 100,1488,15
THERMODYNAMICS DATA
 METHODS SYSTEM=GS, TRANSPORT=PETRO
STREAM
 OUTPUT   FORMAT=1, NSTREAMS=4, STREAMS= F13, F14, F15, F16
 FORMAT   IDNO=1, PAGE, NAME, PHASE, LINE, CPCT(M), LINE, ARATE(M,HR), *
       ARATE(W,LB,HR), TEMP, PRES, LFRAC, LINE, ENTHALPY(T),       *
       ENTROPY(T), DENSITY, TC, PC, VC, ZC, ACENTRIC, LINE,        *
       SSPGR(WATER), SAPI, MW, NBP, CP(W), PAGE, NAME, PHASE, LINE, *
       CRATE(W), LINE, CPCT(W)
$  INPUT STREAMS
 PROPERTY STRM=F13, TEMP=350, PRES=1983, RATE(W)=256.586, ASSAY=WT
 TBP     STRM=F13,*
       DATA 0.4822,304 / 1.6495,421 / 6.2566,520 / 9.7234,601 /    *
          18.8604,716 / 26.8391,808 / 44.2711,911.5 /              *
          61.5871,1003 / 76.2614,1105 / 100,1285.14
 API     AVG=15.183, STRM=F13
 PROPERTY STRM=F14, TEMP=350, PRES=1983, RATE(W)=27.668,                *
       COMP(W)=1,0.78868 / 2,0.03044 / 3,0.01353 / 4,0.02671 /     *
            5,0.02773 / 6,0.02625 / 7,0.04473 / 8,0.02185 /      *
            9,0.01169 / 10,0.00837
UNIT OPERATIONS
 FEED F13, F14
 PROD V=F15, L=F16
 ISO  TEMP=736.8, PRES=1995
END
```

APPENDIX F

OUTPUT FILE FOR PROCESS SIMULATION

VERSION 3.02, VAX 77 TM
SIMULATION SCIENCES INC. PROCESS PAGE 1
PROJECT HDMBIT KWAKRJDS
PROBLEM HTTEMP INPUT JUN/10/93

VIIIA UNIT - STREAM CORRELATION MATRIX

UNIT NO	ID	====== FEED STREAM IDS ======					===== PRODUCT STREAM IDS =====	
4	HD11	F13	F14	-	-	-	F15	F16

VIIIC CALCULATIONAL SEQUENCE IS DEFINED BY INPUT

*** ALL INPUT DATA IN ORDER ***

**** PROBLEM SOLUTION REACHED ****

UNIT ID HD11
NUMBER 1
NAME
TYPE FLASH

FEEDS F13
F14

PRODUCTS F15 (V)
F16 (L)

TEMP, DEG F 736.8000
PRESSURE, PSIA 1995.0000
FRACTION LIQUID 0.06414
DUTY, MM BTU /HR 0.10339

VERSION 3.02, VAX 77 TM
SIMULATION SCIENCES INC. PROCESS PAGE 11
PROJECT HDMBIT KWAKRJDS
PROBLEM HTTEMP SOLUTION JUN/10/93

*** USER-DEFINED STREAM SUMMARY OUTPUT ***

STREAM ID.	F13	F14	F15	F16
STREAM NAME				
STREAM PHASE	LIQUID	VAPOR	VAPOR	LIQUID
COMP. MOLE PERCENTS.				
1 HYDROGEN	0.0000	98.0191	97.2015	27.5007
2 WATER	0.0000	0.4234	0.4067	0.3104
3 HYSULFID	0.0000	0.0995	0.0874	0.1921
4 AMMONIA	0.0000	0.3929	0.3887	0.1241
5 METHANE	0.0000	0.4331	0.4278	0.1451
6 ETHANE	0.0000	0.2187	0.2109	0.1485
7 PROPANE	0.0000	0.2542	0.2439	0.1905
8 BUTANE	0.0000	0.0942	0.0891	0.0887
9 PENTANE	0.0000	0.0406	0.0376	0.0499
10 HEXANE	0.0000	0.0243	0.0219	0.0388
11 NBP - 75	0.0000	0.0000	0.0000	0.0000
12 NBP 256	0.0000	0.0000	0.0000	0.0000
13 NBP 326	3.9918	0.0000	0.1821	0.7001
14 NBP 419	2.1175	0.0000	0.0855	0.5330
15 NBP 551	11.4195	0.0000	0.3121	5.0518
16 NBP 613	6.3807	0.0000	0.1263	3.5249
17 NBP 709	12.4306	0.0000	0.1186	8.7259
18 NBP 797	9.4474	0.0000	0.0355	7.4283
19 NBP 889	17.9606	0.0000	0.0199	14.8166
20 NBP 976	13.3873	0.0000	0.0038	11.2057
21 NBP 1071	9.5353	0.0000	0.0005	8.0139
22 NBP 1164	7.8793	0.0000	0.0001	6.6269
23 NBP 1252	5.4500	0.0000	0.0000	4.5842
24 NBP 1344	0.0000	0.0000	0.0000	0.0000
25 NBP 1434	0.0000	0.0000	0.0000	0.0000
RATE, LB MOLS/HR	0.6297	11.0430	10.9240	0.7487
RATE, LB /HR	256.5860	27.6680	48.8354	235.4186
TEMPERATURE, DEG F	350.0000	350.0000	736.8000	736.8000
PRESSURE, PSIA	1983.0000	1983.0000	1995.0000	1995.0000
MOLE FRAC LIQUID	1.0000	0.0000	0.0000	1.0000
ENTHALPY, MM BTU /HR	0.0251	0.0009	0.0411	0.0883
ENTROPY, M BTU /HR F	0.0800	0.2263	0.2651	0.1424
ACT.DENS, LB /FT3	56.0270	0.5386	0.6628	44.4758
CRIT. TEMP, F	1150.4110	-386.8691	-376.0008	747.6270
CRIT. PRES, PSIA	187.8697	212.5301	212.5935	190.8625
CRIT. VOLUME, FT3/LB MOLE	22.2287	1.0580	1.1642	17.3172
CRIT. COMPRESS. (ZC)	0.2175	0.3041	0.3036	0.2388
ACENTRIC FACTOR	0.9189	-0.2121	-0.2052	0.6386
STD. SPGR, (H2O,60F)	0.9662	0.0856	0.1430	0.9523
STD. API GRAVITY	14.9534	1521.3000	858.0804	17.0907
MOLECULAR WEIGHT	407.4461	2.5055	4.4705	314.4485
NML. BOIL PT., (MOLE) F	839.9493	-415.3532	-407.1068	520.2131
CP, BTU /LB F	0.5542	2.8503	1.8979	0.7290

APPENDIX G

NON-LINEAR NUMERICAL INTEGRATION FORTRAN PROGRAM FOR MOLECULAR WEIGHT REDUCTION MODEL

```
C
C       This is the main program for solving ODE equations and performing
C     nonlinear regressions using the SIMPLEX method simultaneously.
C     This program was developed to obtain the best reaction constants
C     at 735 [F] for the series of irreversible first-order reactions in a plug-flow reactor.
C     All data were obtained for hydrotreating of Whiterocks bitumen over a commercial
C     UNOCAL hydrodemetallation catalyst.....
C
C                                                  By Seokhwan Kwak
C
C
C
C     The molecular weight reduction reaction scheme was examined by lumping
C     HT products into four representive groups, which are
C   -       Resid (b.p. > 538 C)
C   -       Total Gas Oil (275 C < b.p. < 538 C)
C   -       Middle Distillates (C5 < b.p. < 275 C)
C   -       Gases (including NH3, H2S, C1 to C4 Hydrocarbon gases).....
C
C
C
C     The proposed irreversible first order reaction scheme is as follows.....
C
C             Resid--(kro)--> Total Gas Oil --(kod)--> Middle Distillates
C                                  |                          |
C                                  |--(kog)-->  Gases  <--(kdg)--|
C
C     where,
C     kro = rate constant from resid to total gas oil [1/hr] (=X(1))
C     kod = rate constant from total gas oil to middle distillates [1/hr] (=X(2))
C     kog = rate constant from total gas oil to gases [1/hr] (=X(3))
C     kdg = rate constant from middle distillates to gases [1/hr] (=X(4)).....
C
C
C
      IMPLICIT REAL*8 (A-H, O-Z)
      CHARACTER *1 CC, CC1, CC2, CNAME*11
      DIMENSION X(6), XX(7,6), FX(7), C(6), Y(6), Z(6), V(6)
      EXTERNAL F
      WRITE(6,200)
200   FORMAT(2X, 'The name of output file: ', $)
      READ (5,210) CNAME
210   FORMAT(A11)
      OPEN (1, FILE=CNAME, STATUS='NEW')
C
C
C     Input all the initial informations including initial guesses.....
C
      WRITE(6,150)
150   FORMAT(2X, 'The dimension of parameter: ', $)
      READ(5,*) N
      WRITE(6,170)
      READ(5,*) ITMAX
      WRITE(6,190)
```

```
      READ(5,*) EPS
5     CONTINUE
      WRITE(1,220) N, ITMAX, EPS
220   FORMAT('1 ', 'Dimension of parameter:    ', I9,
     *    2X, 'Maximum iteration time:   ', I9,
     *    2X, 'Convergence criterion:    ', E9.2)
      WRITE(6,100)
100   FORMAT(2X, 'The initial guesses:',)
      DO 10 I=1,N
      WRITE(6,110) I
110   FORMAT(5X, 'X(', I2, ')= ? ', $)
      READ(5,*) X(I)
10    CONTINUE
      WRITE(6,120) (X(I), I=1,N)
      WRITE(1,120) (X(I), I=1,N)
120   FORMAT (2X, 'The initial value:',5X, 6D12.4)
C
C
C     Now call subroutine SIMPLEX for solving nonlinear regression, which calls
C     FX in RK4 for solving ODEs simultaneously.....
C
      CALL SIMPLEX(N, ITMAX, EPS, X, XX, FX, C, Y, Z, V, FY, 0, IP1, F)
C
C
C     The subroutine STTEST is used to evaluate the overall performance of the
C     results obtained from this program.  This will include the relative
C     errors like AAD, etc.....
C
      CALL STTEST(N,X,IP1)
C
C
C     If the desired AAD was not obtained in the previous run
C     the following subroutine will rerun the program.....
C
      WRITE(6,130)
130   FORMAT (2X, 'Going on with another initial values? (Y/N) ', $)
      READ(5,140) CC
140   FORMAT(A1)
      IF(CC .EQ. 'Y' .OR. CC .EQ. 'y') THEN
      WRITE(6,160)
160   FORMAT(2X, 'to change the max. iteration time? (Y/N) ', $)
      READ(5,140) CC1
      IF (CC1 .EQ. 'Y' .OR. CC1 .EQ. 'y') THEN
      WRITE(6,170)
170   FORMAT(2X, 'The max. number of iterations: ', $)
      READ (5,*) ITMAX
      ENDIF
      WRITE(6,180)
180   FORMAT(2X, 'to change the convergence criterion? (Y/N) ', $)
      READ(5,140) CC2
      IF (CC2 .EQ. 'Y' .OR. CC2 .EQ. 'y') THEN
      WRITE(6,190)
190   FORMAT(2X, 'The convergence criterion: ', $)
      READ (5,*) EPS
```

```
      ENDIF
      GOTO 5
      ENDIF
      CLOSE (1)
      STOP
      END
C
C
C     The following subroutine is a general SIMPLEX method.....
C
C
      SUBROUTINE SIMPLEX(N, ITMAX, EPS, X, XX, FX, C, Y, Z, V, FY,
     2                                IP, IP1, F)
C
      IMPLICIT REAL *8 (A-H, O-Z)
      CHARACTER ACTION*12, FLIP*5, ACTP*17
      DIMENSION X(N), XX(N+1,N), FX(N+1), C(N), Y(N), Z(N), V(N)
      EXTERNAL F
      DATA R, T, S/1.0D0, 2.0D0, 0.5D0/
      DATA FLIP/'Flip'/
C
C
C     Initialization.....
C
      ITER=0
      LINE=0
      IFLIP=0
      ACTION='          '
      ACTP = '              '
      L=N/7+1
C
C
C     Calculate the coordinate of other N vertices.....
C
      SQ1=SQRT(FLOAT(N+1))-1
      SQ=N*SQRT(2.0D0)
      P=(SQ1+N)/SQ
      Q=SQ1/SQ
      DO 200 I=1,N
      XX(1,I)=X(I)
200   CONTINUE
      DO 210 I=2,N+1
      I1=I-1
      DO 210 J=1,N
      IF (I1 .EQ. J) THEN
      XX(I,J)=X(J)+P
      ELSE
      XX(I,J)=X(J)+Q
      ENDIF
210   CONTINUE
5     CONTINUE
C
C
C     Calculate the function values at every vertex.....
```

```
C
      DO 10 I=1,N+1
      DO 8 J=1,N
      X(J)=XX(I,J)
8     CONTINUE
      CALL F(X,N,FX(I))
10    CONTINUE
C
C
C     Search for the max. and the min. points.....
C
15    CONTINUE
      FMAX=-1.0D38
      FMIN=1.0D38
      DO 17 I=1,N+1
      IF (FX(I) .GT. FMAX) THEN
      FMAX=FX(I)
      IMAX=I
      ENDIF
      IF (FX(I) .LT. FMIN) THEN
      FMIN=FX(I)
      IMIN=I
      ENDIF
17    CONTINUE
C
C
C     Print the title for the intermediate results.....
C
      IF (MOD(LINE,53) .EQ. 0) THEN
C     WRITE(1,1000)
      IF (IP1 .EQ. 1) WRITE(6,1000)
1000  FORMAT('1', 'No of IT', 2X, 'Action', 16X, 'F(min)',
     *      11X, 'X(min)',
     *      /1X, '========', 2X, '======', 16X, '======',
     *      11X, '======',/)
      ENDIF
C
C     Check to see if the action is combined with flip.....
C
      IF (IFLIP .EQ. 1) THEN
      ACTP=FLIP//ACTION
      IFLIP=0
      ELSE
      ACTP=ACTION
      ENDIF
C
C
C     Print the intermediate results: iteration time, action taken,
C     coordinate and function value at the minimum point.....
C
C     WRITE(1,1010) ITER, ACTP, FX(IMIN), (XX(IMIN,J),J=1,N)
      IF (IP1 .EQ. 1)
     *  WRITE(6,1010) ITER, ACTP, FX(IMIN), (XX(IMIN,J),J=1,N)
1010  FORMAT(2X, I4, 5X, A17, D15.6, 2X, /5X, D11.3)
```

```
      ACTP='              '
      LINE=LINE+1
C
C
C     Check to see if the criterion is satisfied, if so, return.....
C
      SS=0.0D0
      DO 170 I=1,N+1
      SS=SS+(FX(I)-FX(IMIN))**2
170   CONTINUE
      SS=SQRT(SS/N)
      IF (SS .LT. EPS) THEN
      FY=FX(IMIN)
      DO 175 I=1,N
      X(I)=XX(IMIN,I)
175   CONTINUE
      WRITE(6,1020) ITER, FY, (X(I),I=1,N)
      WRITE(1,1020) ITER, FY, (X(I),I=1,N)
1020  FORMAT(5X, 'No. of iterations:', I10,
     *   /5X, 'Function value(min):', D20.10/
     *    5X, 'The coordinate:', 5X, (4X, 7D18.10, :, ))
      RETURN
      ENDIF
C
C
C     Check to see if the max. iteration times have been reached, if
C     so, print a message and return.....
C
      IF (ITER .GT. ITMAX) THEN
      DO 180 I=1,N
      X(I)=XX(IMIN,I)
180   CONTINUE
      FY=FX(IMIN)
C     WRITE(1,1030) ITMAX, ITER, FY, (X(I),I=1,N)
      WRITE(6,1030) ITMAX, ITER, FY, (X(I),I=1,N)
1030  FORMAT(//2X,' ** The max. iteration time,', I5, ' has been ',
     *    'reached, but the convergence is not satisfied.',
     *    /5X, 'No. of iterations:', I10,
     *    /5X, 'Function value(min):', D20.10,
     *    /5X, 'The coordinate:',/5X, (4X, 7D18.10, :, /))
      RETURN
      ENDIF
C
C
C     Search the second max. point.....
C
      SS=-1.0D38
      DO 18 I=1,N+1
      IF (I .NE. IMAX) THEN
      IF (FX(I) .GT. SS) THEN
      SS=FX(I)
      IMAXS=I
      ENDIF
      ENDIF
```

```
18      CONTINUE
C
C
C       Calculate the coordinate of the centroid.....
C
        DO 20 I=1,N
        C(I)=0.0D0
20      CONTINUE
        DO 22 I=1,N
        DO 22 J=1,N+1
        IF (J .NE. IMAX) C(I)=C(I)+XX(J,I)
22      CONTINUE
        DO 25 I=1,N
        C(I)=C(I)/N
25      CONTINUE
C
C
C       Print the coordinate and function values at every vertex,
C       and the coordinate of centroid if IP=1.....
C
        IF (IP .EQ. 1) THEN
        WRITE(2,1040) ITER, (C(I),I=1,N)
1040    FORMAT(/2X,'ITERATION TIME:', I10, 5X,'CC:',/5X, F10.3)
        DO 270 I=1,N+1
        JJ=0
        DO 265 J=1,N
        IF (ABS(FX(J)) .LT. 1E-3) THEN
        JJ=1
        GOTO 267
        ENDIF
265     CONTINUE
267     CONTINUE
        IF (JJ .EQ. 0) THEN
        WRITE(2,1060) I, FX(I), (XX(I,J),J=1,N)
        ELSE
        WRITE(2,1050) I, FX(I), (XX(I,J),J=1,N)
        ENDIF
1050    FORMAT(2X, 'FX(', I1, '):', E10.3, 5X, 'XX:', /5X, F10.3)
1060    FORMAT(2X, 'FX(', I1, '):', F10.3, 5X, 'XX:', /5X, F10.3)
270     CONTINUE
        ENDIF
        ITER=ITER+1
C
C
C       Reflection.....
C
        DO 30 I=1,N
        Y(I)=C(I)+R*(C(I)-XX(IMAX,I))
30      CONTINUE
C
C
C       The function value at the new point.....
C
        CALL F(Y,N,FY)
```

```
      IF (FY .LT. FX(IMIN)) THEN
C
C
C     Expansion.....
C
      DO 40 I=1,N
      Z(I)=C(I)+T*(C(I)-XX(IMAX,I))
40    CONTINUE
      CALL F(Z,N,FZ)
      IF (FZ .LT. FY) THEN
C
C
C     The expansion has succeeded.....
C
      DO 45 I=1,N
      XX(IMAX,I)=Z(I)
45    CONTINUE
      FX(IMAX)=FZ
      ACTION='Expansion   '
      GOTO 15
      ELSE
      DO 50 I=1,N
      XX(IMAX,I)=Y(I)
50    CONTINUE
      FX(IMAX)=FY
      ACTION='Reflection  '
      GOTO 15
      ENDIF
      ELSEIF (FY .LT. FX(IMAXS)) THEN
C
C
C     Exchange .....
C
      DO 60 I=1,N
      XX(IMAX,I)=Y(I)
60    CONTINUE
      FX(IMAX)=FY
      ACTION='Exchange    '
      GOTO 15
      ELSE
      IF (FY .LT. FX(IMAX)) THEN
C
C
C     Flip.....
C
      DO 70 I=1,N
      XX(IMAX,I)=Y(I)
70    CONTINUE
      FX(IMAX)=FY
      IFLIP=1
       ENDIF
C
C
C     Contraction.....
```

```
C
      DO 80 I=1,N
      V(I)=C(I)+S*(XX(IMAX,I)-C(I))
80    CONTINUE
      CALL F(V,N,FV)
      IF (FV .LT. FX(IMAX)) THEN
      DO 90 I=1,N
      XX(IMAX,I)=V(I)
90    CONTINUE
      FX(IMAX)=FV
      ACTION='Contraction '
      GOTO 15
      ELSE
C
C
C     Shrink.....
C
      DO 100 I=1,N+1
      DO 100 J=1,N
      XX(I,J)=0.5D0*(XX(I,J)+XX(IMIN,J))
100   CONTINUE
      ACTION='Shrink     '
      GOTO 5
      ENDIF
      ENDIF
      RETURN
      END
C
C
C     The following subroutine is for solving ODEs by Runge-Kutta
C     fourth method.....
C
      SUBROUTINE F(X,N,FX)
      IMPLICIT REAL *8 (A-H,O-Z)
      DIMENSION X(N), CONST(2)
      INCLUDE 'MOLREDTN.DAT'
      DO 5 I=1,N
      XX(I)=X(I)
      IF (XX(I) .LT. 0.0D0) THEN
      FX=1.0D10
      GOTO 20
      ENDIF
5     CONTINUE
      FX=0.0D0
      DO 20 JCOL=1,NT
      TK=TEMP(JCOL)
      Y(1)=Y10
      Y(2)=Y20
      Y(3)=Y30
      Y(4)=Y40
      Y(5)=Y50
      CALL DERIVS (NN,Y,DY)
      JEXP=1
      TIME1=TIME(JEXP,JCOL)
```

```
      DO 10 I=1,MAXS
      CALL RK4(NN,H,Y,DY,YC,Y1)
      IF (ABS(Y(1)-TIME1) .LE. 1.0D-8) THEN
      DIFA=A(JEXP,JCOL)-Y(2)
      DIFB=B(JEXP,JCOL)-Y(3)
      DIFC=C(JEXP,JCOL)-Y(4)
      DIFD=D(JEXP,JCOL)-Y(5)
      DIFA=SIGN(MIN(ABS(DIFA), 1.0D15), DIFA)
      DIFB=SIGN(MIN(ABS(DIFB), 1.0D15), DIFB)
      DIFC=SIGN(MIN(ABS(DIFC), 1.0D15), DIFC)
      DIFD=SIGN(MIN(ABS(DIFD), 1.0D15), DIFD)
      DIFA=DIFA/A(JEXP,JCOL)
      DIFB=DIFB/B(JEXP,JCOL)
      DIFC=DIFC/C(JEXP,JCOL)
      DIFD=DIFD/D(JEXP,JCOL)
      FX=FX+DIFA*DIFA+DIFB*DIFB+DIFC*DIFC+DIFD*DIFD
      JEXP=JEXP+1
      TIME1=TIME(JEXP,JCOL)
      IF(JEXP .GT. NUMBER(JCOL)) GOTO 20
      ENDIF
10    CONTINUE
20    CONTINUE
      RETURN
      END
C
C
C     Here is the ODE solver.....
C
      SUBROUTINE RK4(N,H,Y,DY,YC,Y1)
      IMPLICIT REAL*8 (A-H,O-Z)
      DIMENSION Y(N), DY(N), YC(N), Y1(N), A(4)
      A(1)=0.5D0*H
      A(2)=A(1)
      A(3)=H
      A(4)=H
      DO 1 I=1,N
      Y1(I)=Y(I)
1     CONTINUE
      DO 3 K=1,3
      DO 2 I=1,N
      YC(I)=Y1(I)+A(K)*DY(I)
      Y(I)=Y(I)+A(K+1)*DY(I)/3.0D0
2     CONTINUE
      CALL DERIVS(N,YC,DY)
3     CONTINUE
      DO 4 I=1,N
      Y(I)=Y(I)+A(1)*DY(I)/3.0D0
4     CONTINUE
      CALL DERIVS(N,Y,DY)
      RETURN
      END
C
C
C     This subroutine is for derivatives of the differential equations for
```

```
C       the reaction scheme.
C       where,
C               Y(1) = time
C               Y(2) = Fraction of the Resid in the total HT product
C               Y(3) = Fraction of the Total Gas Oil in the total HT product
C               Y(4) = Fraction of the Middle Distillates in the total HT product
C               Y(5) = Fraction of the Gases in the total HT product
C
C       Also,
C               X(1) = kro
C               X(2) = kod
C               X(3) = kog
C               X(4) = kdg
C
C               DY(1) = dY(1)/dt, DY(2) = dY(2)/dt, DY(3) = dY(3)/dt,
C               DY(4) = dY(4)/dt, DY(5) = dY(5)/dt.....
C
C
        SUBROUTINE DERIVS(N,Y,DY)
        IMPLICIT REAL*8 (A-H,O-Z)
        DOUBLE PRECISION Y(5), DY(5)
        COMMON /DKWAK/TEMP, X(10)
        DO 10 I=2,N
        IF(Y(I) .LT. 0.0D0) Y(I)=0.0D0
        IF(Y(I) .GT. 1.0D0) Y(I)=1.0D0
10      CONTINUE
        DY(1)=1.0D0
        Y2=Y(2)
        Y3=Y(3)
        DY(2)=-X(1)*Y2
        DY(3)=X(1)*Y2-Y3*(X(2)+X(3))
        DY(4)=X(2)*Y2-X(4)*Y(4)
        DY(5)=X(3)*Y3+X(4)*Y(4)
        RETURN
        END
C
C
C       The following subroutine checks the performance of this program.
C       It compares the experimental and calculated value of the estimated
C       kinetic constants and gives the performance ranges.....
C
        SUBROUTINE STTEST(N,X,IP1)
        IMPLICIT REAL*8 (A-H, O-Z)
        DIMENSION X(N)
C       INCLUDE 'MOLREDTN.DAT'
C       DIMENSION DIFFA(NP),DIFFB(NP),DIFFC(NP),DIFFD(NP),DIFFE(NP),
C    1  YAA(NP),YBB(NP),YCC(NP),YDD(NP),YEE(NP),
C    2  PERCTA(NP),PERCTB(NP),PERCTC(NP),PERCTD(NP)
C       DIMENSION DIFA(NT*NP),DIFB(NT*NP),DIFC(NT*NP),DIFD(NT*NP)
C    1  ,DIFE(NT*NP)
C
        DIMENSION DIFFA(5),DIFFB(5),DIFFC(5),DIFFD(5),DIFFE(5),
     1  YAA(5),YBB(5),YCC(5),YDD(5),YEE(5),
     2  PERCTA(5),PERCTB(5),PERCTC(5),PERCTD(5)
```

```
      DIMENSION DIFA(5),DIFB(5),DIFC(5),DIFD(5)
     1  ,DIFE(5)
      INCLUDE 'MOLREDTN.DAT'
C
      DO 5 I=1,N
      XX(I)=X(I)
5     CONTINUE
      ICOUNT=0
      AADA=0.0D0
      AADB=0.0D0
      AADC=0.0D0
      AADD=0.0D0
      DO 200 JCOL=1,NT
      TK=TEMP(JCOL)
      Y(1)=Y10
      Y(2)=Y20
      Y(3)=Y30
      Y(4)=Y40
      Y(5)=Y50
      NUM=NUMBER(JCOL)
      JEXP=1
      TIME1=TIME(JEXP,JCOL)
      CALL DERIVS(NN,Y,DY)
      DO 10 I=1,1000
      CALL RK4(NN,H,Y,DY,YC,Y1)
      IF(ABS(Y(1)-TIME1). LE. 1.0D-8) THEN
      DIFFA(JEXP) = A(JEXP,JCOL)-Y(2)
      DIFFB(JEXP) = B(JEXP,JCOL)-Y(3)
      DIFFC(JEXP) = C(JEXP,JCOL)-Y(4)
      DIFFD(JEXP) = D(JEXP,JCOL)-Y(5)
      ICOUNT=ICOUNT+1
      DIFA(ICOUNT)=DIFFA(JEXP)
      DIFB(ICOUNT)=DIFFB(JEXP)
      DIFC(ICOUNT)=DIFFC(JEXP)
      DIFD(ICOUNT)=DIFFD(JEXP)
      YAA(JEXP)=Y(2)
      YBB(JEXP)=Y(3)
      YCC(JEXP)=Y(4)
      YDD(JEXP)=Y(5)
      PERCTA(JEXP)=DIFFA(JEXP)/A(JEXP,JCOL)*100.0D0
      PERCTB(JEXP)=DIFFB(JEXP)/B(JEXP,JCOL)*100.0D0
      PERCTC(JEXP)=DIFFC(JEXP)/C(JEXP,JCOL)*100.0D0
      PERCTD(JEXP)=DIFFD(JEXP)/D(JEXP,JCOL)*100.0D0
      AADA=AADA+ABS(PERCTA(JEXP))
      AADB=AADB+ABS(PERCTB(JEXP))
      AADC=AADC+ABS(PERCTC(JEXP))
      AADD=AADD+ABS(PERCTD(JEXP))
      JEXP=JEXP+1
      TIME1=TIME(JEXP,JCOL)
      IF(JEXP .GT. NUM) GOTO 20
      ENDIF
10    CONTINUE
20    CONTINUE
C     WRITE(*,100) TK
```

```
      WRITE(1,100) TK
100   FORMAT(/5X,'TEMPERATURE=',F7.2,' K',
     1     /5X, 'RESID FRACTION:')
      WRITE(*,110)
      WRITE(1,110)
110   FORMAT(7X,'TIME',4X,'EXPERIMENTAL',10X,'CALCULATED',7X,
     1  'DIFFERENCE',5X,'PERCENTAGE'/
     2  7X,'----',5X,'--------',13X,'---------',8X,
     3 '- ---------',5X,'----------')
      DO 30 I=1,NUM
      WRITE(6,120) TIME(I,JCOL),A(I,JCOL),YAA(I),DIFFA(I),PERCTA(I)
      WRITE(1,120) TIME(I,JCOL),A(I,JCOL),YAA(I),DIFFA(I),PERCTA(I)
30    CONTINUE
120   FORMAT(3X,F8.1,2X,G13.5,G22.7,G18.7,G13.5)
      WRITE(*,130)
      WRITE(1,130)
130   FORMAT(/5X, 'TOTAL GAS OIL FRACTION:')
      WRITE(*,110)
      WRITE(1,110)
      DO 40 I=1,NUM
      WRITE(*,120) TIME(I,JCOL),B(I,JCOL),YBB(I),DIFFB(I),PERCTB(I)
      WRITE(1,120) TIME(I,JCOL),B(I,JCOL),YBB(I),DIFFB(I),PERCTB(I)
40    CONTINUE
      WRITE(*,140)
      WRITE(1,140)
140   FORMAT(/5X, 'MIDDLE DISTILLATE FRACTION:')
      WRITE(*,110)
      WRITE(1,110)
      DO 50 I=1,NUM
      WRITE(*,120) TIME(I,JCOL),C(I,JCOL),YCC(I),DIFFC(I),PERCTC(I)
      WRITE(1,120) TIME(I,JCOL),C(I,JCOL),YCC(I),DIFFC(I),PERCTC(I)
50    CONTINUE
      WRITE(*,150)
      WRITE(1,150)
150   FORMAT(/5X, 'GASES (NH3, H2S, C1 TO C4):')
      WRITE(*,110)
      WRITE(1,110)
      DO 60 I=1,NUM
      WRITE(*,120) TIME(I,JCOL),D(I,JCOL),YDD(I),DIFFD(I),PERCTD(I)
      WRITE(1,120) TIME(I,JCOL),D(I,JCOL),YDD(I),DIFFD(I),PERCTD(I)
60    CONTINUE
200   CONTINUE
C
C
C     Now calculating each fraction's AADs.....
C
      S1=0.0D0
      DO 70 J=1,NT
      NUM=NUMBER(J)
      DO 70 I=1,NUM
      S1=S1+A(I,J)
      S1=S1+B(I,J)
      S1=S1+C(I,J)
      S1=S1+D(I,J)
```

```
70      CONTINUE
        S1=0.25D0*S1/ICOUNT
        RGS=0.0D0
        DO 80 J=1,NT
        NUM=NUMBER(J)
        DO 80 I=1,NUM
        RGS=RGS+(A(I,J)-S1)**2
        RGS=RGS+(B(I,J)-S1)**2
        RGS=RGS+(C(I,J)-S1)**2
        RGS=RGS+(D(I,J)-S1)**2
80      CONTINUE
        RSDA=0.0D0
        RSDB=0.0D0
        RSDC=0.0D0
        RSDD=0.0D0
        DO 90 I=1,ICOUNT
        RSDA=RSDA+DIFA(I)*DIFA(I)
        RSDB=RSDB+DIFB(I)*DIFB(I)
        RSDC=RSDC+DIFC(I)*DIFC(I)
        RSDD=RSDD+DIFD(I)*DIFD(I)
90      CONTINUE
        RSD=RSDA+RSDB+RSDC+RSDD
        R2=1.0D0-RDS/RGS
        AADA=AADA/ICOUNT
        AADB=AADB/ICOUNT
        AADC=AADC/ICOUNT
        AADD=AADD/ICOUNT
        WRITE(1,170) RSDA,AADA,RSDB,AADB,RSDC,AADC,RSDD,AADD
        WRITE(*,170) RSDA,AADA,RSDB,AADB,RSDC,AADC,
     1                 RSDD,AADD
170     FORMAT(/5X,'  COMP.', 16X, 'SSE', 12X,'AAD',
     1    /5X,'  -----', 16X, '---', 12X,'---',
     2    /8X, 'RESID',8X,2G16.5,/8X,'GAS OIL',6X,2G16.5,
     3    /8X, 'MID.DIT.',5X,2G16.5,/8X,'GASES',8X,2G16.5)
        RETURN
        END
```

REFERENCES

1. Beaton, W.I., and Bertolacini, R.J., Resid Hydroprocessing at Amoco, Catal. Rev.-Sci. Eng., (1991), 33(3&4), 281.
2. Speight, J.G., The Chemistry and Technology of Petroleum, 2nd Ed., Marcel Dekker, New York, (1991).
3. Hoiberg, A.J., Bituminous Materials: Asphalts, Tars, and Pitches, John Wiley and Sons, New York, (1964).
4. Beattie, C.I., Boberg, T.C. and McNab, G.S., Reservoir Simulation of Cyclic Steam Stimulation in the Cold Lake Oil Sands, SPE Regional Mtg., Bakersfield, CA, April, (1989).
5. Johnson, L.A., Jr., Fahy, L.J., Romanowski, L.J., Jr, Thomas, K.P. and Hutchinson, H.L., An Evaluation of a Steam Flood Experiment in a Utah Tar Sand Deposit, J. Pet. Techol., (1982), 1119.
6. Johnson, L.A. Jr., Fahy, L.J., Jr., Barbour, R.V. and Thomas, K.P., Echoing In-Situ Combustion Oil Recovery Project in a Utah Tar Sands, J. Pet. Technol., (1980), 295.
7. Miller, J.D. and Misra, M., Hot Water Process Development for Utah Tar Sand, Fuel Process. Technol., (1982), 6, 27.
8. Rendall, J.S., Solvent Extraction Process, U.S. Pat., (1979), No. 4, 160, 718.
9. Miller, J.D., and Misra, M., Concentration of Utah Tar Sands by a Ambient Floatation Process, Int. J. Miner. Process., (1982), 9, 269.
10. Hanson, F.V., and Oblad, A.G., The Fluidized Bed Pyrolyis of Bitumen-Impregnated Sandstone from the Tar Sand Deposit of Utah., Proc. 4th

UNITAR/UNDP Int. Conf. Heavy Crude Tar Sands, Edmonton, Alberta, (1988), 5, 421.

11. Speight, J.G., The Desulfurization of Heavy Oils and Residua, Marcel Dekker, New York, (1981).
12. Beaton, W.I., Hydrodesulfurization of Petroleum Resids; Chemical Reactions as a Means of Separation - Sulfur Removal, Chem. Process. Eng., (1977), 11, 1.
13. Speight, J.G., Bitumens, Asphalts and Tar Sands, Developments in Petroleum Science, Ed. T.F. Yen and G.V. Chilingarian, No. 7, Elsevier, New York, (1978).
14. Corbett, R.A., Modern Hydrocracking is the Key to Upgrading Processes, Oil Gas J., OGJ SPECIAL, (1989), June 26, 42.
15. Riley, K.L., Effect of Catalyst Properties on Heavy Feed Hydroprocessing, Prepr. - Am. Chem. Soc., Div. Pet. Chem., (1978), 23, 1104.
16. Cha, S., Pyrolysis of Oil Sands from Whiterocks Tar Sand Deposit in a Rotary Kiln, Ph.D. Dissertation, University of Utah, Salt Lake City, UT, (1991).
17. Oblad, A.G., Bunger, J.W., Hanson, F.V., Miller, J.D., Ritzma, H.R., and Seader, J.D., Tar Sand Research and Development at the University of Utah, Ann. Rev. Energy, (1987), 12, 283.
18. Longstaff, D.C., Hydrotreating the Whiterocks Oil Sand Bitumen and Bitumen-Derived Liquid, Ph.D. Dissertation, University of Utah, Salt Lake City, UT, (1992).
19. Massagutov, R.M., Berg, G.A., Kulinich, G.M., and Kirillov, T.S., Kinetics of High-Sulphur Distillate Hydrotreating, Proc. 7th World Pet. Congr., (1967), 4, 177.

20. Tsai, C.H., Longstaff, D.C., Deo, M., Hanson, F.V., and Oblad, A.G., Potential of Jet Fuels from Utah Tar Sand Bitumens and Bitumen-Derived Liquids, Prepr. - Am. Chem. Soc., Div. Pet. Chem., (1992), 37, 523.

21. Hupka, J., Oblad, A.G., and Miller, J.D., Diluent-Assisted Hot-Water Processing of Tar Sands, AOSTRA J. Res., (1987), 3, 95.

22. Gibson, K.R., Green, D.C., and Teichmann, D.P., Technical Challenges to Heavy Oil Conversion, Chem. Eng. Prog., (1983), 79(4), 93.

23. Siewert, H.R., Koenig, A.H., and Ring, T.A., Optimize Design for Heavy Crude, Hydrocarbon Process., (1985), 64(3), 61.

24. Gulf Pub. Co., 1986 Refining Process Handbook, Hydrocarbon Process. (1986), 65(9), 83.

25. Schuetze, B., and Hofmann, H., How to Upgrade Heavy Feeds, Hydrocarbon Process., (1984), 63(2), 75.

26. Murphy, J.R., Whittington, E.L., and Chang, C.P., Review Ways to Upgrade Resids, Hydrocarbon Process., (1979), 58(9), 119.

27. Quann, R.J., Ware, R.A., Hung, C., and Wei, J., Catalytic Hydrodemetallation of Petroleum, Adv. Chem. Eng., (1988), 14, 95.

28. Bridge, A.G., Scott, J.W., and Reed, E.M., Resid Hydroprocessing Options Multiply with New Technology, Oil Gas J., (1975), May 19, 94.

29. Yamamoto, M.D., Deep Desulfurization Works in Japan, Oil Gas J., (1977), May 16, 146.

30. Young. B.J., and Richardson, R.L., Resid Desulfurizer a Year Later, Hydrocarbon Process., (1977), 56(9), 103.

31. Christ, M.A., Shah, G.N., and Sherman, L.G., Broad Range of Resids Upgraded, Oil Gas J., (1979), May 28, 95.

32. Sosnowski, J., Turner, D.W., and Eng., J., Upgrading Heavy Crude to Clean Liquid Products, Chem. Eng. Prog., (1981), 77(2), 51.

33. Fong, H.L., Kushner, D.S., and Scott, R.T., Shell Redox Desulfurization Process Stresses Versatility, Oil Gas J., (1987), May 25, 54.

34. Gulf Pub. Co., Unicracking/HDS, Hydrocarbon Process., (1982), 61(9), 135.

35. Sikonia, J.G., New Data for RCD Unibon, Hydrocarbon Process., (1980), 59(6), 73.

36. Hohnholt, J.F., and Fausto, C.Y., Refinery Maintains Optimum Yields via Resid HDS, Oil Gas J., (1986), January 6, 63.

37. Beaton, W.I., McDaniel, N.K., McWhirter, W.E., Peterson, R.D., and Van Driesen, R.P., Resid Hydrocracker Expands Crude Processing Flexibility, Oil Gas J., (1986), July 7, 47.

38. Van Driesen, R.P., and Fornoff, L.L, Upgrade Resids with LC-Fining, Hydrocarbon Process., (1985), 64(9), 91.

39. Quinn, P.C., and Jeffries, R.B., Why Ebullieted Bed Hydroprocessing (H-Oil) was Chosen, 3rd Int. Conf. Heavy Crude Tar Sands, Long Beach CA, July, (1985).

40. Graeser, J., and Niemann, K., Proven Hydrogenation Process for Upgrading Residua Being Revived in Germany, Oil Gas J., March 22, (1982), 121.

41. Menzies, M.A., Silva, A.E., and Denis, J.M., Hydrocracking Without Catalysis Upgrades Heavy Oil, Chem. Eng., (1981), 88(4), 46.

42. Anderson, R.F., Olson, R.K., Hutchings, L.E., and Penning, R.T., The UOP Aurabon Process: an Update, 2nd Int. Conf. Heavy Crude Tar Sands, Caracas, Venezuela, February, (1982).

43. Sakabe, T., and Yagi, T., Cracking Resid With Spent HDS Catalyst, Hydrocarbon Process., (1979), 58(12), 103

44. Bearden, R., and Aldridge, C.L., Novel Catalyst and Process to Upgrade Heavy Oils, Energy Prog., (1981), 1(1), 44.

45. Sudoh, J., Shiroto, Y., Fukui, Y., and Takeuchi, C., Upgrading of Heavy Oils by Asphaltenic Bottom Cracking, Ind. Eng. Chem. Process Des. Dev., (1984), 23, 641.

46. Blourl, B., Hamdan, F., and Herault, D., Mild Cracking of High-Molecular-Weight Hydrocarbons, Ind. Eng. Chem. Process Des. Dev., (1985), 24, 30.

47. Fisher, I.P., Souhrada, F., and Wood, H.J., New Noncatalytic Heavy-Oil Process Developed in Canada, Oil Gas J., (1982), November 22, 111.

48. Bakshi, A.S., and Lutz, I.H., Adding Hydrogen Donor Visbreaking Improves Distillate Yields, Oil Gas J., (1987), July 13, 84.

49. Schutze, B., and Hofmann, H., Hydropyrolysis of Petroleum Residues and Heavy Crudes, Erdoel-Kohle, Erdgas, Petrochem., (1983), 36(10), 457.

50. Rakow, M.S., and Galderon, M., The Dynacracking Process - An Update, Chem. Eng. Prog., (1981), 77(2), 31.

51. Hus, M., Visbreaking Process Has Strong Revival, Oil Gas J., (1981), April 13, 109.

52. De Baise, R., and Elliot, J.D., Delayed Coking: Latest Trends, Hydrocarbon Process., (1982), 61(5), 99.

53. Busch, R.A., Fluid Coking: Sesoned Process Takes on New Jobs, Oil Gas J., (1970), April 6, 102.

54. Matula, J.P., Weiberg, H.N., and Weissman, W., Flexicoking: an Advanced Fluid Coking Process, Tech. Pap. - 37th Am. Pet. Inst., Div. Refin., New York, (1972).

55. Aiba, T., Kaji, H., Suzuki, T., and Wakamatsu, T., Residue Thermal Cracking by the Eureka Process, Chem. Eng. Prog., (1981), 77(2), 37.

56. Rush, J.B., Twenty Years of Heavy Oil Cracking, Chem. Eng. Prog., (1981), 77(12), 29.

57. Hennler, C.L., Lomas, D.A., and Tajbl, D.G., FCCU Reflects Technological Process to Resid Cracking, Oil Gas J., (1984), May 28, 79.

58. Dean, R.R., Mauleon, J.L., and Letzsch, W.S., Resid Puts FCC Process in New Perspective, Oil Gas J., (1982), October 4, 75.

59. Considine, D.M., Energy Technology Handbook, McGraw-Hill, New York, (1977).

60. Tomita, T., Development of a Steam Reforming Process for Residue, Chem. Econ. Eng. Rev., (1985), 81(6), 54.

61. Billon, A., Peries, J.P., Fehr, E., and Lorenz, E., SDA Key to Upgrading Heavy Crudes, Oil Gas J., (1977), January 24, 43.

62. Ditman, J.G., Deasphalt to Get Feed for Lubes, Hydrocarbon Process., (1973), 52(5), 110.

63. Gulf Pub. Co., Solvent Deasphalting, Hydrocarbon Process., (1986), 65(9), 110.

64. Gearhart, J.A., Solvent Treats Resids, Hydrocarbon Process., (1980), 59(5), 150.

65. Penning, R.T., Vickers, A.G., and Shah, B.R., Extraction Upgrades Resid, Hydrocarbon Process., (1982), 61(5), 145

66. Rhoe, A., Hamilton, G.L., and Suciu, G.D., Residue Solvent Refining-A New Process Performs Deasphalting of Heavy Residues in Crude Distillation Unit Equipment, NPRA Annu. Mtg., Los Angeles, CA, March, (1986).

67. Ohtsuka T., Catalyst for Hydrodesulfurization of Petroleum Residua, Catal. Rev.-Sci. Eng., (1977), 16(2), 291.

68. Richardson, J.T., Magnetic Study of Cobalt Molybdenum Oxide Catalysts, Ind. Eng. Chem. Fundam., (1964), 3(1), 154.

69. Van Zijll Langhout, W.C., Ouwerkerk, C., and Pronk, K.M.A., New Process Hydrotreats Meta-Rich Feedstocks, Oil Gas J., (1980), December 1, 120.

70. Toulhoat, H., Plumail, J.C., Martino, G., and Jacquin, Y., New HDM Catalysts; Design and Performance for Demetallation and Conversion, Prepr. - Am. Chem. Soc., Div. Pet. Chem., (1985), 30, 85.

71. De Bruijn, A., Naka, I., and Sonnemans, J.W.M., Effect of the Noncylindrical Shape of Extrudate on the Hydrodesulfurization of Oil Fractions, Ind. Eng. Chem. Process Des. Dev., (1981), 20, 40.

72. Ciapetta, F.G., and Plank, C.J., Catalysis, Ed. Emmett, P.H., Reinhold, New York, (1954), 1, 315.

73. Beuther, H. and Schmid, B.K., Reaction Mechanisms and Rates in Residue Hydrodesulfurization, 6th World Petrol. Congr., (1963), 3, 297.

74. Agrawal, R., and Wei, J., Hydrodemetallation of Nickel and Vanadium Porphrins. 1. Intrinsic Kinetics 2. Intraparticle Diffusion, Ind. Eng. Chem. Process Des. Dev., (1984), 23, 505, 515.

75. Arey, W.F., Jr., Blackwell III, N.E., and Reichle, A.D., Advances in Desulfurization of Residual Fractions and Asphalts, Proc. 7th World Petrol. Congr., (1967), 4, 167.

76. Kato, J., Shimada, K., Suzuki, M., Ose, H., Ohshima, S., Kuriki, Y., Nishizaki, H., and Kodera, Y., Hydrotreatment of Heavy Fractions of Petroleum; I. Reaction Rate of Hydrodesulfurization of Fuel Oil in a Complete Mixing Type Flow Reactor, Kogyo Kagakushi, (1971), 74(6), 1156.

77. Shah, Y.T., and Paraskos, J.A., Intraparticle Diffusion Effects in Residue Hydrodesulfurization, Ind. Eng. Chem., Process Des. Dev., (1975), 14(4), 368.

78. Parker, M.A., and Williams, B., Industry Steps Up Development of Heavy Oil, Bitumen Reserves, Oil Gas J., (1986), January 6, 41.

79. Montagna, A.A., Shah, Y.T., The Role of Liquid Holdup, Effective Catalyst Wetting, and Backmixing on the Performance of a Trickle Bed Reactor for Residue Hydrodesulfurization, Ind. Eng. Chem., Process Des. Dev., (1979), 14(4), 479.

80. Riley, K.L., The Effect of Catalyst Properties on Heavy Feed Hydroprocessing, General Papers Presented before Am. Chem. Soc., Div. Pet. Chem. Anaheim Mtg, Mar., (1978).

81. Richardson, R.L., Alley, S.K., Consideration of Catalyst Pore Structure and Asphaltenic Sulfur in the Desulfurization of Resids, Prepr. - Am. Chem. Soc., Div. Pet. Chem., (1975), 20, 554.

82. Schuit, G.C.A., and Gates, B.C., Chemistry and Engineering of Catalytic Hydrodesulfurization, AIChE J., (1973), 19(3), 417.

83. Inoguchi, M., Tate, K., Kaneko, Y., Satomi, Y., Inaba, K., Mizutori, T., Kagaya, H., Nishiyama, R., Onishi, S., Nagai, T., Hydrodesulfurization Catalyst of Residual Fuel; 1. Correlation Between Physical Property and Desulfurization Activity of Catalyst, Bull. Jap. Petrol. Inst., (1971), 13(1), 3.

84. Douwes, C. Th., Van Klinken, J., Wijffels, J.B., and Van Zijll Langhout, W.C., Developments in Hydro-conversion Process for Residues, Proc. 10th World Pet. Congr., (1980), 4, 175.

85. Howell, R.L., Hung, C.W., Gibson, K.R., and Chen, H.C., Catalyst Selection Important for Residuum Hydroprocessing, Oil Gas J., (1985), July 29, 121.

86. Plumail, J.C., Jacquin, Y., Martino, G., and Toulhoat, H., Effect of the Pore Size Distribution on the Activities of Alumina Supported Co-Mo Catalysts in the Hydrotreatment of Boscan Crude, Prepr. - Am. Chem. Soc., Div. Pet. Chem., (1983), 28, 562.

87. Hardin, A.H., Ternan, M., and Packwood, R.H., The Effects of Pore Size in MoO_3-CoO-Al_2O_3 Hydroprocessing Catalysts, Prepr. - Am. Chem. Soc., Div. Pet. Chem., (1978), 23, 1450.

88. Hung, C.W., Howell, R.L., and Johnson, D.R., Hydrodemetallation Catalysts, Chem. Eng. Prog. (1986), 82(3), 57.

89. Satterfield, C.N., Trickle-Bed Reactors, AIChE J., (1975), 21(2), 209.

90. Satterfield, C.N, and Way, P.F., The Role of the Liquid Phase in the Performance of a Trickle Bed Reactor, AIChE J., (1972), 18, 305.

91. Koros, R.M., Scale-up Consideration for Mixed Phase Catalytic Reactors, Multiphase Chemical Reactors. Vol. II - Design Methods, NATO Adv. Study Inst. Ser., Ser. E: Appl. Sci., (1981), 52, 455.

92. Schwartz, J.G., Dudukovic, M.D., and Weger, E., The Efficiency of Liquid-Solid Contacting in Trickle-Bed Reactors, Proc. 4th Int. Symp. Chem. React. Eng., Frankfurt, (1976), 382.

93. Mears, D.E., The Role of Liquid Holdup and Effective Wetting in the Performance of Trickle Bed Reactors, Chem. React. Eng. ACS Monogr. Ser., (1974), 133, 218.

94. Satterfield, C.N., and Ozel, F., Direct Solid-Catalyzed Reaction of a Vapor in an Apparently Completely Wetted Trickle Bed Reactor, AIChE J., (1973), 19(6), 1259.

95. Yui, S.M., Hydrotreating of Bitumen-Derived Coker Gas Oil: Kinetics of Hydrodesulfurization, Hydrodenitrogenation, and Mild Hydrocracking, and

Correlations to Predict Product Yields and Properties, AOSTRA J. Res., (1989), 5, 211.

96. Yui, S.M., and Sanford, E.C., Catalytic Hydrotreating of Bitumen Derived Coker Gas Oil: A Modified Kinetic Model for Pilot and Commercial Plants, Prepr. - Can. Symp. Catal., Kingston, Ontario, (1986), June, 30.

97. Henry, H.C., and Gilbert, J.B., Scale up of Pilot Plant for Catalytic Hydroprocessing, Ind. Eng. Chem. Process Des. Dev., (1973), 12, 328.

98. Paraskos, J.A., Frayer, J.A., and Shah, Y.T., Effect of Holdup Incomplete Catalytic Wetting and Backmixing during Hydroprocessing in Trickle Bed Reactors, Ind. Eng. Chem. Process. Des. Dev., (1975), 14, 315.

99. Yui, S.M., Sanford, E.C., Mild Hydrocracking of Bitumen-Derived coker and Hydracker Heavy Gas Oils: Kinetics, Product Yields, and Product Properties, Ind. Eng. Chem. Res., (1989), 28, 1278.

100. Scott, A.H., Liquid Distribution in Packed Towers, Trans. Inst. Chem. Engr., (1935), 13, 211.

101. Levenspiel, O., Chemcial Reaction Engineering, 2nd Ed., Wiley, New York, (1972).

102. Gierman, H., Design of Laboratory Hydrotreating Reactors Scaling Down of Trickle-Flow Reactors, Appl. Catal. (1988), 43, 277.

103. Hochman, J.M., and Effron, E., Two-Phase Cocurrent Downflow in Packed Beds, Ind. Eng. Chem. Fundam., (1969), 8(1), 63.

104. Miller, S.F., and Judson, K., Axial Dispersion in Liquid Flow Through Packed Beds, AIChE J., (1966), 12(4), 767.

105. Schwartz, J.G., Weger, E., and Dudukovic, M.P., Liquid Holdup and Dispersion in Trickle-Bed Reactors, AIChE J., (1976), 22, 953.

106. Satterfield, C.N., Mass Transfer in Heterogeneous Catalysis, MIT Press., Cambridge, MA, (1970).

107. Schwartz, J.G. and Roberts, G.W., Analysis of Trickle Bed Reactors: Liquid Backmixing and Liquid-Solid Contacting., 74th Nat. Mtg. - AIChE, New Orleans, LA, March, (1973).

108. Mears, D.E., The Role of Axial Dispersion in Trickle-flow Laboratory Reactors, Chem. Eng. Sci., (1971), 26, 1361.

109. De Bruijn, Arie, Testing of HDS Catalysts in Small Trickle Phase Reactors, Proc. 6th Int. Congr. Cat., London, (1976), 2, 951.

110. De Wind, M., Plantenga, F.L., Heinerman, J.J.L., and Homan Free, H.W., Upflow versus Downflow Testing of Hydrotreating Catalysts, Appl. Catal., (1988), 43, 239.

111. Takematsu, T., and Parsons, B.I., A Comparison of Bottom Feed and Top-Feed Reaction Systems for Hydrodesulfurization, Bull. Dep. Energy, Mines and Resurces, Mines Branch, Ottawa, Fuels Res. Centre Tech., TB161, (1972).

112. Gates, B.C., Katzer, J.R., and Schuit, G.C.A., Chemistry of Catalytic Processes, McGraw-Hill, New York, (1979).

113. Katzer, J.R., Sivasubramanian, R., Process and Catalyst Needs for Hydrodenitrogenation, Catal. Rev.-Sci. Eng. (1979), 20, 155.

114. Ho, T.C., Hydrodenitrogenation Catalysis, Catal. Rev.-Sci. Eng., (1988), 30(1), 117.

115. Moore, R.T., McCutchan, P., and Young, D.A., Basic Nitrogen Determined by Titration with Perchloric Acid, Anal. Chem., (1951), 23, 1639.

116. Streitwieser, A., Jr., Heathcock, C.H., Introduction to Organic Chemistry, Macmillan, New York, (1976).

117. Girgis, M.J., and Gates, B.C., Reactivities, Reaction Networks, and Kinetics in High-Pressure Catalytic Hydroprocessing, Ind. Eng. Chem. Res., (1991), 30(9), 2021.

118. Olivé, J.L., Biyoko, S., Moulinas, C., Geneste, P., Hydroprocessing of Indole and ortho-Ethylaniline over Sulfided CoMo, NiMo, and NiW Catalysts, Appl. Catal., (1985), 19, 165.

119. Satterfield, C.N., Yang, S.H., Catalytic Hydrodenitrogention of Quinoline in A Trickle-Bed Reactor. Comparison with Vapor Phase Reaction, Ind. Eng. Chem. Process Des. Dev., (1984), 23, 11.

120. Hanon, R.T., Effects of PH_2S, PH_2, and PH_2S/PH_2 on the Hydrodenitrogenaton of Pyridine, Energy Fuels, (1989), 1, 424.

121. Bar Vise, A.J.G., and Whitehead, E.V., Characterization of Vanadium Porphyrins in Petroleum Residues, Prepr. - Am. Chem. Soc., Div. Pet. Chem., (1980), 25, 268.

122. Vrinat, M.L., The Kinetics of the Hydrodesulfurization Process; a Review, Appl. Cat., (1983), 6, 137.

123. Van Parijs, I.A., Hosten, L.H., Froment, G.F., Kinetics of Hydrodesulfurization on a Co-Mo/γ-Al_2O_3 Catalyst. 2. Kinetics of the Hydrogenolysis of Benzothiophene, Ind. Eng. Chem. Prod. Res. Dev., (1986), 25, 437.

124. Houalla, M., Nag, N.K., Sapre, A.V., Broderick, D.H., Gates, B.C., and Kwart, H., Hydrodesulfurization of Methyl Substituted Dibenzothiophenes Catalyzed by Sulfided CoO-MoO_3/γ-Al_2O_3, J. Cat., (1980), 61, 523.

125. Erickson, R.L., Myers, A.T., and Horr. C.A., Associationof Uranium and Other Metals with Crude Oil, Asphalt, and Petroliferous Rock, Bull. Am. Assoc. Pet. Geol., (1954), 38(10), 2200.

126. Reynolds, J.G., Biggs, W.R., and Fetzer, J.C. Characterization of Heavy Residue by Application of a Modified D 2007 Separation and Electron Paramagnetic Resonance, Liq. Fuels Technol., (1985), 3, 73.

127. Dean, R.A., and Whitehead, E.V., The Composition of High Boiling Petroleum Distillates and Residues, Proc. 6th World Pet. Congr., (1963), 5, 261.

128. Sugihara, J.M., Branthaver, G.Y., Wu, G.Y., and Weatherbee,C., Research on Metal Compounds in Petroleum - Present and Future, Prepr. - Am. Chem. Soc., Div. Pet. Chem., (1970), 15, C5.

129. Yen, T.F., The Role of Trace Metals in Petroleum, Ann Arbor Science, Ann Arbor, MI, (1975).

130. Baker, E.W., and Palmer, S.E., The Porphyrins, Ed. D. Dolphin, Vol. 1, CH. 11, Academic Press., New York, (1978).

131. Hung, C.W., and Wei, J., The Kinetics of Porphyrin Hydrodemetallation. 2. Vanadyl Compounds, Ind. Eng. Chem. Process Des. Dev. (1980), 19, 250.

132. Galiasso, R., Garcia, J., Caprioli, L., Pazos, J.M., and Soto, A., Reactions of Porphyrinic and Non Porphyrinic Molecules During Hydrodemetallization of Heavy Crude Oils, Prepr. - Am. Chem. Soc., Div. Pet. Chem., (1985), 30, 50.

133. Ware, R.A., and Wei, J., Catalytic Hydrodemetallation of Nickel Porphyrins II. Effect of Pyridine and of Sulfiding, J. Catal., (1985), 93, 100.

134. Syncrude Canada Ltd., Syncrude Analytical Methods for Oil Sand and Bitumen Processing, 1st Ed., AOSTRA, Edmonton, Alberta, (1979).

135. Dietz, W.A., Response Factors for Gas Chromatographic Analysis, J. Gas Chromatogr., Feb., (1967), 68.

136. API, Boiling Points of Normal Paraffins, °API Project 44, API, (1972).

137. Bance, S., Handbook of Practical Organic Microanalysis, Halsted Press., New York (1980).

138. Sawicki, E., Mulik, J.D., and Wittgenstein, E., Ion Chromatographic Analysis of Environmental Pollutants, Ann Arbor Science, MI, (1978).

139. ASTM D808-91, Standard Test Method for Chlorine in New and Used Petroleum Products (Bomb Method).

140. Childs, C.E., and Henner, E.B., A Direct Comparison of the Pregl, Dumas, Perkin-Elmer, and Hewlett-Packard (F&M) Carbon-Hydrogen-Nitrogen Procedures, Microchem. J., (1970), 15, 590.

141. Price, W.J., Spectrochemical Analysis by Atomic Absorption, Heydon and Son, London, (1979).

142. Lvov, B.V., Atomic Absorption Spectrochemical Analysis, American Elsevier, New York, (1970).

143. Bock, R., A Handbook of Decomposition Methods in Analytical Chemistry, John Wiley and Sons, New York, (1979).

144. Christian, G.D., Atomic Absorption Spectroscopy: Applications in Agriculture, Biology, and Medicine, Wiley-Interscience, New York, (1970).

145. ASTM D 189-88, Standard Test Method for Conradson Carbon Residue of Petroleum Products.

146. Longstaff, D.C., Deo, M.D., and Hanson, F.V., Hydrotreating the Bitumen from the Whiterocks Oil Sand Deposit, FUEL, (1994), In Press.

147. Longstaff, D.C., Deo, M.D., Hanson, F.V., Oblad, A.G., and Tsai, C.H., Hydrotreating the Bitumen-Derived Hydrocarbon Liquid Produced in a Fluidized-Bed Pyrolysis Reactor, FUEL, (1992), 71, 1407.

148. Sung, S., The Fluidized Bed Pyrolysis of Bitumen-Impregnated Sandstone in a Large Diameter Reactor, M.S. Thesis, University of Utah, Salt Lake City, UT, (1988).

149. Kwak, S., Longstaff, D.C., Deo, M.D., and Hanson, F.V., Hydrotreating Process Kinetics for Bitumen and Bitumen-Derived Liquids, FUEL, (1994), In Press.

150. Rueckor, C.M., Hess, R.K., and Akgerman, A., Effect of Partial Wetting on Scale-Up of Laboratory Trickle-Bed Reactors, Chem. Eng. Comm., (1987), 49, 301.

151. Carruthers, J.D., and DiCamillo, D.J., Pilot Plant Testing of Hydrotreating Catalysts; Influence of Catalyst Condition, Bed Loading and Dilution, Appl. Catal., (1988), 43, 253.

152. Grayson, H.G. and Streed, C.W., Vapor-Liquid Equilibria for High Temperature, High Pressure Hydrogen-Hydrocarbon Systems, Proc. 6th World Pet. Conf., (1963), 3, 233.

153. Simulation Sciences Inc., Process Simulation Program - User Added Subroutines, Rev. 3, Fullerton, CA, (1988).

154. Hwang, J., Application of Dynamic Supercritical Fluid Extraction to the Recovery and Upgrading of Complex Hydrocarbon Mixtures, Ph.D. Dissertation, University of Utah, Salt Lake City, UT, (1993).

155. Marquardt, D.W., An Algorithm for Least-Squares Estimation of Nonlinear Parameters, J. Soc. Ind. App. Math, (1963), 11(2), 431.

156. More, J.J., Garbow, B.S., and Hillstrom, K.E., User Guide for MINPACK-1, Argonne Nat. Lab. Rpt., ANL-80-74, Argonne, IL, (1980).

157. Ho, T.C., and Aris, R., One Apparent Second-Order Kinetics, AIChE J., (1987), 33(6), 1050.

158. Wei, J. and Hung, C.W., Differentiating between Two First-Order Reactions and a Single Second-Order Reaction, Ind. Eng. Chem. Process Des. Dev., (1980), 19, 197.

159. Oleck, S.M., and Sherry, H.S., Fresh Water Manganese Nodules as a Catalyst for Demetalizing and Desulfurizing Petroleum Residua, Ind. Eng., Chem. Process. Des. Dev., (1977), 16, 525.

160. Frye, C.G., and Mosby, J.F., Kinetics of Hydrodesulfurization, Chem. Eng. Prog., (1967), 63(9), 66.

161. Van Zoonen, D., and Douwes, T., Effect of Pellet Pore Structure on Catalyst Performance in the Hydrodesulfurization of Straight-Run Gas Oil, J. Inst. Petrol., (1963), 49(480), 383.

162. Köseoglu, R.Ö. and Phillips, C.R., Kinetics and Product Yield Distributions in the $CoO\text{-}MoO_3/Al_2O_3$ Catalysed Hydrocracking of Athabasca Bitumen, FUEL, (1988), 67, 1411.

163. Del Bianco, A., Panariti, N., Anelli, M., Beltrame, P.L., and Carniti, P., Thermal Cracking of Petroleum Residues: 1. Kinetic Analysis of the Reaction, FUEL, (1993), 72, 75.

164. Mosby, J.F., Buttke, R.D., Cox, J.A., and Nikolaides C., Process Characterization of Expanded-Bed Reactors in Series, Chem. Eng. Sci., (1986), 41(4), 989.

165. Abdul-Halim, A.-K.M., Hussain H. Al, Karim H.N.L. and Ihsan, N., Hydrotreating of Qaiyarah Deashpalted Residue, FUEL, (1988), 67, 36

166. Billon, A., Henrich, G., Jacquin, Y. and Peries, J.P., Heavy Solvent Deasphalting+HT - A New Refining Route for Upgrading of Residues and Heavy Crudes, Proc. 11th World Pet. Congr., (1983), 4, 35.

167. Paraskos, J.A., Frayer, J.A., and Shah, Y.T., Effect of Holdup Incomplete Catalyst Wetting and Backmixing during Hydroprocessing in Trickle Bed Reactors, Ind. Eng. Chem. Process Res. Dev., (1975), 14(3), 315.

168. Johnson, A.R., Wolk, R.M., Hippeli, R.F. and Nongbri, G., H-Oil Desulfurization of Heavy Fuels, Adv. Chem. Ser., (1973), 127, 105.

169. Curran, G.P., Struck, R.T., and Gorin, E., Mechanism of the Hydrogen-Transfer Process to Coal and Coal Extract, Ind. Eng. Chem. Process. Des. Dev., (1967), 6, 166.

170. Garg, D., Tarrer, A.R., and Guin, J.A., and Lee, J.M., Hydrotreating of SRC-1 Product, ACS Symp. Ser., (1981), 156, 191.

171. Soni, D.S., and Crynes, B.L., A Comparison of the HDS and HDN Activities of Monolith Alumina Impregnated with Cobalt and Molybdenum and a Commercial Catalyst, ACS Symp. Ser., (1981), 156, 207.

172. Scamangas, A., Papayannakos, N, and Marangozis, J., Catalytic Hydrodesulfurization of Petroleum Residue, Chem. Eng. Sci., (1982), 37, 1810.

173. George, Z.M, Catalytic Upgrading of Liquid Hydrocarbons Derived from Coprocessing of Heavy Oil and Coal, Can. J. Chem. Eng., (1990), 68, 519.

174. Iannibello, A., Marengo, S., Burglo, G., Baldi, G., Sicardi, S., and Specchia, V., Modelling the Hydrotreating Reactions of a Heavy Residual Oil in a Pilot Trickle-Bed Reactor, Ind. Eng. Chem. Process. Des. Dev., (1985), 24, 531.

175. De Bruijn, A., Testing of HDS Catalysts in Small Trickle Phase Reactors, Proc. 6th Int. Congr. Catal., (1976), 2, 951.

176. Higashi, H., Shirono, K., Sato, G., Nishimura, Y., and Egashira, S., Pilot Performance of Combined HDS and HDM Catalysts for Heavy Residue Hydrodemetallization, Prepr. - Am. Chem. Soc., Div. Pet. Chem., (1985), 30(1), 111.

177. Sooter, M.C., Effect of Catalyst Pore Size on Hydrodesulfurization of Coal Derived Liquids, Ph.D. Dissertation, Oklahoma State University, Stillwater, OK, (1974).

178. Diaz-Real, R.A., Mann, R.S., Sambi, I.S., Hydrotreatment of Athabasca Bitumen Derived Gas Oil over Ni-Mo, Ni-W, and Co-Mo Catalysts, Ind. Eng. Chem. Res., (1993), 32, 1354.

179. Bridge, A.G., Reed, E.M., Tamm, P.W., and Cash, D.R., Chevron Hydrotreating Processes Desulfurize Arabian Heavy Residua), AIChE. Sym. Ser., (1975), 71, 148.

180. Oballa, M., Wong, C., Krzywicki, A., Chase, S., Dennis, G., Vandenhengel. W., and Jeffries, R., Hydroprocessing Catalyst Research to Support the Operation of the Bi-Provincial Upgrader in Lloydminster, Proc. Int. Sym. on Heavy Oil and Residue Upgrading and Utilization, Ed. H. Chongren, and H. Chu, Beijing, (1992).

181. Morales, A., Garcia, J.J., Prada, R., Abrams, O., and Katan, L., Mechanism and Kinetic Model for Hydrodemetallation Reations, Proc. 8th Int. Congr. Catal., (1984), 2, 341.

182. Flinn, R.A., Larson, O.A. and Beuther, H., The Kinetics of Hydrodenitrogenation, Prepr. - Am. Chem. Soc., Div. Pet. Chem., (1962), 7, 165.

183. Trytten, L.C., Gray, M.R. and Sanford, E.C., Hydroprocessing of Narrow-Boiling Gas Oil Fractions: Dependence of Reaction Kinetics on Molecular Weight, Ind. Eng. Chem. Res., (1990), 29, 725.

184. Heck, R.H., Rankel, L.A., and DiGuisseppi, F.T., Conversion of Petroleum Resid from Maya Crude: Effects of H-Donors, Hydrogen Pressure and Catalyst, Fuel Process. Technol., (1992), 30, 69.

185. Sanford, E.C., and Chung, K.H., The Mechanism of Pitch Conversion During Coking, Hydrocracking and Catalytic Hydrocracking of Athabasca Bitumen, AOSTRA J. Res., (1991), 7, 37.

186. Miki, Y., Yamadaya, S., Oba, M., and Sugimoto, Y., Role of Catalyst in Hydrocracking of Heavy Oil, J. Catal., (1983), 83, 371.

187. Savage, P.E., and Klein, M.T., Petroleum Asphaltene Thermal Reaction Pathways, Prepr. - Am. Chem. Soc., Div. Pet. Chem., (1985), 30(4), 642.

188. Bunger, J.W., Reactions of Hydrogen During Hydropyrolysis Processing of Heavy Crudes, Prepr. - Am. Chem. Soc., Div. Pet. Chem., (1985), 30(4), 658.